THE MINOR PLANET BULLETIN

BULLETIN OF THE MINOR PLANETS SECTION OF THE ASSOCIATION OF LUNAR AND PLANETARY OBSERVERS

VOLUME 43, NUMBER 1, A.D. 2016 JANUARY-MARCH 1.

PHOTOMETRIC OBSERVATIONS OF MAIN-BELT ASTEROIDS 656 BEAGLE AND 2649 OONGAQ

Adrian Bruno Şonka
Astronomical Institute of the Romanian Academy, 5 Cuţitul de Argint, 040557 Bucharest, ROMANIA
sonka.adrian@gmail.com

Marcel Popescu, Dan Alin Nedelcu
Astronomical Institute of the Romanian Academy

(Received: 2015 September 15)

We present photometric observations for two main-belt asteroids, 656 Beagle and 2649 Oongaq, carried out at Astronomical Institute of Romanian Academy between 2014 September and 2015 March. For 656 Beagle, we found a synodic rotation period of 7.034 ± 0.003 h and for 2649 Oongaq a synodic rotation period of 7.789 ± 0.006 h. Both are in good agreement with recent results.

Main-belt asteroids 656 Beagle and 2649 Oongaq were observed from Bucharest Observatory (073) using a 0.5-m *f*/10 Cassegrain telescope and SBIG STL 11000M CCD camera (binned 2x2) cooled to – 20 °C. The field-of-view was 16x11 arcmin and the pixel scale 0.502 arcsec/pixel. For 656 Beagle, exposures were 60 seconds using a Johnson V filter. 2649 Oongaq was observed by taking unfiltered images with 60 seconds integration time to improve the signal to noise ratio.

For both asteroids, images were calibrated with bias, flats, and darks. Data processing and period analysis were performed using *MPO Canopus*. Differential photometry measurements were performed using the Comp Star Selector (CSS) procedure in *MPO Canopus* which allows selecting up to five comparison stars of near solar color.

656 Beagle has an estimated diameter of 53.17 km (JPL, 2015). We observed it on nine nights between 2015 Feb 16 and Mar 24 (Table I). We obtained a synodic period of 7.034 ± 0.003 h with a maximum amplitude of 0.85 mag.

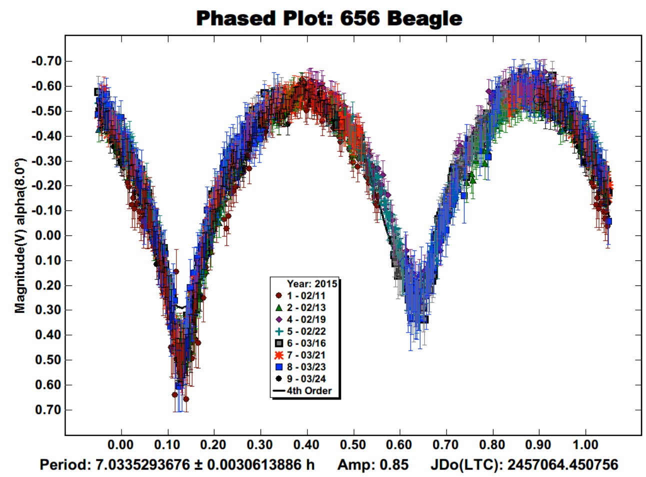

Date/2015	UT start-end	V	Airmass Start-End
Feb 10/11	21:03-00:57	14.0	3.7 - 1.3
Feb 12/13	20:29-01:51	13.9	4.9 - 1.2
Feb 18/19	21:46-01:34	13.8	1.9 - 1.2
Feb 21/22	20:25-01:58	13.7	3.0 - 1.3
Mar 16/16	18:01-23:22	13.9	4.0 - 1.2
Mar 21/22	19:21-00:09	14.0	1.9 - 1.3
Mar 23/24	19:01-00:07	14.1	2.0 - 1.3
Mar 24/25	18:09-22:09	14.1	2.7 - 1.2

Table I. Observation circumstances for 656 Beagle. From left to right, the columns give the date, UT at the start and end of the observing night, apparent V magnitude, the phase angle and the air mass at the beginning and the end of the observations.

2649 Oongaq. Masiero *et al.* (2012) report a diameter of 12 km for this main-belt asteroid. It was observed for nine nights between 2014 Sept 24 and Oct 19 (Table II). Analysis found a synodic period of 7.789 ± 0.006 h with an amplitude of 0.44 mag. The period is in good agreement with the period of 7.786 ± 0.001 h given by Klinglesmith *et al.* (2015). The amplitude observed was 0.44 magnitudes. Note the flat maximum just before the secondary minimum.

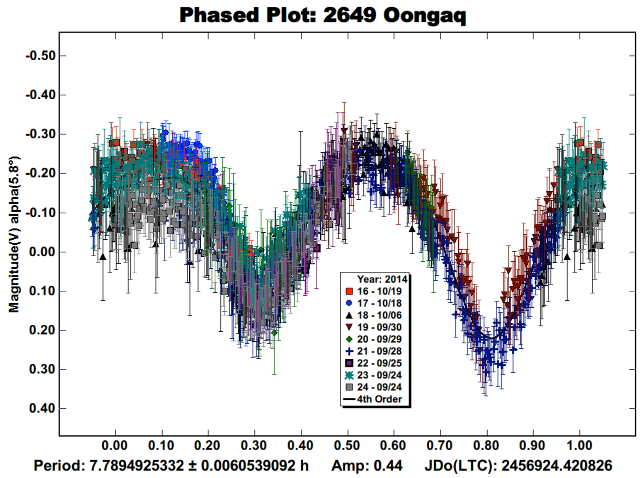

Date/2014	UT start-end	V	Airmass Start-End
Sep 23/24	20:17-00:15	15.3	1.3 - 1.2
Sep 24	19:16-22:55	15.3	4.0 - 1.2
Sep 25	20:55-22:48	15.2	1.9 - 1.2
Sep 28/29	17:56-00:35	15.2	4.0 - 1.0
Sep 29	17:59-21:50	15.1	4.0 - 1.4
Sep 30/01	19:22-00:20	15.1	3.0 - 1.0
Oct 05/06	19:50-01:29	15.0	2.1 - 1.1
Oct 18	20:50-23:15	14.8	1.3 - 1.1
Oct 19	19:22-22:43	14.8	1.8 - 1.2

Table II. Observation circumstances for 2449 Oongaq. From left to right, the columns give the date, UT at the start and end of the observing night, apparent V magnitude, the phase angle and the air mass at the beginning and the end of the observations.

References

Klinglesmith, D.A., Dehart, A., Hanowell, J., Henderickx, S. (2015). "Asteroids at Etscorn Campus Observatory: 2014 September - December." *Minor Planet Bull*. **42**, 101-104.

Masiero, J., Mainzer, A.K., Grav, T., Bauer, J.M., Cutri, R.M., Nugent, C., Cabrera, M.S. (2012). "Preliminary Analysis of WISE/NEOWISE 3-Band Cryogenic and Post-cryogenic Observations of Main Belt Asteroids." *Ap. J. Letters* **759**, L8.

Tedesco, E.F., Noah, P.V., Noah, M., Price, S.D. (2004). "IRAS Minor Planet Survey." IRAS-A-FPA-3-RDR-IMPS-V6.0. NASA Planetary Data System.

ASTEROID PHOTOMETRY FROM THE PRESTON GOTT OBSERVATORY

Dr. Maurice Clark
Department of Physics
Texas Tech University
Lubbock TX 79409
maurice.clark@ttu.edu

(Received: 2015 Aug 9 Revised: 2015 Aug 17)

Asteroid period and amplitude results obtained at the Preston Gott Observatory during the first half of 2015 are presented.

The Preston Gott Observatory is the main astronomical facility of the Texas Tech University. Located about 20 km north of Lubbock, TX, the main instrument is a 0.5-m *f*/6.8 Dall-Kirkham Cassegrain. An SBIG STL-1001E CCD was used with this telescope. Other telescopes used were 0.35-m and 0.30-m Schmidt-Cassegrains (SCT). SBIG ST9XE CCD's were used with these telescopes. All images were unfiltered and were reduced with dark frames and sky flats.

Image analysis was accomplished using differential aperture photometry with *MPO Canopus*. Period analysis was also done in *MPO Canopus*, which implements the algorithm developed by Alan Harris (Harris *et al.*, 1989). Differential magnitudes were calculated using referene stars from the USNO-A 2.0 catalog and the UCAC3 catalog.

Results are summarized in Table I and the lightcurve plots are presented at the end of the paper. The data and curves are presented without additional comment except were circumstances warrant. Column 3 in Table I gives the range of dates of observations and column 4 gives the number of nights on which observations were undertaken.

1361 Leuschneria. Observations of this asteroid were made on five nights. However with the derived period being very close to 12 hours, it was not possible to observe a complete period. More observations are required to confirm the derived period.

3015 Candy. This asteroid was observed on six nights as part of continuing observations to derive the asteroid shape. The derived period was very close to that obtained at previous oppositions. (Clark, 2007; 2011; 2015) Comparison with these earlier observations indicates the possibility that the period may be increasing. Since I first observed the asteroid in 2005, the period has increased from 4.62472 hours to 4.62538 hours, an increase of

#	Name	Date Range yyyy/mm/dd	Sess	Period (h)	P.E. (h)	Amp (mag)	A.E. (mag)
1361	Leuschneria	2015/06/03 - 2015/06/24	5	12.0893	0.0035	0.75	0.05
3015	Candy	2015/04/26 - 2015/06/21	6	4.62501	0.00004	0.66	0.03
6730	Ikeda	2015/05/27 - 2015/06/25	7	16.33408	0.00001	0.54	0.1
7889	1994 LX	2015/06/25 - 2015/07/19	3	2.6889	0.0001	0.30	0.05
9090	Chirotenmondai	*2014/12/15* - 2015/03/15	5	5.6477	0.0002	0.17	0.05
9963	Sandage	2015/05/27 - 2015/06/24	6	4.65053	0.00013	0.43	0.1
13003	Dickbeasley	2015/05/18 - 2015/05/27	3	3.4999	0.0005	0.30	0.05
19327	1996 XH19	2015/05/27 - 2015/06/23	5	3.9878	0.0001	0.57	0.05
19918	1977 PB	2015/04/26 - 2015/05/25	3	7.6897	0.0003	0.92	0.03
67354	2000 KM1	2015/06/23 - 2015/06/25	3	5.76?		0.52?	
136108	Haumea	2015/04/25 - 2015/05/25	3	3.9154	0.0002	0.27	0.03
152679	1998 KU2	2015/06/21 - 2015/06/25	4	4.48??		0.08??	

Table I. Period analysis results.

almost 2.4 seconds. Such a small apparent increase may be just caused by random measurement uncertainty; however, other asteroids observed at multiple oppositions do not show such a constant variation. More observations at future oppositions are planned to see if this apparent period increase is real. A graph of the measured period over time is included at the end of this paper.

6730 Ikeda. This asteroid proved very difficult to analyze. Despite observations being made on seven nights, several possible periods were indicated. The one produced here appeared the one most likely; however, more observations are required to confirm this result.

(67354) 2000 KM1. Observations of this asteroid were made on three nights when it was in the same field as another asteroid I was observing. No definitive period could be derived. The value presented here is as a guide for future observers.

(152679) 1998 KU2. This Apollo-class asteroid was observed on four nights. The scatter in the data appeared to be greater than any amplitude. As a result, no definitive period could be derived. The value presented here is as a guide for future observers.

Acknowledgments

I would like to thank Brian Warner for all of his work with the program *MPO Canopus* and for his efforts in maintaining the CALL website.

References

Clark, M. (2007). “Lightcurve Results For 1318 Nerina, 2222 Lermontov, 3015 Candy, 3089 Oujianquan, 3155 Lee, 6410 Fujiwara, 6500 Kodaira, 8290 1992 NP, 9566 Rykhlova, 42923 1999 SR18, and 2001 FY.” *Minor Planet Bul.* **34,** 19-22.

Clark, M. (2011). “Asteroid Lightcurves from the Preston Gott Observatory.” *Minor Planet Bul.* **39**, 63-65.

Clark, M. (2015). “Asteroid Lightcurves from the Preston Gott Observatory.” *Minor Planet Bul.* **42**, 15-20.

Harris, A.W., Young, J.W., Bowell, E., Martin, L.J., Millis, R.L., Poutanen, M., Scaltriti, F., Zappala, V., Schober, H.J., Debehogne, H., and Zeigler, K.W. (1989). “Photoelectric Observations of Asteroids 3, 24, 60, 261, and 863.” *Icarus* **77**, 171-186.

Warner, B.D. (2011). Collaborative Asteroid Lightcurve Link website. *http://www.minorplanet.info/call.html*

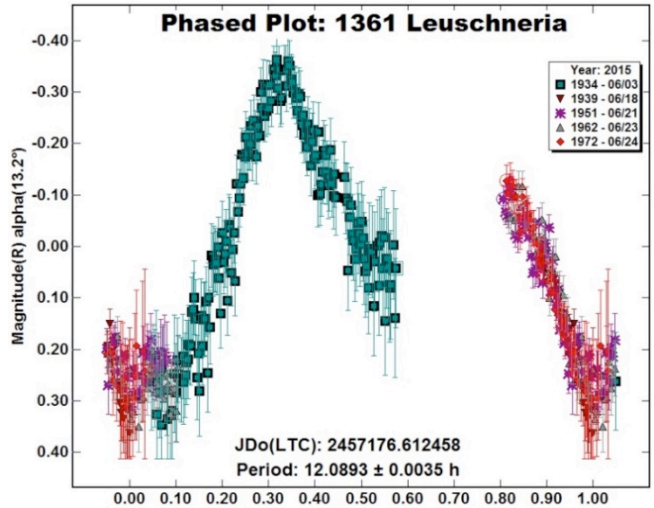

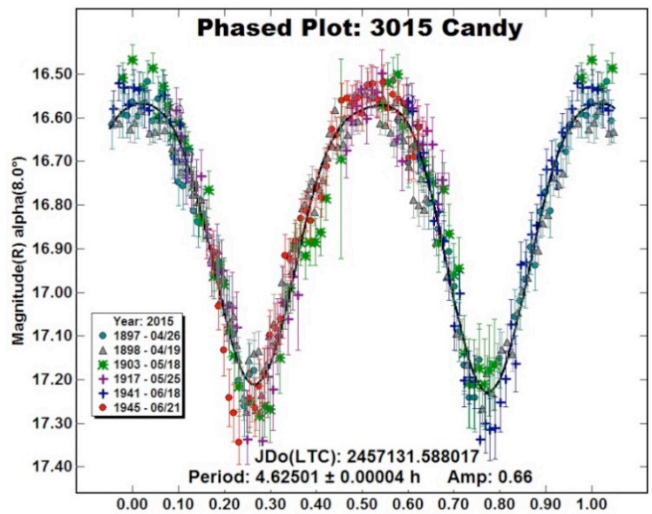

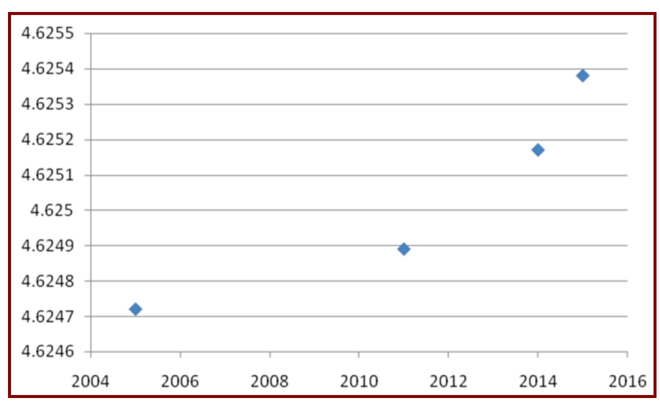

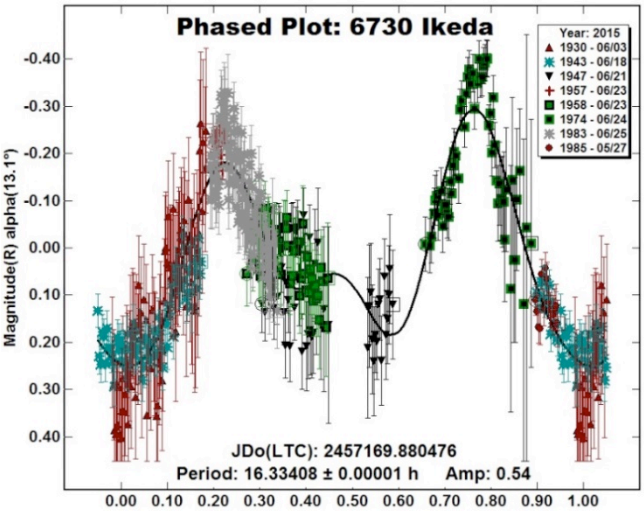
Phased Plot: 6730 Ikeda
Year: 2015
1930 - 06/03
1943 - 06/18
1947 - 06/21
1957 - 06/23
1958 - 06/23
1974 - 06/24
1983 - 06/25
1985 - 05/27
Magnitude(R) alpha(13.1°)
JDo(LTC): 2457169.880476
Period: 16.33408 ± 0.00001 h Amp: 0.54

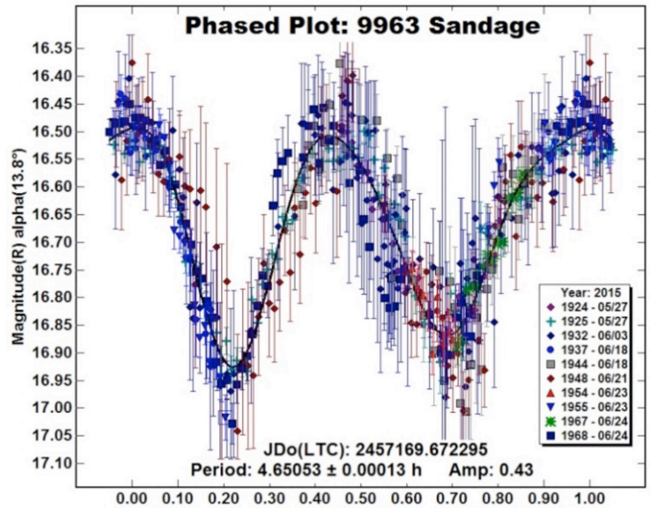
Phased Plot: 9963 Sandage
Year: 2015
1924 - 05/27
1925 - 05/27
1932 - 06/03
1937 - 06/18
1944 - 06/18
1948 - 06/21
1954 - 06/23
1955 - 06/23
1967 - 06/24
1968 - 06/24
Magnitude(R) alpha(13.8°)
JDo(LTC): 2457169.672295
Period: 4.65053 ± 0.00013 h Amp: 0.43

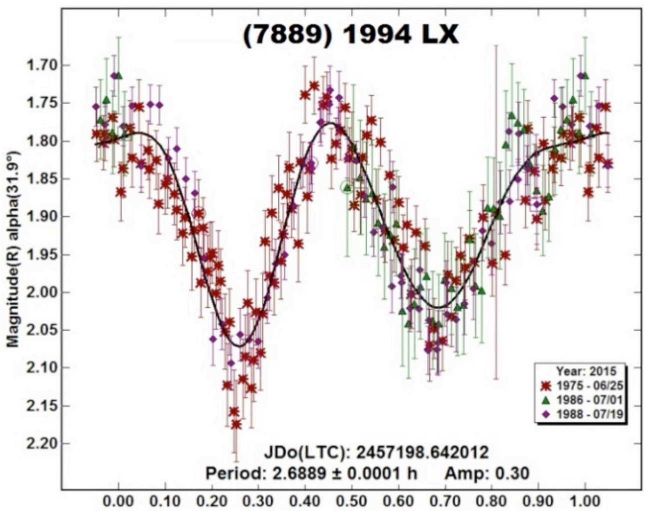
(7889) 1994 LX
Year: 2015
1975 - 06/25
1986 - 07/01
1988 - 07/19
Magnitude(R) alpha(31.9°)
JDo(LTC): 2457198.642012
Period: 2.6889 ± 0.0001 h Amp: 0.30

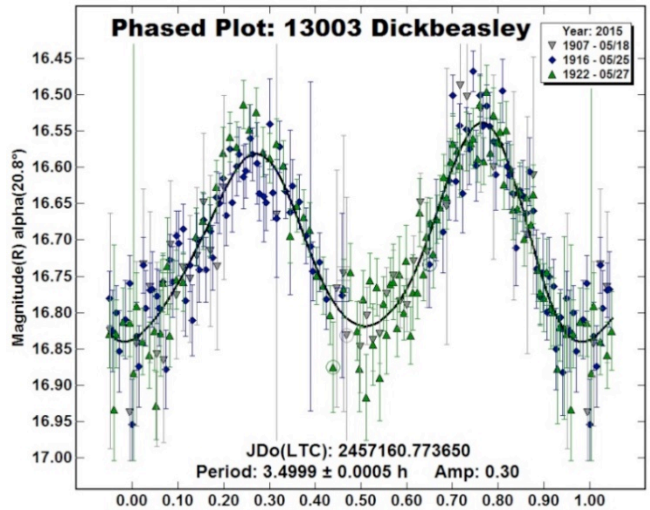
Phased Plot: 13003 Dickbeasley
Year: 2015
1907 - 05/18
1916 - 05/25
1922 - 05/27
Magnitude(R) alpha(20.8°)
JDo(LTC): 2457160.773650
Period: 3.4999 ± 0.0005 h Amp: 0.30

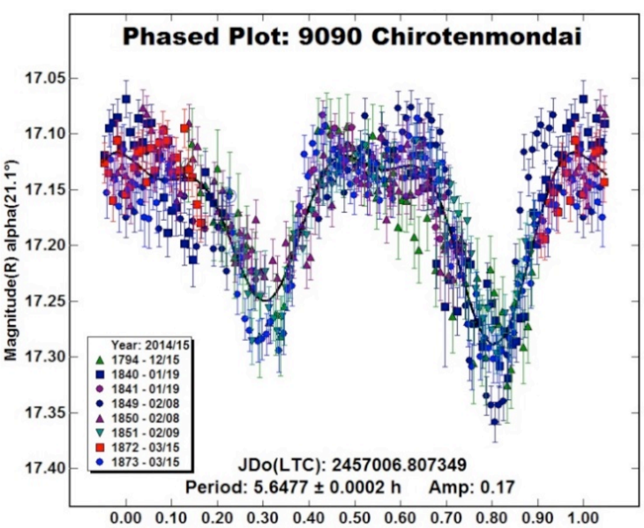
Phased Plot: 9090 Chirotenmondai
Year: 2014/15
1794 - 12/15
1840 - 01/19
1841 - 01/19
1849 - 02/08
1850 - 02/08
1851 - 02/09
1872 - 03/15
1873 - 03/15
Magnitude(R) alpha(21.1°)
JDo(LTC): 2457006.807349
Period: 5.6477 ± 0.0002 h Amp: 0.17

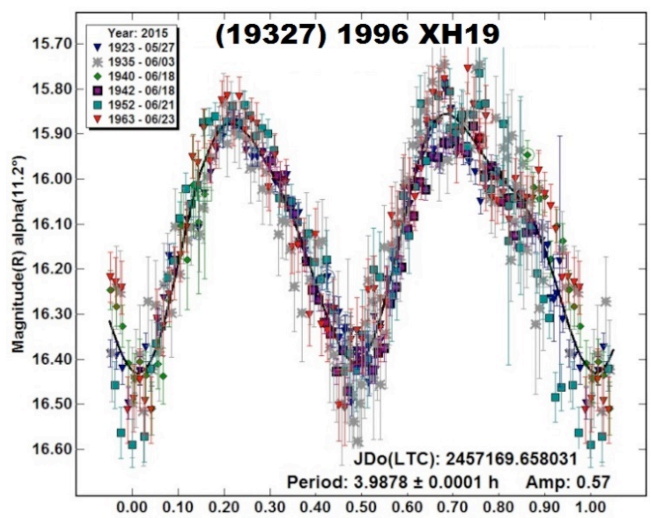
(19327) 1996 XH19
Year: 2015
1923 - 05/27
1935 - 06/03
1940 - 06/18
1942 - 06/18
1952 - 06/21
1963 - 06/23
Magnitude(R) alpha(11.2°)
JDo(LTC): 2457169.658031
Period: 3.9878 ± 0.0001 h Amp: 0.57

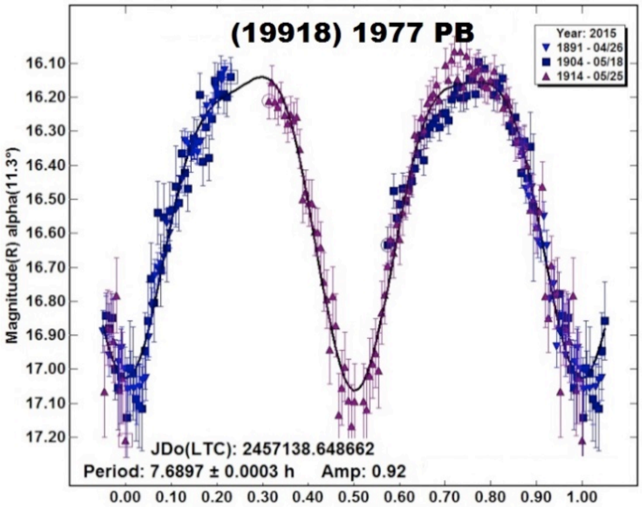

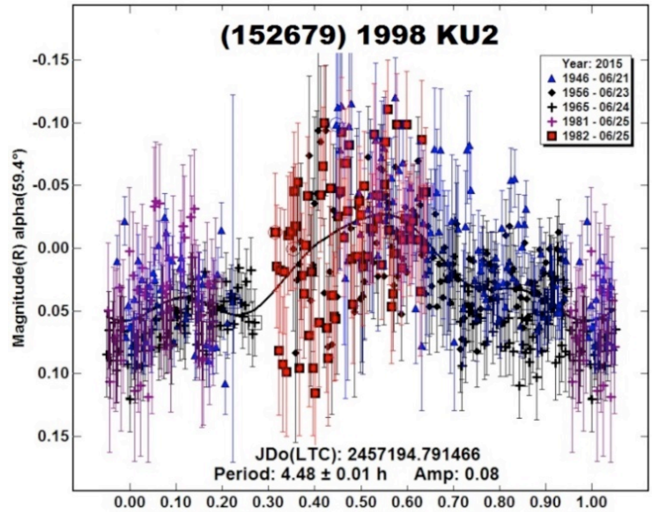

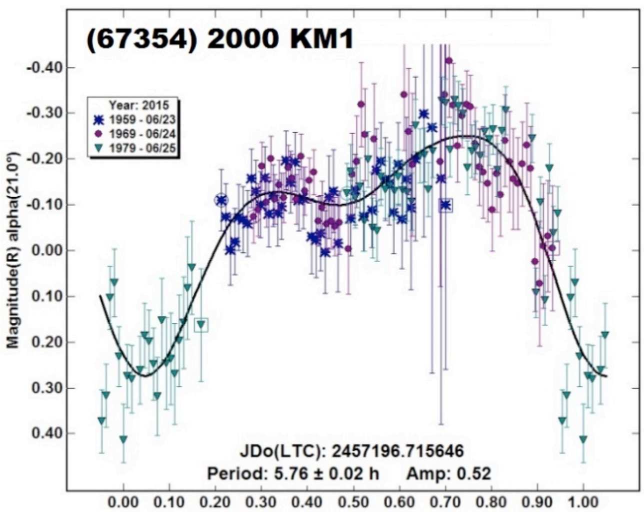

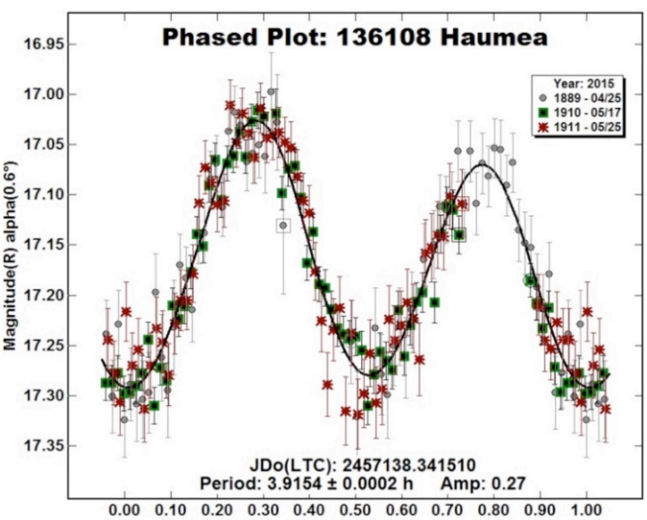

ASTEROID LIGHTCURVE ANALYSIS AT RIVERLAND DINGO OBSERVATORY (RDO)

Kevin Hills
Riverland Dingo Observatory
Moorook 5343, South Australia AUSTRALIA
kevinhills@me.com

(Received: 13 September)

Lightcurves for four asteroids selected from the Collaborative Asteroid Lightcurve Link (CALL) were obtained at RDO in the period 2014 May-November: 1794 Finsen, 2476 Andersen, 3296 Bosque Alegre, and 8159 Fukuoka.

The observations reported here were all obtained using a 0.41-m *f*/9 Ritchey-Chretien telescope, SBIG STL-1001E CCD camera and Johnson-Cousins V filter. All images were bias, dark and flat field corrected and have an image scale of 1.35 arc seconds per pixel. Differential photometry measurements were made in *MPO Canopus* (Warner, 2008). V magnitudes for comparison stars were extracted from the *AAVSO Photometric All-Sky Survey (APASS)* catalog (Henden *et al.*, 2009).

The Asteroid Lightcurve Database (LCDB; Warner *et al.*, 2009) does not contain any previously reported results for the asteroids reported on here.

<u>1794 Finsen</u> is a main-belt asteroid discovered by Bruwer in Hartbeespoort in 1970. A total of 710 data points were obtained over 18 nights during the period 2014 May 7 - August 7 with an average magnitude of 16.0 and average SNR of 36. The data are fit by a period of 12.346 h ± 0.001 h and an amplitude of 0.58 ± 0.04 mag.

<u>2476 Andersen</u> is a main-belt asteroid discovered by Chernykh in Nauchnyj in 1976. A total of 1,351 data points were obtained over nine nights during the period 2014 August 21 - September 5 with an average magnitude of 15.2 and average SNR of 70. The lightcurve shows a period of 8.241 h ± 0.003 h and an amplitude of 0.07 ± 0.02 mag. However, given the low-signal-to-noise, this result should be treated with caution.

3296 Bosque Alegre is a main-belt asteroid discovered by Felix Aguilar Observatory in El Leoncito in 1975. A total of 758 data points were obtained over six nights during the period 2014 September 18 - October 3 with an average magnitude of 15.2 and average SNR of 61. The lightcurve shows a period of 7.778 h ± 0.001 h and amplitude of 0.30 ± 0.02 mag.

8159 Fukuoka is a main-belt asteroid discovered by Endate and Watanabe in Kitami in 1990. A total of 469 data points were obtained over four nights during the period 2014 October 14 - November 18 with an average magnitude of 15.2 and average SNR of 51. The lightcurve shows a period of 5.400 h ± 0.001 h and amplitude of 0.19 ± 0.03 mag.

Acknowledgements

The measurements reported make use of the *AAVSO Photometric All-Sky Survey (APASS)* catalog, which is funded by the Robert Martin Ayers Sciences Fund.

Thank you to Darren Wallace of RDO and his collaborators at New Mexico Skies for maintaining the equipment in Australia.

References

Henden, A.A., Terrell, D., Levine, S.E., Templeton, M., Smith, T.C., Welch, D.L. (2009). *AAVSO Photometric All-Sky Survey (APASS)* catalog. *http://www.aavso.org/download-apass-data*

Warner, B.D. (2008). MPO Software, Canopus version 10, Bdw Publishing, Colorado Springs, CO.

Warner, B.D., Harris, A.W., Pravec, P. (2009). "The Asteroid Lightcurve Database." *Icarus* **202**, 134-146. Updated 2015 Sept. *http://www.minorplanet.info/lightcurvedatabase.html*

Warner, B.D. (2011). Collaborative Asteroid Lightcurve Link website. *http://www.minorplanet.info/call.html*

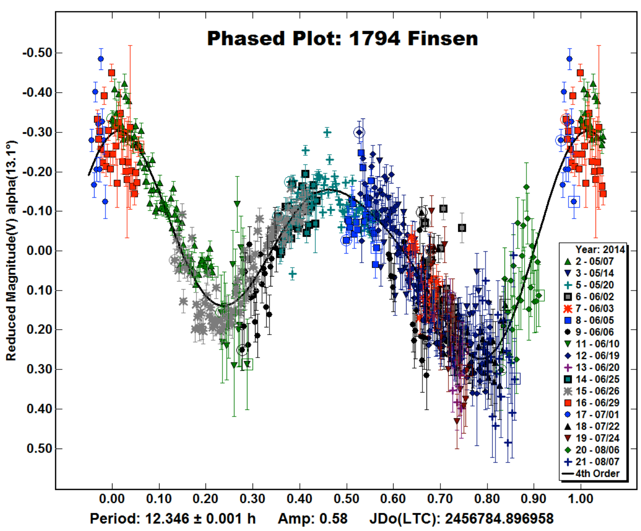

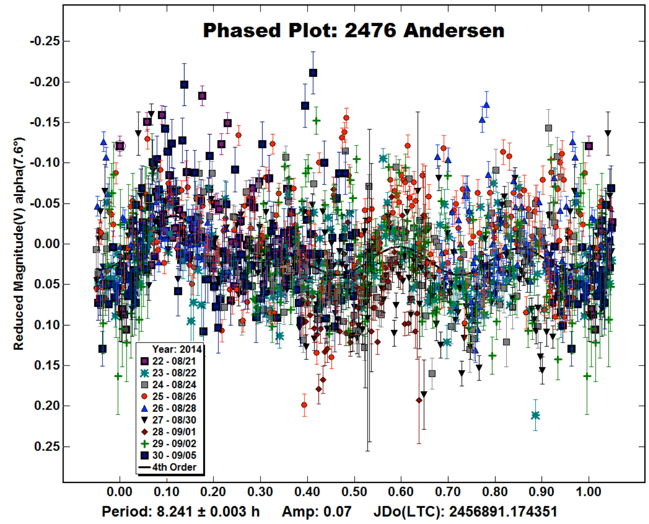

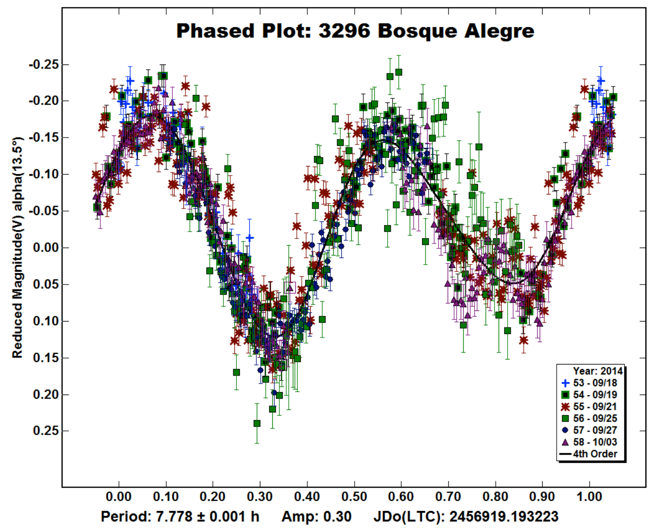

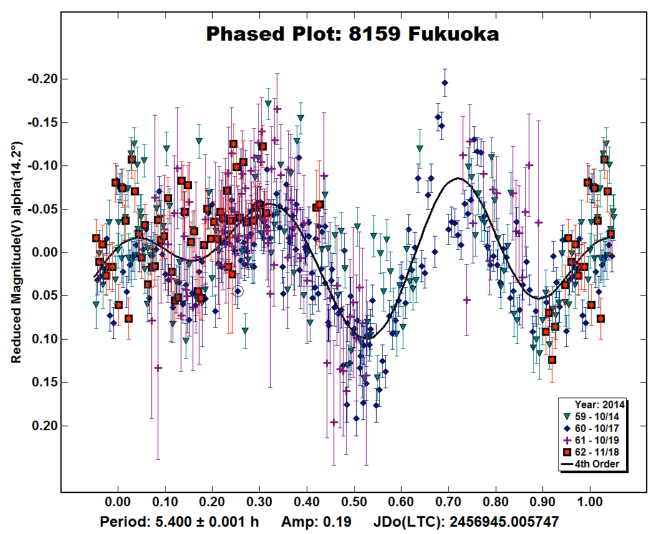

ROTATION PERIOD DETERMINATION FOR (9801) 1997 FX3

Alessandro Marchini, Sara Marullo
Astronomical Observatory, DSFTA - University of Siena (K54)
Via Roma 56, 53100 - Siena, ITALY
alessandro.marchini@unisi.it

Paolo Bacci
Osservatorio Astronomico San Marcello Pistoiese (104)
San Marcello Pistoiese, Pistoia, ITALY

Lorenzo Franco
Balzaretto Observatory (A81), Rome, ITALY

Riccardo Papini
Carpione Observatory (K49)
Spedaletto, Florence, ITALY

Fabio Salvaggio
21047 - Saronno, ITALY

(Received: 2015 September 2)

Photometric observations of the main-belt asteroid (9801) 1997 FX3 in 2015 August revealed a bimodal lightcurve phased to 2.889 ± 0.001 hours as the most likely solution for the asteroid's synodic rotation period.

The main-belt asteroid (9801) 1997 FX3 was discovered on 1997 March 31 by the LINEAR Program at Socorro (MPC 704). The asteroid orbits with a semi-major axis of about 2.647 AU, eccentricity 0.337, and a period of 4.31 years (JPL, 2015). Its absolute magnitude is H = 13.8 (MPC, 2015). WISE satellite infrared radiometry (Masiero *et al.*, 2011) reports a value of H = 14.6 with a diameter of 4.723 ± 0.141 km based on an optical albedo of 0.114 ± 0.035. Using the photometric sparse data from 703 Catalina Sky Survey (CSS, 2015) we derived H = 13.89 ± 0.06 and G = 0.123 ± 0.06 (Fig. 1), which is close to the values found in the JPL Small-Body Database Browser.

A search of the asteroid lightcurve database (LCDB; Warner *et al.*, 2009) indicates that our results appear to be the first reported lightcurve observations and results for this object. The asteroid was reported as a lightcurve photometry opportunity for 2015 August in the *Minor Planet Bulletin* (Warner *et al.*, 2015).

Observations at the Astronomical Observatory of the University of Siena were carried out on eight consecutive nights from 2015 April 6-13 using a 0.30-m *f*/5.6 Maksutov-Cassegrain telescope, SBIG STL-6303E NABG CCD camera, and clear filter; the pixel scale was 2.26 arcsec (2x2 binning). Exposures were 300 seconds. At Saronno Observatory, data were obtained with a 0.23-m *f*/10 (SCT) telescope, SBIG ST8-XME NABG CCD camera, unfiltered; the pixel scale was 1.6 arcsec (2x2 binning). Exposures were 300 seconds. At San Marcello Pistoiese Observatory, data were obtained with a 0.60-m *f*/4 reflector telescope, Apogee Alta NABG CCD camera, unfiltered; the pixel scale was 2 arcsec (1x1 binning) and exposures were 180 seconds.

Images were calibrated with bias, flat, and dark frames. Data processing, including reduction to R band, and period analysis was performed using *MPO Canopus* (BDW Publishing, 2012). Differential photometry measurements were performed using the Comp Star Selector (CSS) utility in *MPO Canopus* that allows selecting of up to five comparison stars of near solar color. Minor adjustments of the nightly zero-points were made in order to minimize the RMS error in the Fourier model lightcurve.

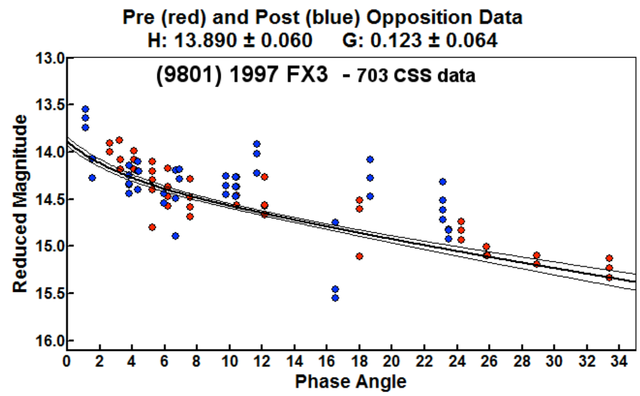

Figure 1. H-G plot using sparse data from the Catalina Sky Survey (MPC 703).

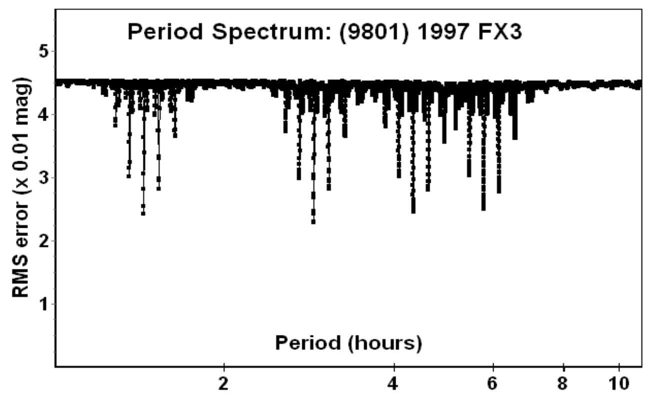

Figure 2. The period spectrum for (9801) 1997 FX3 shows several possible solutions.

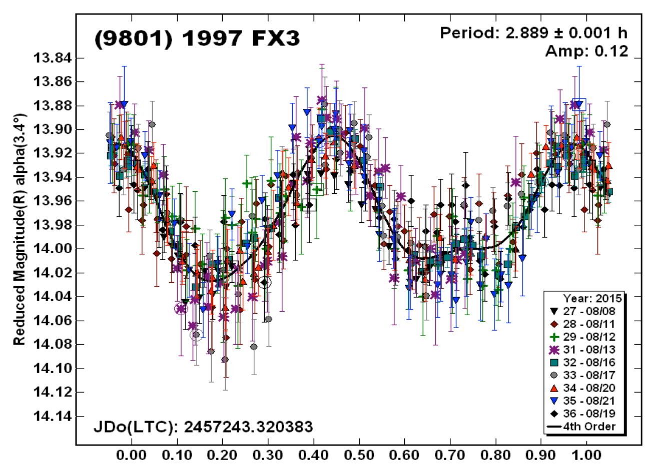

Figure 3. The lightcurve for (9801) 1997 FX3 phased to the adopted period of 2.889 h.

A total of 414 data points were used in the data analysis. Over the interval of about 14 days, the phase angle ranged from 3.3 to 10.1 degrees after the opposition. The period spectrum (RMS vs. period; Fig. 2) shows several possible solutions. We concluded that the most likely solution is a bimodal lightcurve with a synodic period P = 2.889 ± 0.001 hours with an amplitude of 0.12 ± 0.03 mag (Fig. 3).

During period analysis, we found two attenuation events in the lightcurves that cannot be confirmed with the existing data. Observations at future oppositions will be required to verify of the possibility of the asteroid being binary.

Acknowledgments

The authors want to thank Sara Marullo, a student of the course in Physics and Advanced Technologies, who looked after the collection and analysis of data during her internship activities at the Astronomical Observatory of the University of Siena.

References

Catalina Sky Survey (2015). *http://www.lpl.arizona.edu/css/*

JPL (2015). Small-Body Database Browser. *http://ssd.jpl.nasa.gov/sbdb.cgi#top*

Masiero, J.R., Mainzer, A.K., Grav, T., Bauer, J.M., Cutri, R.M., Dailey, J., Eisenhardt, P.R.M., McMillan, R.S., Spahr, T.B., Skrutskie, M.F., Tholen, D., Walker, R.G., Wright, E.L., DeBaun, E., Elsbury, D., Gautier, T., IV, Gomillion, S., Wilkins, A. (2011). "Main Belt Asteroids with WISE/NEOWISE. I. Preliminary Albedos and Diameters." *Ap. J.* **741**, A68.

MPC (2015). MPCORB elements file. *http://www.minorplanetcenter.net/db_search/*

Warner, B.D., Harris, A.W., Pravec, P. (2009). "The asteroid lightcurve database." Icarus **202**, 134-146. Updated 2015 July 22. *http://www.minorplanet.info/lightcurvedatabase.html*

Warner, B.D. (2012). MPO Software, *MPO Canopus* v10.4.1.9. Bdw Publishing. *http://minorplanetobserver.com*

Warner, B.D., Harris, A.W., Ďurech, J., Benner, L.A.M. (2015). "Lightcurve photometry opportunities: 2015 July-September." *Minor Planet Bulletin* **42**, 228-232.

ROTATION PERIOD ANALYSIS FOR ASTEROIDS 1324 KNYSNA AND (7748) 1987 TA

Junda Liu, Yifan Gu
Suzhou High School Of Jiangsu Province
Suzhou,Jiangsu 215007 P.R. CHINA
824841086jdl@gmail.com

(Received: 2015 Aug 21 Revised: 2015 Nov 12)

Analysis of photometric observations shows synodic rotation periods and amplitudes for two main-belt asteroids: 1324 Knysna, P = 2.553 ± 0.001 h, A = 0.10 mag; (7748) 1987 TA, P = 4.22 ± 0.01 h, A = 0.15 mag.

CCD photometric observations of 1324 Knysna and (7748) 1987 TA were made at Lvye Observatory (IAU P34) and iTelescope Observatory (IAU Q62). The instruments of Lvye Observatory were a Skywatcher 0.25-m *f*/4.4 reflector telescope, QHY9 CCD camera at –20°C, binned 2x2, unfiltered. The image scale was 1.99 arc seconds per pixel. The exposure time was 120 s. Observations obtained at iTelescope Observatory were by a Planewave 0.43-m Corrected Dall-Kirkham and FLI ProLine PL4710 CCD camera; the exposure time was 120 s. All images were dark, bias, and flat-corrected by *MaxIm DL v5.23*. Differential photometry and period analysis were made with *MPO Canopus*.

1324 Knysna. The asteroid was discovered at Johannesburg on 1934 Jun 15 by C. Jackson. Its orbit has a semi-major axis of 2.185 AU, eccentricity of 0.1634, and orbital period of 3.23 years (JPL, 2015). Previous works found a synodic rotation period P = 2.5538 ± 0.0005 h (Warner, 2008) and 2.56 ± 0.01 h (Behrend, 2002). The observations were taken on 2015 Jul 28, Aug 8, and Aug 9. 200 data points were used for the analysis. The lightcurve shows a period P = 2.553 ± 0.001 h with an amplitude A = 0.10 mag. This is in good agreement with the earlier works.

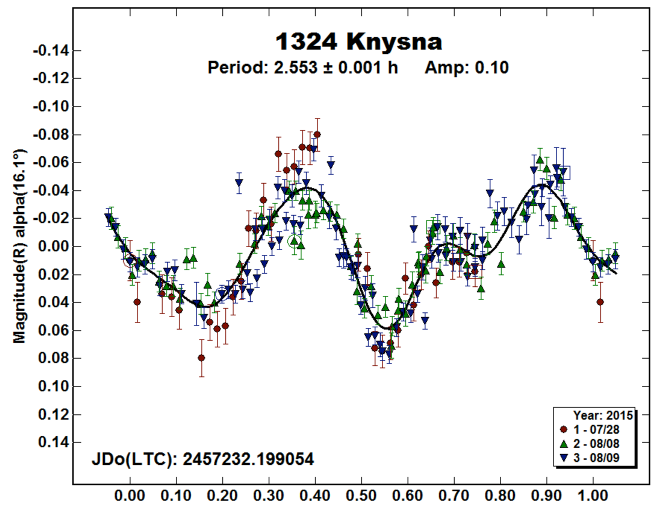

(7748) 1987 TA. This asteroid was discovered at Ojima on 1987 Oct 12 by T. Niijima. and T. Urata. Its orbit has a semi-major axis of 2.313 AU, eccentricity of 0.2427, and orbital period of 3.52 years (JPL, 2015). No previous observations were reported in the LCDB (Warner *et al.*, 2009). Observations were taken at five nights between 2015 Aug 15-20. 321 data points were used for the analysis. The lightcurve shows a period P = 4.22 ± 0.01 h with an amplitude A = 0.15 mag.

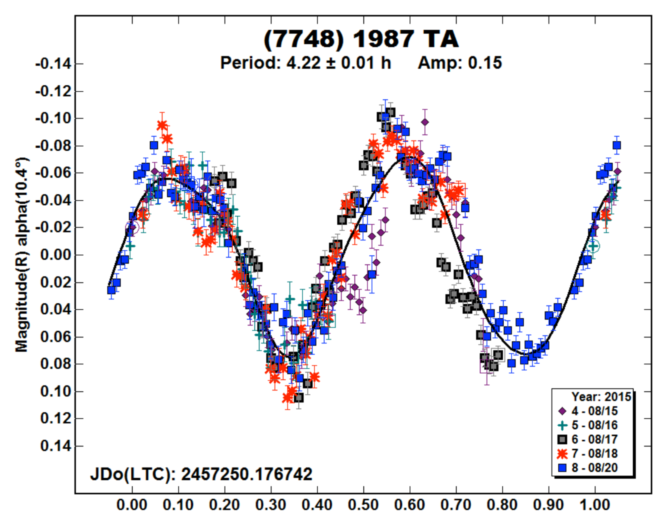

References

Behrend, R. (2002). Observatoire de Geneve web site. *http://obswww.unige.ch/~behrend/page_cou.html*

JPL (2015). Small Body Database Browser. *http://ssd.jpl.nasa.gov/sbdb.cgi*

Warner, B.D. (2008). "Asteroid Lightcurve Analysis at the Palmer Divide Observatory: February-May 2008." *Minor Planet Bul.* **35**, 163-167.

Warner, B.D., Harris, A.W., Pravec, P. (2009). *Icarus* **202**, 134-146. Updated 2015 July 23. *http://www.MinorPlanet.info/lightcurvedatabase.html*

Warner, B.D. (2013). MPO Software, *MPO Canopus* v10.4.3.17. Bdw Publishing, *http://minorplanetobserver.com/*

LIGHTCURVE AND ROTATION PERIOD DETERMINATION FOR (12207) 1981 EU28

Fabio Salvaggio
21047 – Saronno, ITALY
fsalvaggio@gmail.com

Alessandro Marchini
Astronomical Observatory, DSFTA, University of Siena (K54)
via Roma, 56, 53100 – Siena, ITALY

Riccardo Papini
Carpione Observatory (K49)
Spedaletto – Florence, ITALY

(Received: 2015 August 24)

Analysis of photometric observations of the main-belt asteroid (12207) 1981 EU28 made in 2015 August revealed that the most likely synodic rotation period for the asteroid is $P = 4.836 \pm 0.002$ h.

(12207) 1981 EU28 is a main-belt asteroid discovered on 1981 March 1 by S.J. Bus. It is a typical main-belt asteroid in an orbit with a semi-major axis of about 2.227 AU, eccentricity of 0.193, and orbital period of about 3.32 years (JPL, 2015). It was selected from the "Potential Lightcurve Targets" article in the *Minor Planet Bulletin* (Warner, 2015).

Data were obtained at the Astronomical Observatory of the University of Siena with a 0.30-m *f*/5.6 Maksutov-Cassegrain telescope, SBIG STL-6303E NABG CCD camera, and clear filter; the pixel scale was 2.20 arcsec (2x2 binning). Exposures were 300 seconds. At Saronno Observatory, data were obtained with a 0.24-m *f*/10 (SCT) telescope, SBIG ST8-XME NABG CCD camera, and unfiltered; the pixel scale was 1.6 arcsec in (2x2 binning). Exposures were 300 seconds. The collaborative observations resulted in six sessions over a time span of four days with a total of 171 data points. The phase angle ranged from 3.6° to 2.1° before the opposition.

All data images were calibrated with bias, flats and darks. Data processing, including reduction to R band, and period analysis, were performed using *MPO Canopus*. Differential photometry measurements were performed using the Comp Star Selector (CSS) procedure in *MPO Canopus* that allows selecting of up to five comparison stars of near solar color. Minor additional adjustments of the magnitude zero-points were made to find the minimum RMS fit from the Fourier analysis.

The period spectrum (RMS vs. period) favored a bimodal lightcurve with a synodic period of 4.836 ± 0.002 hours and amplitude of 0.26 ± 0.03 mag.

Acknowledgments

The authors want to thank Sara Marullo, a student of the course in Physics and Advanced Technologies, who attended a few of the observing sessions at the Astronomical Observatory of the University of Siena during her internship activities.

References

JPL (2015). Small-Body Database Browser. *http://ssd.jpl.nasa.gov/sbdb.cgi#top*

Warner, B.D., Harris, A.W., Durech, J., Benner, L.A.M. (2015). "Lightcurve Photometry Opportunities: 2015 July – September." *Minor Planet Bulletin* **43**, 228-232.

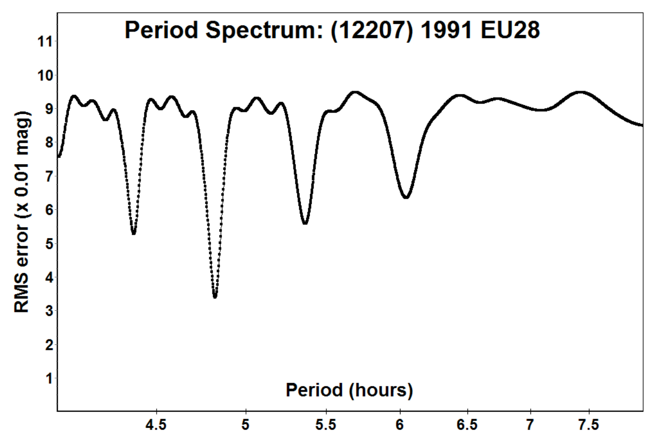

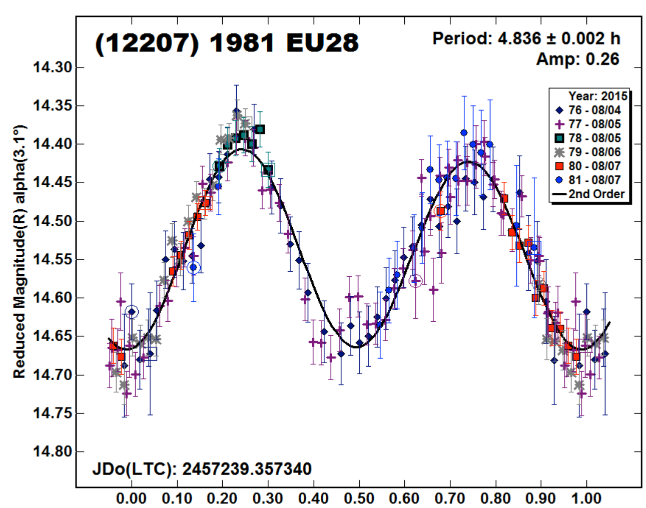

MAIN-BELT ASTEROID LIGHTCURVES FROM CERRO TOLOLO INTER-AMERICAN OBSERVATORY

Robert D. Stephens
Center for Solar System Studies (CS3)/MoreData!
11355 Mount Johnson Ct., Rancho Cucamonga, CA 91737 USA
rstephens@foxandstephens.com

Linda M. French
Illinois Wesleyan University
Bloomington, IL 61702 USA

David James
Cerro Tololo Inter-American Observatory
La Serena, Chile

Kyle Connour
Illinois Wesleyan University
Bloomington, IL USA

Brian D. Warner
Center for Solar System Studies / MoreData! Inc.
Eaton, CO USA

(Received: 15 September)

25 main-belt asteroids were observed from CTIO (Cerro Tololo Inter-American Observatory MPC 807) in May and June 2015. Rotational periods were determined for 22 of them. Three are reported as having a long-period.

Observations of 25 main-belt asteroids were a byproduct of an observing run of Jovian Trojans. Observing time was scheduled for five nights on the 4-Meter Victor Blanco telescope using the Dark Energy Camera. Four fields were selected in the heart of the Trojan cloud and followed for up to six hours each night. Passing clouds shortened the observing runs for several of the nights.

The observing strategy was designed to provide the greatest chance to derive rotational periods for the Trojan asteroids, which worked equally well for the main-belt asteroids found in the same fields. The main difference was that the main-belt asteroids were moving twice as fast as the Trojans, tended to move across chips quicker, and often moved entirely out of the field of view. The Moon was nearly full during the observing run. It travelled through the heart of the Trojan cloud during the observing run. Therefore, fields were carefully selected where the Moon was at least 20 degrees away.

The images were obtained using the 4-meter Blanco telescope and the Dark Energy Camera (DECam). Exposures 300 seconds through the DECam r filter.

Image processing, measurement and period analysis was done using *MPO Canopus* (Bdw Publishing), which incorporates the Fourier analysis algorithm (FALC) developed by Harris (Harris *et al*., 1989). Because there are no reliable star catalogs with magnitudes > 18, night-to-night calibration of the data (generally < ±0.05 mag) was mostly done using the USNO catalog. Some comparison stars were measured using the MPOSC3 catalog provided with *Canopus*, whose stars are converted to approximate Cousins R magnitudes based on 2MASS J-K colors (Warner 2007).

In the lightcurve plots, the "Reduced Magnitude" is Johnson R corrected to a unity distance by applying -5*log (rΔ) to the measured sky magnitudes with r and Δ being respectively, the Sun-asteroid and the Earth-asteroid distances in AU. The magnitudes were normalized to the phase angle given in parentheses using G = 0.15.

With the exception of (27722) 1990 OB2, none of these asteroids had previously reported rotational periods in the Lightcurve Database (LCDB; Warner et al., 2009).

<u>(27722) 1990</u> OB2. Chang *et al.* (2015) reported a period of 11.290 h for (27722) 1990 OB2. That period appears to be a 4:3 alias of our 14.83 h period. Plots of our data phased to both periods are included. We prefer the 14.83 h period because the 11.290 h period has an asymmetric lightcurve and multiple nights do not reproduce the lightcurve shape cleanly.

<u>32231 Uthmann</u>. This asteroid was in the field of view of the DECam for only two nights. Since each night covered one minimum and maximum extrema, we were able to create a likely rotational period of 16.9 h. A Period Spectrum is presented showing possible aliases of 6.2, 8.8, and 13.1 h. The 8.8 h solution is the half period showing one extrema. The 13.1 h solution shows a reasonable bimodal lightcurve. We slightly prefer the 16.9 h period because it is more symmetrical.

<u>(49586) 1999 CD138</u>. With the long period of 144 h, we were able to cover only just over half of the lightcurve during the 5 night run. Two plots are included, one for the half period of 72 h showing some overlap in the coverage, and a lightcurve phased to 144 h showing coverage of about 55 percent of the rotational period.

<u>(54501) 2000 OB52</u>. This asteroid was on-chip for only a single night. However, it was bright and produced a symmetrical light curve.

<u>(75295) 1999 XH30</u>. With this asteroid being on-chip only four nights, and with a rotational period appearing to be close to three Earth rotations, anything approaching complete coverage of the phased lightcurve was impossible. Here, the phased lightcurve at our preferred period of 76.0 h along with a lightcurve phased to the half period of 38.0 h is presented.

<u>(112248) 2002 LG9</u>. The first two nights each covered about one half of the rotational period of this asteroid. With an amplitude of around 0.10 magnitudes, it is possible that the lightcurve could have only a single extremum, or three or more extrema (Harris *et al* 2014). We also present a period spectrum showing possible alias periods of 5, 7, and 15 h.

Acknowledgements

French, Stephens and Connour were visiting astronomers at Cerro Tololo Inter-American Observatory, National Optical Astronomy Observatory, operated by the Association of Universities for Research in Astronomy, under contract with the National Science Foundation. This research was supported by National Science Foundation grant AST-1212115.

References

Chang, C.-K., Ip, W.-H., Lin, H.-W., Cheng, Y.-C., Ngeow, C.-C., Yang, T.-C., Waszczak, A., Kulkarni, S. R., Levitan, D., Sesar, B., Laher, R., Surace, J., Prince, T. A. (2015). "Asteroid Spin-rate Study Using the Intermediate Palomar Transit Factory." *Ap. J. Suppl. Ser.* **219**, A27.

Harris, A.W., Young, J.W., Bowell, E., Martin, L.J., Millis, R.L., Poutanen, M., Scaltriti, F., Zappala, V., Schober, H.J., Debehogne, H., Zeigler, K.W. (1989). "Photoelectric Observations of Asteroids 3, 24, 60, 261, and 863." *Icarus* **77**, 171-186.

Harris, A.W., Pravec, P., Galád, B. Skiff, B., Warner, B., Világi, J., Gajdoš, S., Carbognani, A., Hornoch, K., Kušnirák, P., Cooney, W., Gross, J., Terrell, D., Higgins, D., Bowell, E., Koehn, B. (2014) "On the maximum amplitude of harmonics of an asteroid lightcurve." *Icarus* **235**, 55-59.

Warner, B.D. (2007). "Initial Results from a Dedicated H-G Project." *Minor Planet Bul.* **34**, 113-119.

Warner, B.D., Harris, A.W., Pravec, P. (2009). *Icarus* **202**, 134-146. Updated 2015 September 1. *http://www.minorplanet.info/lightcurvedatabase.html*.

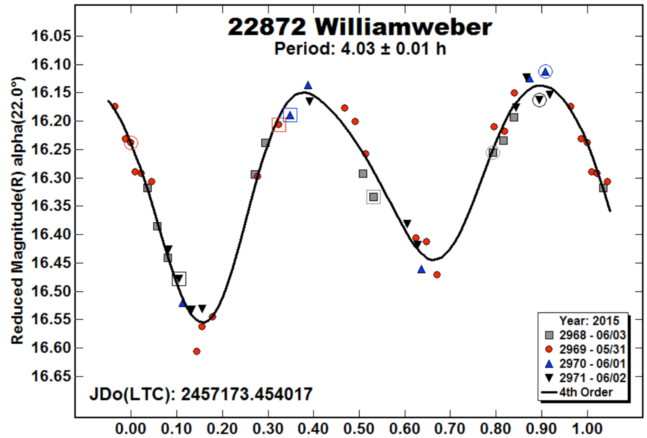

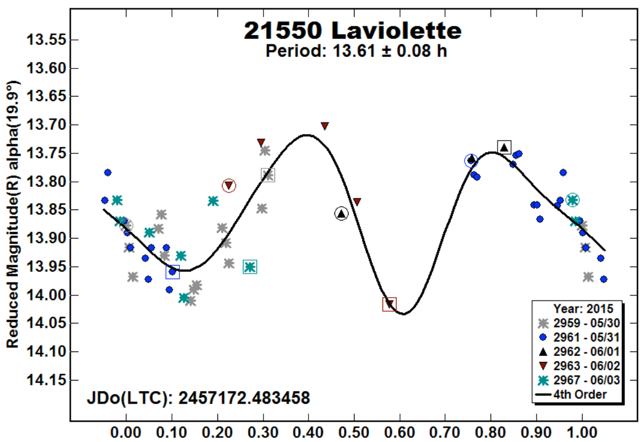

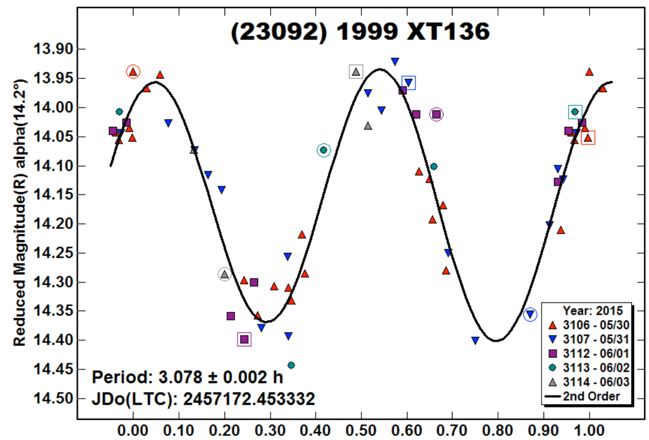

Number	Name	2015 mm\dd	Pts	Phase	L_{PAB}	B_{PAB}	Period	P.E.	Amp	A.E.	Grp
21550	Laviolette	05/30-06/03	51	20.0,20.8	199	-6	13.61	0.08	0.32	0.03	MB-O
22872	Williamweber	05/31-06/03	47	21.4,22.0	200	-6	4.03	0.01	0.42	0.02	FLOR
23092	1999 XT136	05/30-06/03	55	14.2,14.9	205	11	3.078	0.002	0.47	0.03	MB-O
24607	Sevnatu	05/30-06/03	66	17.9,18.6	198	-7	6.08	0.01	0.71	0.02	MB-I
27722	1990 OB2	05/31-06/03	42	13.7,14.2	195	-7	14.85	0.02	0.33	0.03	MB-M
31231	Uthmann	05/30-05/31	45	17.8,18.1	208	10	16.9	0.2	0.14	0.02	MB-I
34111	2000 PZ24	05/30-06/03	58	12.4,13.1	206	11	58.5	2	0.22	0.03	MB-M
49586	1999 CD138	05/30-06/02	49	19.6,20.2	198	-7	144	20	1	0.2	MB-M
51283	2000 KN7	05/31-06/03	41	14.8,15.3	206	11	4.775	0.005	0.32	0.02	MB-M
54501	2000 OB52	05/30	20	18.3	197	-7	5.94	0.08	0.2	0.01	MB-I
66935	1999 WZ1	06/01-06/01	12	14.7,14.7	196	-6	> 24				MB-M
75210	1999 VP192	05/30-06/03	40	20.2,20.9	199	-7	> 150				FLOR
75295	1999 XH30	05/30-06/03	41	20.2,21.3	210	9	76	2	0.35	0.1	FLOR
77216	2001 FO24	06/02-06/03	48	22.6,22.7	200	-6	150	10	1	0.3	MB-O
81975	2000 QH78	05/30-06/03	56	13.2,13.9	205	10	8.03	0.02	0.37	0.02	MB-O
90454	2004 CV	05/30-06/03	60	23.8,24.9	211	10	100	2	0.3	0.03	MB-M
98138	2000 SW42	06/01-06/01	16	23.1,23.1	200	-6	>24				V
111499	2001 YF61	05/30-06/03	59	9.2,15.2	219	8	6.69	0.01	0.32	0.03	MB-O
112248	2002 LG9	05/30-06/03	61	18.5,19.5	207	11	10.74	0.06	0.1	0.02	MB-O
131309	2001 FH158	05/30-06/03	51	22.1,22.9	200	-6	30.2	0.2	0.28	0.05	MB-M
189218	2004 DC37	05/30-06/03	49	21.6,22.7	209	9	41.15	0.45	0.19	0.03	V
199978	2007 JZ1	05/30-06/03	55	18.5,19.5	208	11	57.1	0.7	0.44	0.05	MB-M
211895	2004 JX32	05/31-06/03	55	17.2,17.8	207	10	37	0.3	1.77	0.05	MB-O
212302	2005 NX57	05/30-06/03	46	14.6,15.4	206	11	6.38	0.01	0.35	0.03	MB-O
322377	2011 LJ26	05/30-06/03	46	16.5,17.4	207	10	7.41	0.02	0.34	0.03	MB-M

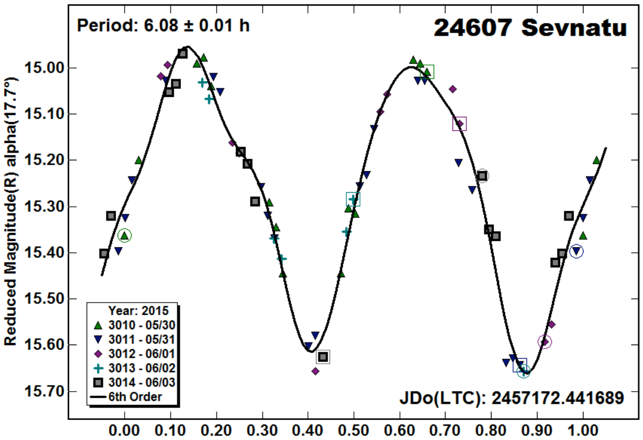
Period: 6.08 ± 0.01 h
24607 Sevnatu
Reduced Magnitude(R) alpha(17.7°)
Year: 2015
3010 - 05/30
3011 - 05/31
3012 - 06/01
3013 - 06/02
3014 - 06/03
6th Order
JDo(LTC): 2457172.441689

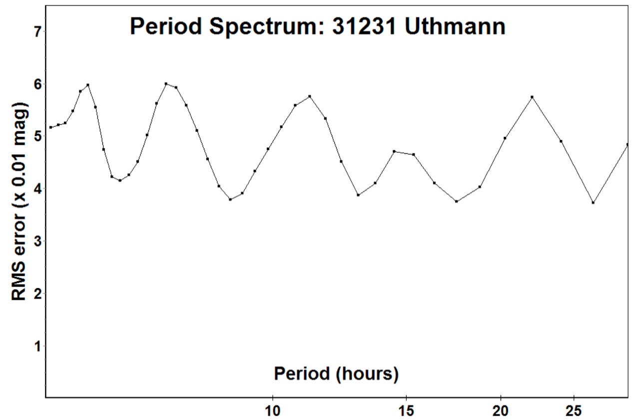
Period Spectrum: 31231 Uthmann
RMS error (x 0.01 mag)
Period (hours)

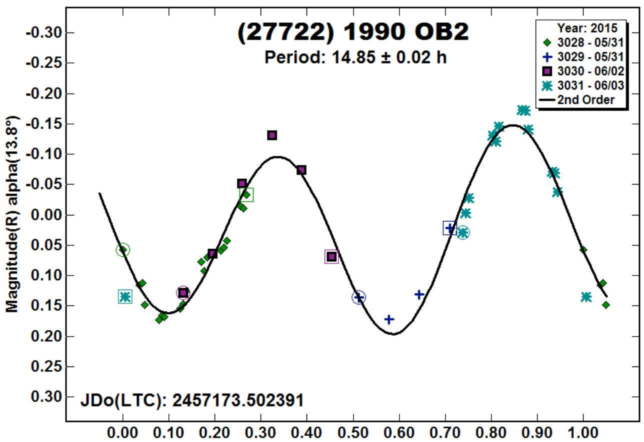
(27722) 1990 OB2
Period: 14.85 ± 0.02 h
Magnitude(R) alpha(13.8°)
Year: 2015
3028 - 05/31
3029 - 05/31
3030 - 06/02
3031 - 06/03
2nd Order
JDo(LTC): 2457173.502391

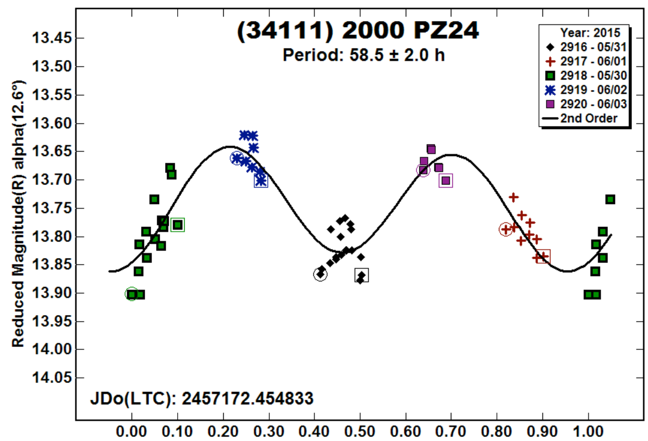
(34111) 2000 PZ24
Period: 58.5 ± 2.0 h
Reduced Magnitude(R) alpha(12.6°)
Year: 2015
2916 - 05/31
2917 - 06/01
2918 - 05/30
2919 - 06/02
2920 - 06/03
2nd Order
JDo(LTC): 2457172.454833

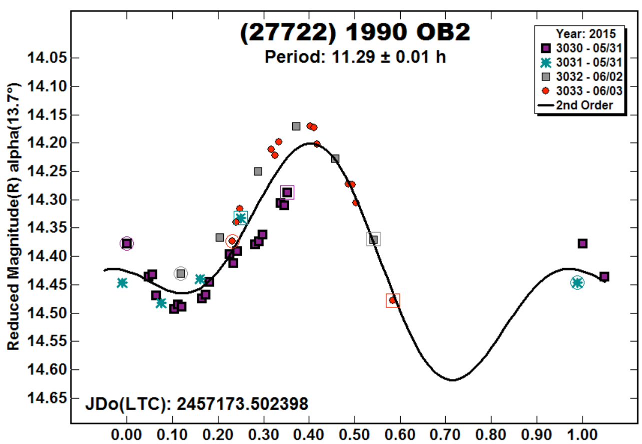
(27722) 1990 OB2
Period: 11.29 ± 0.01 h
Reduced Magnitude(R) alpha(13.7°)
Year: 2015
3030 - 05/31
3031 - 05/31
3032 - 06/02
3033 - 06/03
2nd Order
JDo(LTC): 2457173.502398

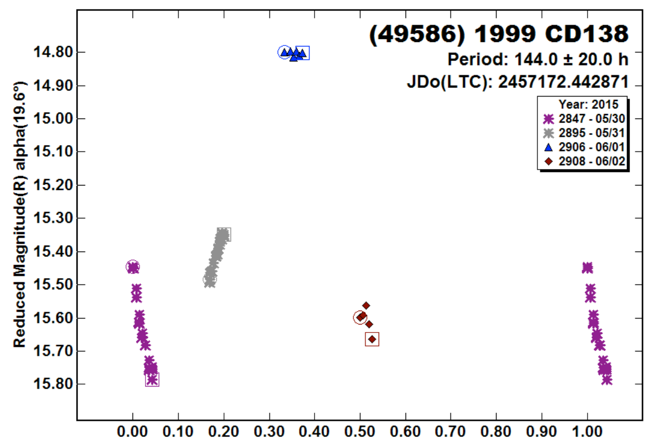
(49586) 1999 CD138
Period: 144.0 ± 20.0 h
JDo(LTC): 2457172.442871
Reduced Magnitude(R) alpha(19.6°)
Year: 2015
2847 - 05/30
2895 - 05/31
2906 - 06/01
2908 - 06/02

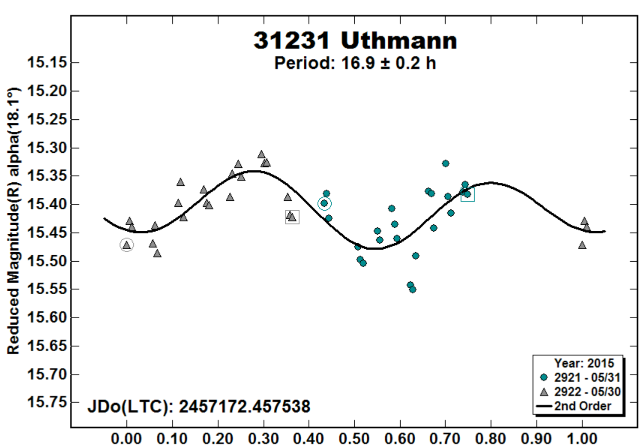
31231 Uthmann
Period: 16.9 ± 0.2 h
Reduced Magnitude(R) alpha(18.1°)
Year: 2015
2921 - 05/31
2922 - 05/30
2nd Order
JDo(LTC): 2457172.457538

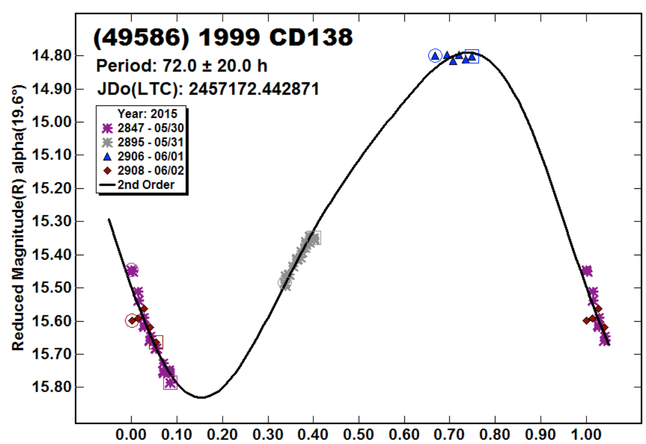
(49586) 1999 CD138
Period: 72.0 ± 20.0 h
JDo(LTC): 2457172.442871
Reduced Magnitude(R) alpha(19.6°)
Year: 2015
2847 - 05/30
2895 - 05/31
2906 - 06/01
2908 - 06/02
2nd Order

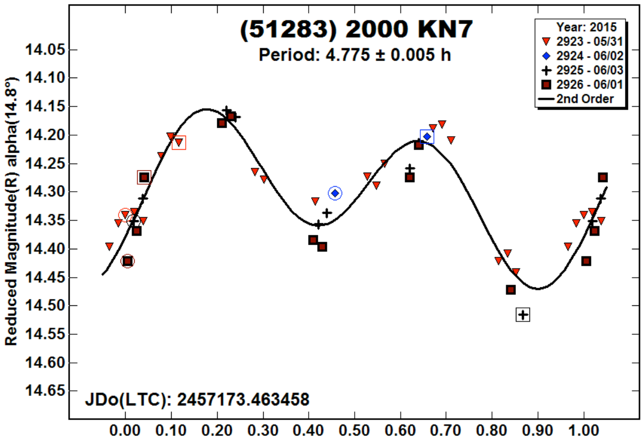
(51283) 2000 KN7
Period: 4.775 ± 0.005 h
Year: 2015
2923 - 05/31
2924 - 06/02
2925 - 06/03
2926 - 06/01
2nd Order
Reduced Magnitude(R) alpha(14.8°)
JDo(LTC): 2457173.463458

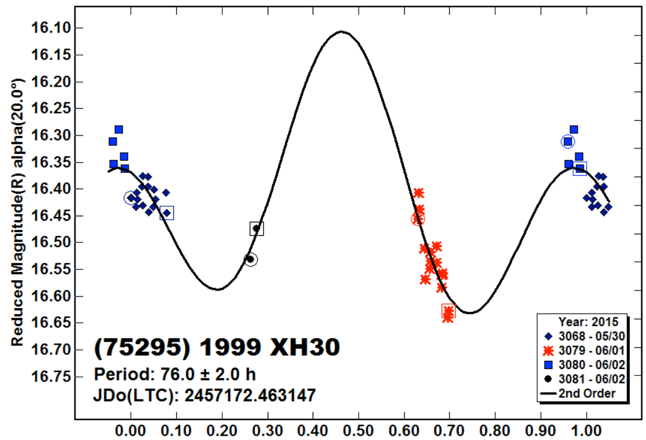
(75295) 1999 XH30
Period: 76.0 ± 2.0 h
JDo(LTC): 2457172.463147
Year: 2015
3068 - 05/30
3079 - 06/01
3080 - 06/02
3081 - 06/02
2nd Order
Reduced Magnitude(R) alpha(20.0°)

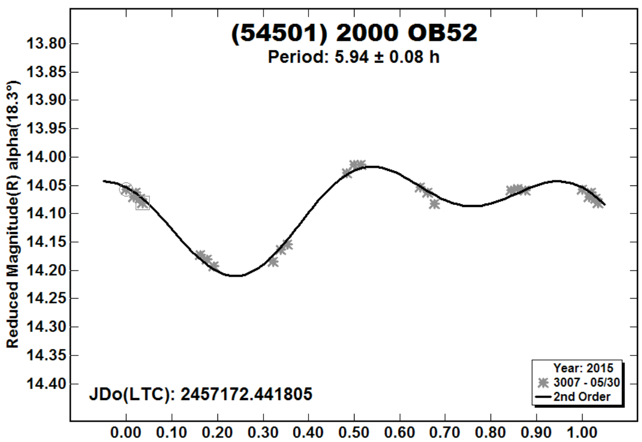
(54501) 2000 OB52
Period: 5.94 ± 0.08 h
Year: 2015
3007 - 05/30
2nd Order
Reduced Magnitude(R) alpha(18.3°)
JDo(LTC): 2457172.441805

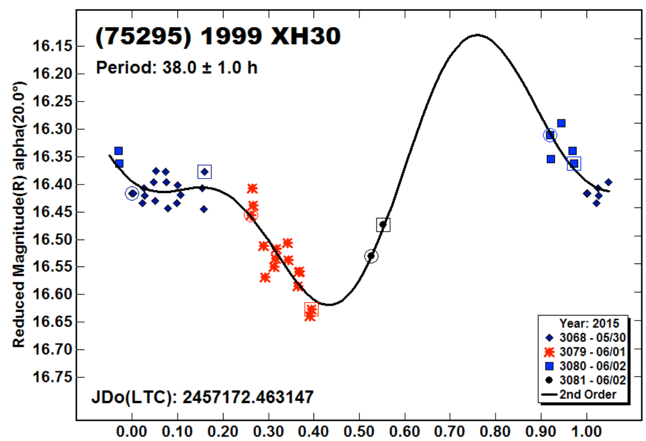
(75295) 1999 XH30
Period: 38.0 ± 1.0 h
Year: 2015
3068 - 05/30
3079 - 06/01
3080 - 06/02
3081 - 06/02
2nd Order
Reduced Magnitude(R) alpha(20.0°)
JDo(LTC): 2457172.463147

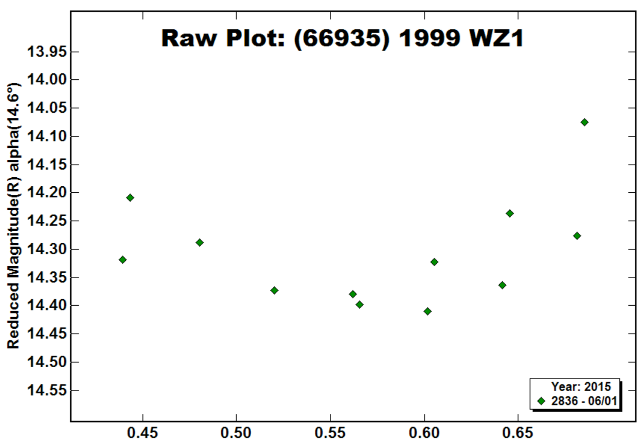
Raw Plot: (66935) 1999 WZ1
Year: 2015
2836 - 06/01
Reduced Magnitude(R) alpha(14.6°)

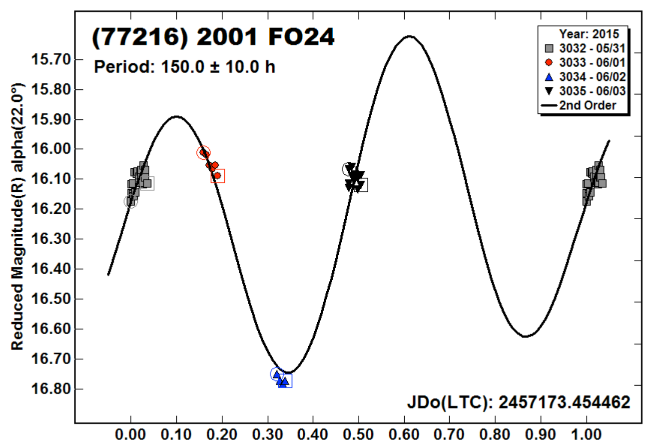
(77216) 2001 FO24
Period: 150.0 ± 10.0 h
Year: 2015
3032 - 05/31
3033 - 06/01
3034 - 06/02
3035 - 06/03
2nd Order
Reduced Magnitude(R) alpha(22.0°)
JDo(LTC): 2457173.454462

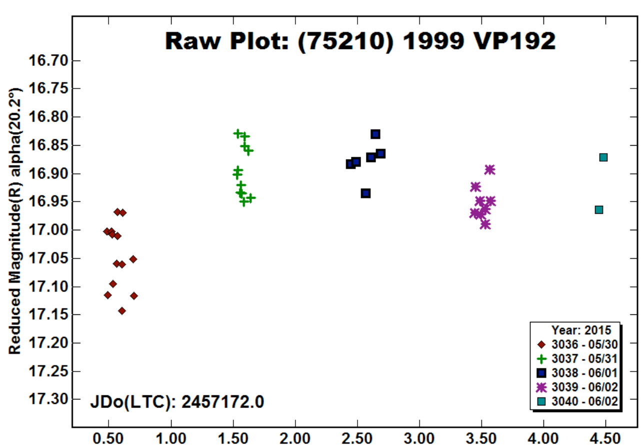
Raw Plot: (75210) 1999 VP192
Year: 2015
3036 - 05/30
3037 - 05/31
3038 - 06/01
3039 - 06/02
3040 - 06/02
Reduced Magnitude(R) alpha(20.2°)
JDo(LTC): 2457172.0

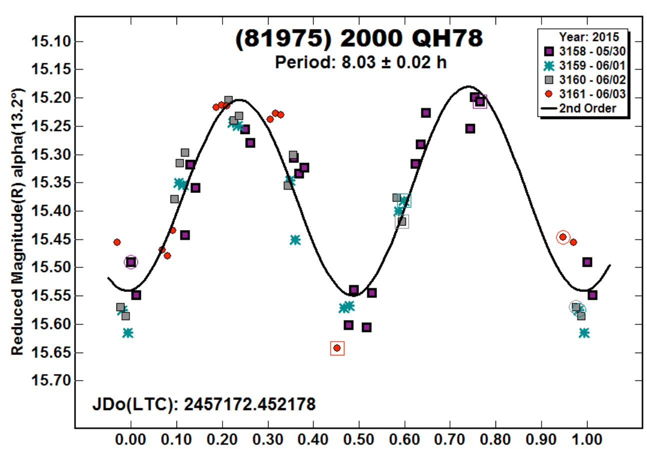
(81975) 2000 QH78
Period: 8.03 ± 0.02 h
Year: 2015
3158 - 05/30
3159 - 06/01
3160 - 06/02
3161 - 06/03
2nd Order
Reduced Magnitude(R) alpha(13.2°)
JDo(LTC): 2457172.452178

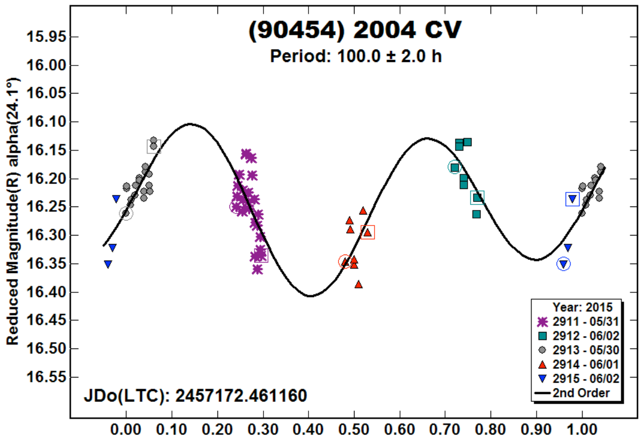
(90454) 2004 CV
Period: 100.0 ± 2.0 h
Reduced Magnitude(R) alpha(24.1°)
Year: 2015
2911 - 05/31
2912 - 06/02
2913 - 05/30
2914 - 06/01
2915 - 06/02
2nd Order
JDo(LTC): 2457172.461160

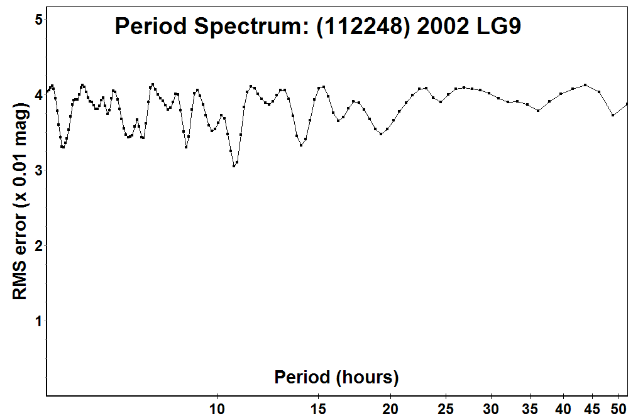
Period Spectrum: (112248) 2002 LG9
RMS error (x 0.01 mag)
Period (hours)

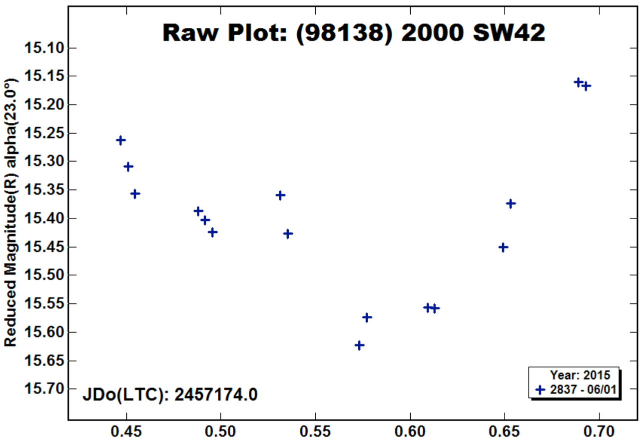
Raw Plot: (98138) 2000 SW42
Reduced Magnitude(R) alpha(23.0°)
Year: 2015
2837 - 06/01
JDo(LTC): 2457174.0

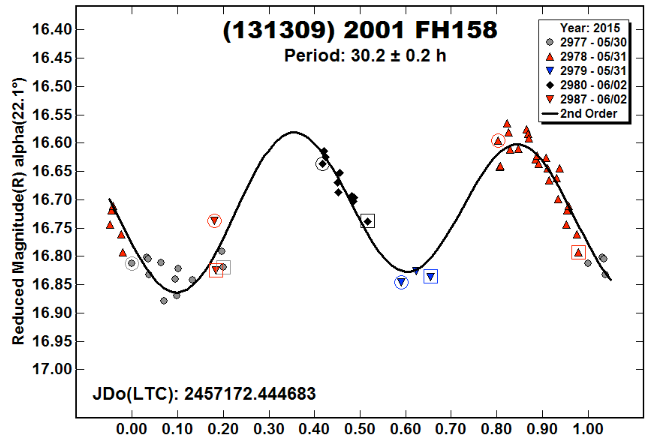
(131309) 2001 FH158
Period: 30.2 ± 0.2 h
Reduced Magnitude(R) alpha(22.1°)
Year: 2015
2977 - 05/30
2978 - 05/31
2979 - 05/31
2980 - 06/02
2987 - 06/02
2nd Order
JDo(LTC): 2457172.444683

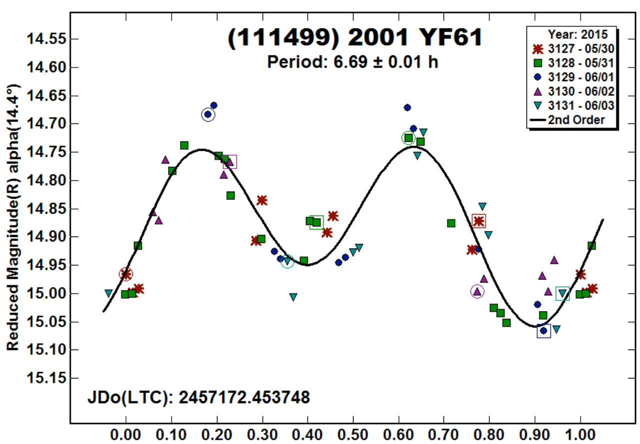
(111499) 2001 YF61
Period: 6.69 ± 0.01 h
Reduced Magnitude(R) alpha(14.4°)
Year: 2015
3127 - 05/30
3128 - 05/31
3129 - 06/01
3130 - 06/02
3131 - 06/03
2nd Order
JDo(LTC): 2457172.453748

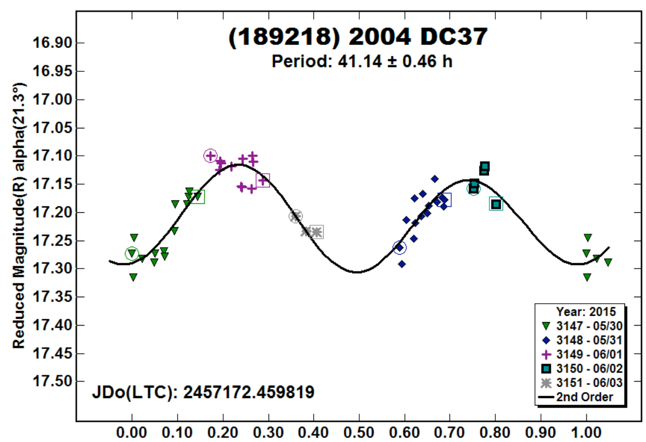
(189218) 2004 DC37
Period: 41.14 ± 0.46 h
Reduced Magnitude(R) alpha(21.3°)
Year: 2015
3147 - 05/30
3148 - 05/31
3149 - 06/01
3150 - 06/02
3151 - 06/03
2nd Order
JDo(LTC): 2457172.459819

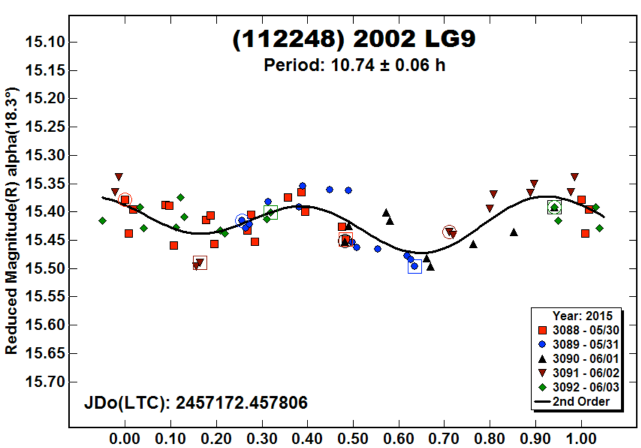
(112248) 2002 LG9
Period: 10.74 ± 0.06 h
Reduced Magnitude(R) alpha(18.3°)
Year: 2015
3088 - 05/30
3089 - 05/31
3090 - 06/01
3091 - 06/02
3092 - 06/03
2nd Order
JDo(LTC): 2457172.457806

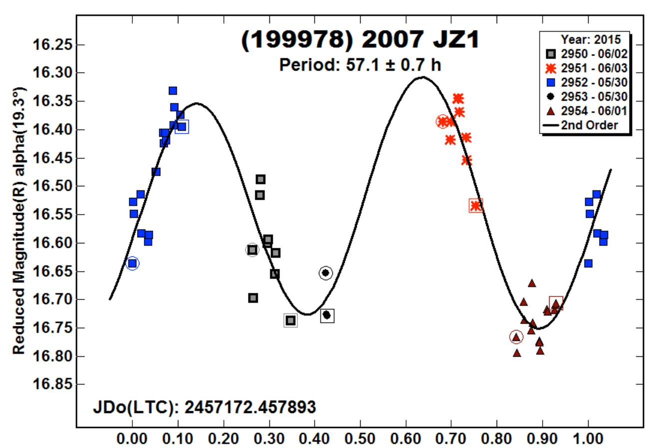
(199978) 2007 JZ1
Period: 57.1 ± 0.7 h
Reduced Magnitude(R) alpha(19.3°)
Year: 2015
2950 - 06/02
2951 - 06/03
2952 - 05/30
2953 - 05/30
2954 - 06/01
2nd Order
JDo(LTC): 2457172.457893

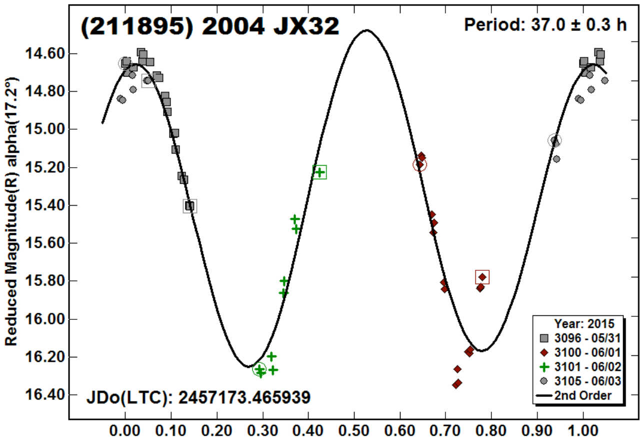

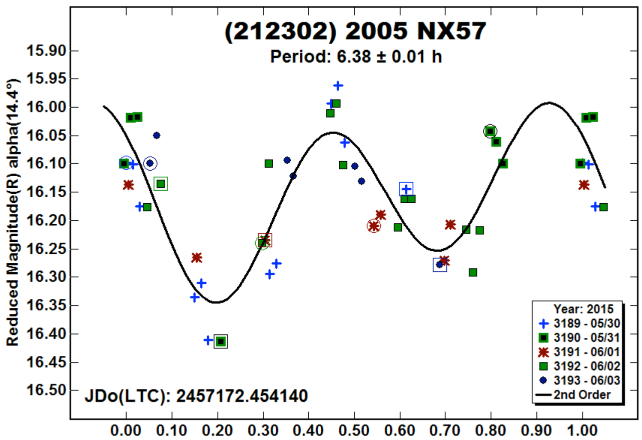

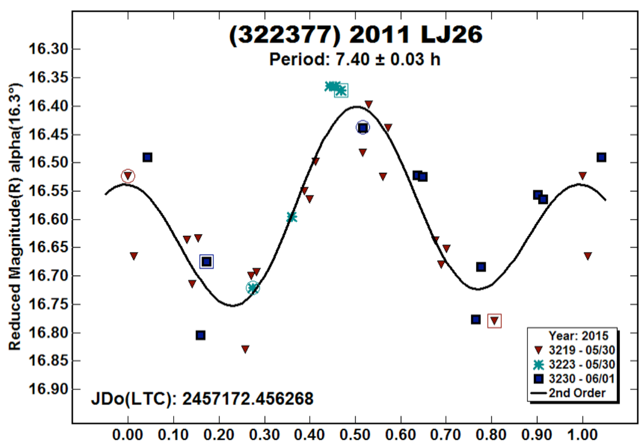

LARGE L5 JOVIAN TROJAN ASTEROID LIGHTCURVES FROM THE CENTER FOR SOLAR SYSTEM STUDIES

Robert D. Stephens
Center for Solar System Studies (CS3)/MoreData!
11355 Mount Johnson Ct., Rancho Cucamonga, CA 91737 USA
rstephens@foxandstephens.com

Daniel R, Coley
Center for Solar System Studies (CS3)
Corona, CA 92883 USA

Linda M. French
Illinois Wesleyan University
Bloomington, IL 61702 USA

(Received: 2015 September 29)

Jovian Trojan asteroids larger than 35 km were studied from the Center for Solar System Studies (CS3, MPC U81). Lightcurves for 24 Trojan asteroids were obtained between January and June 2015.

For three years, CS3 has been conducting a study of Jovian Trojan asteroids. Parts of this study include accumulating data for family rotational studies and future shape model studies. Most of these targets were selected to verify a previous result or because we had one or more sets of data from previous oppositions. For those targeted for shape model studies, dense lightcurves will need to be obtained during several more oppositions as reliable sparse data probably does not exists for Trojan asteroids at 5 AU and a low albedo.

With the exception of 5264 Telephus, all images were made with a 0.4-m or a 0.35-m SCT using an FLI-1001E or a SBIG STL-1001E CCD camera. Images were unbinned with no filter and had master flats and darks applied to the science frames prior to measurement. 5264 Telephus was observed as part of a program observing small Trojan asteroids with the 4-meter Blanco telescope and the Dark Energy Camera (DECam) using a red filter.

Measurements were made using MPO Canopus, which employs differential aperture photometry to produce the raw data. Period analysis was done using MPO Canopus, which incorporates the Fourier analysis algorithm (FALC) developed by Harris (Harris et al., 1989). Night-to-night calibration of the data (generally < ±0.05 mag) was done using field stars converted to approximate Cousins V magnitudes based on 2MASS J-K colors (Warner 2007). The Comp Star Selector feature in MPO Canopus was used to limit the comparison stars to near solar color.

Image processing, measurement and period analysis was done using *MPO Canopus* (Bdw Publishing), which incorporates the Fourier analysis algorithm (FALC) developed by Harris (Harris *et al*., 1989). Night-to-night calibration of the data (generally < ±0.05 mag) was done using field stars converted to approximate Cousins V magnitudes based on 2MASS J-K colors (Warner 2007). The Comp Star Selector feature in *MPO Canopus* was used to limit the comparison stars to near solar color.

In the lightcurve plots, the "Reduced Magnitude" is Johnson R corrected to a unity distance by applying -5*log (rΔ) to the measured sky magnitudes with r and Δ being respectively, the Sun-asteroid and the Earth-asteroid distances in AU. The magnitudes were normalized to the phase angle given in parentheses using G = 0.15.

2260 Neoptolemus. Mottola (Mottola *et al* 2011) previously found a rotational period of 8.180 h. Our result agrees with that previous finding.

2797 Teucer. We studied this asteroid twice before (French *et* al 2011, Stephens *et al* 2014) finding periods of 10.145 h and 10.157 h. The result this year is in good agreement with those findings.

3564 Talthybius. Mottola (Mottola *et al* 2011) studied this Trojan in 1994 reporting a period of 40.59 h. We observed it in 2009 (Stephens 2010) and found a period of 40.44. The result this year of 40.40 h is in good agreement with those prior findings.

(3708) 1974 FV1. Mottola (Mottola *et al* 2011) found a period of 6.553 h in 1993 for this Trojan. Our period of 6.519 h agrees with that result.

3709 Polypoites. This Trojan illustrates the need to re-observe asteroids even when it appears you have a solid solution. In 2010 we observed Polypoites on two nights obtaining what appeared to be a very reasonable, if asymmetric, lightcurve with a 5.71 h period (French *et* al 2011). However, with an amplitude of around 0.12 magnitudes, it is possible that a lightcurve could have only a single extremum, or three or more extrema (Harris *et al* 2014). In 2015 our lightcurve had a slightly larger amplitude and a dramatically different appearance which is inconsistent with a 5.71 h period. The phased lightcurve is still asymmetric and likely dominated by surface features. It has a rotational period 2.5 times that of the 2010 result. We re-phased the 2010 data producing a lightcurve that has almost no overlap for the two nights. We now reject the 5.71 h period in favor of the 14.19 h period. This case illustrates the need to get more than a couple of nights of observations on low amplitude targets that do not have well established rotational periods.

3793 Leonteus. Leonteus is another example where a low amplitude lightcurve can produce alias results when forced to a bimodal solution. We observed this Trojan in 2009, reporting a period of 11.22 h and an amplitude of 0.05 mag. Later, Mottola (Mottola *et al* 2011) reported a period of 5.6225 h from observations obtained in 1994 and 1997. The largest amplitude in the Mottola observations was 0.24 magnitudes suggesting that our 2009 observations were nearly pole on. In 2015, our observations still show an asymmetric lightcurve with a period of 5.62 h and the amplitude now up to 0.11 mag. Re-phasing our 2009 data shows a lightcurve with a single extrema and otherwise no features.

4060 Deipylos. Using sparse photometry from the Palomar Transient Factory, Chang (Waszczak *et al* 2015) reported a period of 11.4905 h for Deipylos. That period appears to be a 5:4 alias of our 9.19 h period. Plots of the Period Spectrum showing possible periods of 7, 10 and 11 h are included. We prefer the 9.19 h period because it produces a symmetric bimodal.

4063 Euforbo. This Trojan has been well observed over the years. Brinsfield (Brinsfield 2011), Mottola (Mottola *et al* 2011), and Chang (Waszczak *et al* 2015) each reported periods near 8.84 h, in agreement with our findings.

4068 Menestheus. We studied this asteroid before (French *et* al 2011, Stephens *et* al 2014) finding a period of 14.341 h. The result this year is in good agreement with those findings.

(4489) 1988 AK. We observed this Trojan in 2009 and 2010 finding periods of 12.6 and 12.58 h (French *et* al 2011). Our period this year agrees with those results.

4709 Ennomos. Mottola (Mottola *et al* 2011) observed Ennomos in 1990 finding a period of 12.275 h. We got two nights of data which were three weeks apart. These showed an 11.12 h period

Number	Name	2015 mm\dd	Pts	Phase	L_{PAB}	B_{PAB}	Period	P.E.	Amp	A.E.	Dia.
2260	Neoptolemus	05/03-05/05	13	5.1,5.3	203	17	8.18	0.01	0.14	0.02	76
2797	Teucer	04/03-04/05	22	5.5,5.2	215	16	10.12	0.01	0.22	0.03	89
3564	Talthybius	02/14-02/27	61	8.0,5.9	186	6	40.4	0.01	0.31	0.02	74
3708	1974 FV1	02/02-02/08	25	8.6,9.3	85	5	6.52	0.003	0.31	0.02	76
3709	Polypoites	04/06-04/10	39	0.8,1.5	193	3	14.19	0.02	0.15	0.02	65
3793	Leonteus	05/01-05/07	98	1.6,2.2	219	8	5.62	0.01	0.11	0.03	112
4060	Deipylos	04/09-04/12	14	3.7,3.3	212	12	9.19	0.01	0.13	0.02	84
4063	Euforbo	05/24-05/26	13	6.0,6.2	217	20	8.84	0.01	0.22	0.02	96
4068	Menestheus	05/03-05/06	10	6.8,7.3	191	6	14.45	0.03	0.3	0.03	68
4489	1988 AK	02/14-03/17	10	8.4,5.2	185	24	12.582	0.001	0.26	0.02	77
4709	Ennomos	02/02-02/13	90	8.4,9.6	86	-9	12.271	0.001	0.46	0.02	91
4834	Thoas	04/26-04/30	17	5.1,5.3	204	25	18.14	0.01	0.39	0.02	72
4836	Medon	04/28-05/02	22	3.4,3.0	229	12	9.818	0.005	0.27	0.02	63
5027	Androgeos	06/01-06/07	19	8.7,9.1	205	26	11.301	0.006	0.65	0.02	60
5126	Achaemenides	12/31-12/31	44	0.0,0.0,0.	0	0	53.02	0.03	0.36	0.02	51
5244	Amphilochos	05/07-05/13	19	4.5,5.6	204	-1	9.766	0.002	0.79	0.02	37
5258	1989 AU1	04/13-04/20	37	2.7,4.1	191	-5	19.85	0.03	0.14	0.02	53
5264	Telephus	05/28-05/31	14	8.9,9.1	213	36	9.54	0.007	0.2	0.03	68
5284	Orsilocus	05/21-06/04	11	6.7,8.3	210	21	10.28	0.01	0.2	0.02	50
5285	Krethon	06/05-06/08	72	7.4,7.6	224	27	12.04	0.02	0.33	0.03	50
7152	Euneus	04/21-04/27	23	2.2,3.3	201	4	9.73	0.02	0.09	0.02	40
11252	Laertes	03/23-03/28	30	2.6,1.7	193	6	9.15	0.01	0.18	0.02	41
15440	1998 WX4	03/29-04/07	52	5.9,5.8,5.	192	30	43.08	0.01	0.11	0.02	63
30102	2000 FC1	04/23-05/09	76	2.8,5.4	202	9	23.95	0.01	0.5	0.03	37

(French *et* al 2012). Shevchenko observed it in 2010 and 2011 reporting a period of 12.2696 (Shevchenko 2012). The result this year confirms the Mottola and Shevchenko results.

4834 Thoas. Mottola (Mottola *et al* 2011) observed Thoas in 1996 finding a period of 18.22 h. We observed it in 2010 (French *et* al 2011) finding a period of 18.192 h. Our result this year of 18.14 h is in good agreement with those results.

4836 Medon. Mottola (Mottola *et al* 2011) observed Medon in 1991 and 2009 finding periods of 9.838 h and 9.840 h respectively. Our period this year of 9.818 is in good agreement with those results.

5027 Androgeos. Mottola (Mottola *et al* 2011) observed Androgeos in 1992 finding a period of 11.355 h. Our period of 11.301 is in agreement with that result.

5126 Achaemenides. There are no previously reported rotational periods in the Lightcurve Database (LCDB; Warner et al., 2009) for this asteroid.

5244 Amphilochos. Using sparse photometry from the Palomar Transient Factory, Chang (Waszczak *et al* 2015) reported a period of 9.7872 h for Amphilochos. Our period of 9.766 h is substantially the same.

(5258) 1989 AU1. There are no previously reported rotational periods in the Lightcurve Database (LCDB; Warner et al., 2009). This Trojan has a low amplitude asymmetric lightcurve. We have included a Period Spectrum showing possible aliases at 12 h and 30 h. We prefer the 19.85 h solution because each nightly session covered over a quarter of the phased lightcurve and most segments of the lightcurve are covered by two or three nights.

5264 Telephus. Telephus was observed by Mottola (Mottola *et al* 2011) in 1994 who reported a period of 9.518 h. Our period of 9.540 h agrees with that result.

5284 Orsilocus. We studied Orsilocus in 2013 (French *et* al 2013) finding a period of 10.31 h. The results this year agrees with that period.

5285 Krethon. We studied Krethon before (French *et* al 2013) finding a period of 12.04 h. Since the period is very similar to one half the Earth's rotation, it is impossible for a single station to get a complete phased lightcurve. However, our result this year is consistent with a bimodal lightcurve and in agreement with the 2013 result.

7152 Euneus. We observed Euneus in 2009 but could not determine a period because the lightcurve was flat and featureless (French *et al* 2013). The observations in 2015 also resulted in a very low amplitude suggesting a spheroid shape. The Period Spectrum suggests periods near 8, 10 and 12 hours. The best of these produces a bimodal lightcurve with a period of 9.72 h. We prefer this period, recognizing that the low amplitude means that the lightcurve is not necessarily bimodal. We phased the 2013 data to the 9.72 h period and produced a lightcurve that is essentially flat to within the noise of the data, implying that this Trojan was near pole-on at the time.

11252 Laertes. There are no previously reported rotational periods in the Lightcurve Database (LCDB; Warner et al., 2009) for this Trojan.

(15440) 1998 WX4. We observed this Trojan in 2013 and 2014 (French *et al* 2013, Stephens *et al* 2014). In both cases, the raw lightcurves spanning multiple nights were featureless. This year the lightcurve showed an amplitude of 0.11 magnitudes with an asymmetric bimodal shape. The usual warnings about low amplitude lightcurves and re-observing at later oppositions apply.

(30102) 2000 FC1. There are no previously reported rotational periods in the Lightcurve Database (LCDB; Warner et al., 2009). This is possibly because the rotational period appears to be very close to that of the Earth. That being the case, no doubt observations may exist on dusty hard drives elsewhere. We observed this Trojan on four nights spanning 16 days, covering the same portion of the phased lightcurve each time. We are able to estimate the rotational period of 23.95 h by solving for half period of 11.98 h. It will take a coordinated campaign by observatories located around the globe to obtain a complete lightcurve.

Acknowledgements

This research was supported by National Science Foundation grant AST-1212115. The purchase of the FLI-1001E CCD camera was made possible by a 2013 Gene Shoemaker NEO Grant from the Planetary Society.

References

Brinsfield, J.W. (2011). "Asteroid Lightcurve Analysis at the Via Capote Observatory: 4th Quarter 2010." *Minor Planet Bul.* **38**, 73-74.

French, L.M., Stephens, R.D., Lederer, S.M., Coley, D.R., Rohl, D.A. (2011). "Preliminary Results from a Study of Trojan Asteroids." *Minor Planet Bul.* **38**, 116-120.

French, L.M., Stephens, R.D., Coley, D.R., Megna, R., Wasserman, L.H. (2012) "Photometry of 17 Jovian Trojan Asteroids." *Minor Planet Bul.* **39**, 183-187.

French, L.M., Stephens, R.D., Coley, D.R., Wasserman, L.H., Vilas, F., La Rocca, D. (2013). "A Troop of Trojans: Photometry of 24 Jovian Trojan Asteroids." *Minor Planet Bul.* **40**, 198-203.

Harris, A.W., Pravec, P., Galád, B., Skiff, B., Warner, B., Világi, J., Gajdoš, S., Carbognani, A., Hornoch, K., Kušnirák, P., Cooney, W., Gross, J., Terrell, D., Higgins, D., Bowell, E., Koehn, B. (2014) "On the maximum amplitude of harmonics of an asteroid lightcurve." *Icarus* **235**, 55-59.

Harris, A.W., Young, J.W., Bowell, E., Martin, L.J., Millis, R.L., Poutanen, M., Scaltriti, F., Zappala, V., Schober, H.J., Debehogne, H., Zeigler, K.W. (1989). "Photoelectric Observations of Asteroids 3, 24, 60, 261, and 863." *Icarus* **77**, 171-186.

Mottola, S., Di Martino, M., Erikson, A., Gonano-Beurer, M., Carbognani, A., Carsenty, U., Hahn, G., Schober, H., Lahulla, F., Delbò, M., Lagerkvist, C., (2011). "Rotational Properties of Jupiter Trojans. I. Light Curves of 80 Objects." *Astron. Jrnl.* **170**, 32.

Shevchenko, V.G., Slyusarev, I.G., Belskaya, I.N. (2012). "Albedo of the Trojan Asteroid 4709 Ennomos." *Asteroids, Comets, Meteors* **2012**, Proceedings of the conference held May 16-20, 2012 in Niigata, Japan.

Stephens, R.D. (2010). "Trojan Asteroids Observed from GMARS and Santana Observatories: 2009 October – December." *Minor Planet Bul.* **37**, 47-48.

Stephens, R.D., Coley, D.R., French, L.M. (2014). “Trojan Asteroids Observed from CS3: 2014 January-May.” *Minor Planet Bul.* **41**, 210-212.

Warner, B.D., (2007). “Initial Results from a Dedicated H-G Project.” *Minor Planet Bul.* **34**, 113-119.

Warner, B.D., Harris, A.W., Pravec, P. (2009). *Icarus* **202**, 134-146. Updated 2015 February 7. *http://www.minorplanet.info/lightcurvedatabase.html.*

Waszczak, A., Chang, C., Ofek, E.O., Laher, R., Masci, F., Levitan, D., Surace, J., Cheng, Y., Ip, W., Kinoshita, D., Helou, G., Prince, T.A., Kulkarni, S. (2015) “Asteroid lightcurves from the Palomar Transient Factory survey: Rotation periods and phase functions from sparse photometry.” *Astron. Jrnl.* **150**, 75.

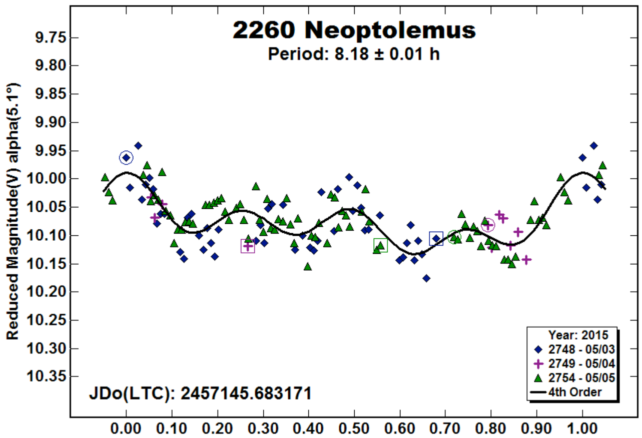

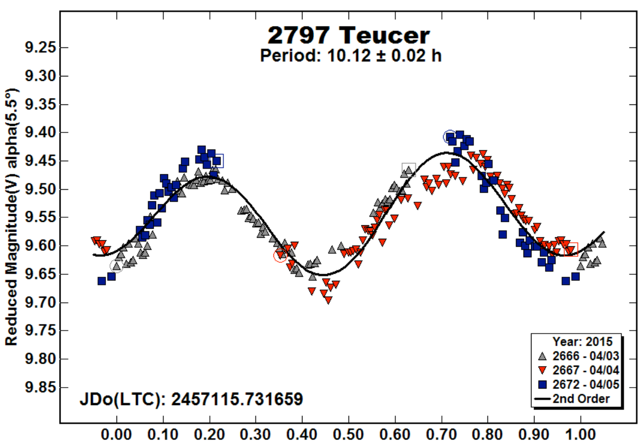

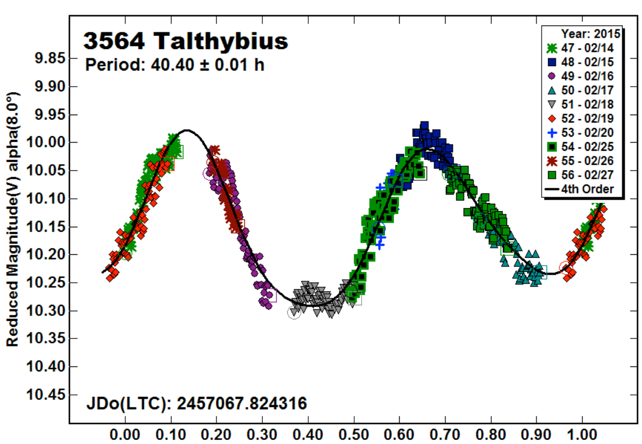

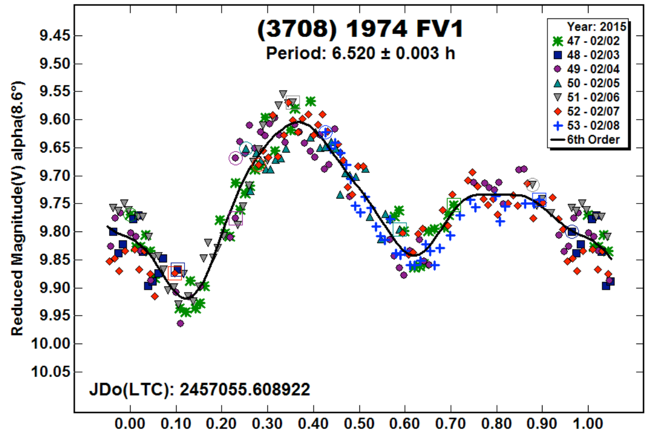

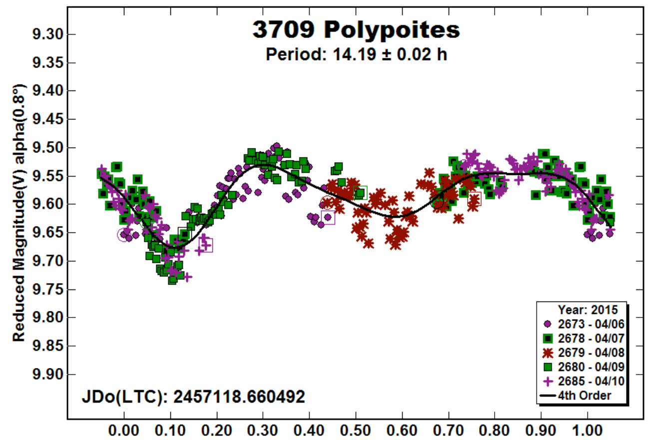

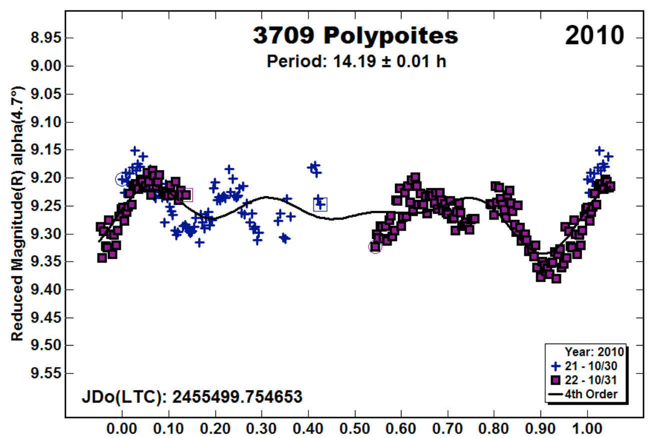

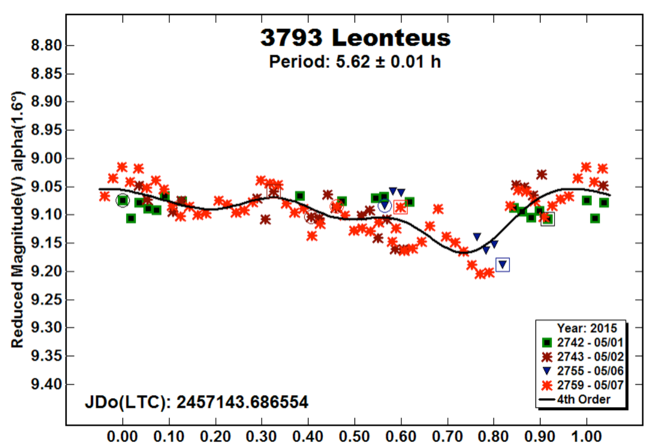

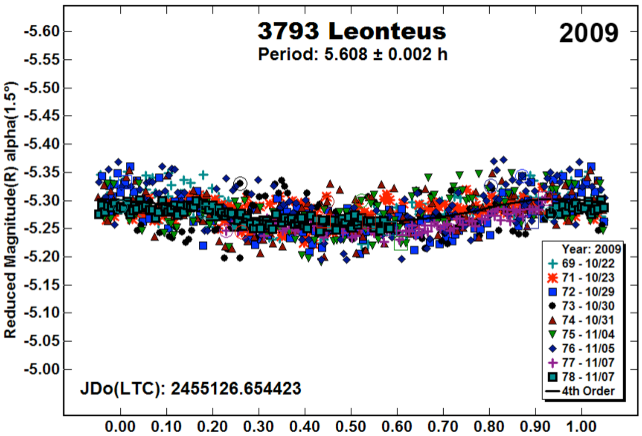
3793 Leonteus
2009
Period: 5.608 ± 0.002 h
Reduced Magnitude(R) alpha(1.5°)
Year: 2009
69 - 10/22
71 - 10/23
72 - 10/29
73 - 10/30
74 - 10/31
75 - 11/04
76 - 11/05
77 - 11/07
78 - 11/07
4th Order
JDo(LTC): 2455126.654423

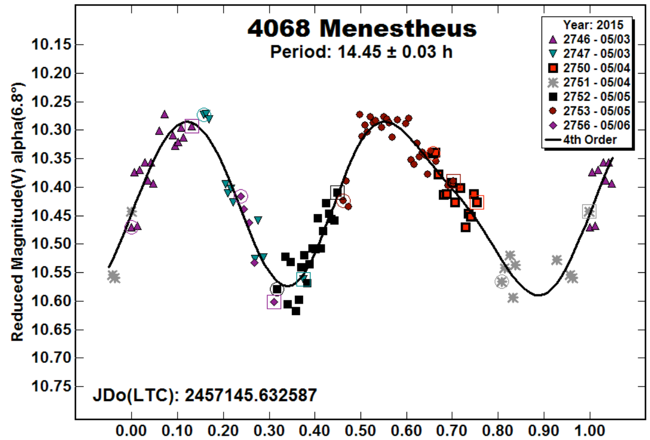
4068 Menestheus
Period: 14.45 ± 0.03 h
Reduced Magnitude(V) alpha(6.8°)
Year: 2015
2746 - 05/03
2747 - 05/03
2750 - 05/04
2751 - 05/04
2752 - 05/05
2753 - 05/05
2756 - 05/06
4th Order
JDo(LTC): 2457145.632587

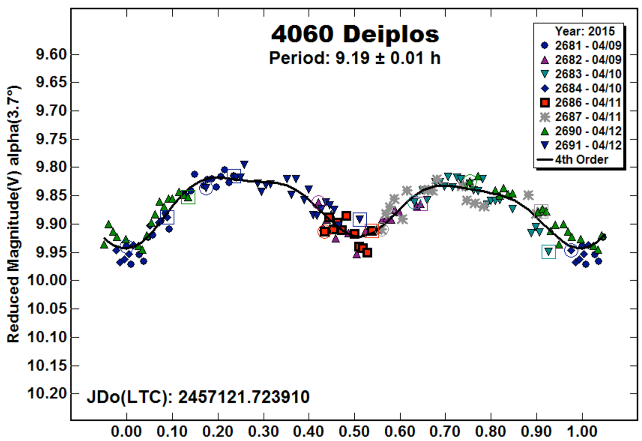
4060 Deiplos
Period: 9.19 ± 0.01 h
Reduced Magnitude(V) alpha(3.7°)
Year: 2015
2681 - 04/09
2682 - 04/09
2683 - 04/10
2684 - 04/10
2686 - 04/11
2687 - 04/11
2690 - 04/12
2691 - 04/12
4th Order
JDo(LTC): 2457121.723910

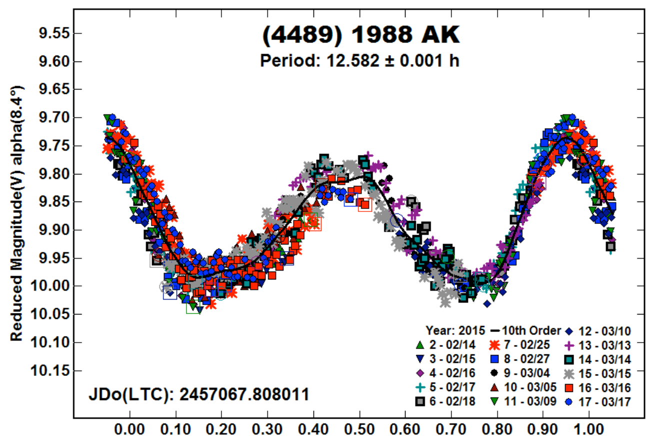
(4489) 1988 AK
Period: 12.582 ± 0.001 h
Reduced Magnitude(V) alpha(8.4°)
Year: 2015
10th Order
2 - 02/14
3 - 02/15
4 - 02/16
5 - 02/17
6 - 02/18
7 - 02/25
8 - 02/27
9 - 03/04
10 - 03/05
11 - 03/09
12 - 03/10
13 - 03/13
14 - 03/14
15 - 03/15
16 - 03/16
17 - 03/17
JDo(LTC): 2457067.808011

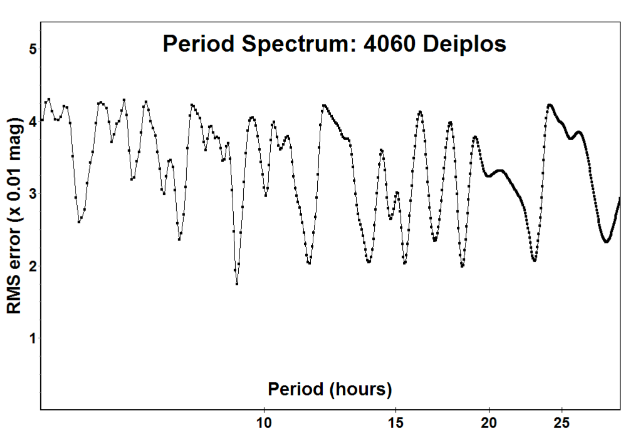
Period Spectrum: 4060 Deiplos
RMS error (x 0.01 mag)
Period (hours)

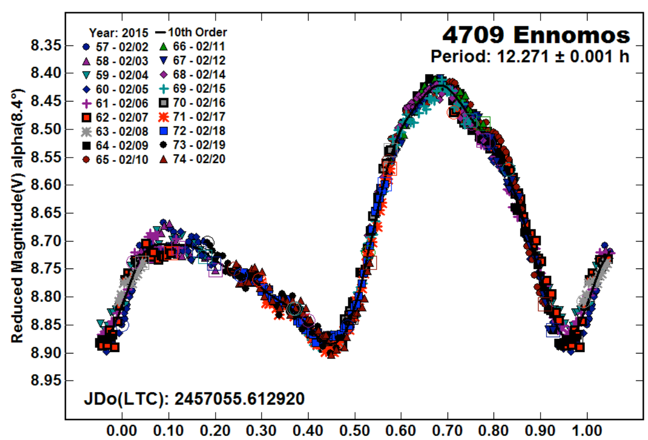
4709 Ennomos
Period: 12.271 ± 0.001 h
Reduced Magnitude(V) alpha(8.4°)
Year: 2015
10th Order
57 - 02/02
58 - 02/03
59 - 02/04
60 - 02/05
61 - 02/06
62 - 02/07
63 - 02/08
64 - 02/09
65 - 02/10
66 - 02/11
67 - 02/12
68 - 02/14
69 - 02/15
70 - 02/16
71 - 02/17
72 - 02/18
73 - 02/19
74 - 02/20
JDo(LTC): 2457055.612920

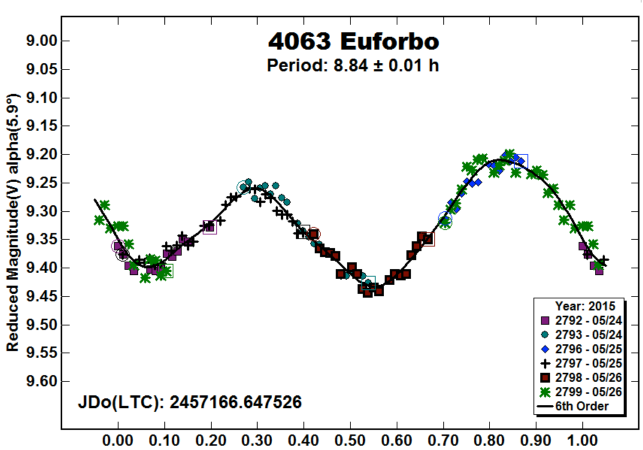
4063 Euforbo
Period: 8.84 ± 0.01 h
Reduced Magnitude(V) alpha(5.9°)
Year: 2015
2792 - 05/24
2793 - 05/24
2796 - 05/25
2797 - 05/25
2798 - 05/26
2799 - 05/26
6th Order
JDo(LTC): 2457166.647526

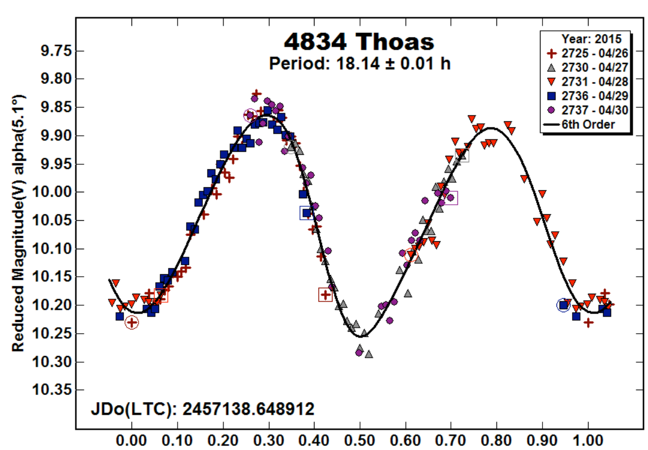
4834 Thoas
Period: 18.14 ± 0.01 h
Reduced Magnitude(V) alpha(5.1°)
Year: 2015
2725 - 04/26
2730 - 04/27
2731 - 04/28
2736 - 04/29
2737 - 04/30
6th Order
JDo(LTC): 2457138.648912

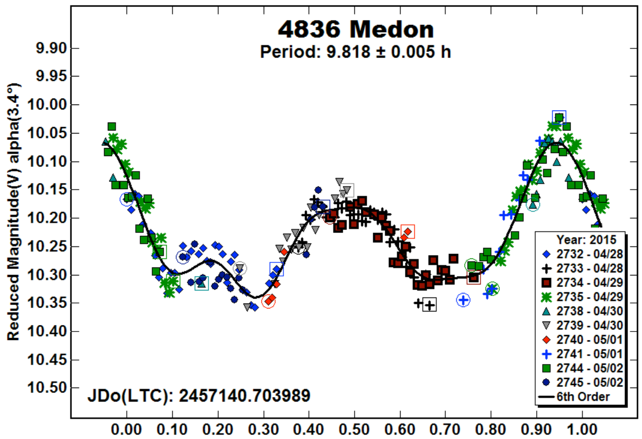
4836 Medon
Period: 9.818 ± 0.005 h
Reduced Magnitude(V) alpha(3.4°)
Year: 2015
2732 - 04/28
2733 - 04/28
2734 - 04/29
2735 - 04/29
2738 - 04/30
2739 - 04/30
2740 - 05/01
2741 - 05/01
2744 - 05/02
2745 - 05/02
6th Order
JDo(LTC): 2457140.703989

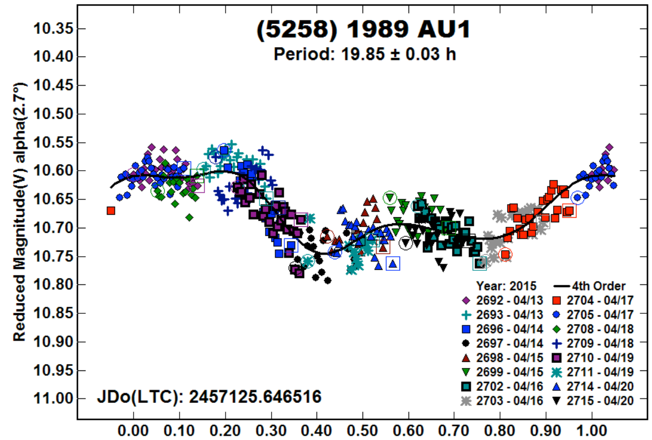
(5258) 1989 AU1
Period: 19.85 ± 0.03 h
Reduced Magnitude(V) alpha(2.7°)
Year: 2015
4th Order
2692 - 04/13
2704 - 04/17
2693 - 04/13
2705 - 04/17
2696 - 04/14
2708 - 04/18
2697 - 04/14
2709 - 04/18
2698 - 04/15
2710 - 04/19
2699 - 04/15
2711 - 04/19
2702 - 04/16
2714 - 04/20
2703 - 04/16
2715 - 04/20
JDo(LTC): 2457125.646516

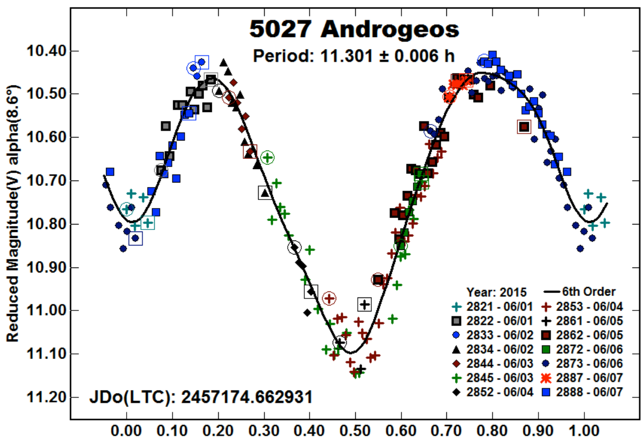
5027 Androgeos
Period: 11.301 ± 0.006 h
Reduced Magnitude(V) alpha(8.6°)
Year: 2015
6th Order
2821 - 06/01
2853 - 06/04
2822 - 06/01
2861 - 06/05
2833 - 06/02
2862 - 06/05
2834 - 06/02
2872 - 06/06
2844 - 06/03
2873 - 06/06
2845 - 06/03
2887 - 06/07
2852 - 06/04
2888 - 06/07
JDo(LTC): 2457174.662931

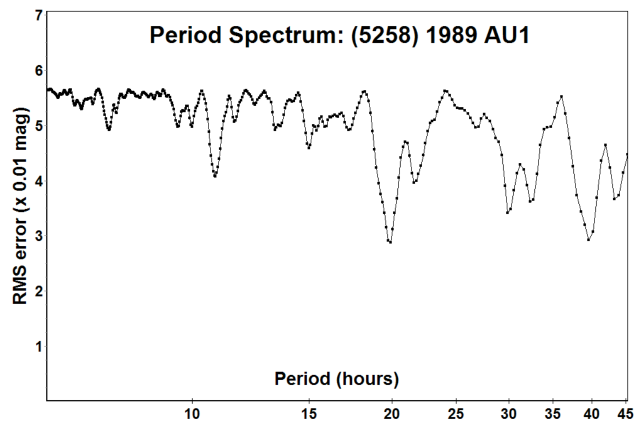
Period Spectrum: (5258) 1989 AU1
RMS error (x 0.01 mag)
Period (hours)

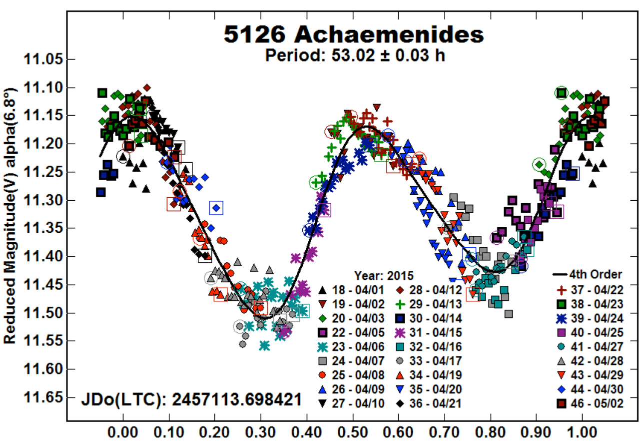
5126 Achaemenides
Period: 53.02 ± 0.03 h
Reduced Magnitude(V) alpha(6.8°)
Year: 2015
4th Order
18 - 04/01
28 - 04/12
37 - 04/22
19 - 04/02
29 - 04/13
38 - 04/23
20 - 04/03
30 - 04/14
39 - 04/24
22 - 04/05
31 - 04/15
40 - 04/25
23 - 04/06
32 - 04/16
41 - 04/27
24 - 04/07
33 - 04/17
42 - 04/28
25 - 04/08
34 - 04/19
43 - 04/29
26 - 04/09
35 - 04/20
44 - 04/30
27 - 04/10
36 - 04/21
46 - 05/02
JDo(LTC): 2457113.698421

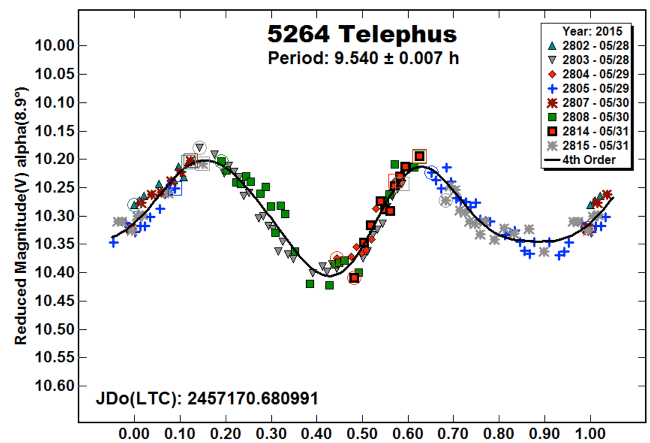
5264 Telephus
Period: 9.540 ± 0.007 h
Reduced Magnitude(V) alpha(8.9°)
Year: 2015
2802 - 05/28
2803 - 05/28
2804 - 05/29
2805 - 05/29
2807 - 05/30
2808 - 05/30
2814 - 05/31
2815 - 05/31
4th Order
JDo(LTC): 2457170.680991

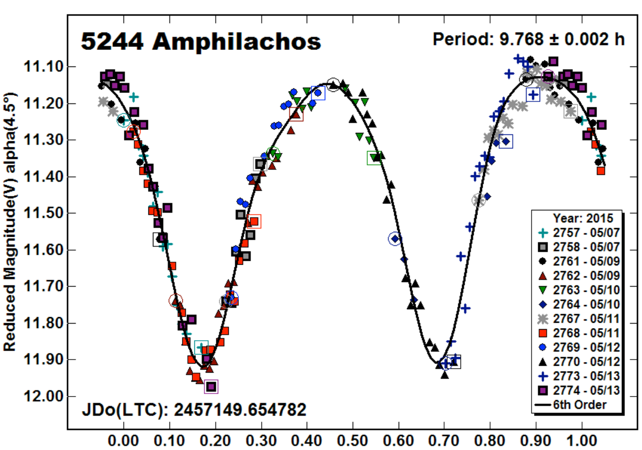
5244 Amphilachos
Period: 9.768 ± 0.002 h
Reduced Magnitude(V) alpha(4.5°)
Year: 2015
2757 - 05/07
2758 - 05/07
2761 - 05/09
2762 - 05/09
2763 - 05/10
2764 - 05/10
2767 - 05/11
2768 - 05/11
2769 - 05/12
2770 - 05/12
2773 - 05/13
2774 - 05/13
6th Order
JDo(LTC): 2457149.654782

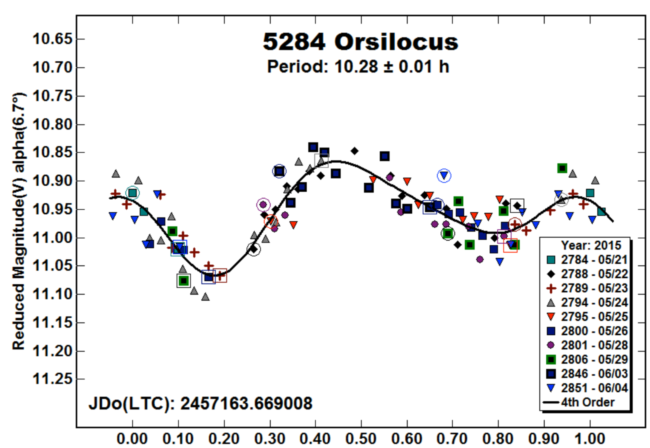
5284 Orsilocus
Period: 10.28 ± 0.01 h
Reduced Magnitude(V) alpha(6.7°)
Year: 2015
2784 - 05/21
2788 - 05/22
2789 - 05/23
2794 - 05/24
2795 - 05/25
2800 - 05/26
2801 - 05/28
2806 - 05/29
2846 - 06/03
2851 - 06/04
4th Order
JDo(LTC): 2457163.669008

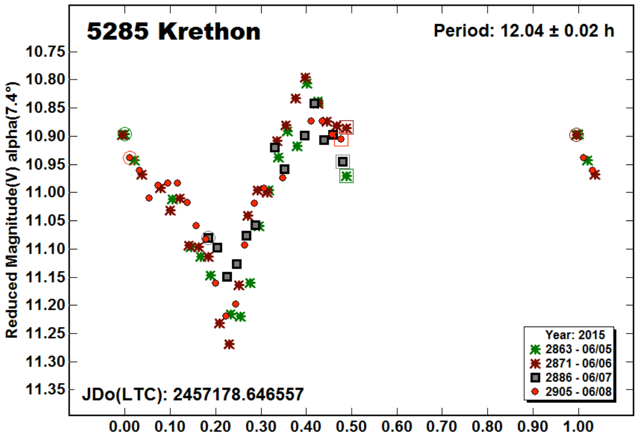
5285 Krethon
Period: 12.04 ± 0.02 h
Reduced Magnitude(V) alpha(7.4°)
Year: 2015
2863 - 06/05
2871 - 06/06
2886 - 06/07
2905 - 06/08
JDo(LTC): 2457178.646557

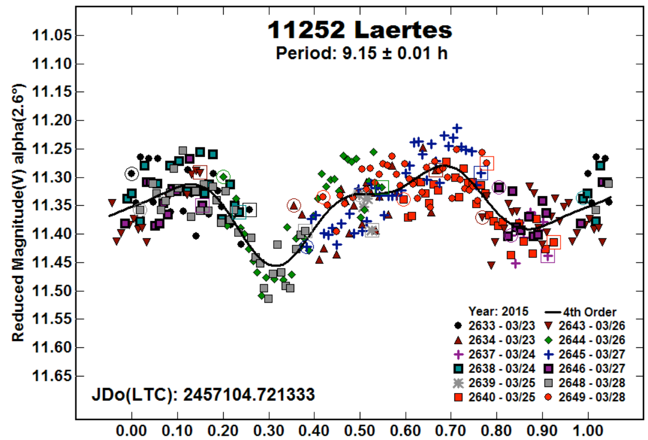
11252 Laertes
Period: 9.15 ± 0.01 h
Reduced Magnitude(V) alpha(2.6°)
Year: 2015
4th Order
2633 - 03/23
2634 - 03/23
2637 - 03/24
2638 - 03/24
2639 - 03/25
2640 - 03/25
2643 - 03/26
2644 - 03/26
2645 - 03/27
2646 - 03/27
2648 - 03/28
2649 - 03/28
JDo(LTC): 2457104.721333

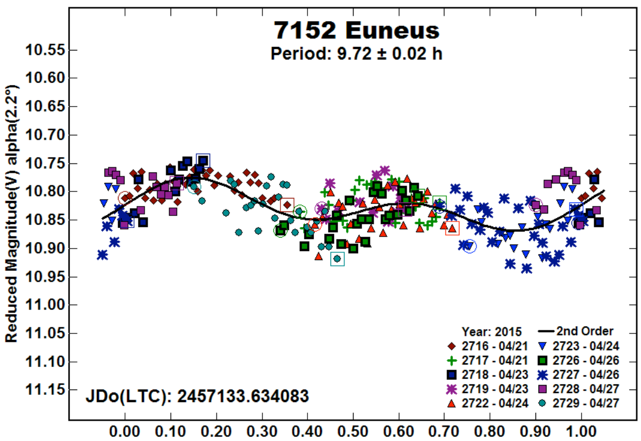
7152 Euneus
Period: 9.72 ± 0.02 h
Reduced Magnitude(V) alpha(2.2°)
Year: 2015
2nd Order
2716 - 04/21
2717 - 04/21
2718 - 04/23
2719 - 04/23
2722 - 04/24
2723 - 04/24
2726 - 04/26
2727 - 04/26
2728 - 04/27
2729 - 04/27
JDo(LTC): 2457133.634083

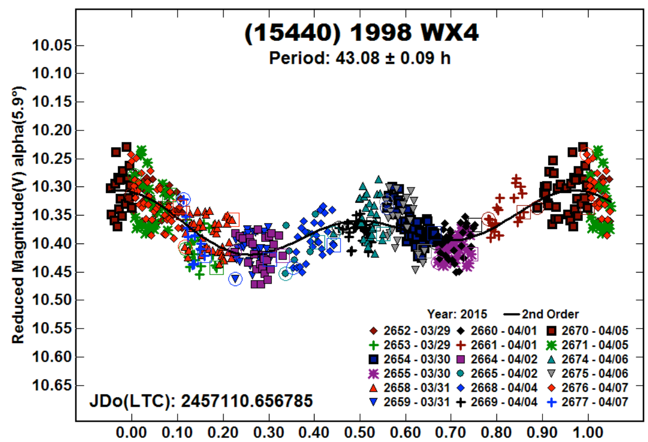
(15440) 1998 WX4
Period: 43.08 ± 0.09 h
Reduced Magnitude(V) alpha(5.9°)
Year: 2015
2nd Order
2652 - 03/29
2653 - 03/29
2654 - 03/30
2655 - 03/30
2658 - 03/31
2659 - 03/31
2660 - 04/01
2661 - 04/01
2664 - 04/02
2665 - 04/02
2668 - 04/04
2669 - 04/04
2670 - 04/05
2671 - 04/05
2674 - 04/06
2675 - 04/06
2676 - 04/07
2677 - 04/07
JDo(LTC): 2457110.656785

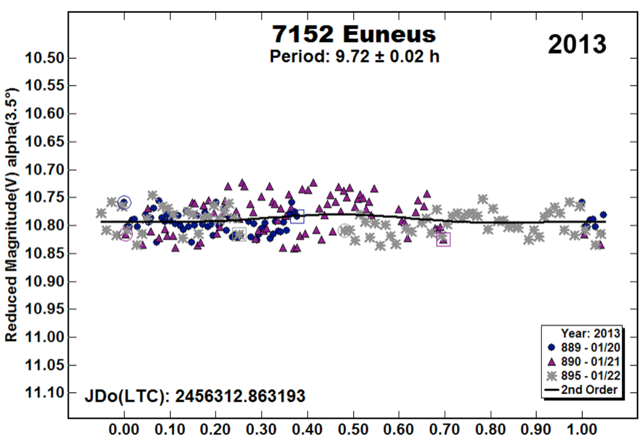
7152 Euneus
2013
Period: 9.72 ± 0.02 h
Reduced Magnitude(V) alpha(3.5°)
Year: 2013
889 - 01/20
890 - 01/21
895 - 01/22
2nd Order
JDo(LTC): 2456312.863193

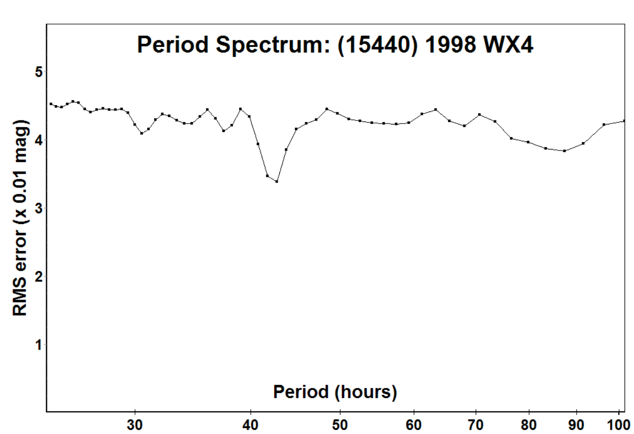
Period Spectrum: (15440) 1998 WX4
RMS error (x 0.01 mag)
Period (hours)

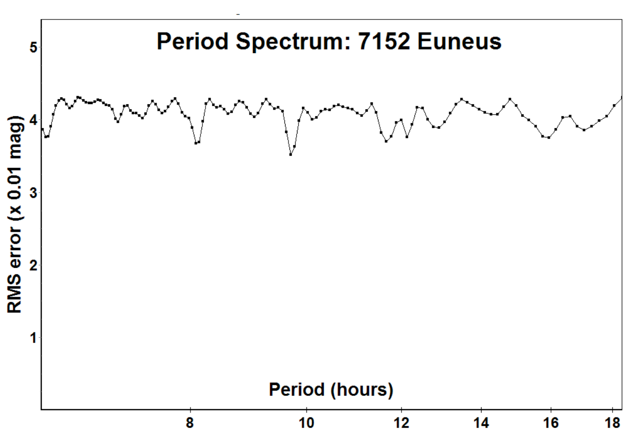
Period Spectrum: 7152 Euneus
RMS error (x 0.01 mag)
Period (hours)

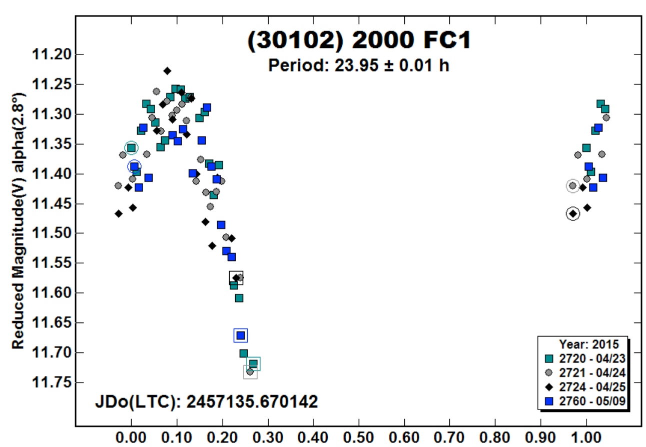
(30102) 2000 FC1
Period: 23.95 ± 0.01 h
Reduced Magnitude(V) alpha(2.8°)
Year: 2015
2720 - 04/23
2721 - 04/24
2724 - 04/25
2760 - 05/09
JDo(LTC): 2457135.670142

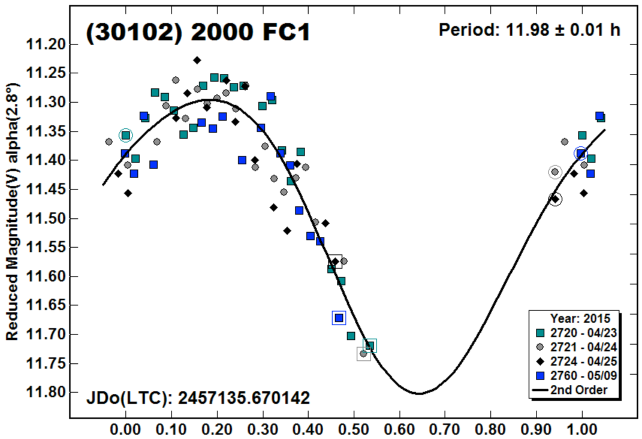

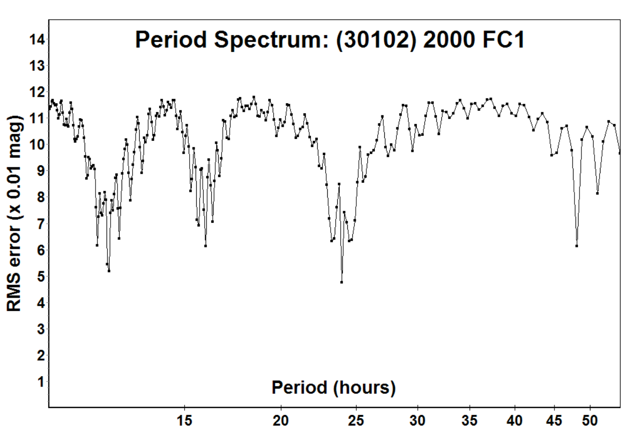

LIGHTCURVE OBSERVATIONS OF (348400) 2005 JF21: AN NEA BINARY

Robert D. Stephens
Center for Solar System Studies (CS3) / MoreData!
11355 Mount Johnson Ct.
Rancho Cucamonga, CA 91737 USA
rstephens@foxandstephens.com

Brian D. Warner
Center for Solar System Studies – Palmer Divide Station
Eaton, CO USA

(Received: 23 September)

CCD photometric observations were made of the near-Earth asteroid (348400) 2005 JF21 in 2015 June and August. Initial analysis in June did not find any signs of a satellite. Follow-up analysis in August using both data sets found indications that the asteroid was binary with a primary period of 2.41 h and an orbital period for the satellite of about 14.3 h. In mid-August, analysis of radar observations at Goldstone (Naidu *et al.*, 2015) confirmed that the asteroid is a binary.

CCD photometric observations of the near-Earth asteroid (348400) 2005 JF21 were made at the Center for Solar System Studies (CS3) in 2015 June and August. Table I gives the equipment used by each author while Table II gives the observing circumstances for each date.

Observer	Telescope		CCD
RDS	C14	0.35-m SCT	STL-1001E
	16S	0.40-m SCT	FLI-1001E
BDW	ECL	0.35-m SCT	STL-1001E

Table I. Equipment used. SCT = Schmidt-Cassegrain.

Date mm/dd	Obs	Scope	α	L_{PAB}	B_{PAB}
06/14	RDS	C14	22.0	269	+18
06/15	RDS	C14	22.0	269	+18
06/20	RDS	16S	22.3	271	+18
06/21	RDS	16S	22.4	271	+18
06/22	RDS	16S	22.5	272	+18
08/02	BDW	ECL	36.5	289	+7
08/03	BDW	ECL	36.7	290	+6
08/04	BDW	ECL	36.9	291	+5
08/05	BDW	ECL	37.0	291	+4
08/06	BDW	ECL	37.2	292	+3

Table II. Observation details. The last three columns give, respectively, the solar phase angle and the phase angle bisector longitude and latitude (see Harris *et al.*, 1984).

Stephens' initial analysis of his data found a period of P = 7.189 h. This stood until Warner made in observations in August using the recently released CMC-15 catalog (*http://svo2.cab.inta-csic.es/vocats/cmc15/*). This catalog provides Sloan r´ and 2MASS (*http://www.ipac.caltech.edu/2mass/*) JHK magnitudes. V and R magnitudes were derived from these values using the formulae by Dymock and Miles (2009). This catalog was adopted with the hope of taking advantage of the better internal consistency over the MPOSC catalog supplied with *MPO Canopus*, which had BVRI magnitudes derived from the 2MASS J-K magnitudes using formulae developed by Warner (2007).

In this case, the hopes were not realized since the initial analysis of the August data showed a large amplitude, long period component without adjusting nightly zero points by more than 0.5 mag. When comparison star magnitudes were taken from the MPOSC, all but one session aligned to within 0.03 mag without adjustments. The discrepancy is not fully explained except to say that both catalogs required converting magnitudes from one magnitude system to another. Such conversions are subject to numerous conditions for accuracy.

Warner's revised analysis lead to finding a period of about 2.4 hours. Stephens could not fit his data to that period "unless it is a binary." This quickly prompted additional analysis. During this time in mid-August, Naidu *et al.* (2015) reported that radar observations had confirmed that the asteroid was a binary, possibly even a trinary.

Figures 1 and 2 show the June (Stephens) data after performing a dual-period search in *MPO Canopus*. The lightcurve for *P2* shows hints of mutual events (occultations and/or eclipses) that would be caused by the first satellite. Given the weak detection of the second satellite by radar, there was essentially no chance that it could be observed photometrically because the variations in the lightcurve would be lost in the noise.

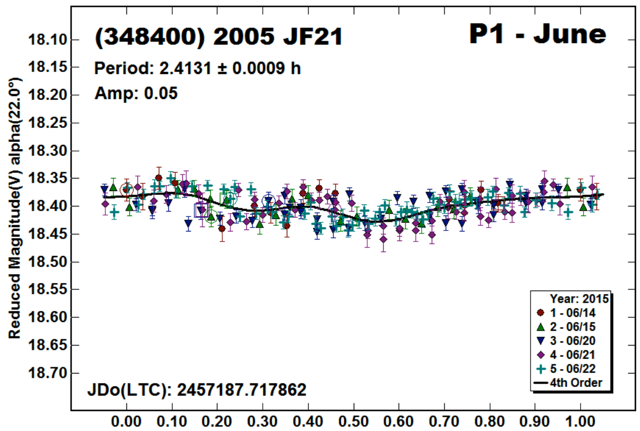

Figure 1. The lightcurve for the primary of 2005 JF21 based only the data from June (Stephens).

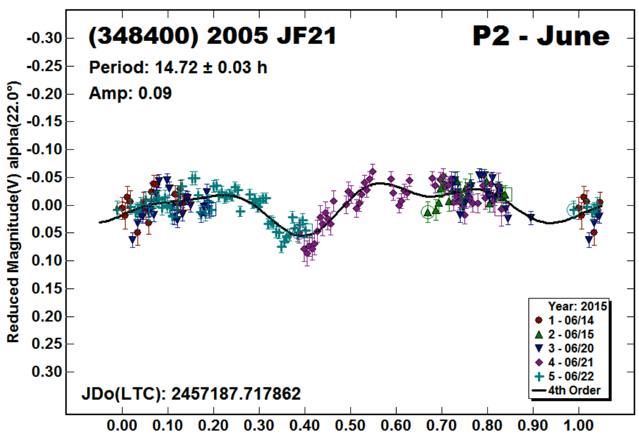

Figure 2. The lightcurve for 2005 JF21 based only on data from June (Stephens). There are hints of mutual events at about 0.4 and 0.9 phase.

Analysis of the August (Warner) data using the comp star magnitudes from MPOSC found $P1$ = 2.4157 ± 0.0007 h and $P2$ = 14.74 ± 0.03 h (Figures 3 and 4). The signs of mutual events are not as strong in the August data. However, both show indications of a satellite that is probably tidally locked to the orbital period.

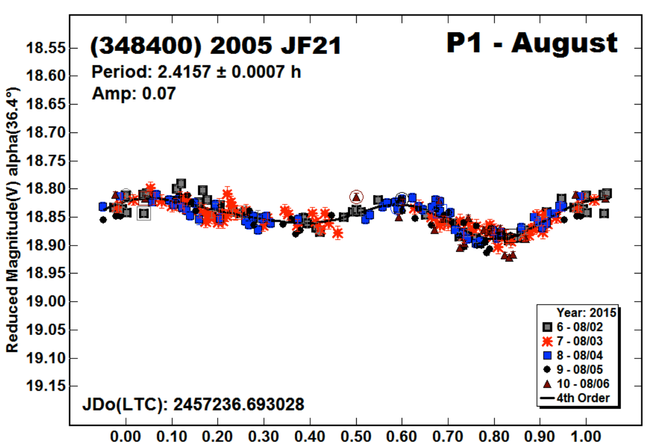

Figure 3. The lightcurve for the primary of 2005 JF1 using only the August (Warner) data.

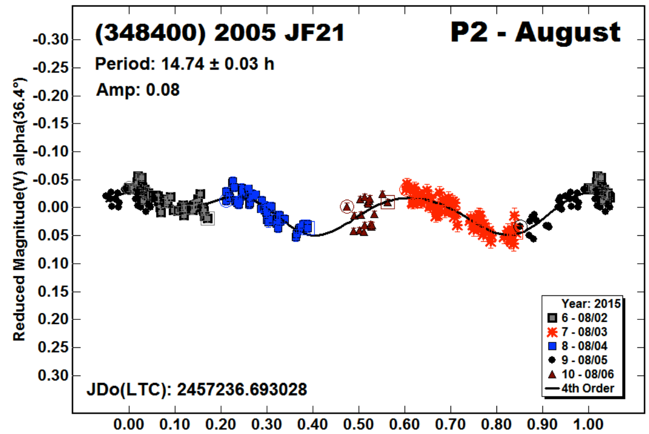

Figure 4. The lightcurve for the satellite of 2005 JF21 using only the August (Warner) data does not show indications of events but does show a constant variation.

Despite the significant change in phase angle and phase angle bisector (viewing aspect) between the two data sets, they were combined to see if a refined solution could be found, one that gave better evidence for the satellite. The resulting lightcurves and periods are shown in Figures 5 and 6. In Figure 6, the mutual events are a little better defined, which allows estimating the satellite-to-primary size ratio, D_S/D_P. This is given by

$$D_S/D_P \geq \sqrt{1 - 10^{-0.4\Delta m}}$$

where Δm is the attenuation, in magnitudes, of the secondary (shallower) event. The value is a minimum in this case because the purported event (at 0.90 phase in Figure 6) is not "flat-bottomed," *i.e.*, it is not a total event. Assuming a value of Δm = 0.04 mag, this gives $D_S/D_P \geq 0.19 \pm 0.02$.

The radar data (Naidu *et al.*, 2015) could not estimate a size ratio because the first satellite was not resolved on the images of about 150-meter resolution.

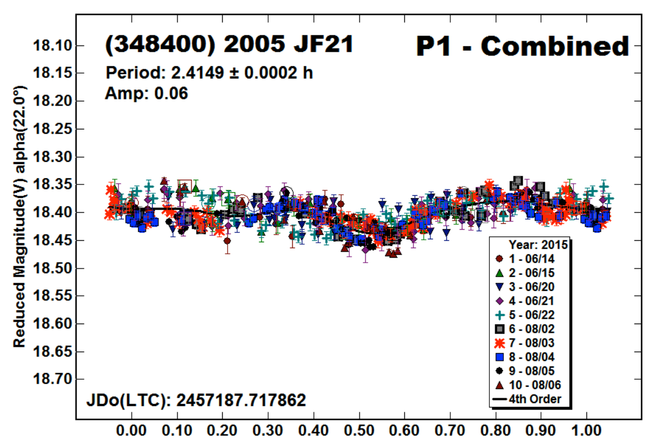

Figure 5. The lightcurve of the primary of 2005 JF21 using the combined data set.

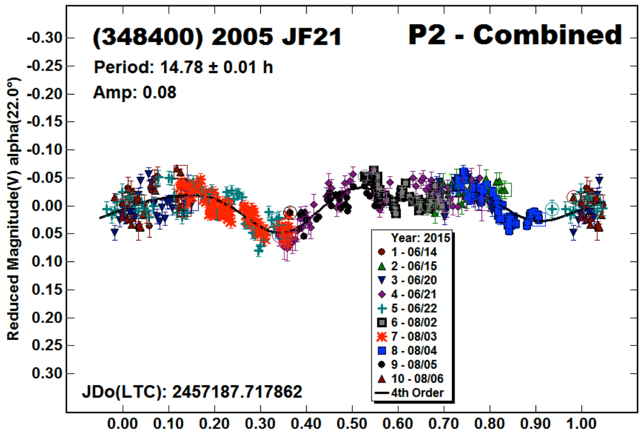

Figure 6. Using the combined data set for 2005 JF21, the mutual events are a little more apparent and can lead to an estimate for the size ratio of the satellite to primary.

The photometry data alone were not enough to *confirm* that 2005 JF21 was a binary, although there were very strong indications of such. The radar data allowed a definitive confirmation. The combined data sets may allow an improved analysis of the system, as would additional time-series data that might be available from other observers.

Acknowledgements

Funding for PDS observations, analysis and publication was provided by NASA grant NNX13AP56G. Work on the asteroid lightcurve database (LCDB) was also funded in part by National Science Foundation Grant AST-1210099.

The purchase of the RDS FLI-1001E CCD camera was made possible by a 2013 Gene Shoemaker NEO Grant from the Planetary Society.

This research was made possible in part based on data from CMC15 Data Access Service at CAB (INTA-CSIC) and the AAVSO Photometric All-Sky Survey (APASS), funded by the Robert Martin Ayers Sciences Fund.

References

Dymock, R., Miles, R. (2009). "A method for determining the V magnitude of asteroids from CCD images." *J. Br. Astron. Assoc.* **119**, 149-156.

Harris, A.W., Young, J.W., Scaltriti, F., Zappala, V. (1984). "Lightcurves and phase relations of the asteroids 82 Alkmene and 444 Gyptis." *Icarus* **57**, 251-258.

Naidu, S.P., Benner, L.A.M., Brozovic, M., Giorgini, J.D., Jao, J.S., Lee, C.G., Snedeker, L.G., Lawrence, K.J. (2015) "(348400) 2005 JF21." *CBET* **4139**, 1.

Warner, B.D. (2007). "Initial Results of a Dedicated H-G Program." *Minor Planet Bul.* **34**, 113-119.

LIGHTCURVE AND ROTATION PERIOD DETERMINATION FOR (31450) 1999 CU9 AND (91252) 1999 CS49

Fabio Salvaggio
21047 – Saronno, ITALY
fsalvaggio@gmail.com

Alessandro Marchini
Astronomical Observatory, DSFTA - University of Siena (K54)
via Roma, 56, 53100 – Siena, ITALY

Riccardo Papini
Carpione Observatory (K49)
San Casciano in Val di Pesa (FI), ITALY

(Received: 2015 October 8 Revised: 2015 November 30)

Photometric observations of the main-belt asteroids (31450) 1999 CU9 and (91252) 1999 CS49 were conducted in 2015 September. Analysis of the data for 1999 CU9 found a bimodal lightcurve phased to a synodic period of $P = 3.413 \pm 0.002$ hours while the data for 1999 CS49 lead to a bimodal lightcurve with a synodic period of $P = 3.357 \pm 0.001$ hours.

(31450) 1999 CU9 is a main-belt asteroid discovered on 1999 February 14 by John Broughton at Reedy Creek Observatory (Australia). It is a typical main-belt asteroid in an orbit with a semi-major axis of about 2.39 AU, eccentricity 0.26, and orbital period of about 3.70 years (JPL, 2015). According to the WISE satellite infrared radiometry (Masiero *et al.*, 2011), its absolute magnitude is $H = 13.0$.

Data were obtained at the Astronomical Observatory of the University of Siena with a 0.30-m *f*/5.6 Maksutov-Cassegrain telescope, SBIG STL-6303E NABG CCD camera, and clear filter; the pixel scale was 2.26 arcsec binning 2x2. Exposures were 300 seconds. Observations were made on five nights from 2015 September 2-7 with a total of 257 useful data points collected. The phase angle ranged from 6.5° to 5.3° before opposition.

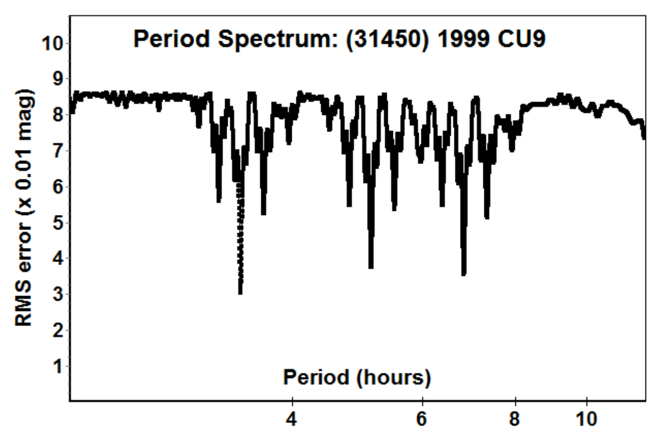

The period spectrum (RMS vs. period) shows several possible solutions. We concluded that the most likely solution was a bimodal lightcurve with a synodic period of 3.413 ± 0.002 hours and an amplitude of 0.24 ± 0.03 mag.

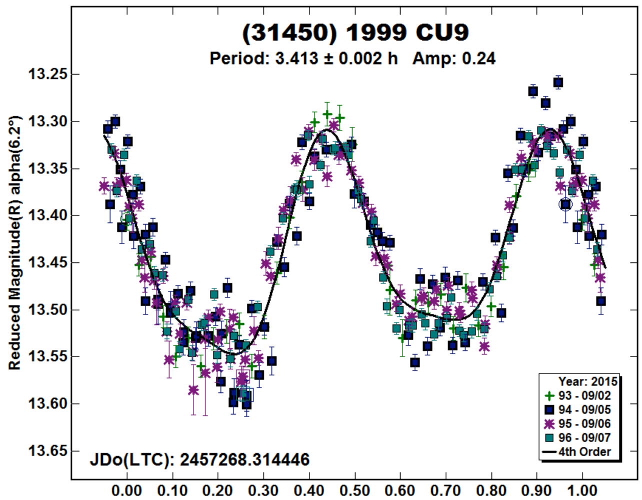

(91252) 1999 CS49 is a main-belt asteroid discovered on 1999 February 10 by the LINEAR survey. It is a typical main-belt asteroid in an orbit with a semi-major axis of about 2.36 AU, eccentricity of 0.24, and orbital period of about 3.63 years (JPL, 2015). According to the WISE satellite infrared radiometry (Masiero *et al.*, 2011), its absolute magnitude is $H = 13.8$.

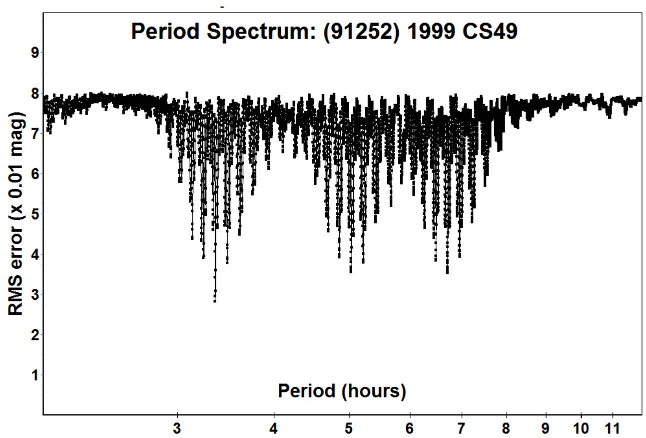

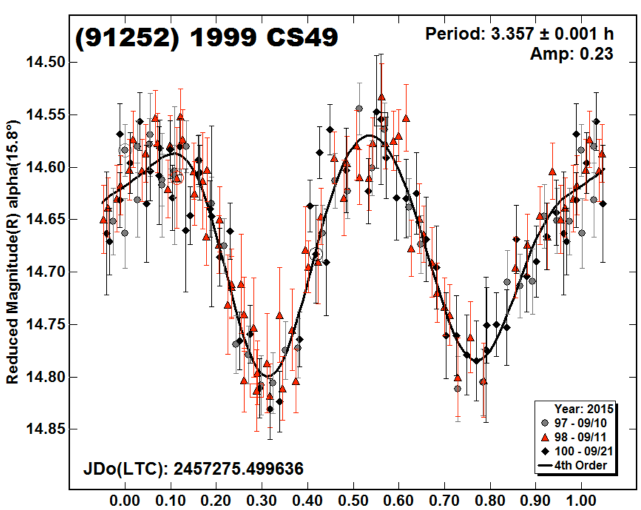

Data were obtained at the Astronomical Observatory of the University of Siena with the same equipment used for (31450) 1999 CU9, with exposure times of 300 seconds. Observations were made on three nights from 2015 September 9-21 with a total of 159 useful data points collected over the interval of 12 days. The phase angle ranged from 16.8° to 11.2° before opposition.

The period showed three groups of solutions. This was due to the 10-day gap between the second and third sessions which resulted in an uncertainty about the number of rotations that occurred within the gap. We concluded that the most likely solution is a bimodal lightcurve with a period of 3.357 ± 0.001 hours and amplitude of 0.23 ± 0.03 mag.

References

JPL (2015). Small-Body Database Browser. *http://ssd.jpl.nasa.gov/sbdb.cgi#top*

Masiero, J.R., Mainzer, A.K., Grav, T., Bauer, J.M., Cutri, R.M., Dailey, J., Eisenhardt, P.R.M., McMillan, R.S., Spahr, T.B., Skrutskie, M.F., Tholen, D., Walker, R.G., Wright, E.L., DeBaun, E., Elsbury, D., Gautier, T., IV, Gomillion, S., Wilkins, A. (2011). "Main Belt Asteroids with WISE/NEOWISE. I. Preliminary Albedos and Diameters." *Ap. J.* **741**, A68.

[NOTE ADDED IN PROOF: 2015 November 30]

After our 2015 October 8 submission of this manuscript, we note that Pray et al. (2015; *IAUC* 4157, dated 2015 October 26) report photometric lightcurve evidence that (31450) 1999 CU9 is a binary. In light of this discovery by Pray et al., we subsequently realize that during our 2015 September 6 observing session, three photometric measurements of our own were interpreted by us to be spurious and we discarded them from our analysis. Those points are included in an updated figure, appended below, which may corroborate the binary discovery by Pray et al.

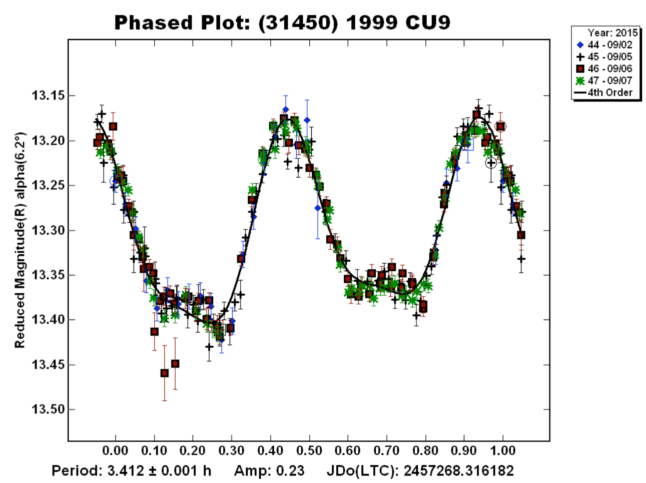

SAVE THE LIGHTCURVES! AN UPDATE ON THE ALCDEF PROJECT

Brian D. Warner
Center for Solar System Studies / MoreData!
446 Sycamore Ave.
Eaton, CO 80615 USA
brian@MinorPlanetObserver.com

(Received: 26 September)

The Asteroid Lightcurve Data Exchange Format (ALCDEF) project has been in development for more than five years. To date, almost 2.5 million time-series data points for more than 11400 asteroids have been submitted to the ALCDEF database hosted on the Minor Planet Center web site. These raw time-series observations have helped researchers produce hundreds of shape and spin axis models. The recent introduction of the S-ALCDEF (Simple-ALCDEF) page is hoped to encourage that even more data be submitted and so expedite and facilitate research efforts that depend on these type of data.

A Brief History of ALCDEF

In the past decade, the number of asteroid lightcurves has grown almost exponentially, mostly due to the efforts of backyard astronomers and students working with small college observatories. Two recent papers involving professional surveys (Waszczak *et al.* 2015, Chang *et al.*, 2015) added more than 10,000 lightcurves to the asteroid lightcurve database (LCDB; Warner *et al.*, 2009).

The rotation periods derived from these lightcurves have helped change the picture of the Solar System dramatically by providing conclusive evidence of the YORP effect (Yarkovsky–O'Keefe–Radzievskii–Paddack; Rubincam, 2000), which is the thermal re-radiation of sunlight that affects the rotation rates (*e.g.*, Pravec *et al.*, 2008) and spin axis orientations of asteroids (*e.g.*, Hanus *et al*., 2013). The availability of the raw data that led to the lightcurves has also allowed a significant increase in the number of shape models (which include spin axis orientation). Beyond the mere curiosity of knowing the shapes of various asteroids, these models have also helped refine theories and ideas on YORP, asteroid densities, and binary formation mechanisms, among others.

These advancements are due in large measure to the availability of the underlying raw time-series data, which are required for the modeling process. However, there remains a fundamental issue: the lack of a *universally-accepted, central repository* similar to the one for astrometric data as managed by the Minor Planet Center. Without such a repository, a researcher may have to contact a number of people and scour several web sites in order to find all available lightcurve photometry. This can be a poor use of resources.

The idea of a central repository for asteroid time-series photometry is not new. Magnusson *et al*. (1993) made one of the earlier significant efforts towards this goal by outlining the Uppsala Asteroid Database, which stored time-series data going back to the 1950's for hundreds of asteroids. The final version of this was produced by Lagerkvist *et al*. (1993). An update was done in 2011 (NASA, 2011) where the data lines were put into their own ASCII tables, apart from the metadata tables. However, not all data in the Uppsala catalog can be taken at face value.

While the 2011 update appears to have standardized all dates to be light-time corrected and magnitudes to unity distances using geo- and heliocentric distances, many other pitfalls are to be found. Quoting from the metadata table for one asteroid but which appears to be common to many if not all asteroids,

> *Some observation sets ... may have an artificial Julian date, which may be set near 0.0, since the observation time is unknown or the lightcurve is a composite of several observation sets made at different times ... Some observation sets have unknown constants added to their magnitudes.*

In other words, some of the dates may be offsets from a zero point that are based on a presumed period that may be wrong. This is a critical problem when modeling since the asteroid-Sun and asteroid-Earth geometries are an essential element in the process. Having the wrong dates, especially if based on incorrect periods, will lead to bad models.

The issue with the magnitudes can be mitigated by using the values as relative magnitudes, not absolute, when modeling. However, for those data that are actually absolute, *i.e.*, standardized apparent magnitudes reduced to unity distances, their value is diminished. The lightcurve inversion modeling process cannot constrain the z-axis of an xyz ellipsoid unless all the data are absolute. It might be possible to "unscrew" the catalog data into original data, but this may involve guess work or, at the very least, referring to the original paper, if available, to try to understand the data's pedigree. This takes time, lots of time, which is a rare commodity for most researchers.

There was an attempt to extend the Uppsala Database with the Standard Asteroid Photometric Catalog (Piironen *et al.*, 2001). That site does not appear to have been active for several years.

At the Division of Planetary Sciences meeting in 2010 (Stephens *et al.*, 2010; Warner *et al.*, 2011), a renewed effort for establishing a central repository was introduced along with a standardized reporting format: the Asteroid Lightcurve Data Exchange Format (ALCDEF). The critical elements of ALCDEF were that

1. Metadata and data were in a single, simple ASCII file (ASCII values < 128). Information for more than one observing run for a given asteroid and even multiple asteroids could be contained in a single file.
2. The format followed a "FITS-like" structure, *i.e.*, keyword=value, including the photometric data.
3. The data were *raw photometry*, *i.e.*, they were not reduced to unity distances nor were arbitrary offsets to magnitudes added, such as might be done during period analysis. In other words, if the data were not differentials from a common zero point, they represented the apparent sky magnitude of the asteroid at the time of the observation. If the magnitudes were offsets, then the common zero point could be indicated in a comment line.
4. The data used full Julian Dates for the mid-time of each observation. The J.D. were not offsets from an arbitrary zero point nor based on a presumed period (the S-ALCDEF standard – see below – allows importing partial or full JD or MJD values).

5. The metadata section included a number of required keywords, *e.g.*, object number and name, mid-date of observations, data set contributor name and contact information, etc. The standard also included a number of optional keywords that would further define the data for use by other researchers.

Initially the data were stored on a public web site maintained by the author but this was not an adequate long-term solution. A conversation in 2009 with then MPC Directory Timothy Spahr eventually led to a web page on the MPC site in 2010 that was developed by MPC staff member Michael Rudenko with the assistance of Assistant Director Gareth Williams.

In 2014, the author began work with MPC staff members Dr. Jose-Luis Galache, Jim Davies, and Michael Rudenko to produce a new version of the web site that would be developed by the author using PHP code and MySQL database. The new code would include additional cross-checks of incoming data to assure its quality and avoid contradictions, *e.g.*, trying to submit data for *(8132) Vesta*. Data retrieval of only newly added objects or a subset of lightcurves was another enhancement to the original site. The new site is now available at

http://www.minorplanetcenter.net/light_curve

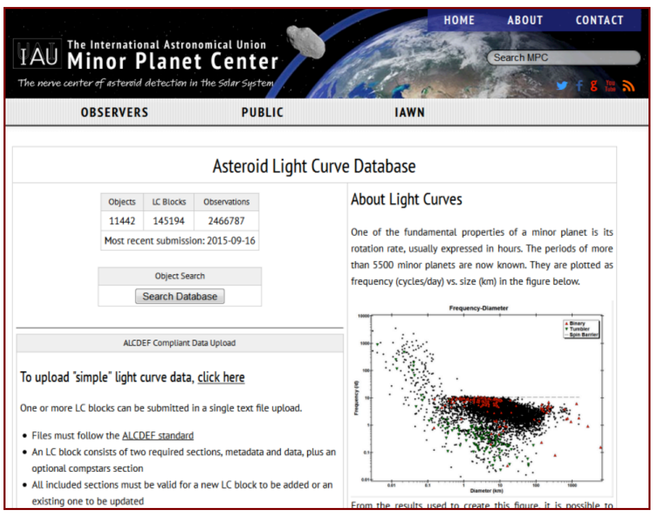

Figure 1. The home page of the ALCDEF database on the Minor Planet Center web site.

As of mid-September 2015, the ALCDEF database included almost 2.5 million individual observations for more than 11,400 objects. This includes the raw data from the Waszczak *et al.* (2015) paper that used *sparse* photometry (about 50-75 data points on 4 nights).

The home page calls it the "Asteroid Light Curve Database." Unfortunately, this is the same name given to the database of rotation periods commonly referred to as the LCDB (Warner *et al.*, 2009). The author and MPC are working on resolving this conflict. Until that happens, to avoid confusion, this database should be referred to as the ALCDEF (pronounced ALK def) database.

The ALCDEF home page allows the user to

1. Search the ALCDEF and/or LCDB databases by number, name, or designation.

2. Upload data files to the ALCDEF database.

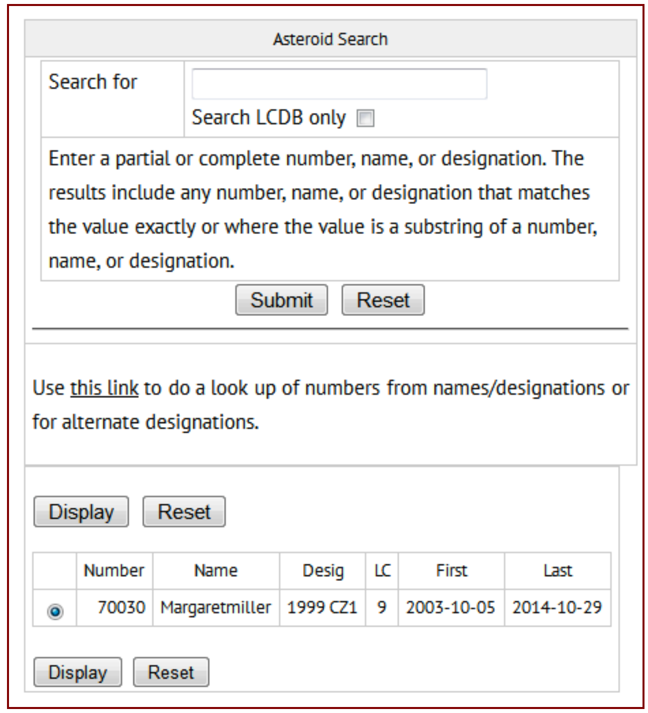

Figure 2. The search page after looking for an asteroid number of 70030.

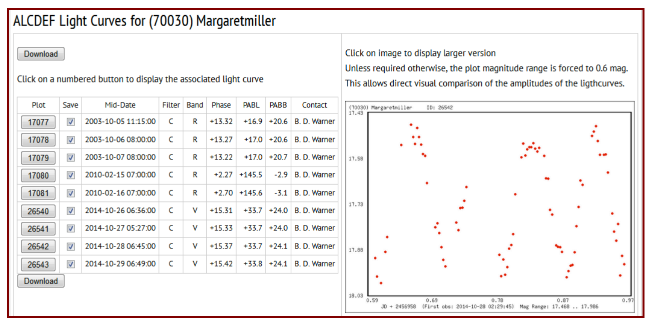

Plot	Save	Mid-Date	Filter	Band	Phase	PABL	PABB	Contact
17077	☑	2003-10-05 11:15:00	C	R	+13.32	+16.9	+20.6	B. D. Warner
17078	☑	2003-10-06 08:00:00	C	R	+13.27	+17.0	+20.6	B. D. Warner
17079	☑	2003-10-07 08:00:00	C	R	+13.22	+17.0	+20.7	B. D. Warner
17080	☑	2010-02-15 07:00:00	C	R	+2.27	+145.5	-2.9	B. D. Warner
17081	☑	2010-02-16 07:00:00	C	R	+2.70	+145.6	-3.1	B. D. Warner
26540	☑	2014-10-26 06:36:00	C	V	+15.31	+33.7	+24.0	B. D. Warner
26541	☑	2014-10-27 05:27:00	C	V	+15.33	+33.7	+24.0	B. D. Warner
26542	☑	2014-10-28 06:45:00	C	V	+15.37	+33.7	+24.1	B. D. Warner
26543	☑	2014-10-29 06:49:00	C	V	+15.42	+33.8	+24.1	B. D. Warner

Figure 3. A screen shot showing the ALCDEF entries for asteroid 70030 Margaretmiller.

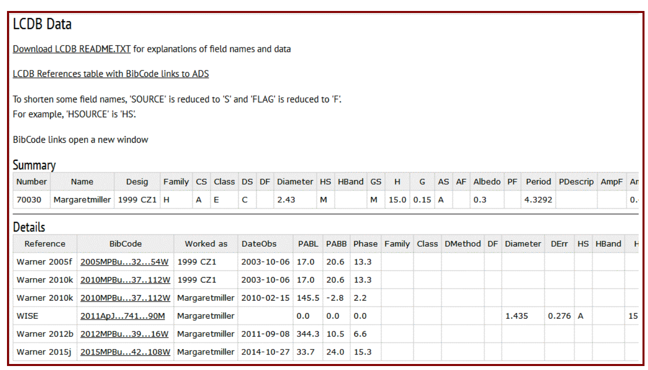
LCDB Data

Download LCDB README.TXT for explanations of field names and data

LCDB References table with BibCode links to ADS

To shorten some field names, 'SOURCE' is reduced to 'S' and 'FLAG' is reduced to 'F'.
For example, 'HSOURCE' is 'HS'.

BibCode links open a new window

Summary

Number	Name	Desig	Family	CS	Class	DS	DF	Diameter	HS	HBand	GS	H	G	AS	AF	Albedo	PF	Period	PDescrip	AmpF	Ar
70030	Margaretmiller	1999 CZ1	H	A	E	C		2.43	M		M	15.0	0.15	A		0.3		4.3292			0.

Details

Reference	BibCode	Worked as	DateObs	PABL	PABB	Phase	Family	Class	DMethod	DF	Diameter	DErr	HS	HBand	H
Warner 2005f	2005MPBu...32...54W	1999 CZ1	2003-10-06	17.0	20.6	13.3									
Warner 2010k	2010MPBu...37..112W	1999 CZ1	2003-10-06	17.0	20.6	13.3									
Warner 2010k	2010MPBu...37..112W	Margaretmiller	2010-02-15	145.5	-2.8	2.2									
WISE	2011ApJ...741...90M	Margaretmiller		0.0	0.0	0.0					1.435	0.276	A		15
Warner 2012b	2012MPBu...39...16W	Margaretmiller	2011-09-08	344.3	10.5	6.6									
Warner 2015j	2015MPBu...42..108W	Margaretmiller	2014-10-27	33.7	24.0	15.3									

Figure 4. This partial screen shot shows some of the entries from the LCDB for 70030 Margaretmiller.

3. Download the latest full archive or only data added since the last full archive. The full archive is updated approximately every three months.

Figure 2 shows the search page after searching for '70030'. Only one result was found and was eventually selected. The caseinsensitive search will find embedded strings as well. For example, if the search had been for ‘Fred’, the list would contain, among others, 678 Fredegundis and 1575 Winifred. The default is to search and display matching records in the ALCDEF database. If no ALCDEF matches are found, the LCDB is searched independently. It is possible to search only the LCDB by checking the “Search LCDB only” box.

Referring to Figure 2, if no matching object exists in the ALCDEF tables but does in the LCDB, then the list will include only the number, name, and MPC designation. If there is at least one matching object in the ALCDEF database, the last three columns give the number of lightcurves and the earliest/latest observation dates. When an ALCDEF object is selected and the user clicks the <Display> button, an LCDB search is done and, if the object is found, the LCDB information will be included in the display page.

Figures 3 and 4 show screen shots of the results for 70030 Margaretmiller (the author’s wife). This asteroid was in the ALCDEF and LCDB tables. In Figure 3, the list of available “lightcurve blocks” is shown. Clicking on a numbered button plots the data in the lightcurve block. All plots are forced to a magnitude range of 0.6 mag, unless the data for a given block exceed that range. This allows a direct visual inspection of the amplitude changes at different viewing aspects.

Below the lightcurve is a plot (Figure 5) showing the phase angle bisector longitude of the chosen block as a red symbol while any other blocks are displayed with grayed symbols.

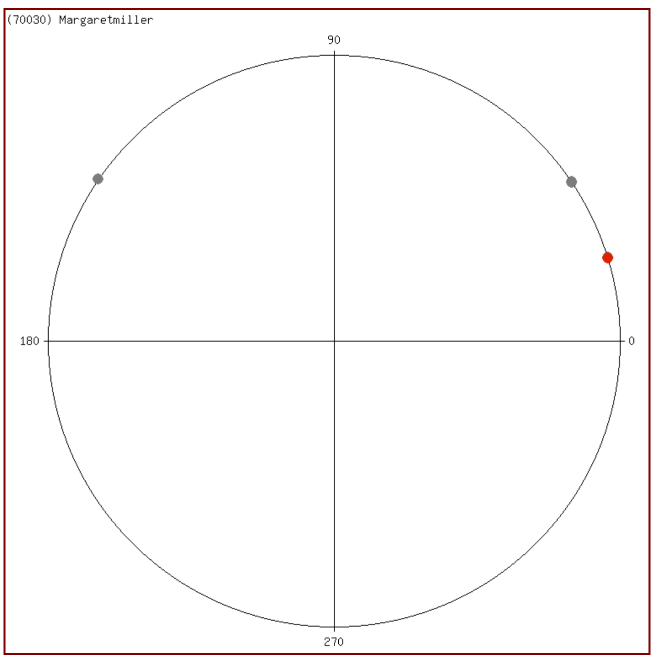

Figure 5. The phase angle bisector longitude (L_{PAB}) plot shows the value for each of the available lightcurves. The values are ecliptic longitude with 0° being the Vernal Equinox.

This feature allows an observer to check if the phase angle bisector longitude (L_{PAB}) at the time of new observations will differ significantly from previous data sets; this would make them even more useful for modeling. However, even if the observations are near existing L_{PAB} values, they may extend the total date range of observations and so help refine the sidereal rotation period. That, in turn, could lead to determining if the asteroid’s rotation period is changing, which a signature of YORP.

Clicking on a lightcurve or L_{PAB} plot displays a larger version. This is a PNG file that can be saved, typically using the browser’s “save image as” popup menu item.

After checking the boxes next to the lightcurve blocks for which data are wanted, clicking the <Download> button generates an ASCII file in ALCDEF form that can be saved to a local computer.

Figure 4 shows a partial screen shot of the LCDB entries for 70030 Margaretmiller. Clicking on the BibCode reference in a given line opens a new window and takes the user to the SAO/NASA ADS page for that reference where, in many cases, the original paper is available for download.

Further Encouragement – S-ALCDEF

To upload data from the main ALCDEF page requires that the metadata and data follow the ALCDEF standard. Programs such as *MPO Canopus*, written by the author, include provisions for writing such files from the original data. However, many other programs do not and there is a wealth of legacy data that might also be uploaded if there were a simpler format.

In mid-2015, the Simple-ALCDEF (S-ALCDEF) standard was introduced by the author. In its simplest form, S-ALCDEF requires only four lines other than the data lines. For example, assuming all the data in the file are for the same asteroid (bold text highlights the four lines),

```
#First night
STARTBLOCK
STARTDATA
2457210.698517|+18.377|+0.121
2457210.700769|+18.489|+0.136
2457210.703026|+18.354|+0.121
...
ENDDATA
ENDBLOCK

#Second Night
STARTBLOCK
STARTDATA
2457210.776946|+17.375|+0.055
2457210.777695|+17.419|+0.058
...
ENDDATA
ENDBLOCK
```

Lines preceded by the hashtag (#) are ignored. The hashtag can also be embedded in a line. Starting with the hashtag, it and all characters after it on that line are ignored, making it possible to include a comment about a specific line in the file.

Of course, the system must know for which object the data apply and this is provided in one of two forms on the S-ALCDEF page,

http://www.minorplanetcenter.net/light_curve2/alcdef_SimpleUpload.php

The “Required Data” form applies to *all* lightcurve blocks. This includes the submitting author’s name and contact information and the delimiter character between fields in the data lines. A universal comment of up to 400 characters can also be included.

The “Base Data” section includes default entries for every lightcurve block, unless a specific block overrides one or more of the entries. The overrides are applied only to the block in which they are found; the remaining defaults from the form are applied to the block. An example of this would be when the object changes. For example,

```
#First asteroid
STARTBLOCK
OBJECTNUMBER=1
OBJECTNAME=Ceres
...
#Second asteroid
STARTBLOCK
OBJECTNUMBER=70030
```

The override lines *must* use the full ALCDEF standard keyword and provide data in the form and format expected. There are many themes and variations allowed. However, the main point is to keep the data files as simple as possible in order to allow quick and easy conversion from legacy files and formats.

The ALCDEF site has a link to the full documentation for the ALCDEF and S-ALCDEF standards, which includes additional examples for S-ALCDEF. The direct link to the PDF is:

http://www.minorplanetcenter.net/light_curve2/docs/ALCDEF_Standard.pdf

Further Developments

The ALCDEF standard was presented briefly by Steve Chesley of JPL at the 2015 August meeting of the International Astronomical Union in Honolulu. The intent was to gauge interest in ALCDEF eventually becoming the official standard for asteroid time-series data. Any action along those lines will likely be years from now, if at all.

A proposed new standard for astrometry was also introduced at the IAU meeting. This is a considerably more evolved process and may see adoption before long. That standard adopts one of two formats, one being XML. In order to be in step with the astrometry standard and to minimize programming efforts by the users, the author is looking into providing the necessary methods on the web site to process XML-formatted data and the required documentation for end-users. The current format would *not* be abandoned as part of this development.

Other site enhancements to make it easier to use and provide additional data are also under consideration or development.

Closing Remarks

The ALCDEF and S-ALCDEF standards and MPC web site provide a straight-forward way to archive raw asteroid time-series data that are readily available and critical to researchers. However, the ALCDEF database is far from universally-accepted and used.

For example, all data presented in articles in *Astronomy and Astrophysics* must be archived in the Centre de Donnée astronoimiques de Stransbourg (Lub, 2015; CDS, Strasbourg Astronomical Data Center). This is not going to change nor should it do so. It's also unlikely that a researcher is going to prepare his data for more than one archive database, even though in this case there may not be significant differences in the files submitted to CDS and ALCDEF; it might be something for those submitting to CDS (or ALCDEF) to consider.

There are many other repositories of raw data, many on private web sites or in the computer equivalent of "dusty filing cabinets." It's hoped that the introduction of S-ALCDEF will encourage even more submissions to the system.

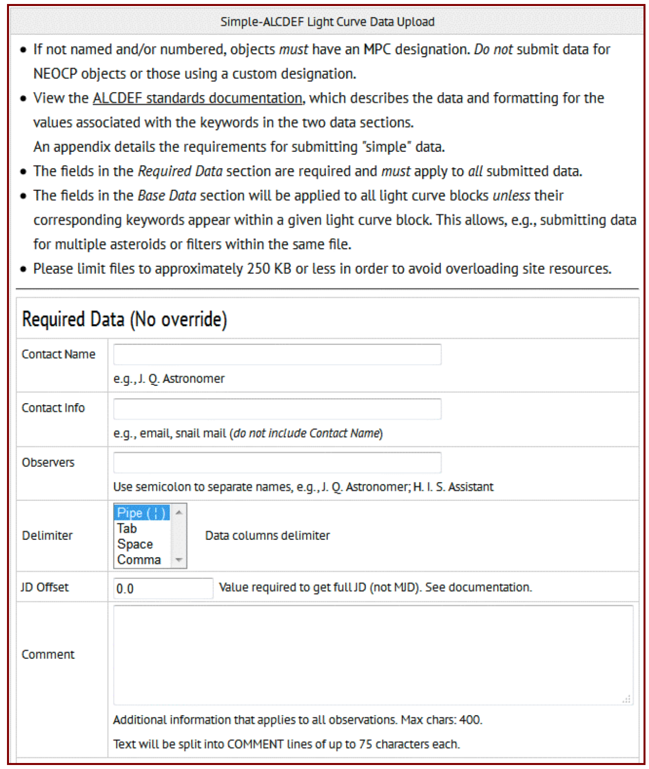

Figure 6. This screen shot shows the "Required Data" section on the S-ALCDEF page. The data in this section *must* apply to *all* lightcurve blocks.

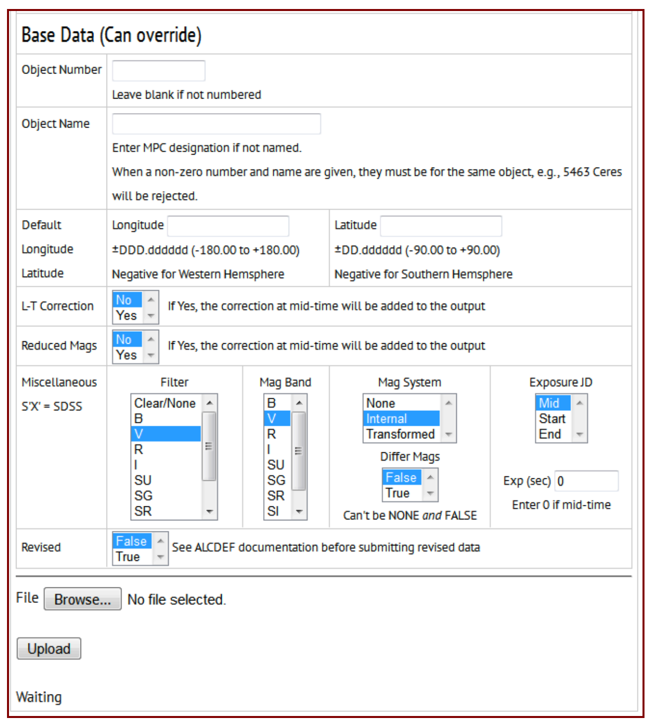

Figure 7. This screen shot shows the "Base Data" section on the S-ALCDEF page. These are default entries for all lightcurve blocks but one or more can be overridden within a given block by including the necessary lines between STARTBLOCK and STARTDATA.

While a single universally-accepted repository is preferable, a minimum number, each with long-term stability that extends beyond those who currently own and/or maintain it, is a good alternative and is encouraged.

Questions and comments about the ALCDEF project are welcome; they can be sent to the author's email address.

Acknowledgements

Work on the asteroid lightcurve database (LCDB) and ALCDEF database is funded by NASA grant NNX13AP56G and by National Science Foundation Grant AST-1507535.

References

Chang, C.-K., Ip, W.-H., Lin, H.-W., Cheng, Y.-C., Ngeow, C.-C., Yang, T.-C., Waszczak, A., Kulkarni, S.R., Levitan, D., Sesar, B., Laher, R., Surace, J., Prince, T.A. (2015). "Asteroid Spin-rate Study Using the Intermediate Palomar Transient Factory." *Ap. J. Suppl. Ser.* **219**, A27.

Hanuš, J., Brož, M., Durech, J., Warner, B.D., Brinsfield, J., Durkee, R., Higgins, D., Koff, R.A., Oey, J., Pilcher, F., Stephens, R., Strabla, L.P., Ulisse, Q., Girelli, R. (2013). "An anisotropic distribution of spin vectors in asteroid families." *Astron. Astrophys.* **559**, A134.

Lagerkvist, C.-I., Magnusson, P., Belskaya, I., Erikson, A., Dahlgren, M., Barucci, M.A. (1993). "Asteroid Photometric Catalog, Third Update." Uppsala Astronomical Observatory, Uppsala.

Lub, J. (2015). "Editorial." *Astron. Astrophys*. **581**, E1.

Magnusson, P., Lagerkvist, C.-I., Dahlgren, M., Erikson, A. (1993). "The Uppsala Asteroid Database." in ACM 1993, Proceedings of the 160th International Astronomical Union. A. Milani, M. Di Martino, A. Cellino, eds. pp 471-476. Kluwer Academic Publishers.

NASA (2011). Update to Uppsala Asteroid Database. Planetary Data Systems catalog EAR-A-3-DDR-APC-LIGHTCURVE-V1.1. Available on-line:
https://pds.nasa.gov/ds-view/pds/viewProfile.jsp?dsid=EAR-A-3-DDR-APC-LIGHTCURVE-V1.1

Piironen, J., Lakgerkvist, C.-I., Torppa, J., Kaasalainen, M., Warner B. (2001). "Standard Asteroid Photometric Catalog." DPS Meeting #33. *B.A.A.S.* **33**, 1562.
http://asteroid.astro.helsinki.fi/apc

Pravec, P., Harris, A.W., Vokrouhlický, D., Warner, B.D., Kušnirák, P., Hornoch, K., Pray, D.P., Higgins, D., Oey, J., Galád, A., Gajdoš, Š., Kornoš, L., Világi, J., Husárik, M., Krugly, Yu.N., Shevchenko, V., Chiorny, V., Gaftonyuk, N., Cooney, W.R., Gross, J., Terrell, D., Stephens, R.D., Dyvig, R., Reddy, V., Ries, J.G., Colas, F., Lecacheux, J., Durkee, R., Masi, G., Koff, R.A., Goncalves, R. (2008). "Spin rate distribution of small asteroids." *Icarus* **197**, 497-504.

Rubincam, D.P. (2000). "Relative Spin-up and Spin-down of Small Asteroids." *Icarus* **148**, 2-11.

Stephens, R.D., Warner, B.D., Harris, A.W. (2010). "A Proposed Standard for Reporting Asteroid Lightcurve Data." DPS meeting #42. *B.A.A.S.* **42**, 1035.

Warner, B.D., Harris, A.W., Pravec, P. (2009). "The Asteroid Lightcurve Database." *Icarus* **202**, 134-146. Updated 2015 Sept. *http://www.minorplanet.info/lightcurvedatabase.html*

Warner, B.D., Stephens, R.D., Harris, A.W. (2011). "Save the Lightcurves." *Minor Planet Bull*. **38**, 172-174.

Waszczak, A., Chang, C.-K., Ofek, E.O., Laher, R., Masci, F., Levitan, D., Surace, J., Cheng, Y.-C., Ip, W.-H., Kinoshita, D., Helou, G., Prince, T.A., Kulkarni, S. (2015). "Asteroid Light Curves from the Palomar Transient Factory Survey: Rotation Periods and Phase Functions from Sparse Photometry." *Astron. J.* **150**, A75.

LIGHTCURVE ANALYSIS OF NEA 2015 HM10

Brian D. Warner
Center for Solar System Studies – Palmer Divide Station
446 Sycamore Ave.
Eaton, CO USA 80615
brian@MinorPlanetObserver.com

William H. Ryan
Magdalena Ridge Observatory
New Mexico Institute of Mining and Technology
Socorro, NM USA 87801

(Received: 2015 September 30)

Independent CCD photometry observations by the authors of the near-Earth asteroid 2015 HM10 were made in 2015 July. Analysis of both data sets found a synodic rotation period of approximately 0.376 h and amplitude of 1.47 ± 0.05 mag.

CCD photometric observations of the near-Earth asteroid 2015 HM10 were made in early 2015 July at the Magdalena Ridge Observatory (MRO) and the Center for Solar System Studies – Palmer Divide Station (CS3). Both sets of observations were made in support of radar observations by providing rotation periods and astrometry and, more generally, as part of on-going programs to determine physical characteristics of near-Earth asteroids (see, *e.g.*, Ryan and Ryan, 2015). The MRO data were collected early in the asteroid's apparition under less than ideal conditions to provide the critical spin rate information necessary to optimize radar observations.

Date 2015/mm/dd	Obs	α	L_{PAB}	B_{PAB}
07/01	MRO	100.0	227	-4
07/10	CS3	85.4	331	+7
07/11	CS3	80.8	330	+6

Table I. Observation details. The last three columns give, respectively, the solar phase angle and the phase angle bisector longitude and latitude.

Observations at MRO were made using the 2.4-m *f*/8.8 telescope, located in the Magdalena Mountains of New Mexico, using a VR filter (V and R). Exposures were 45 seconds. Approximately 1.4 hours of data were obtained at air masses X = 2.5 to 3.8 with thin cirrus clouds and a full moon. The images were bias-subtracted and flat-fielded, and on-chip differential photometry was performed using IRAF (Tody, 1993). The V magnitudes were calibrated using magnitudes from the MPOSC catalog, which converts 2MASS J-K magnitudes to BVRI using formulae developed by Warner (2007). These were checked for consistency using SDSS transformations (Jester *et al.*, 2005). The data were corrected to unit geocentric and heliocentric distances and then analyzed using the techniques described by Harris *et al.* (1989).

Observations at CS3 were made using a 0.30-m Schmidt-Cassegrain telescope (SCT) and Finger Lakes ML-1001E CCD camera. The images were dark-subtracted and flat-fielded using *MPO Canopus* (Warner, 2015). The 60-second unfiltered images were converted to V magnitudes using comparison star magnitudes from the MPOSC catalog and differential photometry. Period analysis was also done in *MPO Canopus*, which implements the FALC Fourier analysis algorithm (Harris *et al.*, 1989).

Analysis

Figure 1 shows the lightcurve derived from the data obtained at MRO. While the absolute calibration errors are on the order of 0.05 mag, the low photon statistics and high background levels resulted in differential errors on the order of 0.1-0.3 mag. Even so, these were relatively small in comparison to the amplitude of the lightcurve and so allowed finding a reliable synodic period of *P* = 0.376 ± 0.002 h.

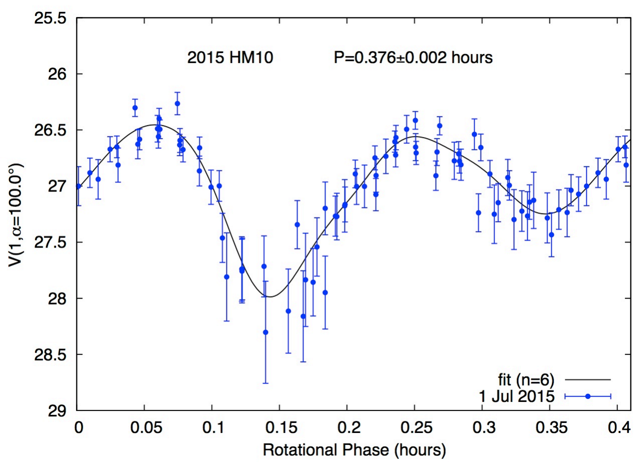

Figure 1. The lightcurve for 2015 HM10 based on data from Magdalena Ridge Observatory.

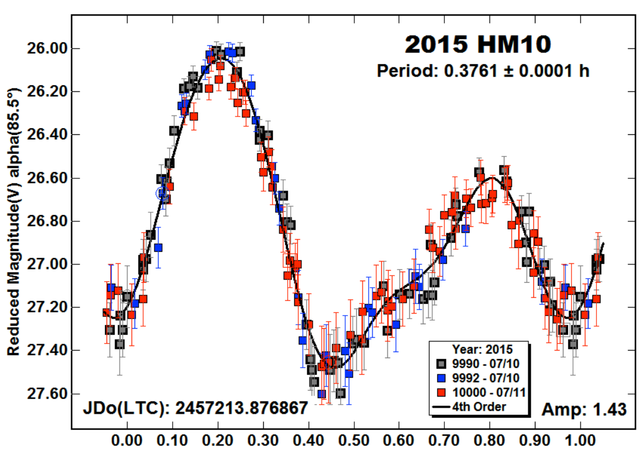

Figure 2. The lightcurve of 2015 HM10 based on data from CS3. Note the significant change in the shape from that in Figure 1 due to changing phase and viewing aspect.

Figure 2 shows the lightcurve derived from two nights of observations at CS3. Analysis found a period of 0.3761 ± 0.0001 h. The formal error was about 5x less (0.00002 h), but the span of the observations called for a less precise solution. The CS3 data had photon statistical errors on the order of 0.1 mag. Even though the CS3 scope was about 8x smaller in diameter, it had the advantages of the asteroid being about 2.3 magnitudes brighter, observations were at air masses X = 1.1-1.9, and the moon was almost new.

While the amplitudes of the two lightcurves were similar, ~1.47 ± 0.05 mag, the shape changed significantly over the 10-day interval between the two data sets. These differences will be helpful when modeling the asteroid's shape and spin in combination with radar data.

Acknowledgements

Funding for PDS observations, analysis and publication was provided by NASA grant NNX13AP56G. Funding for work at MRO was provided by the Arecibo/MRO cooperative agreement under NASA grant NNX13AQ46G. This research was made possible in part based on data from CMC15 Data Access Service at CAB (INTA-CSIC) and the AAVSO Photometric All-Sky Survey (APASS), funded by the Robert Martin Ayers Sciences Fund.

References

Harris, A.W., Young, J.W., Bowell, E., Martin, L.J., Millis, R.L., Poutanen, M., Scaltriti, F., Zappala, V., Schober, H.J., Debehogne, H., Zeigler, K.W. (1989). "Photoelectric Observations of Asteroids 3, 24, 60, 261, and 863." *Icarus* **77**, 171-186.

Jester, S., Schneider, D.P., Richards, G.T., Green, R.F., Schmidt, M., Hall, P.B., Strauss, M.A., Vanden Berk, D.E., Stoughton, C., Gunn, J.E., Brinkmann, J., Kent, S.M., Smith, J.A., Tucker, D.L., Yanny, B. (2005). "The Sloan Digital Sky Survey View of the Palomar-Green Bright Quasar Survey." *Astron. J.* **130**, 873-895.

Ryan, W.H., Ryan, E.V. (2015). "Target-of-Opportunity characterization of sub-200 meter Near-Earth Asteroids." *Proceedings of the 4th IAA Planetary Defense Conference*, in press.

Tody, D. (1993). "IRAF in the Nineties." in *Astronomical Data Analysis Software and Systems II*, A.S.P Conference Ser. **52**, eds. Hanisch, R.J., Brissenden, R.J.V., Barnes, J., p. 173 ff.

Warner, B.D. (2007). "Initial Results of a Dedicated H-G Program." *Minor Planet Bul.* **34**, 113-119.

Warner, B.D. (2015). *MPO Canopus* v10.7.0.

ASTEROID-DEEPSKY APPULSES IN 2016

Brian D. Warner
Center for Solar System Studies
446 Sycamore Ave.
Eaton, CO 80615
brian@MinorPlanetObserver.com

(Received: 2015 October 1)

The following list is a very small subset of the results of a search for asteroid-deepsky appulses for 2016, presenting only the highlights for the year based on close approaches of brighter asteroids to brighter DSOs. The complete set of predictions is available at

http://www.minorplanet.info/ObsGuides/Appulses/DSOAppulses.htm

For any event not covered, the Minor Planet Center's web site at *http://www.minorplanetcenter.net/cgi-bin/checkmp.cgi* allows you to enter the location of a suspected asteroid or supernova and check if there are any known targets in the area.

The table gives the following data:

Date/Time	Universal Date (MM DD) and Time of closest approach
#/Asteroid	The number and name of the asteroid
RA/Dec	The J2000 position of the asteroid
AM	The approximate visual magnitude of the asteroid
Sep/PA	The separation in arcseconds and the position angle from the DSO to the asteroid
DSO	The DSO name or catalog designation
DM	The approximate total magnitude of the DSO
DT	The type of DSO: OC = Open Cluster; GC = Globular Cluster; G = Galaxy
SE/ME	The elongation in degrees from the sun and moon respectively
MP	The phase of the moon: 0 = New, 1.0 = Full. Positive = waxing; Negative = waning

Date	UT	#	Name	RA	Dec	AM	Sep	PA	DSO	DM	DT	SE	ME	MP
01 03	09:31	386	Siegena	02:54.78	-10 03.3	11.8	178	116	NGC 1140	12.5	G	113	154	-0.39
01 03	23:05	6	Hebe	12:25.24	+04 59.9	10.8	238	348	NGC 4378	11.7	G	99	28	-0.34
01 05	05:30	140	Siwa	07:22.53	+22 06.6	12.9	157	10	NGC 2365	12.4	G	175	118	-0.23
01 09	22:53	171	Ophelia	09:05.39	+18 18.8	12.4	16	204	NGC 2749	11.8	G	155	154	0.00
01 09	**23:18**	**261**	**Prymno**	**10:46.71**	**+11 49.7**	**12.7**	**88**	**300**	**M96**	**9.3**	**G**	**130**	**129**	**0.00**
01 14	10:07	344	Desiderata	11:49.83	+26 29.4	13.2	222	276	NGC 3912	12.4	G	124	156	0.23
01 16	01:08	25	Phocaea	10:18.50	-17 55.9	12.8	203	334	NGC 3200	12.0	G	126	140	0.40
02 05	22:13	6	Hebe	12:33.88	+07 42.2	10.3	202	256	NGC 4526	9.7	G	131	96	-0.09
02 12	04:23	357	Ninina	10:47.73	+13 59.5	13.5	43	41	NGC 3377	10.4	G	164	147	0.17
02 14	08:56	148	Gallia	12:16.01	+13 57.1	12.5	301	65	NGC 4212	11.2	G	144	135	0.40
03 02	23:23	6	Hebe	12:22.60	+11 47.4	9.9	129	224	NGC 4313	11.6	G	158	83	-0.40
03 06	**00:03**	**27**	**Euterpe**	**06:08.90**	**+24 22.0**	**10.6**	**122**	**0**	**M35**	**5.1**	**OC**	**106**	**147**	**-0.12**
03 06	19:19	36	Atalante	08:00.86	+39 49.2	12.6	320	98	NGC 2493	12.0	G	125	149	-0.07
03 11	10:32	6	Hebe	12:16.12	+13 12.8	9.8	299	40	NGC 4216	10.0	G	165	152	0.08
03 14	01:32	753	Tiflis	13:48.20	+03 55.2	13.0	189	207	NGC 5300	11.4	G	147	141	0.32
03 14	22:17	270	Anahita	09:25.80	+11 22.1	12.6	251	201	NGC 2874	12.5	G	146	65	0.42
03 15	01:31	270	Anahita	09:25.71	+11 22.6	12.6	219	202	NGC 2872	11.9	G	145	63	0.43
04 01	07:39	6	Hebe	11:58.47	+16 07.8	9.9	222	209	NGC 4014	12.3	G	156	115	-0.43
04 01	18:50	346	Hermentaria	12:54.99	+08 00.0	11.5	260	201	NGC 4795	12.1	G	167	105	-0.38
04 03	20:27	89	Julia	13:49.31	-36 04.9	11.1	56	176	ESO 383-G087	10.5	G	147	106	-0.18
04 08	09:07	382	Dodona	13:20.45	-20 34.4	12.3	161	14	NGC 5087	11.4	G	167	164	0.01
04 09	16:57	346	Hermentaria	12:48.56	+08 33.0	11.6	189	17	NGC 4698	10.6	G	162	136	0.08
04 10	11:45	585	Bilkis	12:04.50	+01 55.0	13.1	2	44	NGC 4073	11.4	G	159	117	0.14
04 30	16:36	456	Abnoba	13:15.06	-16 35.4	12.1	65	56	NGC 5037	12.2	G	161	114	-0.44
05 01	09:50	346	Hermentaria	12:33.70	+09 13.2	12.0	129	0	NGC 4522	12.3	G	141	141	-0.36
05 12	23:32	804	Hispania	13:21.81	-27 26.5	12.3	35	21	NGC 5101	10.6	G	151	75	0.43
06 01	07:11	346	Hermentaria	12:27.04	+07 57.4	12.5	229	68	NGC 4416	12.4	G	112	163	-0.20
06 05	21:44	751	Faina	22:28.49	-24 56.2	13.2	326	196	NGC 7284	11.9	G	105	114	0.01
07 04	02:40	188	Menippe	18:52.99	-08 47.4	12.1	336	196	NGC 6712	8.2	GC	166	169	0.00
07 04	08:37	462	Eriphyla	18:55.03	-22 36.3	12.7	349	350	Pal 9	9.2	GC	180	176	0.00
07 04	12:24	615	Roswitha	17:59.90	-28 12.2	13.3	70	181	Tr 31	9.8	OC	166	164	0.00
07 06	11:11	625	Xenia	18:17.73	-12 37.8	12.5	58	148	Tr 32	12.2	OC	165	143	0.05
07 10	14:32	224	Oceana	17:32.39	-32 31.7	12.2	269	15	NGC 6374	9.0	OC	154	81	0.37
08 02	17:16	787	Moskva	23:20.83	+08 12.3	13.1	122	110	NGC 7626	11.1	G	135	134	0.00
08 03	02:11	462	Eriphyla	18:31.95	-23 33.1	13.5	249	171	NGC 6642	8.8	GC	146	143	0.00
08 08	10:03	625	Xenia	17:59.60	-17 24.0	13.1	5	90	NGC 6507	9.6	OC	134	69	0.29
09 01	12:59	631	Philippina	00:21.49	+22 22.2	13.4	181	156	NGC 83	12.5	G	141	143	0.00
09 01	21:42	141	Lumen	18:03.71	-30 03.3	12.9	116	131	NGC 6522	8.6	GC	111	105	0.00
09 02	01:26	631	Philippina	00:21.21	+22 20.6	13.4	24	158	NGC 80	12.1	G	142	148	0.01
09 02	**16:37**	**454**	**Mathesis**	**21:40.45**	**-23 15.6**	**13.2**	**281**	**172**	**M30**	**7.5**	**GC**	**158**	**143**	**0.02**
09 26	18:08	117	Lomia	00:22.21	+10 25.5	12.0	207	177	NGC 95	12.5	G	171	126	-0.17
11 01	16:27	65	Cybele	01:37.18	+05 57.4	12.0	284	339	NGC 632	12.3	G	165	144	0.04
11 06	00:40	326	Tamara	21:49.74	-34 52.5	13.5	51	304	NGC 7135	11.7	G	94	34	0.32
11 28	03:32	218	Bianca	04:36.65	+00 05.6	12.9	212	347	NGC 1620	12.3	G	158	157	-0.02
12 01	15:53	163	Erigone	00:42.69	-01 31.8	13.3	17	325	NGC 227	12.1	G	119	96	0.04
12 22	11:25	375	Ursula	08:13.01	+36 19.3	12.6	326	14	NGC 2543	11.9	G	149	79	-0.36
12 23	18:21	57	Mnemosyne	01:24.56	+01 48.6	12.1	280	353	NGC 521	11.7	G	108	168	-0.25
12 24	08:51	679	Pax	09:32.16	+21 28.8	13.1	32	251	NGC 2903	9.0	G	134	80	-0.20

UNUSUAL PROPERTIES FOR THE NEA (436724) 2011 UW158

Bruce L. Gary
5320 E. Calle Manzana
Hereford, AZ 85615
BLGary@umich.edu

(Received: 2 October Revised: 21 November)

Near-Earth Asteroid 2011 UW158 was observed for 3.5 months with the Hereford Arizona Observatory 0.35-m telescope during the 2015 apparition. A phase curve slope of 0.023 ± 0.001 mag/deg was determined from r'-mag measurements for a phase angle range of 17 to 90 deg. This slope is used to estimate albedo = 0.39 ± 0.09, H = 19.93 ± 0.11, and diameter D = 220 ± 40 m. The UW158 rotation period = 0.61072 h, which is greater than the "spin barrier" of the "rotation frequency vs. diameter" diagram, thus requiring internal cohesion.

Introduction

Near-Earth Asteroid (436724) 2011 UW158 has been referred to as the "platinum asteroid" because of widespread news coverage purporting that it was worth $5.4 trillion for the platinum that it contained. Aside from this humorous story about its monetary value, UW158 turns out to have substantial scientific value because of its fast rotation in relation to its size.

The first observation of UW158, on 2015 Jun 17, was motivated by a listing of it as a target for JPL and Arecibo radar observations during its close approach in July. It was described as a candidate for a future human mission, based on a favorable orbit, and the radar web sites included a request for photometric observations prior to the scheduled radar observations. The specific need was for a rotation period for radar bandwidth planning purposes. The June 17 lightcurve showed that the rotation period was ~ ½ h. This was surprising since the H-G phase curve model used H = 19.5, based on 2011 discovery observations, and an asteroid this bright is usually larger than ~ 250 m. But it's extremely rare for asteroids this large to rotate with a period < 2.2 hours. The two known exceptions are thought to be bodies having significant internal cohesion since a non-cohesive rubble pile of their size would "fly apart." Smaller cohesion-less rubble pile asteroids can rotate faster without flying apart, but not larger ones.

The second observation, on Jun 20, confirmed the short rotation period (36.665 min). One key question became "Is the effective diameter really > 250 m?" To answer this question photometrically it would be necessary to verify that H wasn't significantly fainter than 19.5 (*e.g.*, H > 20.5), or that albedo wasn't much greater than assumed (*e.g.*, >0.50), or some combination of these two assumptions. This goal was the motivation for creating a phase curve that could be used to evaluate both parameters.

The phase curve model of Belskaya and Shevchenko (2000), hereafter B&S, has been shown to be capable of doing this for large asteroids (D > 10 km) observed for phase angles (α) less than ~24 deg. Main-belt asteroids don't have phase curve information beyond α ~ 24 deg due to their orbit size, so it's possible that the B&S relationship applies beyond this α limit. Indeed, the moon's phase curve is linear (consistent with B&S) out to 45 deg (Gary, 2015d) and probably also out to 60 deg (Hapke, 2015). If B&S is valid for these larger α, then it could be used for near-Earth asteroids (NEAs), who's viewing geometry is often limited to α > 24 deg. With regard to asteroid size, there is no information showing that the B&S relationships <u>can't</u> be used for smaller asteroids, but there is also no confirmation that it can be. If both supposed limitations of the B&S model could be overcome by showing that a small asteroid, observed at large α, conform to the B&S model, then it would become an important new tool for the photometric study of NEAs. Since radar observations of UW158 were planned, it was decided that this would be a good opportunity for evaluating the range of situations for which B&S can be used. In addition, UW158 showed promise as an asteroid that could be scientifically important because of its location in the "spin frequency/size" diagram.

Observations

A Meade 0.35-m fork-mounted Schmidt-Cassegrain telescope was used with a SBIG ST-10 XME CCD camera, binned 2x2. Hereford Arizona Observatory (MPC code G95) is located at 1420 m altitude in Hereford, AZ. Control of the telescope, dome, focuser, camera and offset autoguider was accomplished using *MaxIm DL* and 100-foot cabling in buried conduit. Image analysis was also performed using *MaxIm DL*. For each field-of-view, a median combine of all good-quality images was subtracted from individual images; these star-subtracted images were photometrically measured using an artificial star for reference. The images without star-subtraction were then photometrically measured, using the same artificial star for reference, but also including about two dozen stars designated as check stars. Both photometric CSV-files were imported into a spreadsheet; the star-subtracted mags for the moving asteroid were used with the non-star subtracted mags for the check stars, which served as candidate reference stars within the spreadsheet. This star-subtracting procedure has the advantage of greatly reducing the effect of background stars in the resulting lightcurve. Details of the observing, image analysis and spreadsheet procedures are given in Gary (2014, 2015a).

Unfiltered observations were calibrated using r'-mag's of APASS stars (in the UCAC4 catalog). CCD transformation corrections were accomplished using a plot of reference star instrumental magnitude minus true (APASS) magnitude versus star color (g'-r'). This assured that each lightcurve segment was calibrated with an accuracy estimated to be < 0.010 mag. On one date, g'r'i'z' filters were used to estimate the asteroid's colors. On two dates, observations were made with g'r'i' bands for the same purpose. On three dates, a SA-100 transmission grating was used to obtain spectra with ~ 50:1 resolution between 420 and 820 nm.

Sample Lightcurves

Figure 1 is a sample lightcurve showing a typical pair of different maxima per rotation.

Figure 2 is a phase-folded (rotation) lightcurve for the same data compared with data from four weeks earlier.

Notice in Fig. 2 that at rotation phase ~ 0.50 the r'-mag's agree; the shape and brightness changes are limited to the other rotation phases. This is due to the maximum brightness during a rotation corresponding to one of the two broadside views (maximum solid angle), the lesser maximum corresponding to the opposite broadside view, while the minima are views closer to end-on. This illustrates the importance of choosing a rotation phase with maximum brightness for creating a phase curve.

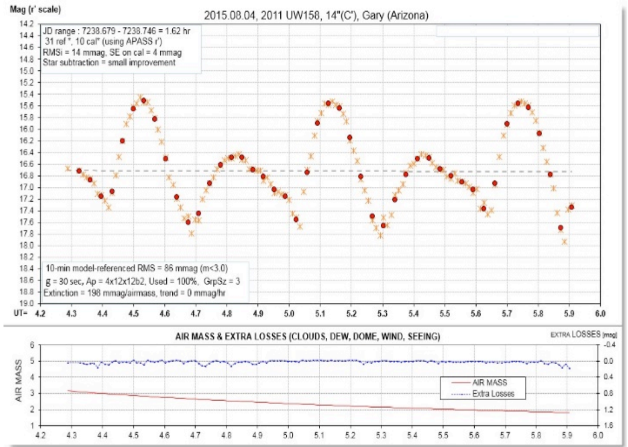

Figure 1. Lightcurve for Aug 4 (upper panel) showing 2.6 rotations. The lower panel shows air mass and un-modeled atmospheric losses due to clouds, dew, seeing, wind, etc.

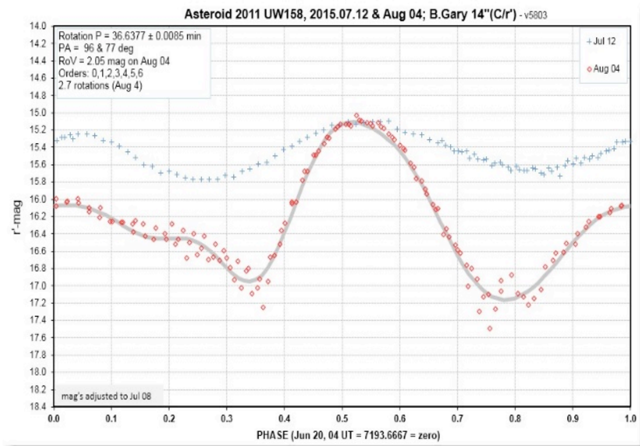

Figure 2. Phase-folded lightcurve for two dates showing change in amplitude and shape. The r'-mags have been adjusted to a standard date (Jul 8) using an H-G model with *G* = 0.15 to help in detecting which parts of the rotation have undergone change.

The entire set of rotation lightcurves show maxima at the same two rotation phases, as well as minima at similar rotation phases, and this shows that UW158 is not a tumbler.

Amplitude of Variation

It is evident in Fig. 2 that the rotation lightcurve amplitude *(A),* defined as peak-to-peak, varies greatly with date and that *A* can be large (2.05 mag). Figure 3 is a plot of *A* vs. date, with a smooth (high-order polynomial) fit.

The asteroid's closest approach to Earth occurred on Jul 20, when it was 6.4 times the moon's average distance. At this time it was moving fast along the 180 deg arc that is close to a great circle on the celestial sphere.

Whenever an asteroid moves through a 180 deg arc, there should be one location when it is viewed with an inclination (angle between line-of-sight and rotational axis) of 90 deg., *i.e.,* viewed within the asteroid's rotational equatorial plane. This will occur when *A* is maximum, provided shadowing is not important. *A* was maximum on Aug 4 (lightcurve shown in Fig. 2). It is likely that after Aug 4, with *A* decreasing monotonically, our view was of the asteroid's other hemisphere.

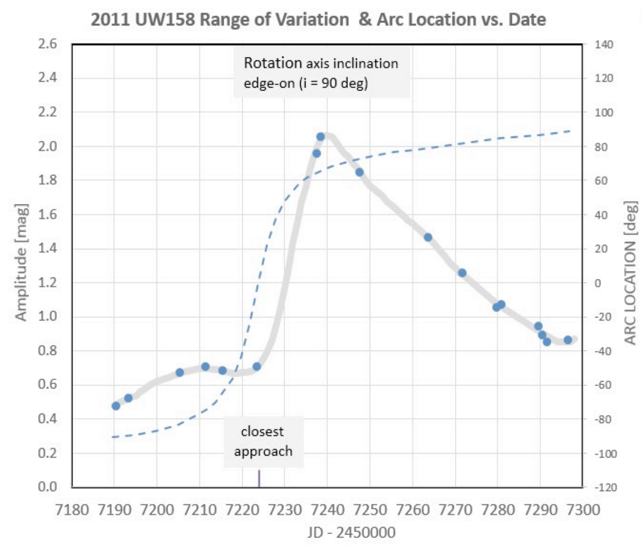

Figure 3. Rotation lightcurve amplitude (symbols) with a smooth fit, and location along the arc on the celestial sphere traversed during this 110-day interval (dashed trace).

Note that the Aug 4 value for *A* = 2.05 mag corresponds to a brightness ratio of 6.6:1. In other words, as the asteroid rotated (when our view was within the asteroid's equatorial plane), the solid angle could have varied by as much as 6.6 to 1. The association of brightness with solid angle assumes two things: 1) albedo is uniform across the surface, and 2) shadowing effects are small. Shadowing becomes important at large α, and α was 77 deg on Aug 4. If shadowing wasn't important on this date, then UW158 would be ~6.6 times longer than it is wide. But if shadowing was important for the end-on view (minimum brightness, rotation phases 0.34 and 0.78 in Fig. 2), then the ratio of dimensions would be smaller than 6.6:1.

Orientation of Rotational Axis

It is reasonable to begin with the assumption that UW158 resembles an ellipsoid, shown in Fig. 4, having radii a, b and c, where c/b = 6.6 (2.05 mag). An additional first assumption will be that dimensions "a" and "b" are the same.

A pole-on view will project the maximum solid angle for all rotation phases, given by π × b × c / d, where d = distance from Earth. An equatorial view will project a solid angle that ranges from π × a × b / d to π × a × c / d. If a = b, we can convert rotation brightness ratio to inclination. The actual equation is quite complicated, so let's use a tube-model approximation for the ratio of maximum-to-minimum solid angle (brightness) as a function of inclination *(i)*:

$$R(i) = x / (\sin i + x (\cos i)) \quad (1)$$

$$\text{where } x = c/b = c/a \ (i.e.,\ a = b) \quad (2)$$

For UW158, we know that *i* = 90 deg on about Aug 4, when R(*i*) = 6.6 (assuming uniform surface albedo and no shadowing effects). For example, the Jul 20 observation with *A* = 0.70, would then correspond to *i* = 67 deg. When each observation is converted to an *i* value, it is possible to draw arcs on the celestial sphere and their intersection will be one of the rotational axis pole positions. We don't yet know whether rotation is prograde or retrograde, so there will be two RA/DE pole locations. One pole position, according to this analysis, is at RA/DE = 17:30/+10. The shortcoming of this

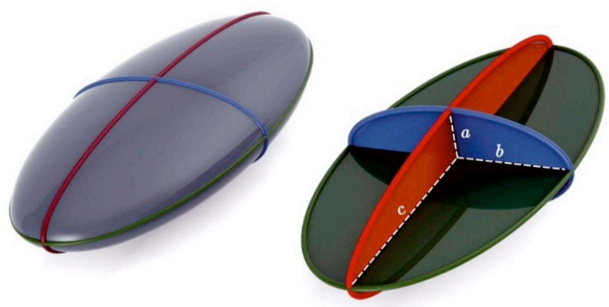

Figure 4. Ellipsoid with radii a, b, and c viewed with inclination ~45 deg (assuming rotational axis is parallel to "a").

method for deriving a rotational axis orientation is its shadowing assumptions. A better approach is to employ a shape-adjusting program designed specifically for fitting lightcurves made at specific viewing geometries; such an analysis is beyond the scope of this observational work.

Phase Curve: Albedo and Size

Creating a phase curve is most safely done for spherical asteroids, since their brightness won't be affected by changes in solid angle as α varies. If UW158 had a circular cross-section orthogonal to the long axis (*i.e.*, a = b in Fig. 4), then during each rotation there would be two equal brightness maxima corresponding to the same solid angle broadside view. The rotation lightcurve in Fig. 2 shows unequal maxima for Aug 4, thus revealing that the shape of UW158 is not the simple ellipsoid preferred for phase curve interpretation. The following phase curve analysis will be subject to this limitation.

UW158 was discovered on 2011 Oct 25 and must have been observed on several dates for determining an orbit. Apparently there were no lightcurve observations, so we don't have *A* information or a rotation-maximum V-mag. If we assume that these astrometric observations were made at random rotation phases, we can use the adopted H-G model to estimate rotation-average V-mag for the α range of those observations (~14-21 deg). V-mag can be converted to r'-mag by subtracting 0.23 ± 0.08 (Gary, 2105e), based on the asteroid's color as described below. It is assumed that rotation-maximum was between 0.1 and 0.6 mag brighter than rotation-average during the 2011 discovery observations.

Fig. 5 is a phase curve plot. The 2011 discovery r'-mags are plotted at their α range, with a rhombus-shaped symbol representing an estimate for rotation-maximum r'-mag. The 17 measurements for 2015 were made using the same observatory and the same analysis and calibration procedures, so they should share the same systematic calibration errors. The H-G model meant to represent rotation-maximum r'-mag (dashed trace) does not adequately fit all of the measurements. For α > 80 deg, the measured r'-mag is brighter while for α < 50 deg, the r'-mag is fainter. A greater *G* value would fit the data slightly better. However, there is greater interest in fitting the observations with a phase curve model that can be used to estimate geometric albedo and size.

B&S analyzed 33 well-studied main belt asteroids using a 3-term phase effect model first introduced by Shevchenko (1996, 1997):

$$V(\alpha) = Vo + b\times\alpha - a/(1+\alpha) \quad (3)$$

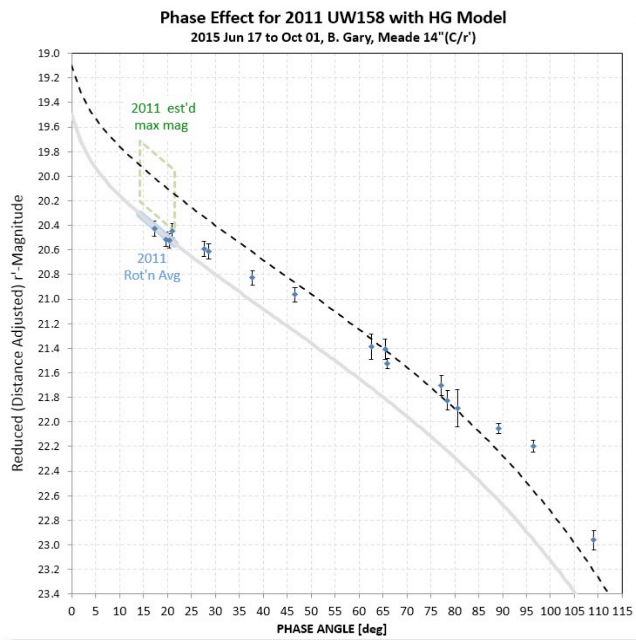

Figure 5. Rotation maximum r' magnitudes, adjusted to standard distance for 17 dates in 2015, with two H-G model fits: 1) *H* = 19.5, *G* = 0.15, and 2) *H* = 19.1, *G* = 0.15. The models are meant to fit rotation-average and rotation-maximum brightness, respectively. The symbols at α = 14–21 deg are estimated r'-mag for the 2011 discovery observations.

where V(α) is V-mag at phase angle α, Vo is V-mag at zero phase, "b" is phase coefficient (a slope term) fitted to V(α) measurements and "a" is an "opposition effect" (OE) amplitude term. B&S found that there was a strong correlation between the phase coefficient "b" and albedo, and also an inverted U-shape relationship between the OE amplitude term "a" and albedo. Their equation relating phase coefficient "b" and V-mag albedo at α = 0, ρ_v, is:

$$b = 0.013(2) - 0.024(2) * \log(p_v) \quad (4)$$

where "b" has units of mag/deg and p_v is fractional geometric albedo. Hereafter, I will use the term "albedo" to be the same as p_v.

In Fig. 6, the observation date notations show that the first observation (Jun 17) was at α = 62 deg, with α increasing to 109 deg (Jul 20), and then decreasing to 17 deg (Oct 01). It is noteworthy that on the occasions when measurements were made at the same α, but a month or more apart, there is r'-mag agreement.

The B&S model has a straight line slope parameter b = 0.0228 ± 0.0008 mag/deg. Substituting this b value in the above equation (4) yields geometric albedo p_v = 0.39 ± 0.09.

Since information for α close to zero is not present the size of OE isn't measured. We shall use the B&S relation between OE and albedo. For an albedo of 0.39, they find that the OE term a = 0.29 ± 0.02 mag. The solid trace in Fig. 6 includes the OE component.

Comparing Figures 5 and 6, the B&S model fits the measurements much better, with a good fit out to α = 96 deg. The measurement at α = 109 deg can be discounted as being affected by shadowing.

The B&S model fit has r' = 19.70 ± 0.05 at α = 0. Converting to V-mag yields 19.93 ± 0.11, which corresponds to *H*. Asteroid size can now be calculated using the standard equation:

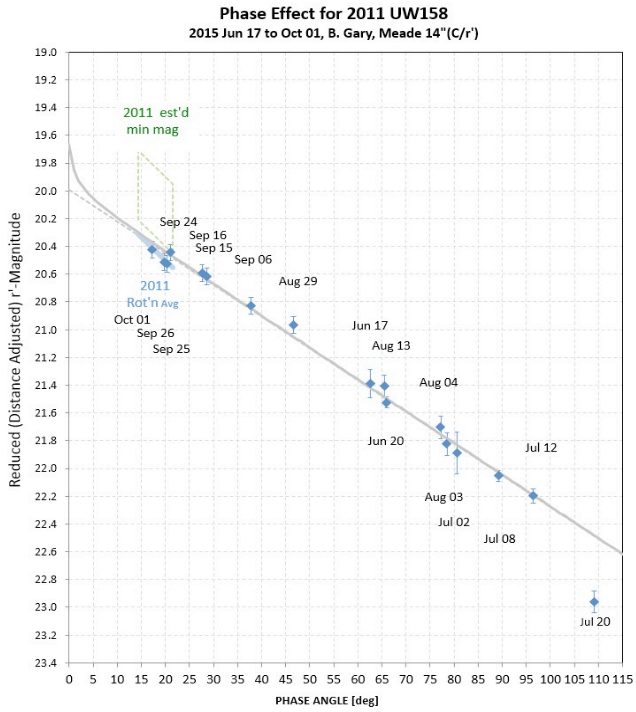

Figure 6. Same as Fig. 5, but with the B&S model fit. Observing date annotations are included.

D [km] = (1329 / sqrt(albedo)) × 10^(-0.2×H) (3)

where albedo is a fraction. Setting H = 19.93 ± 0.11, and albedo = 0.39 ± 0.09, yields diameter = 220 ± 40 m. This is an equivalent diameter, corresponding to a circle with the same solid angle as that presented by a broadside view.

Whereas the B&S relationships were established for large asteroids with and α < 24 deg, it is encouraging that the Fig. 6 phase curve for a smaller asteroid that was observed for α > 17 deg exhibits such a good-quality fit using the B&S straight-line model. If a departure from a straight line model exists, it should manifest itself as a growing departure from linearity as α increases; there is no hint of this in the observations. Thus, one goal for the observations has been met: it is a "suggestive conclusion" of this work that the B&S phase curve model can be used for α >> 24 deg.

Claiming that the B&S relationships are valid for asteroids smaller than ~ 10 km is equivalent to claiming that the regolith covering of asteroids is similar for smaller asteroids. One approach for assessing the reasonableness of this hypothesis is to compare the size for UW158 obtained from radar observations with the size obtained photometrically using the B&S model.

Radar Size

JPL and the Arecibo Observatory observed UW158 using radar in mid-July, during closest approach. Fig. 7 is a frame from an Arecibo Observatory animation (P.A. Taylor, pers. comm.).

Arecibo Observatory radar images reveal an elongated shape that I estimate to be equivalent to an ellipsoid with 200 x 600 m outer dimensions (Fig. 7). The rectangular equivalent dimensions appear to be 160 x 500 m. We should keep in mind that one of the radar dimensions (160 m) is "depth," not a lateral dimension, so it is not directly related to solid angle. If we adopt 160 m for the missing (lateral) dimension, then we can calculate a size for deriving solid

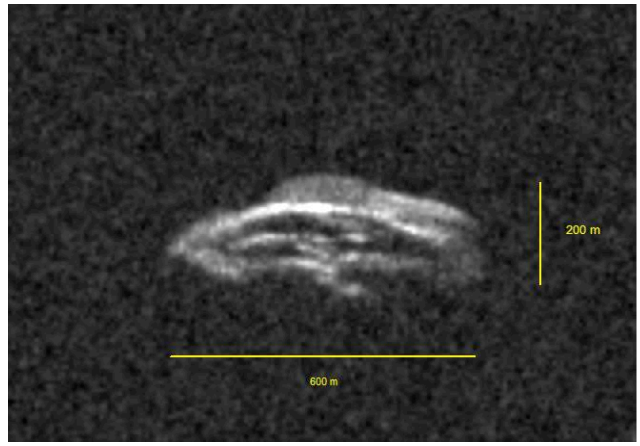

Figure 7. Arecibo Observatory radar image (one of a series of images from an animation showing rotation).

angle. The dimensions 160 x 500 m are equivalent to a circle with diameter 320 ± 50 m (where an arbitrary SE = 40 m per dimension is adopted). This equivalent diameter differs from the "photometric" diameter of 220 ± 40 m by an amount of 100 ± 65 m, which is not statistically significant. This can be viewed as supporting the argument that the B&S relationships can be used for small asteroids (and also determined by measurements at large α). This is a second "suggestive conclusion" of this work.

Rubble Pile vs. Solid Rock

Fig. 8 is in common use for characterizing the physical state of asteroids, based on their rotation spin-rate and size (estimated from H and albedo). Region A is where asteroids are small enough that inter-grain forces plus gravity are sufficient to hold the asteroid together for a wide range of spin frequencies. In other words, rubble piles as well as rocks may exist in Region A. Region B is where asteroids are rotating slowly enough (P > 2.2 h) that gravity is sufficient to hold rubble pile asteroids together; rock asteroids are also permitted. In Region C non-cohesive rubble piles are "forbidden" because they should fly apart (assuming plausible densities). In other words, only bodies where the constituents have significant cohesion, or are comprised of unfractured solid rock, should exist in Region C. The oft-cited 250 m size boundary was initially inspired by the pattern of avoidance in Region C, which was completely unpopulated until the discovery of 2001 OE84 by Pravec *et al.* (2002). Given that asteroid sizes are usually determined using estimated (or assumed) albedo, the locations of data points in this diagram should be viewed as horizontally oblong, causing the 250 m boundary to be better thought of as merely a most probable value within a range of sizes (as indicated using a shaded band in Fig. 8).

The radar dimensions (160 x 500 m, broadside view) are equivalent to a circular diameter of ~320 m (for broadside view), and a spherical equivalent volume with a diameter of ~290 m. According to the photometric solution, based on a phase curve with a B&S interpretation, all of the radar dimensions should be multiplied by ~ 0.70 ± 0.15. Because of UW158's elongated shape, the surface is located at distances from the rotation axis that can be as small as 100 m and as large as 600 m (represented by the rectangle in Fig. 8). The UW158 surface therefore straddles the 250 m "size barrier." This means that we should consider the possibility that the ends of UW158 are experiencing a centrifugal force sufficient for loose regolith particles to "fly off," leaving the ends bare rock, while the rest of the surface has the physical plausibility to retain regolith.

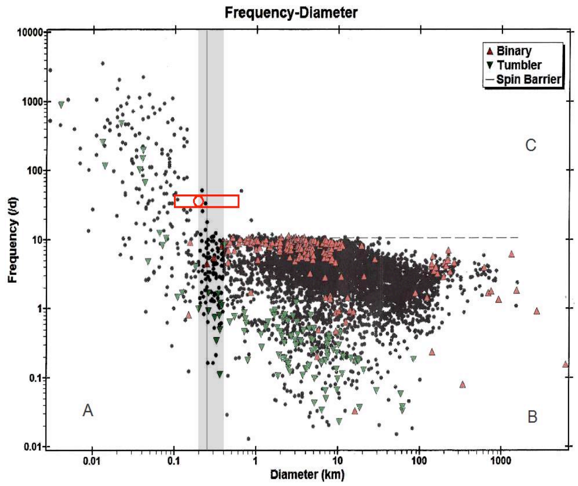

Figure 8. Plot of asteroid spin rate vs. diameter (based on Warner et al., 2009). The horizontal dashed line is the “spin barrier” and the vertical band defines a size boundary separating rubble piles permitted (to left) and cohesive or solid rock interiors only (to right) for spin rates above the spin barrier. A spherical version of UW158 is shown as a circle, within a rectangle representing a range of diameters corresponding to the smallest to the largest dimension for UW158.

Visible Spectrum

UW158 was observed with g’r’i’z’ filters on Jul 2. The goal was to search for evidence of an I-band absorption feature at 0.92 microns. Details of these observations can be found at Gary (2015b). Fig. 9 shows the magnitudes at these four bands converted to flux, allowing for comparison with the sun’s flux spectrum. The asteroid’s spectral energy distribution (SED) is similar to the Sun’s except for a possible I-band absorption feature at 0.92 microns (due to olivine and pyroxene). The presence of such an absorption feature is not statistically significant but merely suggestive.

On Aug 13, g’r’i’ observations were also conducted. The average slope of “relative reflectivity” across this range of wavelengths was close to zero. This slope is uncertain due to the confounding effect of exposures with each filter not occurring simultaneously in the presence of fast changes of brightness.

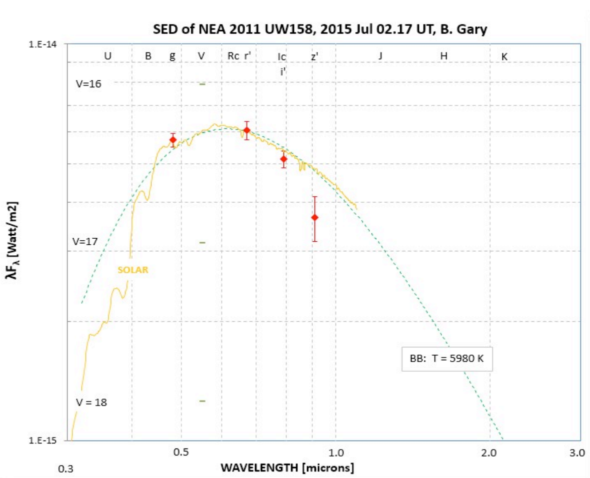

Figure 9. Jul 2 g’r’i’z’ magnitudes, converted to fluxes vs. wavelength (SED, spectral energy distribution), showing possible evidence for an I-band absorption feature at 0.92 microns.

On Jul 9 and 11, a SA-100 transmission grating was used to measure the UW158 visible spectrum with a spectral resolution of ~50. On each date, three solar-like stars were used for reference. The observing sequence, image processing and spreadsheet analysis are described in more detail at Gary (2015b,c). This spectrum is more uninfluenced by brightness variations due to rotation, since all wavelengths are measured simultaneously, so it should take preference over the spectrum based on g’r’i’ observations. The SA-100 spectrum shows a slightly red color, with B-V = +0.77 ± 0.10. Using this color allows the following conversion: V = r’ + 0.23 ± 0.08 (Gary, 2015e).

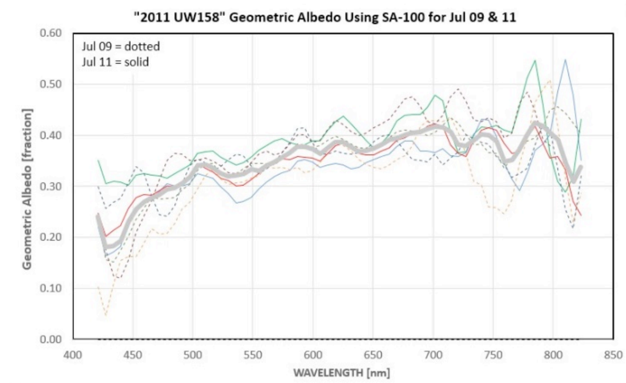

Figure 10. Transmission grating spectra of UW158 on two dates: Jul 9 and 11. The measurements are plotted as geometric albedo on the assumption of diameter being 220 meters.

A consensus albedo spectrum from the transmission grating observations on two dates is shown in Fig. 10, where geometric albedo is plotted for a 220 m diameter. Note that the geometric albedo at r’-band (~ 620 nm) is ~0.38 ± 0.03, in agreement with the phase curve analysis of 0.39 ± 0.09. The I-band absorption feature at 920 nm cannot be seen because sensitivity limited spectral coverage to < 820 nm.

Discussion and Conclusion

The 2011 UW158 phase curve, observed with a single telescope and reduction procedure, has been interpreted using the Belskaya and Shevchenko (2000) relationships to derive a geometric albedo of 0.39 ± 0.09 and an effective diameter of 220 ± 40 meters (for the rotation maximum brightness view). This albedo is confirmed using SA-100 transmission grating observations, calibrated using solar-like stars. The broadside dimensions are consistent with radar observations.

Since UW158 rotates with a period of 0.61072 h, it is “located” in a diagram of “spin rate vs. diameter” where rubble piles are permitted. This location in the spin/diameter diagram assumes a spherical diameter with volume equivalent to the estimated dimensions. However, UW158 is highly elongated, with a diameter ratio of at least 3.5 (based on both radar and photometry), so the ends of the asteroid are located far enough from the spin axis that they are in a spin/diameter region where non-cohesive rubble piles are “forbidden.” Thus, while regolith particles may plausibly exist around the asteroid mid-section, the asteroid ends could be bare rock. Indeed, aside from a partial regolith coverage, UW158 must have a cohesive interior or be comprised by a solid rock; otherwise, the ends would fly away due to centrifugal force exceeding the gravitational one.

Future apparitions of UW158 won’t be as favorable as this one for another 93 years. Nevertheless, because of its uniqueness, even the less favorable apparitions at intervals of 2.056 years (*e.g.,* 2017 Sep with V ~ 20.7) will provide opportunities for additional observations with large telescope apertures for elucidating the nature of fast-spinning, rocky asteroids.

Acknowledgements

Asteroid ephemeris information was provided by Caltech's Jet Propulsion Laboratory web site: *http://ssd.jpl.nasa.gov/horizons*. Calibration with SDSS magnitudes in the UCAC4 catalog was made possible through the use of the AAVSO Photometric All-Sky Survey (APASS), funded by the Robert Martin Ayers Sciences Fund. I want to record my appreciation to Dr. Arne Henden for initiating the APASS project; this is a sentiment I feel every morning after a night's observations as I select APASS stars for calibration. Radar images were kindly provided by the Arecibo Observatory, which is operated by SRI International under a cooperative agreement with the National Science Foundation (AST-1100968), and in alliance with Ana G. Méndez-Universidad Metropolitana, and the Universities Space Research Association. The Arecibo planetary radar program is supported by the National Aeronautics and Space Administration under Grant Nos. NNX12AF24G and NNX13AQ46G issued through the Near-Earth Object Observations program. The "spin frequency/diameter" diagram (Fig. 8) is a modification of a graph at the IAU Minor Planet Center web site, which is based on data from the asteroid lightcurve database (Warner *et al.*, 2009).

References

Belskaya, I.N., Shevchenko, V.B. (2000). "Opposition Effect of Asteroids." *Icarus*, **147**, 94-105.

Gary, B.L. (2014). *Exoplanet Observing for Amateurs*, Hereford, AZ: Reductionist Publications.

Gary, B.L. (2015a). *http://brucegary.net/asteroids/*

Gary, B.L. (2015b). *http://www.brucegary.net/UW158/*

Gary, B.L. (2015c). *http://brucegary.net/SA/*

Gary, B.L. (2015d). *http://www.brucegary.net/UW158/#Moon*

Gary, B.L. (2015e). *http://www.brucegary.net/mags/#Examples*

Hapke, B., Denevi. B., Sato, H., Braden, S., Robson, M. (2015). *http://onlinelibrary.wiley.com/doi/10.1029/2011JE003916/full*

Pravec, P., Kusnirak, P., Sarounova, L., Harris, A.W., Binzel, R. P., Rivkin, A.S. (2002). "Large Coherent Asteroid 2001 OE84", *Proc. Asteroids, Comets, Meteors (ACM 2002)*, Jul 29 – Aug 02, Tech. Univ. Berlin, Berlin, Germany (ESA SP-500).

Shevchenko, V.G, (1996). "Analysis of the Asteroid Phase Dependencies of Brightness." *Lunar Planet Sci.* **27**, 1193.

Shevchenko, V.G. (1997). "Analysis of Asteroid Brightness-Phase Relations." *Solar System Res.* **31**, 219-234.

Warner, B.D., Harris, A.W., Pravec, P. (2009). "The Asteroid Lightcurve Database." *Icarus* **202**, 134-146. Updated 2015 Sept. *http://www.minorplanet.info/lightcurvedatabase.html*

POLE AND SHAPE FOR THE NEA (436724) 2011 UW158

Albino Carbognani
Astronomical Observatory
of the Aosta Valley Autonomous Region (OAVdA)
Lignan 39, 11020 Nus (Aosta), ITALY
albino.carbognani@gmail.com

Bruce L. Gary
Hereford Arizona Observatory
Hereford, Arizona, USA

Julian Oey
Blue Mountains Observatory
Leura, AUSTRALIA

Giorgio Baj
Astronomical Station of Monteviasco
Varese, ITALY

Paolo Bacci
Astronomical Observatory of San Marcello Pistoiese
Pistoia, ITALY

(Received: 2015 Oct 7)

The near-Earth asteroid (436724) 2011 UW158 was followed by an international team of observers on 31 nights between 2015 Jun 17 and Sep 26. By using the standard lightcurve inversion method with the combined photometry data set, we obtained a unique spin axis solution with ecliptic coordinates $\lambda = 290° \pm 3°$, $\beta = -39° \pm 2°$, a sidereal period $P_S = 0.610752 \pm 0.000001$ h, and a shape model qualitatively consistent with radar observations.

Asteroids of size $D \geq 0.15$ km generally do not have periods $P \leq 2.2$ h, a limit known as the *cohesionless spin-barrier*. This barrier can be explained by the rubble-pile structure model. According to this model, the asteroids are made up of collisional breakup fragments bound together only by mutual gravitational force (Pravec and Harris 2000). The exceptions to this "rule," called large super-fast rotators (LSFR), are very few; 2001 OE84, (335433) 2005 UW163, and 2011 XA3 are the best known examples. The presence of these objects was theorized for the first time by Holsapple (2007). His analysis shows that the cohesion necessary to bind together a rubble-pile asteroid under the spin-barrier value is low, but he does not specifically propose a theory for how cohesion could arise. These results have been confirmed and enriched by subsequent theoretical studies, such as by Sànchez and Scheeres (2014), in which a model for the origin of the cohesion forces within a regolith has been proposed. The presence of cohesion forces begins to be important only for objects with diameter $D < 10$ km. So, for small bodies (0.15 km $< D < 10$ km) with rubble-pile structure, the presence of even a very small amount of strength allows much more rapid spin than the simple cohesionless spin-barrier value.

The asteroid 2011 UW158 is a near-Earth asteroid and potentially hazardous object. It was discovered on 2011 Oct 25 by the Pan-STARRS observatory at Haleakala (Hawaii, USA). A flyby with the Earth occurred on 2015 Jul 19 at a distance of 0.0164 AU, so this object also became a radar target for Goldstone and Arecibo. This asteroid, with a synodic period of about 37 minutes and an absolute magnitude of about 19.5 (*D* = 240-740 m) is an example of LSFR. This short period was first found by Bruce Gary on 2015 Jun 17 (see his paper elsewhere in this issue) and independently by Julian Oey on Jul 1. Table I shows the instruments used while Table II lists the observing sessions that produced lightcurves used for this analysis. The photometric coverage was dense because our purpose was to determine the pole of rotation and convex shape using the standard lightcurve (LC) inversion method (Kaasalainen *et al*. 2001; Kaasalainen and Torppa, 2001).

In most cases, it is not possible to get a reasonable solution for a pole using LC inversion with photometric observations from one apparition. It may be possible to get an initial solution if, as in the case of ours observations, the total span covers several rotations and a large range of phase angles, the synodic period is well-established, and the photometric data are of good quality. It is also helpful if the viewing aspect, as measured by the phase angle bisector, goes through a relatively large range as well. In our case the range of observed phase angle is 62° to 109° and 109° to 20°; the amplitudes of angle bisector are ΔL_{PAB} = 137° and ΔB_{PAB} = 64° (Fig. 1).

Observer	Telescope	CCD camera
Bacci	Ref. 0.60-m f/4	Apogee Alta 1024
Baj	RC 0.25-m f/8	SBIG-ST10
Carbognani	RC 0.81-m f/7.9	FLI 1001E
Gary	SC 0.35-m f/10	SBIG-ST10XME
Oey	CDK 0.61-m f/6.8	Apogee U42

Table 1. Observers, telescopes and CCD camera used.

Obs.	yyyy/mm/dd	Phase (°)	LPAB (°)	BPAB (°)	A (mag)
Gary	2015/06/17	62.3	230.7	-12.9	0.50
Gary	2015/06/20	65.7	231.9	-12.5	0.52
Oey	2015/07/01	79.0	236.4	-9.3	0.67
Oey	2015/07/02	80.3	236.8	-9.3	0.67
Oey	2015/07/03	81.6	237.1	-8.8	0.73
Oey	2015/07/06	85.8	238.1	-6.7	0.76
Oey	2015/07/08	88.9	238.6	-4.7	0.71
Gary	2015/07/08	88.9	238.6	-4.7	0.70
Gary	2015/07/12	96.0	239.4	2.3	0.70
Gary	2015/07/20	109.3	269.9	50.6	0.92
Baj	2015/07/23	101.9	314.6	50.5	1.92
Bacci	2015/08/01	82.0	341.4	30.0	2.38
Carb.	2015/08/02	80.4	342.4	29.0	1.96
Gary	2015/08/03	78.9	343.3	28.1	1.95
Gary	2015/08/04	77.5	344.1	27.3	2.05
Carb.	2015/08/11	68.3	348.9	23.4	1.96
Gary	2015/08/13	65.8	350.1	22.6	1.84
Bacci	2015/08/14	64.6	350.7	22.3	1.82
Carb.	2015/08/19	58.6	353.4	20.8	1.62
Bacci	2015/08/20	57.4	353.9	20.5	1.65
Gary	2015/08/29	47.0	357.9	18.6	1.46
Baj	2015/09/05	39.1	0.5	17.3	1.27
Gary	2015/09/06	38.1	0.9	17.2	1.25
Baj	2015/09/06	38.1	0.9	17.2	1.17
Baj	2015/09/08	35.9	1.5	16.8	1.34
Gary	2015/09/15	28.3	3.7	15.7	1.07
Gary	2015/09/16	27.8	4.0	15.5	1.08
Oey	2015/09/21	23.5	5.4	14.7	0.95
Gary	2015/09/24	21.2	6.2	14.3	0.94
Gary	2015/09/25	20.5	6.5	14.1	0.89
Gary	2015/09/26	19.9	6.7	13.9	0.85

Table 2. Observational circumstances. The columns from left to right are observer, observation date, phase angle (α), phase angle bisector ecliptic coordinates (L_{PAB}, B_{PAB}), and LC amplitude. Note the large LC amplitudes (≥ 2 mag) found on some dates. The data for α, L_{PAB} and B_{PAB} are from the JPL HORIZONS web site.

These ranges are sufficiently broad for trying to determine pole orientation and shape. The LC inversion process was performed using *MPO LCInvert* v11.1.0.2 (Bdw Publishing), which implements the core algorithms developed by Kaasalainen and then converted to C language by Josef Durech.

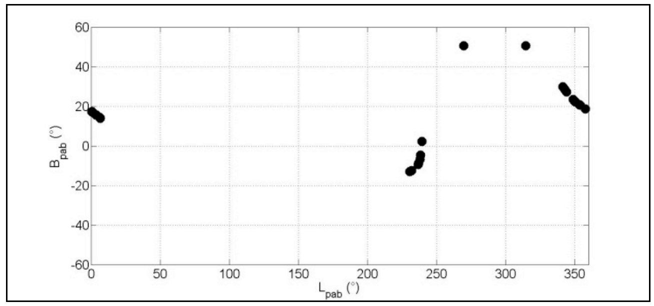

Figure 1. Distribution of phase angle bisector (PAB) for 2011 UW158. Data is from Table 2.

Period Search

The inversion process started by finding the sidereal rotation period of the asteroid. A search in *MPO LCInvert* was confined to 0.6100 to 0.6115 h, a range that includes the synodic period found in the single phased LC, with weight 0.5. However, inclusion of all observations listed in Table II leads to χ^2 values that are quite high. After some tests, we found that by restricting observations to those by Gary (in this way the range of the phase angle remains unchanged) and those before Aug 15 for the other observers, the χ^2 values were reduced to reasonable values.

The search process found an isolated, deep, and flat minimum in the plot of χ^2 vs. sidereal period (Fig. 2). A renormalization was not necessary since reduced χ^2 ~ 1.0 (*i.e.*, N = 24 and sum χ^2 is also ~24). The minimum appears asymmetrical, *i.e.* the descending branch is less steep than the ascending branch. For this reason we assumed the value of the point to the right, 0.6107643 h, for the starting period in the pole search.

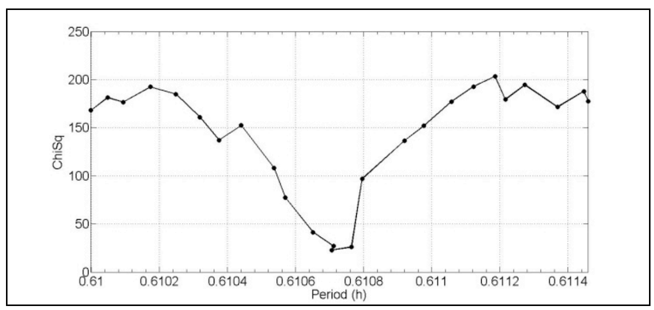

Figure 2. ChiSq vs period for 2011 UW158.

Pole Search

For the pole orientation search, we started using the "Medium" search option in LCInvert (312 fixed pole positions with 15° longitude-latitude steps). The previously found sidereal period was set to "float" and the weight parameter = 0.8. The pole search found one cluster of solutions centered around ecliptic coordinates λ = 285° and β = –45° with a sidereal period *P* = 0.61075717 h. Fig. 3 shows the distribution of log(χ^2) values.

A final search for a spin axis solution was made using the lowest value in this island. Here the longitude and latitude were allowed to float, as was the period. The spin axis parameters were then used to generate a final shape and spin axis model. Refining the pole search, using the "Fine" option of LCInvert software (49 fixed pole steps with 10° longitude-latitude pairs) and the previous period/longitude/latitude set to "float", we found the best solution to be ecliptic coordinates $\lambda = 290° \pm 3°$ and $\beta = -39° \pm 2°$ (near the star alpha Pavonis), with an averaged sidereal period $Ps = 0.610752 \pm 0.000001$ h. The uncertainty in λ, β, and sidereal period are chosen to be the mean standard deviation of the 49 single solution of the fine pole search. Since the ecliptic latitude of the rotations axis is negative, the asteroid has a retrograde rotation, *i.e.,* it rotates clockwise when viewed from the ecliptic north pole. The study of the prograde-retrograde spin distribution of near-Earth asteroids is important, *e.g.*, for the model of orbital drift of these bodies (La Spina *et al*., 2004). Of course this is a preliminary solution, but our confidence in the final solution is bolstered by the fact that the first half of the data (up to and including Aug 14), shown as Fig. 4, gave only two possible solutions, one of which is the same solution using all data.

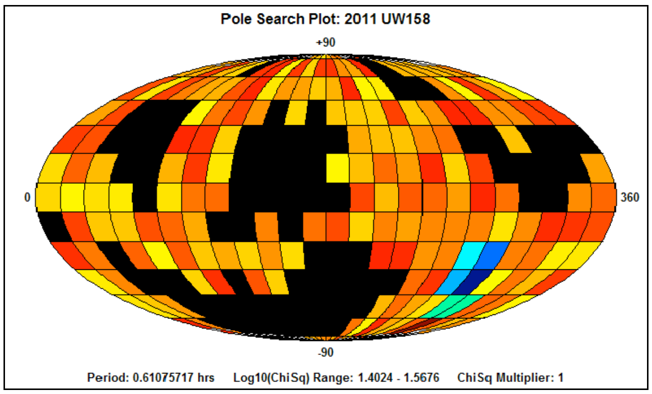

Figure 3. Results of the "medium" pole search as a map of χ^2 on the ecliptic sky. The deep blue region represents the pole location with the lowest Chi-square which increases as the color goes from light blue to green to yellow to orange and finally to deep red. Black regions indicate where the code produced an invalid result (NAN, not a number).

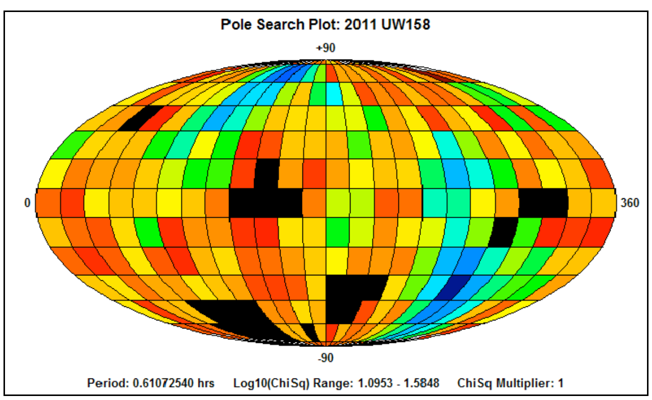

Figure 4. Distribution of χ^2 using only the first half of lightcurve data (up to Aug 14), using the "medium" pole search. One of the two possible solutions is the one found in the final analysis of the data.

Shape Model

The best shape model for this asteroid (the n. 24 in our data processing), shows a rather elongated object in rotation around the minor axis (Fig's 5 and 6). This result is consistent from the physical point of view and in agreement with the large LC amplitudes (>2 mag) found on some dates. This shape is also in agreement with the radar observations (Fig. 7). We tested the shape model by comparing synthetic lightcurves with observed ones shown as Fig's 8, 9, 10 and 11. We chose four dates, representative of the whole period of observation. The shape model produces synthetic lightcurves that are in good agreement with observed lightcurves.

Acknowledgements

This research has made use of the NASA's Astrophysics Data System, JPL's Small-Body Database Browser, and JPL's HORIZONS system. Research at the Astronomical Observatory of the Aosta Valley Autonomous Region was supported by the 2013 Shoemaker NEO Grant. Work at the Blue Mountains Observatory was supported by the 2015 Shoemaker NEO Grant.

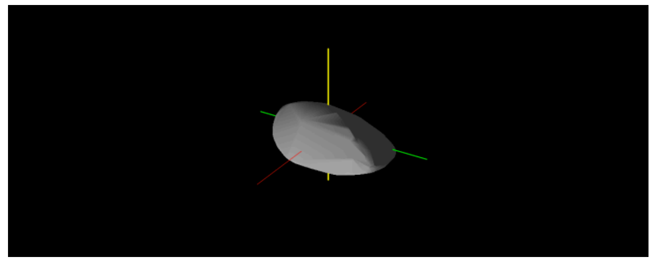

Figure 5. The 3-D best model for 2011 UW158, with pole in $\lambda = 295°$, $\beta = -40°$ (a/b=1.3, a/c=2.3, b/c=1.7).

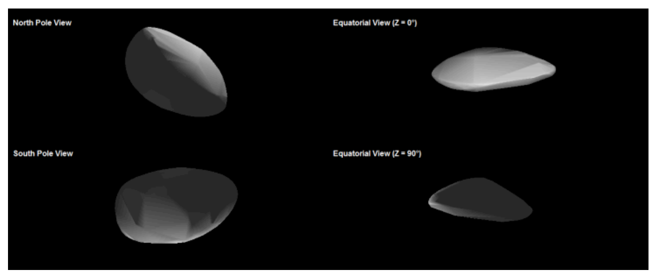

Figure 6. Multi-view of the best 3-D model for 2011 UW158.

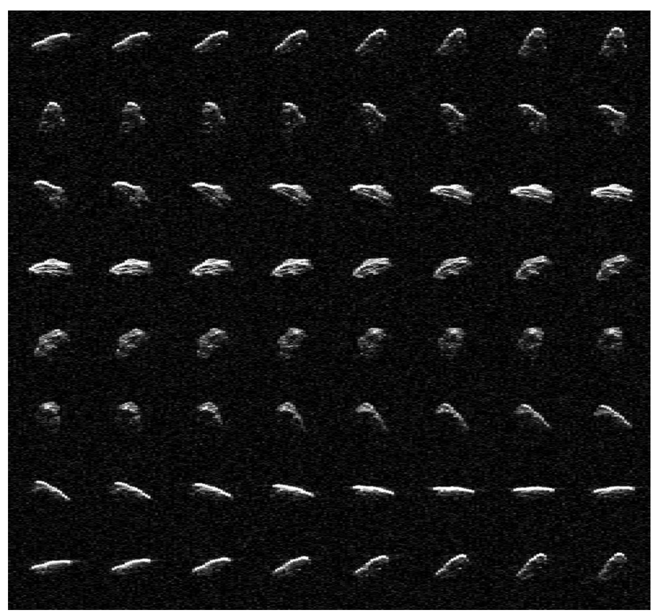

Figure 7. Delay-Doppler images of 2011 UW158 obtained on 2015 July 18 from Goldstone using DSS-14 to transmit and Green Bank Telescope to receive. Resolution is 7.5 m x 5 Hz. Range increases down and Doppler frequency increases to the right. The images span a little more than 1 rotation of the object (Goldstone Radar Team).

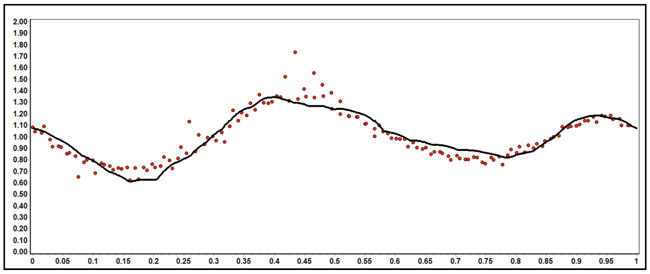

Figure 8. Comparison of the shape model synthetic LC with the observed LC on 2015 Jul 12.

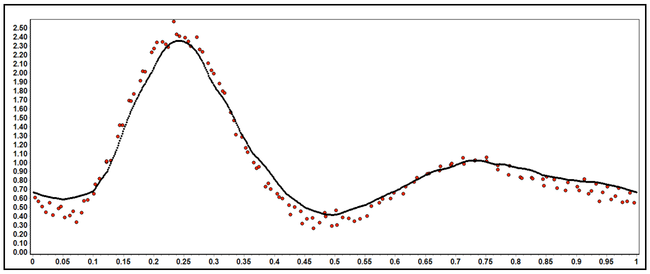

Figure 9. Comparison of the shape model synthetic LC with the observed LC on 2015 Aug 04.

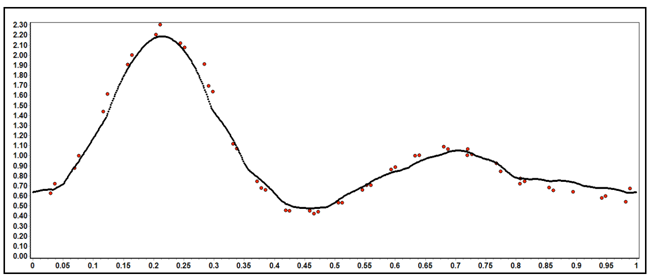

Figure 10. Comparison of the shape model synthetic LC with the observed LC on 2015 Aug 14.

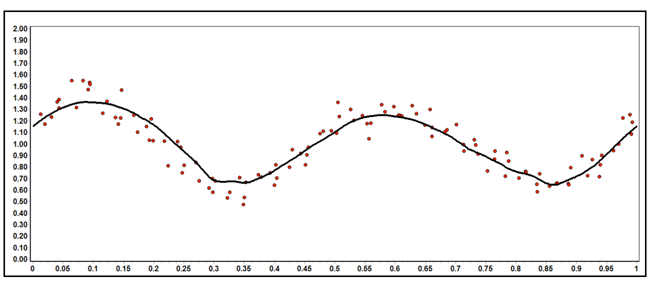

Figure 11. Comparison of the shape model synthetic LC with the observed LC on 2015 Sep 24.

References

Bdw Publishing (2015). *http://www.minorplanetobserver.com/MPOSoftware/MPOLCInvert.htm*

Holsapple, K.A. (2007). "Spin limits of Solar System bodies: From the small fast-rotators to 2003 EL61." *Icarus*, **187**, 500-509.

La Spina, A., Paolicchi, P., Kryszczynksa, A., Pravec P. (2004). "Retrograde spins of near-Earth asteroids from the Yarkovsky effect." *Nature* **428**, 400-401.

Kaasalainen M., Torppa, J., Muinonen, K. (2001). "Optimization methods for asteroid lightcurve inversion. II. The complete inverse problem." *Icarus* **153**, 37-51.

Kaasalainen M., Torppa J. (2001). "Optimization methods for asteroid lightcurve inversion. I. Shape determination." *Icarus*, **153**, 24-36.

Pravec, P., Harris, A.W. (2000). "Fast and Slow Rotation of Asteroids." *Icarus*, **148**, 12-20.

Sànchez, P., Scheeres D.J. (2014). "The Strength of Regolith and Rubble Pile Asteroids." *Meteoritics and Planetary Science*, **49**, 788-811.

MINOR PLANETS AT UNUSUALLY FAVORABLE ELONGATIONS IN 2016

Frederick Pilcher
4438 Organ Mesa Loop
Las Cruces, NM 88011 USA
fpilcher35@gmail.com

(Received: 10 October)

A list is presented of minor planets which are much brighter than usual at their 2016 apparitions.

The minor planets in the lists which follow will be much brighter at their 2016 apparitions than at their average distances at maximum elongation. Many years may pass before these planets will be again as bright as in 2016. Observers are encouraged to give special attention to those which lie near the limit of their equipment.

These lists have been prepared by an examination of the maximum elongation circumstances of minor planets computed by the author for all years through 2060 with a full perturbation program written by Dr. John Reed, and to whom he expresses his thanks. Elements are from EMP 1992, except that for all planets for which new or improved elements have been published subsequently in the Minor Planet Circulars or in electronic form, the newer elements have been used. Planetary positions are from the JPL DE-200 ephemeris, courtesy of Dr. E. Myles Standish.

Any planets whose brightest magnitudes near the time of maximum elongation vary by at least 2.0 in this interval and in 2016 will be within 0.3 of the brightest occuring, or vary by at least 3.0 and in 2016 will be within 0.5 of the brightest occuring; and which are visual magnitude 14.5 or brighter, are included. For planets brighter than visual magnitude 13.5, which are within the range of a large number of observers, these standards have been relaxed somewhat to include a larger number of planets. Magnitudes have been computed from the updated magnitude parameters published in MPC28104-28116, on 1996 Nov. 25, or more recently in the Minor Planet Circulars.

Oppositions may be in right ascension or in celestial longitude. Here we use still a third representation, maximum elongation from the Sun, instead of opposition. Though unconventional, it has the advantage that many close approaches do not involve actual opposition to the Sun near the time of minimum distance and greatest brightness and are missed by an opposition-based program. Other data are also provided according to the following tabular listings: Minor planet number, date of maximum elongation from the Sun in format yyyy/mm/dd, maximum elongation in degrees, right ascension on date of maximum elongation, declination on date of maximum elongation, both in J2000 coordinates, date of brightest magnitude in format yyyy/mm/dd, brightest magnitude, date of minimum distance in format yyyy/mm/dd, and minimum distance in AU.

Ten numbered minor planets are predicted to make close approaches to Earth at magnitude 14.5 or brighter. A special table is provided at the end of this paper.

Users should note that when the maximum elongation is about 177° or greater, the brightest magnitude is sharply peaked due to enhanced brightening near zero phase angle. Even as near as 10 days before or after minimum magnitude the magnitude is generally about 0.4 greater. This effect takes place in greater time interval for smaller maximum elongations. There is some interest in very small minimum phase angles. For maximum elongations E near 180° at Earth distance Δ, an approximate formula for the minimum phase angle ϕ is $\phi=(180°-E)/(\Delta+1)$.

Table I. Numerical Sequence of Favorable Elongations

Planet	Max Elon D	Max E	RA	Dec	Br Mag D	Br Mag	Min Dist D	Min Dist
5	2016/02/15	179.2°	9h54m	+13°	2016/02/15	8.7	2016/02/15	1.095
18	2016/10/22	160.7°	2h22m	- 6°	2016/10/21	8.0	2016/10/18	0.830
28	2016/03/07	173.7°	11h24m	+10°	2016/03/07	10.0	2016/03/04	1.435
35	2016/04/28	170.1°	14h10m	-23°	2016/04/28	11.3	2016/04/27	1.326
52	2016/02/13	177.0°	9h47m	+16°	2016/02/13	10.0	2016/02/11	1.813
56	2016/08/15	167.5°	21h21m	- 2°	2016/08/14	10.3	2016/08/09	1.010
57	2016/10/18	177.2°	1h39m	+ 7°	2016/10/18	10.7	2016/10/19	1.823
60	2016/11/27	174.3°	4h17m	+15°	2016/11/27	10.1	2016/12/01	1.032
67	2016/09/13	173.8°	23h15m	+ 1°	2016/09/12	10.3	2016/09/06	1.044
79	2016/11/03	177.6°	2h39m	+13°	2016/11/03	9.6	2016/11/03	0.988
85	2016/08/12	159.9°	21h 2m	+ 4°	2016/08/13	10.2	2016/08/13	1.161
99	2016/05/19	171.9°	15h41m	-27°	2016/05/19	11.7	2016/05/19	1.139
132	2016/02/08	125.4°	9h15m	-39°	2016/02/14	11.2	2016/02/16	0.800
138	2016/07/16	174.6°	19h46m	-26°	2016/07/16	10.7	2016/07/18	1.057
157	2016/12/16	170.8°	5h41m	+32°	2016/12/17	12.9	2016/12/19	1.126
161	2016/07/15	162.4°	19h56m	-38°	2016/07/16	11.5	2016/07/18	1.076
185	2016/09/07	171.4°	23h22m	-13°	2016/09/07	10.7	2016/09/08	1.423
188	2016/07/04	165.9°	18h52m	- 8°	2016/07/05	12.1	2016/07/07	1.307
193	2016/12/05	154.8°	4h34m	+47°	2016/12/05	11.5	2016/12/04	0.890
217	2016/07/13	163.5°	19h15m	- 5°	2016/07/15	12.0	2016/07/20	1.037
226	2016/08/06	179.4°	21h 4m	-16°	2016/08/06	11.8	2016/08/02	1.179
228	2016/09/18	175.8°	23h38m	+ 2°	2016/09/18	13.1	2016/09/11	0.687
278	2016/05/20	179.4°	15h50m	-19°	2016/05/20	12.2	2016/05/17	1.439
284	2016/06/28	167.6°	18h31m	-10°	2016/06/29	11.5	2016/07/01	0.839
305	2016/01/22	172.7°	8h 9m	+12°	2016/01/22	12.0	2016/01/21	1.527
319	2016/09/27	179.4°	0h14m	+ 1°	2016/09/27	13.4	2016/10/01	1.836
322	2016/09/19	165.2°	23h24m	+12°	2016/09/20	11.4	2016/09/20	1.117
323	2016/12/29	179.3°	6h35m	+23°	2016/12/29	11.2	2016/12/17	0.958
335	2016/06/17	171.2°	17h44m	-14°	2016/06/17	11.1	2016/06/20	1.061
341	2016/10/09	177.3°	1h 3m	+ 3°	2016/10/09	11.9	2016/09/30	0.888
347	2016/01/21	168.1°	8h25m	+31°	2016/01/22	11.8	2016/01/26	1.318
360	2016/12/17	165.8°	5h40m	+ 9°	2016/12/16	11.9	2016/12/14	1.535
361	2016/11/22	167.7°	3h43m	+32°	2016/11/23	12.8	2016/11/24	2.196
382	2016/04/14	168.6°	13h15m	-20°	2016/04/15	12.3	2016/04/17	1.610
404	2016/06/07	172.4°	17h 1m	-15°	2016/06/06	11.4	2016/06/01	1.160
428	2016/10/06	179.0°	0h52m	+ 4°	2016/10/06	12.8	2016/10/08	0.911
432	2016/05/27	170.3°	16h18m	-11°	2016/05/27	10.9	2016/05/29	1.029
437	2016/08/17	165.3°	21h30m	+ 0°	2016/08/17	11.8	2016/08/16	0.795
448	2016/10/25	178.3°	2h 3m	+10°	2016/10/25	13.9	2016/10/19	1.773
464	2016/07/19	175.4°	20h 3m	-25°	2016/07/20	12.5	2016/07/26	1.434
465	2016/04/17	172.2°	13h31m	-18°	2016/04/18	12.8	2016/04/20	1.471
516	2016/05/31	154.6°	16h10m	-46°	2016/05/29	10.5	2016/05/26	1.018
518	2016/10/15	179.6°	1h22m	+ 9°	2016/10/15	13.1	2016/10/05	1.151
544	2016/07/01	175.0°	18h44m	-28°	2016/07/01	12.2	2016/07/02	1.183
585	2016/03/24	179.1°	12h16m	- 0°	2016/03/24	12.5	2016/03/22	1.164
604	2016/11/20	174.8°	3h38m	+24°	2016/11/20	12.4	2016/11/17	1.554
620	2016/10/01	177.9°	0h26m	+ 5°	2016/10/01	13.4	2016/09/26	1.142
632	2016/07/15	176.4°	19h44m	-24°	2016/07/15	14.1	2016/07/09	1.241
645	2016/11/21	170.5°	3h42m	+29°	2016/11/22	13.8	2016/11/23	1.796
654	2016/01/29	157.3°	8h40m	- 4°	2016/01/29	10.1	2016/01/30	0.815
664	2016/08/14	173.1°	21h25m	- 7°	2016/08/13	13.4	2016/08/07	1.608
668	2016/10/23	179.1°	1h51m	+12°	2016/10/23	14.5	2016/10/14	1.374
670	2016/09/04	177.0°	22h48m	- 4°	2016/09/04	12.4	2016/09/07	1.295
685	2016/08/27	171.9°	22h14m	- 2°	2016/08/27	13.0	2016/08/23	0.805
699	2016/10/28	162.8°	1h30m	+27°	2016/10/21	13.1	2016/10/07	0.773
703	2016/11/12	178.5°	3h14m	+16°	2016/11/12	13.4	2016/11/09	0.901
718	2016/03/26	173.6°	12h29m	+ 3°	2016/03/26	12.9	2016/03/30	1.496
722	2016/05/27	175.7°	16h18m	-25°	2016/05/28	13.7	2016/06/03	0.950
779	2016/07/27	169.5°	20h21m	- 8°	2016/07/27	10.5	2016/07/31	1.094
786	2016/05/21	168.4°	16h 2m	- 8°	2016/05/21	12.3	2016/05/20	1.681
787	2016/09/10	172.3°	23h 0m	+ 2°	2016/09/10	12.5	2016/09/06	1.257
814	2016/12/02	166.9°	4h36m	+ 8°	2016/11/30	11.7	2016/11/24	1.348
817	2016/01/11	174.5°	7h21m	+16°	2016/01/10	13.5	2016/01/05	1.313
822	2016/11/13	179.5°	3h15m	+17°	2016/11/13	13.7	2016/11/17	0.996
880	2016/08/27	152.7°	21h50m	+16°	2016/08/31	14.1	2016/09/03	1.135
889	2016/12/08	166.5°	5h 2m	+ 9°	2016/12/07	13.1	2016/12/03	1.006
918	2016/08/31	177.0°	22h36m	- 5°	2016/08/31	13.3	2016/08/31	1.317
922	2016/09/10	171.7°	22h59m	+ 2°	2016/09/09	14.1	2016/09/06	1.178
934	2016/09/23	164.6°	23h42m	+14°	2016/09/24	12.9	2016/09/26	1.206
942	2016/12/11	177.5°	5h16m	+25°	2016/12/11	14.4	2016/12/07	1.766
980	2016/07/10	178.4°	19h21m	-20°	2016/07/11	10.7	2016/07/18	1.410
984	2016/09/19	168.9°	23h31m	+ 9°	2016/09/19	11.7	2016/09/20	1.265
985	2016/08/11	175.2°	21h21m	-10°	2016/08/12	13.4	2016/08/19	0.695
986	2016/07/21	169.0°	20h19m	-30°	2016/07/22	13.1	2016/07/27	1.705
999	2016/09/08	165.4°	22h41m	+ 7°	2016/09/08	13.3	2016/09/06	1.054
1089	2016/11/25	178.9°	4h 7m	+19°	2016/11/25	13.0	2016/11/25	0.946
1096	2016/06/27	175.5°	18h28m	-27°	2016/06/27	12.7	2016/07/04	1.221
1108	2016/06/06	156.9°	17h31m	- 0°	2016/06/10	14.0	2016/06/16	0.968
1204	2016/08/06	175.9°	21h11m	-20°	2016/08/06	12.4	2016/08/08	0.588
1222	2016/06/21	163.4°	18h11m	- 6°	2016/06/23	13.8	2016/06/27	1.169
1251	2016/08/09	179.3°	21h18m	-15°	2016/08/09	13.1	2016/08/13	1.352
1293	2016/08/05	166.4°	20h49m	- 3°	2016/08/07	14.5	2016/08/12	0.634
1360	2016/06/20	141.2°	17h23m	-61°	2016/06/19	13.9	2016/06/19	1.182
1419	2016/11/05	178.1°	2h44m	+13°	2016/11/05	13.1	2016/11/08	1.034
1438	2016/08/16	176.6°	21h40m	-10°	2016/08/16	14.5	2016/08/22	1.533
1555	2016/09/14	173.1°	23h20m	+ 3°	2016/09/14	13.4	2016/09/16	0.954
1590	2016/05/03	179.5°	14h42m	-16°	2016/05/03	13.3	2016/05/10	0.985
1631	2016/08/15	165.7°	21h56m	-27°	2016/08/15	13.4	2016/08/16	0.763
1650	2016/06/06	175.4°	17h 3m	-18°	2016/06/06	13.4	2016/06/07	1.026
1660	2016/04/22	179.3°	13h58m	-12°	2016/04/22	13.8	2016/04/10	1.070
1665	2016/01/09	173.5°	7h24m	+28°	2016/01/08	13.5	2016/01/07	0.940
1682	2016/08/20	179.4°	22h 0m	-11°	2016/08/20	13.8	2016/08/21	0.800
1685	2016/02/26	120.0°	6h37m	- 0°	2016/01/30	13.0	2016/01/22	0.157
1687	2016/12/03	178.3°	4h38m	+20°	2016/12/03	13.5	2016/11/30	1.640
1771	2016/11/15	170.0°	3h33m	+ 8°	2016/11/15	13.5	2016/11/14	1.600
1821	2016/07/06	179.0°	19h 4m	-23°	2016/07/06	14.5	2016/07/07	0.885
1863	2016/03/02	131.9°	13h36m	-19°	2016/03/20	14.7	2016/03/27	0.237
1937	2016/06/28	171.9°	18h37m	-31°	2016/06/28	13.9	2016/07/02	1.025
1945	2016/09/15	175.8°	23h42m	- 6°	2016/09/15	14.3	2016/09/12	1.098
2016	2016/10/12	179.8°	1h12m	+ 7°	2016/10/12	14.4	2016/10/09	1.559
2044	2016/11/15	179.0°	3h21m	+17°	2016/11/15	13.9	2016/11/26	0.724
2102	2016/12/27	115.6°	3h43m	-27°	2016/12/29	14.1	2016/12/30	0.138
2109	2016/08/19	175.6°	21h47m	- 8°	2016/08/19	13.8	2016/08/24	1.025
2134	2016/04/07	172.4°	12h58m	-14°	2016/04/06	14.1	2016/03/30	1.238
2183	2016/06/23	176.8°	18h10m	-26°	2016/06/23	13.5	2016/07/06	1.075
2189	2016/07/26	177.3°	20h20m	-16°	2016/07/26	14.3	2016/08/02	0.936
2235	2016/01/18	150.0°	7h33m	- 8°	2016/01/18	14.5	2016/01/18	1.626
2259	2016/06/15	177.2°	17h34m	-26°	2016/06/15	13.9	2016/06/20	0.886
2375	2016/06/09	166.6°	17h10m	- 9°	2016/06/07	14.2	2016/06/04	1.642
2510	2016/07/30	174.9°	20h48m	-23°	2016/07/30	13.7	2016/07/31	0.799
2536	2016/08/05	173.6°	20h56m	-10°	2016/08/06	14.5	2016/08/14	0.896
2544	2016/03/19	139.7°	11h16m	-38°	2016/03/24	14.5	2016/03/27	0.947
2651	2016/08/26	165.2°	22h50m	-23°	2016/08/29	14.1	2016/09/06	1.357
2754	2016/09/27	166.3°	23h56m	+14°	2016/09/27	14.5	2016/09/26	0.718
2786	2016/10/27	169.1°	1h57m	+23°	2016/10/27	14.4	2016/10/25	1.165
2848	2016/12/04	178.6°	4h43m	+23°	2016/12/04	14.5	2016/11/29	1.698
3034	2016/07/20	169.7°	20h 7m	-30°	2016/07/21	13.8	2016/07/25	0.860
3103	2016/07/07	116.7°	22h50m	+ 9°	2016/07/28	14.3	2016/08/02	0.189
3105	2016/09/11	173.0°	23h32m	-10°	2016/09/11	14.3	2016/09/08	0.823
3353	2016/06/08	165.7°	17h30m	- 9°	2016/06/09	14.5	2016/06/10	0.710
3500	2016/07/20	177.2°	20h 1m	-23°	2016/07/20	13.8	2016/07/25	0.815
3687	2016/09/13	156.1°	22h40m	+17°	2016/09/12	14.3	2016/09/10	1.228
3913	2016/02/21	176.1°	10h 7m	+ 7°	2016/02/21	13.8	2016/02/29	0.955
3925	2016/08/28	176.3°	22h23m	- 6°	2016/08/28	14.2	2016/09/01	1.614
3935	2016/12/25	172.5°	6h16m	+30°	2016/12/24	14.2	2016/12/18	1.097
4049	2016/08/11	177.0°	21h31m	-17°	2016/08/11	14.2	2016/08/10	1.221
4293	2016/12/13	173.1°	5h22m	+30°	2016/12/13	14.4	2016/12/17	1.190
4369	2016/10/10	156.8°	0h25m	+28°	2016/10/09	14.0	2016/10/08	0.989
4517	2016/08/14	170.9°	21h50m	-22°	2016/08/14	14.5	2016/08/12	0.774
4775	2016/09/12	168.4°	23h28m	+ 7°	2016/09/10	12.7	2016/09/05	0.308
4844	2016/06/10	177.5°	17h17m	-20°	2016/06/10	14.1	2016/06/08	0.998
4937	2016/06/20	176.5°	17h56m	-26°	2016/06/20	14.1	2016/06/19	1.181
5331	2016/09/13	156.0°	0h18m	-24°	2016/09/20	13.6	2016/09/27	0.816
5349	2016/10/18	132.9°	2h29m	+55°	2016/11/04	14.3	2016/11/08	0.732
5661	2016/08/05	178.6°	21h 4m	-18°	2016/08/05	14.1	2016/08/05	2.026
5971	2016/07/22	176.0°	20h 6m	-16°	2016/07/22	14.2	2016/07/21	1.158
6016	2016/10/04	179.4°	0h43m	+ 4°	2016/10/04	13.9	2016/09/29	0.844
6398	2016/02/05	173.0°	9h29m	+21°	2016/02/06	14.5	2016/02/14	1.003
6610	2016/12/13	174.1°	5h24m	+29°	2016/12/13	14.5	2016/12/09	0.954
6916	2016/07/13	165.3°	19h33m	-36°	2016/07/12	14.5	2016/07/09	1.149
7456	2016/08/07	170.4°	21h31m	-24°	2016/08/07	14.4	2016/08/08	0.830
7717	2016/01/28	173.6°	8h42m	+24°	2016/01/28	14.5	2016/01/30	0.778
13123	2016/05/26	176.4°	16h11m	-17°	2016/05/26	14.3	2016/06/07	1.025
14465	2016/08/12	174.3°	21h40m	-19°	2016/08/12	13.9	2016/08/14	0.883
20789	2016/11/27	179.2°	4h11m	+20°	2016/11/27	14.4	2016/11/29	0.965
20826	2016/08/05	116.7°	17h28m	-72°	2016/03/22	14.4	2016/04/06	0.337
58143	2016/10/14	173.0°	1h26m	+ 1°	2016/10/13	14.2	2016/10/04	0.926
85990	2016/01/17	161.2°	6h47m	+11°	2016/01/09	14.5	2016/01/06	0.033
96590	2016/11/28	152.9°	3h29m	- 2°	2016/11/23	13.2	2016/11/15	0.120
154244	2016/05/27	171.5°	16h35m	-13°	2016/07/17	13.8	2016/07/22	0.068
164121	2016/10/29	130.9°	5h39m	+18°	2016/10/30	10.9	2016/10/31	0.035

Table II. Temporal Sequence of Favorable Elongations

Planet	Max Elon D	Max E	RA	Dec	Br Mag D	Br Mag	Min Dist D	Min Dist
1665	2016/01/09	173.5°	7h24m	+28°	2016/01/08	13.5	2016/01/07	0.940
817	2016/01/11	174.5°	7h21m	+16°	2016/01/10	13.5	2016/01/05	1.313
85990	2016/01/17	161.2°	6h47m	+11°	2016/01/09	14.5	2016/01/06	0.033
2235	2016/01/18	150.0°	7h33m	- 8°	2016/01/18	14.5	2016/01/18	1.626
347	2016/01/21	168.1°	8h25m	+31°	2016/01/22	11.8	2016/01/26	1.318
305	2016/01/22	172.7°	8h 9m	+12°	2016/01/22	12.0	2016/01/21	1.527
7717	2016/01/28	173.6°	8h42m	+24°	2016/01/28	14.5	2016/01/30	0.778
654	2016/01/29	157.3°	8h40m	- 4°	2016/01/29	10.1	2016/01/30	0.815
6398	2016/02/05	173.0°	9h29m	+21°	2016/02/06	14.5	2016/02/14	1.003
132	2016/02/08	125.4°	9h15m	-39°	2016/02/14	11.2	2016/02/16	0.800
52	2016/02/13	177.0°	9h47m	+16°	2016/02/13	10.0	2016/02/11	1.813
5	2016/02/15	179.2°	9h54m	+13°	2016/02/15	8.7	2016/02/15	1.095
3913	2016/02/21	176.1°	10h 7m	+ 7°	2016/02/21	13.8	2016/02/29	0.955
1685	2016/02/26	120.0°	6h37m	- 0°	2016/01/30	13.0	2016/01/22	0.157
1863	2016/03/02	131.9°	13h36m	-19°	2016/03/20	14.7	2016/03/27	0.237
28	2016/03/07	173.7°	11h24m	+10°	2016/03/07	10.0	2016/03/04	1.435
2544	2016/03/19	139.7°	11h16m	-38°	2016/03/24	14.5	2016/03/27	0.947
585	2016/03/24	179.1°	12h16m	- 0°	2016/03/24	12.5	2016/03/22	1.164
718	2016/03/26	173.6°	12h29m	+ 3°	2016/03/26	12.9	2016/03/30	1.496
2134	2016/04/07	172.4°	12h58m	-14°	2016/04/06	14.1	2016/03/30	1.238
382	2016/04/14	168.6°	13h15m	-20°	2016/04/15	12.3	2016/04/17	1.610
465	2016/04/17	172.2°	13h31m	-18°	2016/04/18	12.8	2016/04/20	1.471
1660	2016/04/22	179.3°	13h58m	-12°	2016/04/22	13.8	2016/04/10	1.070
35	2016/04/28	170.1°	14h10m	-23°	2016/04/28	11.3	2016/04/27	1.326
1590	2016/05/03	179.5°	14h42m	-16°	2016/05/03	13.3	2016/05/10	0.985
99	2016/05/19	171.9°	15h41m	-27°	2016/05/19	11.7	2016/05/19	1.139
278	2016/05/20	179.4°	15h50m	-19°	2016/05/20	12.2	2016/05/17	1.439
786	2016/05/21	168.4°	16h 2m	- 8°	2016/05/21	12.3	2016/05/20	1.681
13123	2016/05/26	176.4°	16h11m	-17°	2016/05/26	14.3	2016/06/07	1.025
432	2016/05/27	170.3°	16h18m	-11°	2016/05/27	10.9	2016/05/29	1.029
154244	2016/05/27	171.5°	16h35m	-13°	2016/08/06	13.8	2016/07/22	0.068
722	2016/05/27	175.7°	16h18m	-25°	2016/05/28	13.7	2016/06/03	0.950
516	2016/05/31	154.6°	16h10m	-46°	2016/05/29	10.5	2016/05/26	1.018
1108	2016/06/06	156.9°	17h31m	- 0°	2016/06/10	14.0	2016/06/16	0.968
1650	2016/06/06	175.4°	17h 3m	-18°	2016/06/06	13.4	2016/06/07	1.026
404	2016/06/07	172.4°	17h 1m	-15°	2016/06/06	11.4	2016/06/01	1.160
3353	2016/06/08	165.7°	17h30m	- 9°	2016/06/09	14.5	2016/06/10	0.710
2375	2016/06/09	166.6°	17h10m	- 9°	2016/06/07	14.2	2016/06/04	1.642
4844	2016/06/10	177.5°	17h17m	-20°	2016/06/10	14.1	2016/06/08	0.998
2259	2016/06/15	177.2°	17h34m	-26°	2016/06/15	13.9	2016/06/20	0.886
335	2016/06/17	171.2°	17h44m	-14°	2016/06/17	11.1	2016/06/20	1.061
1360	2016/06/20	141.2°	17h23m	-61°	2016/06/19	13.9	2016/06/19	1.182
4937	2016/06/20	176.5°	17h56m	-26°	2016/06/20	14.1	2016/06/19	1.181
1222	2016/06/21	163.4°	18h11m	- 6°	2016/06/23	13.8	2016/06/27	1.169
2183	2016/06/23	176.8°	18h10m	-26°	2016/06/23	13.5	2016/07/06	1.075
1096	2016/06/27	175.5°	18h28m	-27°	2016/06/27	12.7	2016/07/04	1.221
284	2016/06/28	167.6°	18h31m	-10°	2016/06/29	11.5	2016/07/01	0.839
1937	2016/06/28	171.9°	18h37m	-31°	2016/06/28	13.9	2016/07/02	1.025
544	2016/07/01	175.0°	18h44m	-28°	2016/07/01	12.2	2016/07/02	1.183
188	2016/07/04	165.9°	18h52m	- 8°	2016/07/05	12.1	2016/07/07	1.307
1821	2016/07/06	179.0°	19h 4m	-23°	2016/07/06	14.5	2016/07/07	0.885
3103	2016/07/07	116.7°	22h50m	+ 9°	2016/07/28	14.3	2016/08/02	0.189
980	2016/07/10	178.4°	19h21m	-20°	2016/07/11	10.7	2016/07/18	1.410
217	2016/07/13	163.5°	19h15m	- 5°	2016/07/15	12.0	2016/07/20	1.037
6916	2016/07/13	165.3°	19h33m	-36°	2016/07/12	14.5	2016/07/09	1.149
161	2016/07/15	162.4°	19h56m	-38°	2016/07/16	11.5	2016/07/18	1.076
632	2016/07/15	176.4°	19h44m	-24°	2016/07/15	14.1	2016/07/09	1.241
138	2016/07/16	174.6°	19h46m	-26°	2016/07/16	10.7	2016/07/18	1.057
464	2016/07/19	175.4°	20h 3m	-25°	2016/07/20	12.5	2016/07/26	1.434
3034	2016/07/20	169.7°	20h 7m	-30°	2016/07/21	13.8	2016/07/25	0.860
3500	2016/07/20	177.2°	20h 1m	-23°	2016/07/20	13.8	2016/07/25	0.815
986	2016/07/21	169.0°	20h19m	-30°	2016/07/22	13.1	2016/07/27	1.705
5971	2016/07/22	176.0°	20h 6m	-16°	2016/07/22	14.2	2016/07/21	1.158
2189	2016/07/26	177.3°	20h20m	-16°	2016/07/26	14.3	2016/08/02	0.936
779	2016/07/27	169.5°	20h21m	- 8°	2016/07/27	10.5	2016/07/31	1.094
2510	2016/07/30	174.9°	20h48m	-23°	2016/07/30	13.7	2016/07/31	0.799
1293	2016/08/05	166.4°	20h49m	- 3°	2016/08/07	14.5	2016/08/12	0.634
2536	2016/08/05	173.6°	20h56m	-10°	2016/08/06	14.5	2016/08/14	0.896
5661	2016/08/05	178.6°	21h 4m	-18°	2016/08/05	14.1	2016/08/05	2.026
20826	2016/08/05	116.7°	17h28m	-72°	2016/03/22	14.4	2016/04/06	0.337
226	2016/08/06	179.4°	21h 4m	-16°	2016/08/06	11.8	2016/08/02	1.179
1204	2016/08/06	175.9°	21h11m	-20°	2016/08/06	12.4	2016/08/08	0.588
7456	2016/08/07	170.4°	21h31m	-24°	2016/08/07	14.4	2016/08/08	0.830
1251	2016/08/09	179.3°	21h18m	-15°	2016/08/09	13.1	2016/08/13	1.352
985	2016/08/11	175.2°	21h21m	-10°	2016/08/12	13.4	2016/08/19	0.695
4049	2016/08/11	177.0°	21h31m	-17°	2016/08/11	14.2	2016/08/10	1.221
85	2016/08/12	159.9°	21h 2m	+ 4°	2016/08/13	10.2	2016/08/13	1.161
14465	2016/08/12	174.3°	21h40m	-19°	2016/08/12	13.9	2016/08/14	0.883
664	2016/08/14	173.1°	21h25m	- 7°	2016/08/13	13.4	2016/08/07	1.608
4517	2016/08/14	170.9°	21h50m	-22°	2016/08/14	14.5	2016/08/12	0.774
56	2016/08/15	167.5°	21h21m	- 2°	2016/08/14	10.3	2016/08/09	1.010
1631	2016/08/15	165.7°	21h56m	-27°	2016/08/15	13.4	2016/08/16	0.763
1438	2016/08/16	176.6°	21h40m	-10°	2016/08/16	14.5	2016/08/22	1.533
437	2016/08/17	165.3°	21h30m	+ 0°	2016/08/17	11.8	2016/08/16	0.795
2109	2016/08/19	175.6°	21h47m	- 8°	2016/08/19	13.8	2016/08/24	1.025
1682	2016/08/20	179.4°	22h 0m	-11°	2016/08/20	13.8	2016/08/21	0.800
2651	2016/08/26	165.2°	22h50m	-23°	2016/08/29	14.1	2016/09/06	1.357
685	2016/08/27	171.9°	22h14m	- 2°	2016/08/27	13.0	2016/08/23	0.805
880	2016/08/27	152.7°	21h50m	+16°	2016/08/31	14.1	2016/09/03	1.135
3925	2016/08/28	176.3°	22h23m	- 6°	2016/08/28	14.2	2016/09/01	1.614
918	2016/08/31	177.0°	22h36m	- 5°	2016/08/31	13.3	2016/08/31	1.317
670	2016/09/04	177.0°	22h48m	- 4°	2016/09/04	12.4	2016/09/07	1.295
185	2016/09/07	171.4°	23h22m	-13°	2016/09/07	10.7	2016/09/08	1.423
999	2016/09/08	165.4°	22h41m	+ 7°	2016/09/08	13.3	2016/09/06	1.054
787	2016/09/10	172.3°	23h 0m	+ 2°	2016/09/10	12.5	2016/09/06	1.257
922	2016/09/10	171.7°	22h59m	+ 2°	2016/09/09	14.1	2016/09/06	1.178
3105	2016/09/11	173.0°	23h32m	-10°	2016/09/11	14.3	2016/09/08	0.823
4775	2016/09/12	168.4°	23h28m	+ 7°	2016/09/10	12.7	2016/09/05	0.308
67	2016/09/13	173.8°	23h15m	+ 1°	2016/09/12	10.3	2016/09/06	1.044
3687	2016/09/13	156.1°	22h40m	+17°	2016/09/12	14.3	2016/09/10	1.228
5331	2016/09/13	156.0°	0h18m	-24°	2016/09/20	13.6	2016/09/27	0.816
1555	2016/09/14	173.1°	23h20m	+ 3°	2016/09/14	13.4	2016/09/16	0.954
1945	2016/09/15	175.8°	23h42m	- 6°	2016/09/15	14.3	2016/09/12	1.098
228	2016/09/18	175.8°	23h38m	+ 2°	2016/09/18	13.1	2016/09/11	0.687
322	2016/09/19	165.2°	23h24m	+12°	2016/09/20	11.4	2016/09/20	1.117
984	2016/09/19	168.9°	23h31m	+ 9°	2016/09/19	11.7	2016/09/20	1.265
934	2016/09/23	164.6°	23h42m	+14°	2016/09/24	12.9	2016/09/26	1.206
319	2016/09/27	179.4°	0h14m	+ 1°	2016/09/27	13.4	2016/10/01	1.836
2754	2016/09/27	166.3°	23h56m	+14°	2016/09/27	14.5	2016/09/26	0.718
620	2016/10/01	177.9°	0h26m	+ 5°	2016/10/01	13.4	2016/09/26	1.142
6016	2016/10/04	179.4°	0h43m	+ 4°	2016/10/04	13.9	2016/09/29	0.844
428	2016/10/06	179.0°	0h52m	+ 4°	2016/10/06	12.8	2016/10/08	0.911
341	2016/10/09	177.3°	1h 3m	+ 3°	2016/10/09	11.9	2016/09/30	0.888
4369	2016/10/10	156.8°	0h25m	+28°	2016/10/09	14.0	2016/10/08	0.989
2016	2016/10/12	179.8°	1h12m	+ 7°	2016/10/12	14.4	2016/10/09	1.559
58143	2016/10/14	173.0°	1h26m	+ 1°	2016/10/13	14.2	2016/10/04	0.926
518	2016/10/15	179.6°	1h22m	+ 9°	2016/10/15	13.1	2016/10/05	1.151
57	2016/10/18	177.2°	1h39m	+ 7°	2016/10/18	10.7	2016/10/19	1.823
5349	2016/10/18	132.9°	2h29m	+55°	2016/11/04	14.3	2016/11/08	0.732
18	2016/10/22	160.7°	2h22m	- 6°	2016/10/21	8.0	2016/10/18	0.830
668	2016/10/23	179.1°	1h51m	+12°	2016/10/23	14.5	2016/10/14	1.374
448	2016/10/25	178.3°	2h 3m	+10°	2016/10/25	13.9	2016/10/19	1.773
2786	2016/10/27	169.1°	1h57m	+23°	2016/10/27	14.4	2016/10/25	1.165
699	2016/10/28	162.8°	1h30m	+27°	2016/10/21	13.1	2016/10/07	0.773
164121	2016/10/29	130.9°	5h39m	+18°	2016/10/30	10.9	2016/10/31	0.035
79	2016/11/03	177.6°	2h39m	+13°	2016/11/03	9.6	2016/11/03	0.988
1419	2016/11/05	178.1°	2h44m	+13°	2016/11/05	13.1	2016/11/08	1.034
703	2016/11/12	178.5°	3h14m	+16°	2016/11/12	13.4	2016/11/09	0.901
822	2016/11/13	179.5°	3h15m	+17°	2016/11/13	13.7	2016/11/17	0.996
1771	2016/11/15	170.0°	3h33m	+ 8°	2016/11/15	13.5	2016/11/14	1.600
2044	2016/11/15	179.0°	3h21m	+17°	2016/11/15	13.9	2016/11/26	0.724
604	2016/11/20	174.8°	3h38m	+24°	2016/11/20	12.4	2016/11/17	1.554
645	2016/11/21	170.5°	3h42m	+29°	2016/11/22	13.8	2016/11/23	1.796
361	2016/11/22	167.7°	3h43m	+32°	2016/11/23	12.8	2016/11/24	2.196
1089	2016/11/25	178.9°	4h 7m	+19°	2016/11/25	13.0	2016/11/25	0.946
60	2016/11/27	174.3°	4h17m	+15°	2016/11/27	10.1	2016/12/01	1.032
20789	2016/11/27	179.2°	4h11m	+20°	2016/11/27	14.4	2016/11/29	0.965
96590	2016/11/28	152.9°	3h29m	- 2°	2016/11/23	13.2	2016/11/15	0.120
814	2016/12/02	166.9°	4h36m	+ 8°	2016/11/30	11.7	2016/11/24	1.348
1687	2016/12/03	178.3°	4h38m	+20°	2016/12/03	13.5	2016/11/30	1.640
2848	2016/12/04	178.6°	4h43m	+23°	2016/12/04	14.5	2016/11/29	1.698
193	2016/12/05	154.8°	4h34m	+47°	2016/12/05	11.5	2016/12/04	0.890
889	2016/12/08	166.5°	5h 2m	+ 9°	2016/12/07	13.1	2016/12/03	1.006
942	2016/12/11	177.5°	5h16m	+25°	2016/12/11	14.4	2016/12/07	1.766
4293	2016/12/13	173.1°	5h22m	+30°	2016/12/13	14.4	2016/12/17	1.190
6610	2016/12/13	174.1°	5h24m	+29°	2016/12/13	14.5	2016/12/09	0.954
157	2016/12/16	170.8°	5h41m	+32°	2016/12/17	12.9	2016/12/19	1.126
360	2016/12/17	165.8°	5h40m	+ 9°	2016/12/16	11.9	2016/12/14	1.535
3935	2016/12/25	172.5°	6h16m	+30°	2016/12/24	14.2	2016/12/18	1.097
2102	2016/12/27	115.6°	3h43m	-27°	2016/12/29	14.1	2016/12/30	0.138
323	2016/12/29	179.3°	6h35m	+23°	2016/12/29	11.2	2016/12/17	0.958

Table III. Numerical Sequence of Close Approaches

Planet	Max Elon D	Max E	RA	Dec	Br Mag D	Br Mag	Min Dist D	Min Dist
1685	2016/02/26	120.0°	6h37m	- 0°	2016/01/30	13.0	2016/01/22	0.157
1863	2016/03/02	131.9°	13h36m	-19°	2016/03/20	14.7	2016/03/27	0.237
2102	2016/12/27	115.6°	3h43m	-27°	2016/12/29	14.1	2016/12/30	0.138
3103	2016/07/07	116.7°	22h50m	+ 9°	2016/07/28	14.3	2016/08/02	0.189
4775	2016/09/12	168.4°	23h28m	+ 7°	2016/09/10	12.7	2016/09/05	0.308
20826	2016/08/05	116.7°	17h28m	-72°	2016/03/22	14.4	2016/04/06	0.337
85990	2016/01/17	161.2°	6h47m	+11°	2016/01/09	14.5	2016/01/06	0.033
96590	2016/11/28	152.9°	3h29m	- 2°	2016/11/23	13.2	2016/11/15	0.120
154244	2016/05/27	171.5°	16h35m	-13°	2016/07/17	13.8	2016/07/22	0.068
164121	2016/10/29	130.9°	5h39m	+18°	2016/10/30	10.9	2016/10/31	0.035

LIGHTCURVE RESULTS FOR ASTEROIDS 900 ROSALINDE, 4666 DIETZ, AND 6302 TENGUKOGEN

Meaghann Stoelting, David R. DeGraff
Stull Observatory
Alfred University
1 Saxon Drive
Alfred, NY USA 14802
mls9@alfred.edu, degraff@alfred.edu

(Received: 2015 October 15)

In the summer of 2011, we made CCD observations of three asteroids to find their rotation periods. For 900 Rosalinde we found a period of 16.648 ± 0.009 h. For 4666 Dietz we found a period of 2.947 ± 0.003 h, and for 6302 Tengukogen we found a period of 3.092 ± 0.014 h.

Between 2011 June 2-9, we observed three asteroids at Stull Observatory using a 0.4-m *f*/8 DFM Ritchey-Chrétien telescope. The telescope was equipped with an SBIG STL-1001 CCD camera. Our goal was to measure a lightcurve for each asteroid in order to determine its rotation period and amplitude.

We used an R filter for all the observations, with exposure times between 2 and 3 minutes depending on the magnitude of the asteroid. *MPO Canopus* v10.4.7.6 (Warner, 2015) was used for all photometric reductions. The maximum of five comparison stars of roughly solar color were selected. Since photometric conditions are very rare in western New York, being downwind from the Great Lakes, we had no color data and so used only differential magnitudes. We found the rotation periods and amplitudes for the lightcurves using the Fourier fitting technique by Harris (Harris *et al.* 1989) as implemented in *MPO Canopus* (Warner, 2015).

900 Rosalinde is a main belt-asteroid discovered by M. Wolf at Heidelberg Observatory in Germany on 1918 August 10 and has an absolute magnitude H = 11.74 (SBD, 2015). We observed it over four nights between 2011 June 4-9 and obtained a period of 16.648 ± 0.009 h with an amplitude of 0.33 mag. This agrees with the results reported by Binzel (1987). We were able to use the amplitude to constrain the shape of the asteroid. Assuming an equatorial view, 900 Rosalinde has a minimum elongation of 1.36:1.

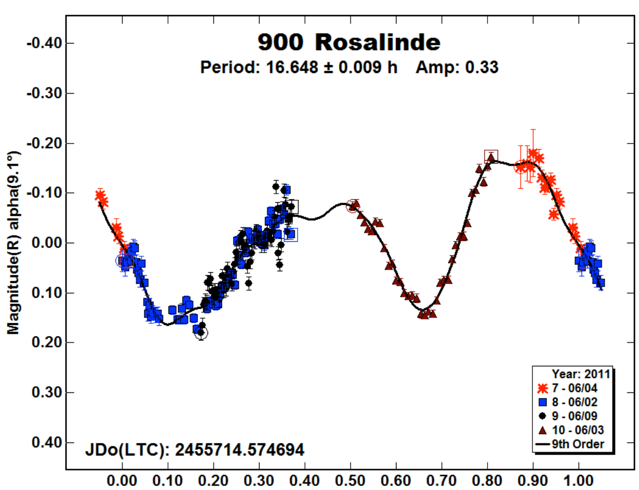

4666 Dietz was discovered on 1986 May 4 by C.S Shoemaker at Palomar Observatory. It is a main-belt asteroid with an absolute magnitude H = 12.7 (SBD, 2015). We observed the asteroid on two nights, 2015 June 2 and 3. Our analysis found a period of 2.947 ± 0.003 h. The period and amplitude of our data are consistent with previous results that were also recorded in 2011: (Behrend, 2011; Ferrero, 2011, Pravec *et al.*, 2011; and Skiff, 2011). The amplitude of 0.26 mag suggests a minimum elongation of 1.26.

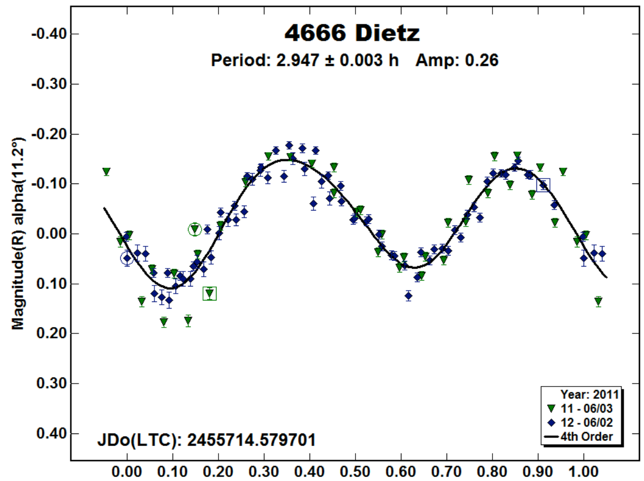

6302 Tengukogen is a main-belt asteroid that was discovered on 1989 Februrary 2 by T. Seki at Geisei Observatory in Japan. It is also known as 1989 CF and has an absolute magnitude H = 13.2 (SBD, 2015). At the time of submission, there were no entries for this asteroid in the Lightcurve Database (LCDB; Warner *et al.*, 2009). This asteroid was observed on 2011 June 3 and 4. After combining the data, we determined a period of 3.09 ± 0.01 h and an amplitude of 0.46 mag.

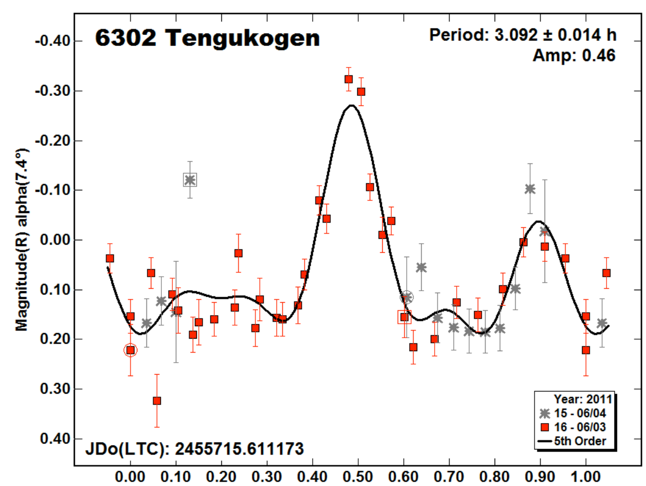

This is an unusual lightcurve with its rapidly brightening peak, but we are convinced that it is a true feature since it occurred twice on the first night of observation and the asteroid did not bypass a star at the time. We calculated a minimum elongation of 1.54 using the amplitude obtained from the lightcurve, but the unusual shape suggests a more interesting profile.

Acknowledgements

We would like to recognize former Alfred University Summer Research students Peter Jones and Casey Dunphy for taking the photometric data of the asteroids in 2011.

References

Behrend, R. (2011). *http://obswww.unige.ch/~behrend/page5cou.html*

Binzel, R.P. (1987). "A photoelectric survey of 130 asteroids." *Icarus* **72**, 135-208.

Ferrero, A. (2011). "Lightcurve Determination of 3151 Talbot and 4666 Dietz." *Minor Planet Bulletin* **38**, 223-224.

Harris, A.W., Young, J.W., Bowell, E., Martin, L.J., Millis, R.L., Poutanen, M., Scaltriti, F., Zappala, V., Schober, H.J., Debehogne, H., Zeigler, K.W. (1989). "Photoelectric Observations of Asteroids 3, 24, 60, 261, and 863." *Icarus* **77**, 171-186.

JPL (2015). Small Body Database Browser. *http://ssd.jpl.nasa.gov/sbdb.cgi#top*

Skiff, B.A. (2011). Posting on CALL web site. http://www.minorplanet.info/call.html

Warner, B.D., Harris, A.W., Pravec, P. (2009). "The asteroid lightcurve database." *Icarus* **202,** 134-146. Updated 2015 February 7. *http://www.minorplanet.info/lightcurvedatabase.html*

Warner, B.D. (2015). *MPO Canopus* software. *http://www.minorplanetobserver.com/MPOSoftware/MPOCanopus.htm*

LIGHTCURVE ANALYSIS OF ASTEROIDS FROM BLUE MOUNTAINS OBSERVATORY IN 2014

Julian Oey
Blue Mountains Observatory (MPC Q68)
94 Rawson Pde. Leura, NSW, AUSTRALIA
julianoey1@optusnet.com.au

(Received: 2015 October 4)

Photometric observations of a number of asteroids were done from Blue Mountains Observatory in 2014. The observations were made in support of the binary asteroid and asteroid pairs campaigns by Petr Pravec, and to obtain new data at favorable apparitions for asteroids with poorly defined lightcurves.

CCD photometric observations were made throughout 2014 from Blue Mountains Observatory where three telescope systems were used. Table I lists the equipment used for the observations. Additional information can be found at the BMO website (BMO, 2014). Unless otherwise specified, all images were taken unfiltered with exposures per image of 300 sec to maximize SNR but at the same time to provide sufficient data point frequency for the more common rotational periods of 2-8 hours.

Data measurement and reduction were done using *MPO Canopus* v10. Period analysis used the Fourier analysis algorithm (FALC) developed by Harris (Harris *et al*., 1989). Calibration of the data (generally < ±0.05 mag) was done using field stars converted to approximate Cousins V magnitudes based on 2MASS J-K colors (Warner, 2007). The Comp Star Selector feature in *MPO Canopus* was used to limit comparison stars to near solar color.

788 Hohensteina was observed by Oey *et al*. (2008) with a result of P = 37.176 h. The data were obtained from 20 sessions over a period of nearly two months with insignificant changes due to changing phase angle. Two observers from different longitudes were used for the campaign and both used an unlinked differential photometry method. In at least one case, a single 14-hour session was created by matching the end of one session with the start of the other, which helped determine the synodic period.

The asteroid was re-observed by the author in 2014 without realizing that Stephens *et al*. (2015) has also conducted an observation campaign and found a period of 29.94 h or 40.87 h with an amplitude of 0.10 mag or 0.15 mag, respectively. Oey's 2014 data were established using the *MPO Canopus* Comp Star Selector utility. Unfortunately no clear result was found.

The inability to find a unique period pointed to the possibility that the asteroid was tumbling. However, the objective was to constrain a primary (or dominant) period. To that end, the nightly zero points were adjusted to within the acceptable calibration error of the catalog, *i.e.*, about ± 0.05 mag, so that each session's slope matched reasonably well. From this, two distinct lightcurves were found, one with a period of 33.02 h and the other with a period of 43.48 h; both have an amplitude of about 0.18mag.

This result differs from that obtained by Stephens *et al.* (2015) and from Oey (2008). These divergent results reinforce the need for a more concerted observing campaign in the future. However, with a small amplitude, relatively long period, and suspected tumbling, the strategy will need to include high-precision linked data and successive long sessions covering widely spaced geographical locations.

749 Malzovia, 1706 Dieckvoss, 1796 Riga, and 2002 Euler were selected from CALL website (Warner, 2014) due to their favorable apparition.

1741 Giclas and 2110 Moore-Sitterly were part of the Photometric Search for Asynchronous Binary Asteroid (PSABA; Pravec, 2014) target selection; however, the selection criteria were also in support of NEO Source paired asteroid project (Pravec *et al*., 2010). 1741 Giclas was observed for one night with the data leading to a period of 3.107 ± 0.001 h. 2110 Moore-Sitterly was found to have a single period of 3.3445 ± 0.0001 h.

2478 Tokai, 2691 Sersic, and 10208 Germanicus. Observations of these previously discovered binary asteroids were made mainly to capture the mutual events (eclipses or occultation) due to the satellite. Complete data sets were obtained by other observers during the same apparitions and were pooled at the Photometric Search for Asynchronous Binary Asteroid (PSABA) web site (Pravec, 2014).

(4555) Josefaperez and (6944) 1979 MR3 were target asteroids that fit the PSABA selection criteria. When a lightcurve shows one or more attenuations but no definitive period for the events could be found, the given asteroid is considered a binary suspect.

4563 Kahnia, 4765 Wasserberg, (8107) 1995 BR4, (8091) 1992 BG, (10597) 1996 TR10, (25327) 1999 JB63, (388468) 2007 DB83, (27300) 2000 AA168, and (56437) 2000 GZ46 were observed as part of the PSABA campaign. They were all found to be singly periodic.

(5510) 1988 RF7 and (20470) 1999 NZ5 happened to be within the same field of view while observing other main targets. Both were in the primary target fields only one or two nights. The periods found were not conclusive and serve only as a guide for future observations.

<u>(5647) 1990 TZ</u> was observed as a routine favorable opposition target selection. During the observing campaign, six consecutive nights of observation were made when the asteroid was near the stationary point in its path across the sky. This provided an opportunity for differential photometry using the same comparison stars for all observing runs. There was a gradual brightening over the six nights that indicated the possibility of secondary period. The brightening due to opposition effect was ruled out since it was one month post-opposition.

<u>6181 Bobweber</u> showed a very small (0.03 mag) attenuation and was considered as binary non-detection. Such asteroids are designated for follow up at a future apparition.

<u>(18082) 2000 GB136</u> was also selected from CALL website. After four nights of observations, it was clear that the rotation period of 11.94 ± 0.02 h was close to being commensurate with the rotation period of the Earth. In such cases, a complete lightcurve and secure period can often be found only with a collaboration among two or more observers at widely-spaced longitudes.

<u>18787 Kathermann</u> was another target meeting the PSABA selection criteria. It was found to have a period of 41.801 ± 0.004 h. So far, all slow-rotating asteroids have been found to be non-binary; the available data were insufficient to determine if the asteroid was a tumbler (Pravec *et al.* 2005).

<u>(39796) 1997 TD</u> had no previously reported period. Despite a sparse data set, analysis of the data from four nights suggested that the asteroid had an estimated rotation period of 40.7 ± 0.1 h and an amplitude of 0.38 ± 0.03 mag.

References

BMO (2014). Blue Mountains Observatory Website *https://www.bluemountainsobservatory.com.au/asteroid/ observatory.html*

Harris, A.W., Young, J.W., Bowell, E., Martin, L.J., Millis, R.L., Poutanen, M., Scaltriti, F., Zappala, V., Schober, H.J., Debehogne, H., Zeigler, K.W. (1989). "Photoelectric Observations of Asteroids 3, 24, 60, 261, and 863." *Icarus* **77**, 171-186.

Oey, J. (2008). "Lightcurve Analysis of Asteroids from Kingsgrove and Leura Observatories in the 2nd half of 2007". Minor Planet Bulletin ***35,*** *132–135*.

Pravec, P., Harris, A.W., Scheirich, P., Kušnirák, P., Šarounová, L., Hergenrother, C.W., Mottola, S., Hicks, M.D., Masi, G., Krugly, Yu.N., Shevchenko, V.G., Nolan, M.C., Howell, E.S., Kaasalainen, M., Galád, A., Brown, P., DeGraff, D.R., Lambert, J.V., Cooney Jr, W.R., Foglia, S. (2005). "Tumbling Asteroids". *Icarus* **173**, 108-131.

Pravec, P., Vokrouhlicky, D., Polishook, D., Scheeres, D.J., Harris, A.W., Galad, A., Vaduvescu, O., Pozo, F., Barr, A., Longa, P., Vachier, F., Colas, F., Pray, D.P., Pollock, J., Reichart, D., Ivarsen, K., Haislip, J., LaCluyze, A., Kušnirák, P., Henych, T., Marchis, F., Macomber, B., Jacobson, S.A., Krugly, Yu.N., Sergeev, A.V., Leroy, A. (2010). "Formation of asteroid pairs by rotational fission." *Nature* **466**, 1085-1088.

Pravec, P. (2014). "Photometric Survey of Asynchronous Binary Asteroids." *http://www.asu.cas.cz/~asteroid/binastphotsurvey.htm*

Stephens, R.D. (2008). "Long period asteroids observed from GMARS and SANTANA observatories." *Minor Planet Bulletin* **35**, 21-22.

Stephens, R.D., Coley, D., Warner ,B.D. (2015). "A lightcurve for 788 Hohensteina." *Minor Planet Bulletin* **42,** 13-15.

Warner, B.D. (2007). "Initial Results from a Dedicated H-G Project." *Minor Planet Bulletin* **34**, 113-119.

Warner, B.D. (2014). CALL website *http://www.minorplanet.info/PHP/call_OppLCDBQuery.php*

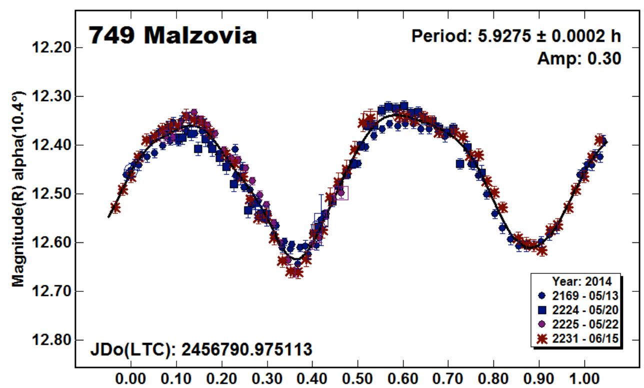

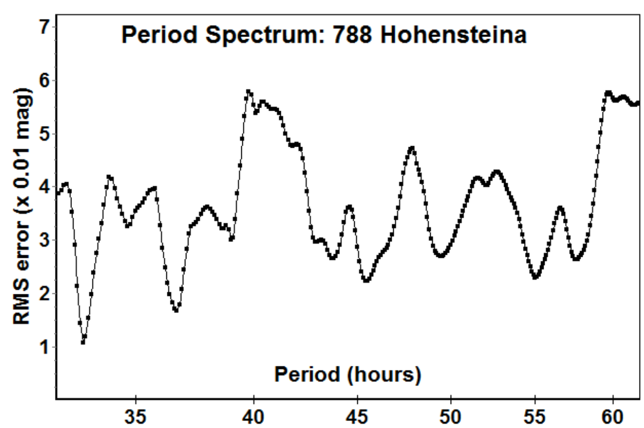

Observatory	Diameter (code)	f/ ratio	Camera	Pixels (microns)	Binning	Scale arcsec/pix
Kingsgrove (E19)	0.25m (10i)	11	ST-402ME (SBIG)	9	1x1	1.41
BMO (Q68)	0.35m (14i)	6	ST8-XME (SBIG)	9	1x1	0.88
BMO (Q68)	0.61m (24if)	6.8	U16M (Apogee)	27	3x3	1.40
BMO (Q68)	0.61m (24ib)	6.8	U42 (Apogee)	13.5	1x1	0.70

Table I. Observatory and telescope/camera systems used.

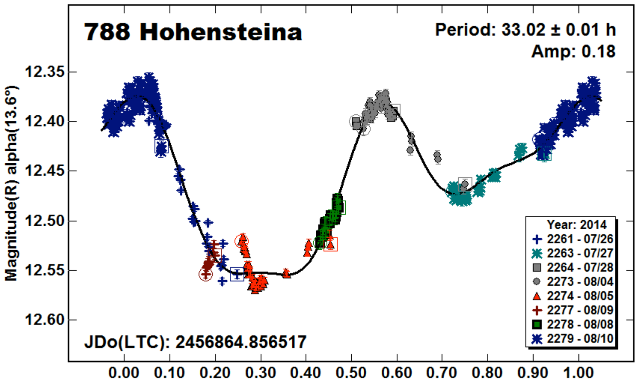
788 Hohensteina
Period: 33.02 ± 0.01 h
Amp: 0.18
Magnitude(R) alpha(13.6°)
Year: 2014
2261 - 07/26
2263 - 07/27
2264 - 07/28
2273 - 08/04
2274 - 08/05
2277 - 08/09
2278 - 08/08
2279 - 08/10
JDo(LTC): 2456864.856517

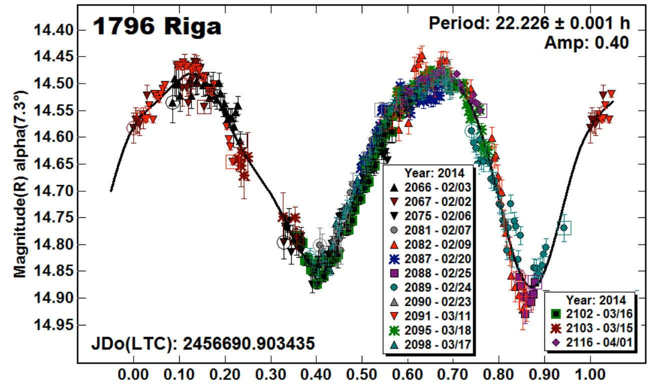
1796 Riga
Period: 22.226 ± 0.001 h
Amp: 0.40
Magnitude(R) alpha(7.3°)
Year: 2014
2066 - 02/03
2067 - 02/02
2075 - 02/06
2081 - 02/07
2082 - 02/09
2087 - 02/20
2088 - 02/25
2089 - 02/24
2090 - 02/23
2091 - 03/11
2095 - 03/18
2098 - 03/17
Year: 2014
2102 - 03/16
2103 - 03/15
2116 - 04/01
JDo(LTC): 2456690.903435

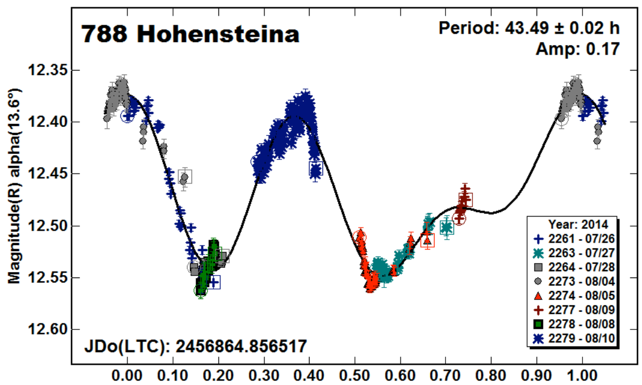
788 Hohensteina
Period: 43.49 ± 0.02 h
Amp: 0.17
Magnitude(R) alpha(13.6°)
Year: 2014
2261 - 07/26
2263 - 07/27
2264 - 07/28
2273 - 08/04
2274 - 08/05
2277 - 08/09
2278 - 08/08
2279 - 08/10
JDo(LTC): 2456864.856517

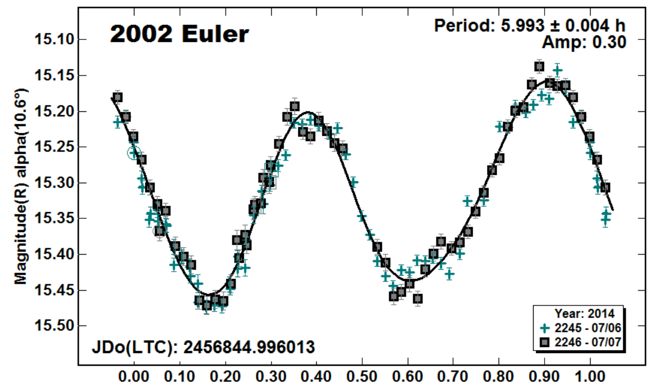
2002 Euler
Period: 5.993 ± 0.004 h
Amp: 0.30
Magnitude(R) alpha(10.6°)
Year: 2014
2245 - 07/06
2246 - 07/07
JDo(LTC): 2456844.996013

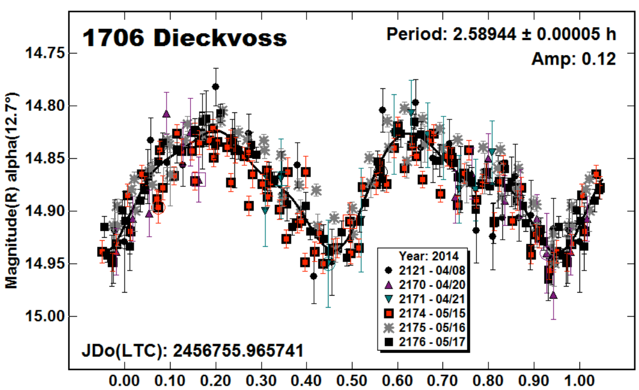
1706 Dieckvoss
Period: 2.58944 ± 0.00005 h
Amp: 0.12
Magnitude(R) alpha(12.7°)
Year: 2014
2121 - 04/08
2170 - 04/20
2171 - 04/21
2174 - 05/15
2175 - 05/16
2176 - 05/17
JDo(LTC): 2456755.965741

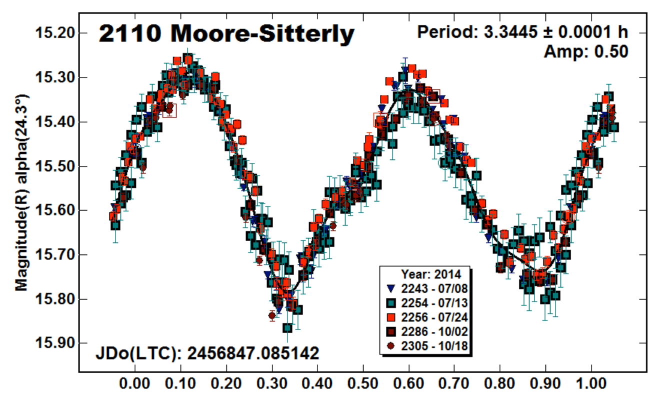
2110 Moore-Sitterly
Period: 3.3445 ± 0.0001 h
Amp: 0.50
Magnitude(R) alpha(24.3°)
Year: 2014
2243 - 07/08
2254 - 07/13
2256 - 07/24
2286 - 10/02
2305 - 10/18
JDo(LTC): 2456847.085142

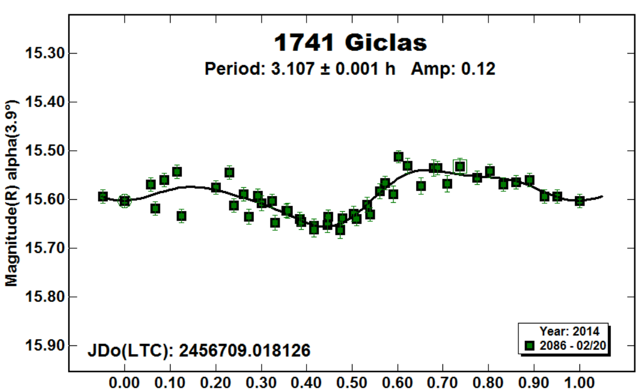
1741 Giclas
Period: 3.107 ± 0.001 h Amp: 0.12
Magnitude(R) alpha(3.9°)
Year: 2014
2086 - 02/20
JDo(LTC): 2456709.018126

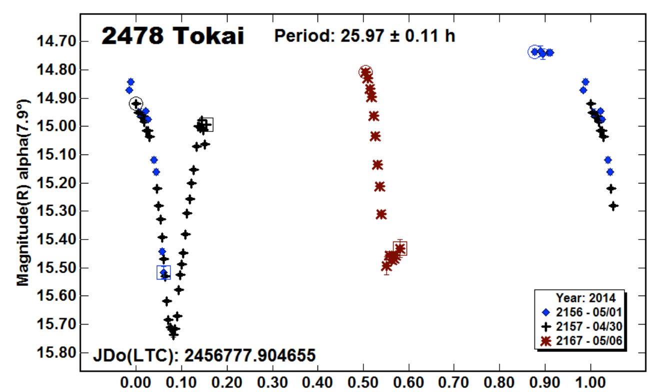
2478 Tokai
Period: 25.97 ± 0.11 h
Magnitude(R) alpha(7.9°)
Year: 2014
2156 - 05/01
2157 - 04/30
2167 - 05/06
JDo(LTC): 2456777.904655

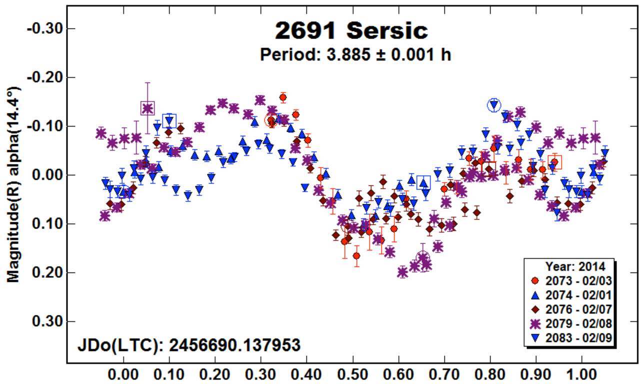
2691 Sersic
Period: 3.885 ± 0.001 h
Magnitude(R) alpha(14.4°)
Year: 2014
2073 - 02/03
2074 - 02/01
2076 - 02/07
2079 - 02/08
2083 - 02/09
JDo(LTC): 2456690.137953

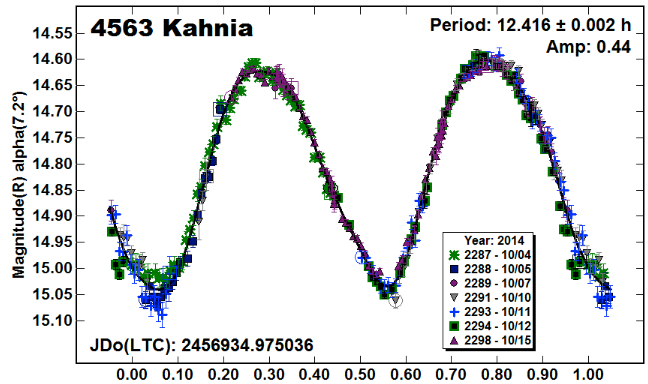
4563 Kahnia
Period: 12.416 ± 0.002 h
Amp: 0.44
Magnitude(R) alpha(7.2°)
Year: 2014
2287 - 10/04
2288 - 10/05
2289 - 10/07
2291 - 10/10
2293 - 10/11
2294 - 10/12
2298 - 10/15
JDo(LTC): 2456934.975036

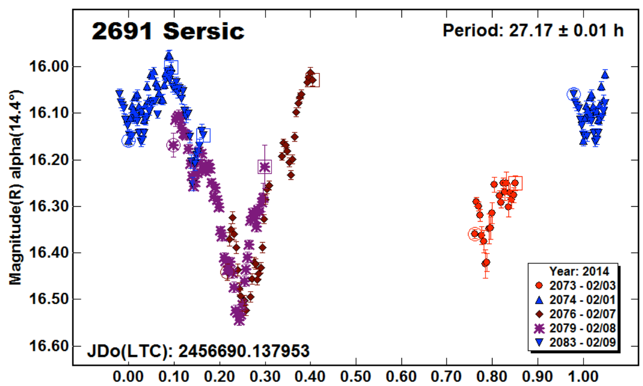
2691 Sersic
Period: 27.17 ± 0.01 h
Magnitude(R) alpha(14.4°)
Year: 2014
2073 - 02/03
2074 - 02/01
2076 - 02/07
2079 - 02/08
2083 - 02/09
JDo(LTC): 2456690.137953

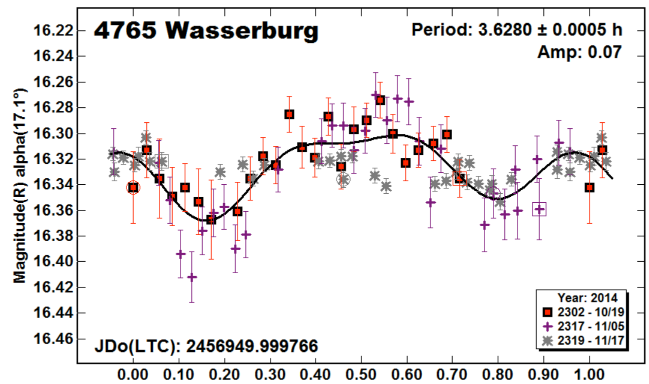
4765 Wasserburg
Period: 3.6280 ± 0.0005 h
Amp: 0.07
Magnitude(R) alpha(17.1°)
Year: 2014
2302 - 10/19
2317 - 11/05
2319 - 11/17
JDo(LTC): 2456949.999766

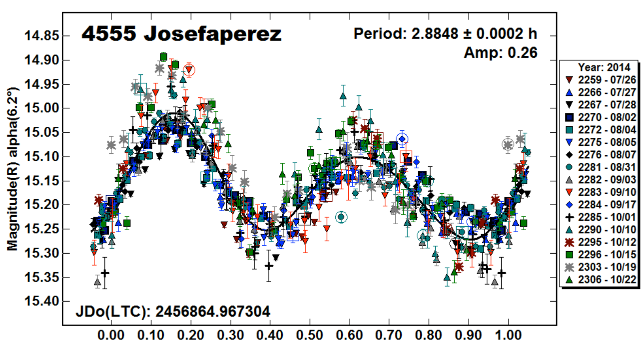
4555 Josefaperez
Period: 2.8848 ± 0.0002 h
Amp: 0.26
Magnitude(R) alpha(6.2°)
Year: 2014
2259 - 07/26
2266 - 07/27
2267 - 07/28
2270 - 08/02
2272 - 08/04
2275 - 08/05
2276 - 08/07
2281 - 08/31
2282 - 09/03
2283 - 09/10
2284 - 09/17
2285 - 10/01
2290 - 10/10
2295 - 10/12
2296 - 10/15
2303 - 10/19
2306 - 10/22
JDo(LTC): 2456864.967304

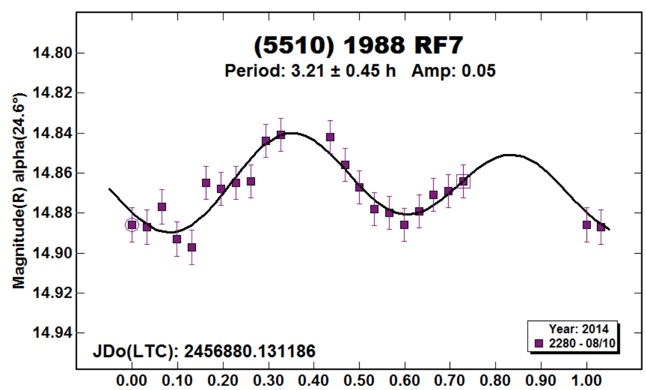
(5510) 1988 RF7
Period: 3.21 ± 0.45 h Amp: 0.05
Magnitude(R) alpha(24.6°)
Year: 2014
2280 - 08/10
JDo(LTC): 2456880.131186

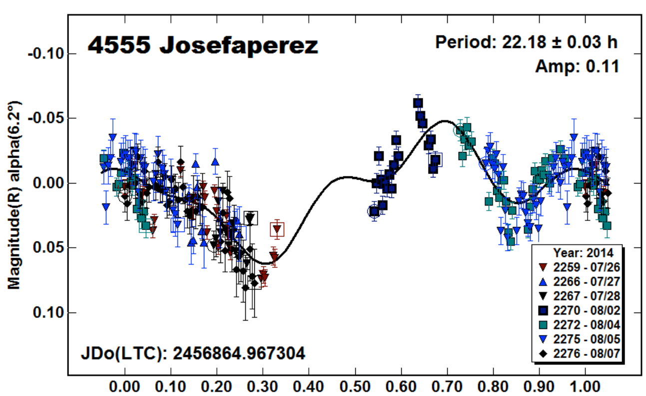
4555 Josefaperez
Period: 22.18 ± 0.03 h
Amp: 0.11
Magnitude(R) alpha(6.2°)
Year: 2014
2259 - 07/26
2266 - 07/27
2267 - 07/28
2270 - 08/02
2272 - 08/04
2275 - 08/05
2276 - 08/07
JDo(LTC): 2456864.967304

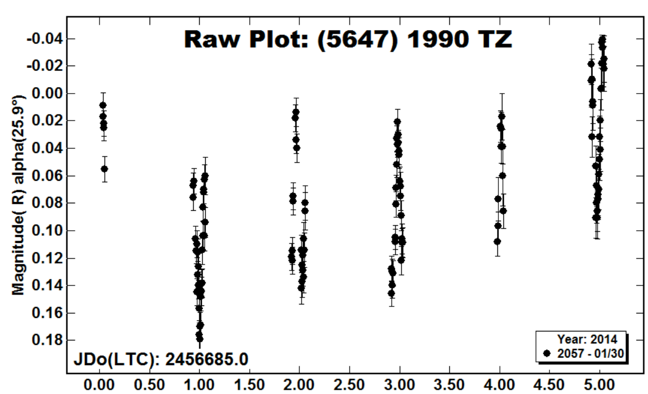
Raw Plot: (5647) 1990 TZ
Magnitude(R) alpha(25.9°)
Year: 2014
2057 - 01/30
JDo(LTC): 2456685.0

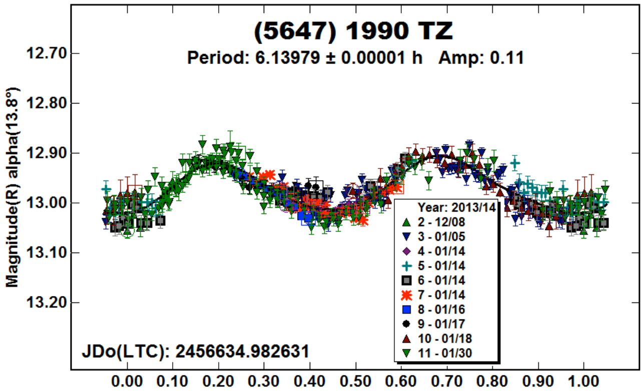
(5647) 1990 TZ
Period: 6.13979 ± 0.00001 h Amp: 0.11
Magnitude(R) alpha(13.8°)
Year: 2013/14
2 - 12/08
3 - 01/05
4 - 01/14
5 - 01/14
6 - 01/14
7 - 01/14
8 - 01/16
9 - 01/17
10 - 01/18
11 - 01/30
JDo(LTC): 2456634.982631

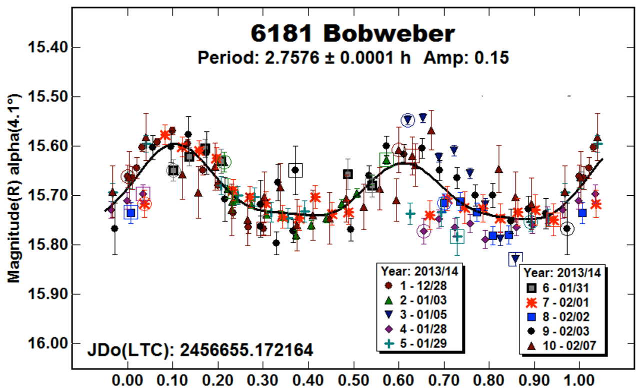
6181 Bobweber
Period: 2.7576 ± 0.0001 h Amp: 0.15
Magnitude(R) alpha(4.1°)
Year: 2013/14
1 - 12/28
2 - 01/03
3 - 01/05
4 - 01/28
5 - 01/29
Year: 2013/14
6 - 01/31
7 - 02/01
8 - 02/02
9 - 02/03
10 - 02/07
JDo(LTC): 2456655.172164

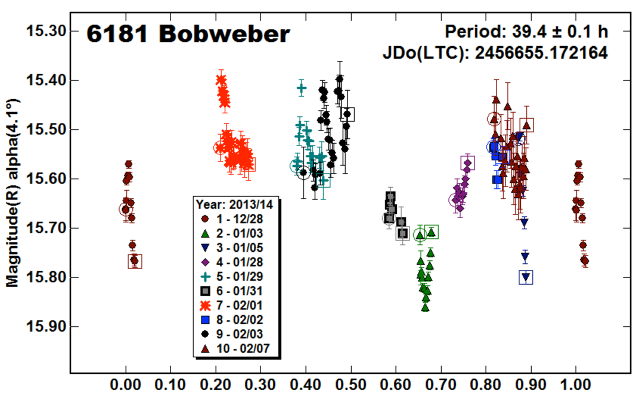
6181 Bobweber
Period: 39.4 ± 0.1 h
JDo(LTC): 2456655.172164
Magnitude(R) alpha(4.1°)
Year: 2013/14
1 - 12/28
2 - 01/03
3 - 01/05
4 - 01/28
5 - 01/29
6 - 01/31
7 - 02/01
8 - 02/02
9 - 02/03
10 - 02/07

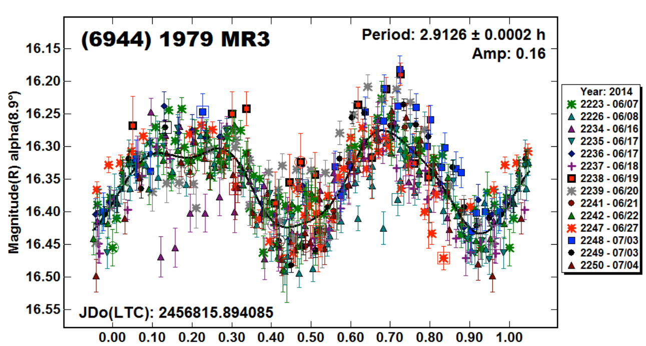
(6944) 1979 MR3
Period: 2.9126 ± 0.0002 h
Amp: 0.16
Magnitude(R) alpha(8.9°)
Year: 2014
2223 - 06/07
2226 - 06/08
2234 - 06/16
2235 - 06/17
2236 - 06/17
2237 - 06/18
2238 - 06/19
2239 - 06/20
2241 - 06/21
2242 - 06/22
2247 - 06/27
2248 - 07/03
2249 - 07/03
2250 - 07/04
JDo(LTC): 2456815.894085

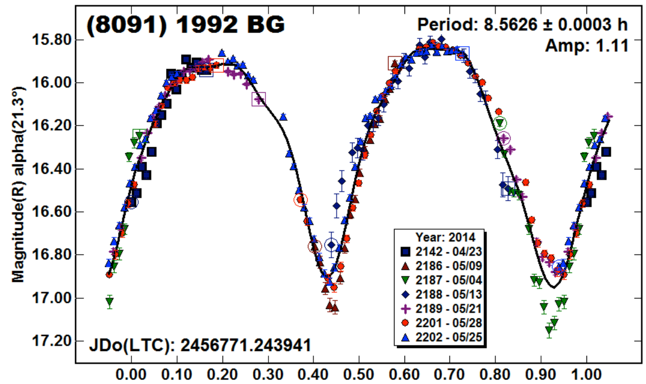
(8091) 1992 BG
Period: 8.5626 ± 0.0003 h
Amp: 1.11
Magnitude(R) alpha(21.3°)
Year: 2014
2142 - 04/23
2186 - 05/09
2187 - 05/04
2188 - 05/13
2189 - 05/21
2201 - 05/28
2202 - 05/25
JDo(LTC): 2456771.243941

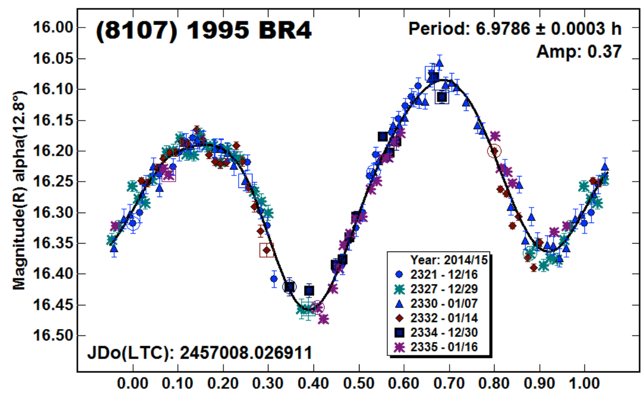
(8107) 1995 BR4
Period: 6.9786 ± 0.0003 h
Amp: 0.37
Magnitude(R) alpha(12.8°)
Year: 2014/15
2321 - 12/16
2327 - 12/29
2330 - 01/07
2332 - 01/14
2334 - 12/30
2335 - 01/16
JDo(LTC): 2457008.026911

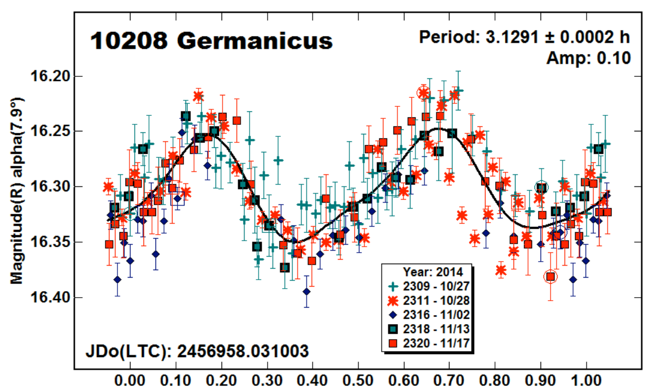
10208 Germanicus
Period: 3.1291 ± 0.0002 h
Amp: 0.10
Magnitude(R) alpha(7.9°)
Year: 2014
2309 - 10/27
2311 - 10/28
2316 - 11/02
2318 - 11/13
2320 - 11/17
JDo(LTC): 2456958.031003

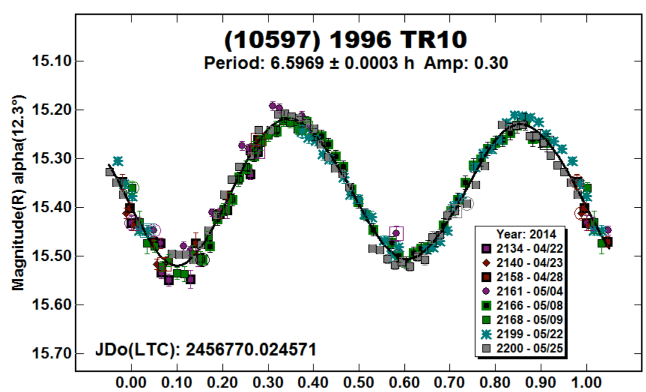
(10597) 1996 TR10
Period: 6.5969 ± 0.0003 h Amp: 0.30
Magnitude(R) alpha(12.3°)
Year: 2014
2134 - 04/22
2140 - 04/23
2158 - 04/28
2161 - 05/04
2166 - 05/08
2168 - 05/09
2199 - 05/22
2200 - 05/25
JDo(LTC): 2456770.024571

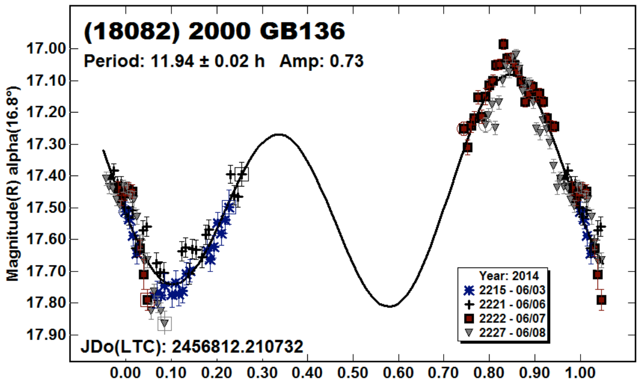
(18082) 2000 GB136
Period: 11.94 ± 0.02 h Amp: 0.73
Magnitude(R) alpha(16.8°)
Year: 2014
2215 - 06/03
2221 - 06/06
2222 - 06/07
2227 - 06/08
JDo(LTC): 2456812.210732

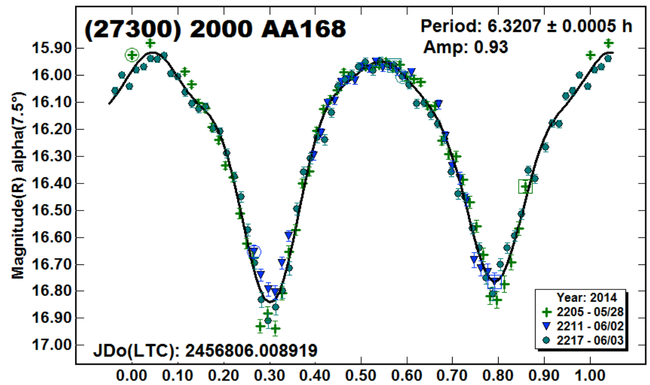
(27300) 2000 AA168
Period: 6.3207 ± 0.0005 h
Amp: 0.93
Magnitude(R) alpha(7.5°)
Year: 2014
2205 - 05/28
2211 - 06/02
2217 - 06/03
JDo(LTC): 2456806.008919

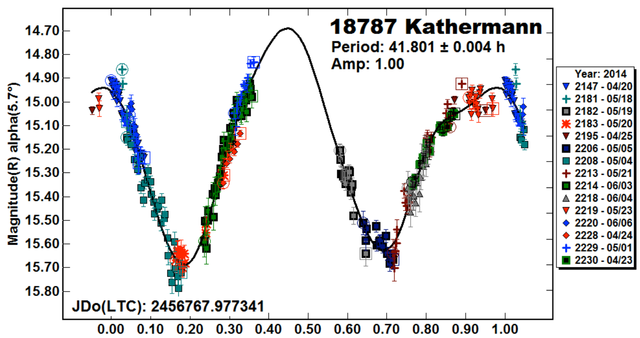
18787 Kathermann
Period: 41.801 ± 0.004 h
Amp: 1.00
Magnitude(R) alpha(5.7°)
Year: 2014
2147 - 04/20
2181 - 05/18
2182 - 05/19
2183 - 05/20
2195 - 04/25
2206 - 05/05
2208 - 05/04
2213 - 05/21
2214 - 06/03
2218 - 06/04
2219 - 05/23
2220 - 06/06
2228 - 04/24
2229 - 05/01
2230 - 04/23
JDo(LTC): 2456767.977341

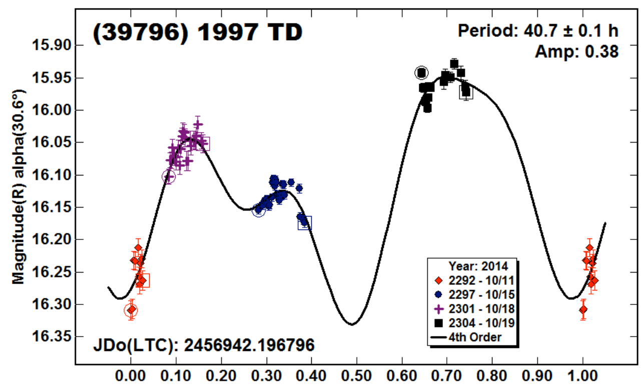
(39796) 1997 TD
Period: 40.7 ± 0.1 h
Amp: 0.38
Magnitude(R) alpha(30.6°)
Year: 2014
2292 - 10/11
2297 - 10/15
2301 - 10/18
2304 - 10/19
4th Order
JDo(LTC): 2456942.196796

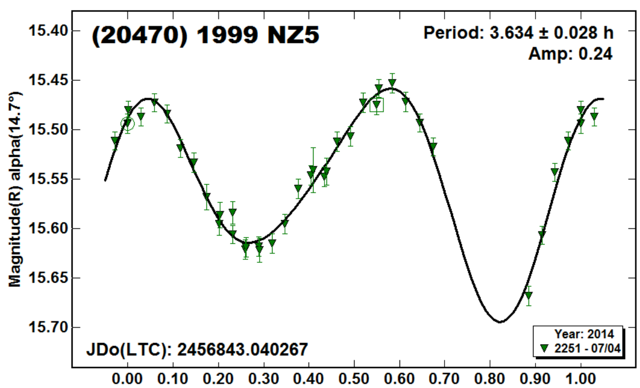
(20470) 1999 NZ5
Period: 3.634 ± 0.028 h
Amp: 0.24
Magnitude(R) alpha(14.7°)
Year: 2014
2251 - 07/04
JDo(LTC): 2456843.040267

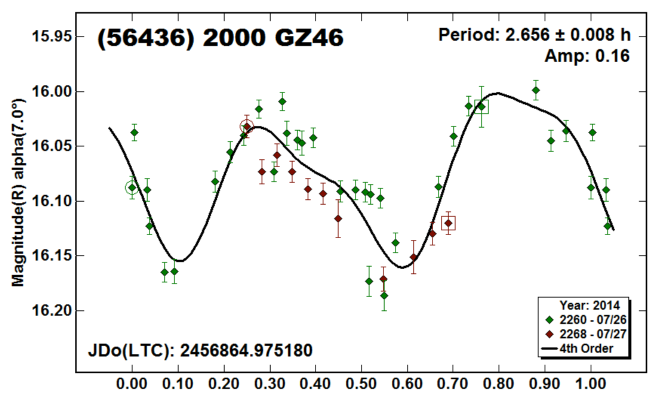
(56436) 2000 GZ46
Period: 2.656 ± 0.008 h
Amp: 0.16
Magnitude(R) alpha(7.0°)
Year: 2014
2260 - 07/26
2268 - 07/27
4th Order
JDo(LTC): 2456864.975180

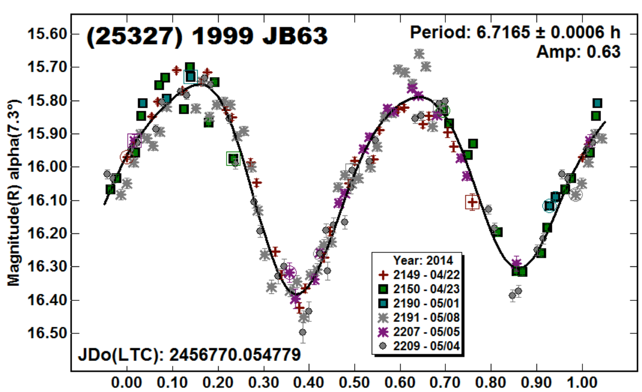
(25327) 1999 JB63
Period: 6.7165 ± 0.0006 h
Amp: 0.63
Magnitude(R) alpha(7.3°)
Year: 2014
2149 - 04/22
2150 - 04/23
2190 - 05/01
2191 - 05/08
2207 - 05/05
2209 - 05/04
JDo(LTC): 2456770.054779

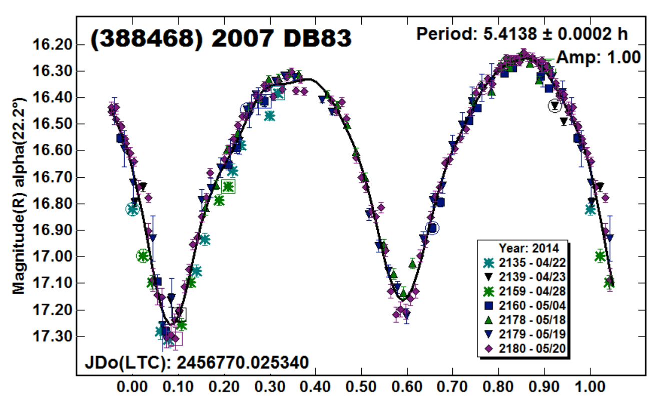
(388468) 2007 DB83
Period: 5.4138 ± 0.0002 h
Amp: 1.00
Magnitude(R) alpha(22.2°)
Year: 2014
2135 - 04/22
2139 - 04/23
2159 - 04/28
2160 - 05/04
2178 - 05/18
2179 - 05/19
2180 - 05/20
JDo(LTC): 2456770.025340

#	Name	mm/dd 2014 start-end	Inst	Period (h)	PE	Amp (mag)	AE	H	Dia (km)	Phase	L_{PAB}	B_{PAB}
788	Hohensteina	07/26 08/10	14i	33.02 43.49	0.01 0.02	0.18 0.17	0.05 0.05	8.6	105.15	13.4 16.5	274	17
749	Malzovia	05/13 06/15	10i	5.9275	0.0002	0.30	0.02	11.82	13.55	10.7	245	6.4
1706	Dieckvoss	04/08 05/17	14i	2.58944	0.00005	0.12	0.03	12.9	8.26	13.0 11.0	217.2 220.2	-2.6 -2.3
1741	Giclas	02/20	24if	3.107	0.001	0.12	0.02	11.4	28.96	4.1	160.9	3.4
1796	Riga	02/03 04/01	14i	22.226	0.001	0.40	0.05	9.84	59.4	7.3 15.0	142	-20 -15.8
2002	Euler	07/06 07/07	14i	5.993	0.004	0.30	0.02	12.3	10.86	20	298	10
2110	Moore-Sitterly	07/08	14i	3.3445	0.0001	0.50	0.02	13.2	7.18	24.5	321.6	0.3
2691	Sersic	02/03 02/09	24if	3.885 27.17*	0.001 0.01	0.20 0.50	0.05 0.05	13.1	7.51	26.5 24.5	198.2 204.6	-3.3
2478	Tokai	04/30 05/06	24if	25.97 *	0.11	1.0	0.1	12	12.47	7.0 10.0	206.9 207.2	-1.8 -1.6
4555	Josefaperez	07/26 10/22	14i	2.8848	0.0002	0.26	0.02	13.8	5.44	6.4 30.6	307.9 328.1	6.4 -0.8
4563	Kahnia	10/04 10/15	14i	12.416	0.002	0.44	0.02	13.2	7.18	7.4 4.9	18.6 19.5	-6.6 -6.8
4765	Wasserburg	10/19 11/17	14i	3.6280	0.0005	0.07	0.02	13.7	5.7	17.3 11.3, 11.7	45.7 45.8	-21 -16.8
5647	1990 TZ	13/12/08 14/01/30	10i	6.13979	0.00001	0.11	0.02	12	12.47	13.9 26.5	88.7 96.2	-14.3 -24
5510	1988 RF7	08/10	14i	3.21	0.45	0.05	0.01	13.4	6.54	24.8	347.4	-6.6
6181	Bobweber	13/12/28 14/02/07	14i	2.7576 39.4 *	0.0001 0.1	0.15 0.30	0.01 0.05	12.5	6.25	4.4 17.7	101.7 104.7	4.4 1.7
6944	1979 MR3	06/07 07/04	24if	2.9126	0.0002	0.16	0.04	14.2	4.53	8.6 20.2	245.6 248.4	8.9 7.3
8091	1992 BG	04/23 05/25	24if	8.5626	0.0003	1.11	0.03	13.7	5.7	21.4 10.1	246.7 250.4	13.6 14.2
8107	1995 BR4	12/16 01/16	24if	6.9786	0.0003	0.37	0.01	13.8	5.44	13.0 4.3, 7.2	104 105.6	-7.6 -6.4
10208	Germanicus	10/27 11/17	14i	3.1291	0.0002	0.10	0.02	14.4	4.13	8.2 4.9	45.6 46.6	0.2 -0.6
10597	1996 TR10	04/22 05/25	14i	6.5969	0.0003	0.30	0.01	13	7.87	12.5 8.9, 12.5	228.4 230.2	13.3 14.8
18082	2000 GB136	06/03 06/08	14i	11.94	0.02	0.73	0.01	14.2	4.53	17.0 14.8	278.7 279.4	-3.2 -3.6
18787	Kathermann	04/20 06/06	14i	41.801	0.004	1.00	0.05	14.6	3.77	5.9 22.1	213.6 219.5	7.6 2.9
25327	1999 JB63	04/22 05/08	24if	6.7165	0.0006	0.63	0.03	13.9	5.2	7.3 9.8	213.7 214.6	11.5 9.9
20470	1999 NZ5	07/04	14i	3.634	0.028	0.24	0.02	13.5	6.25	14.8	299.8	12.5
27300	2000 AA168	05/28 06/03	24if	6.3207	0.0005	0.93	0.03	13.7	5.7	7.5	247.1	12.8
39796	1997 TD	10/15 10/19	24ib	40.7	0.1	0.38	0.03	15.7	2.27	28.6	44.3	-19.7
56436	2000 GZ46	07/26	24if	2.656	0.008	0.16	0.04	14.7	3.6	7.1	307.3	8.1
388468	2007 DB83	04/22 05/20	14i	5.4138	0.0002	1.00	0.02	18.29	0.69	22.6 0.3, 3.8	223.6 236.5	11.5 -1.6

Table II. 24i: 0.61-m+U42, 14i: SCT 0.35-m, 10i: SCT 0.2-5m. *Orbital period of the satellite of the binary asteroid. The Phase column gives the solar phase angle on the first and last date. If there are three values, the phase angle reached a minimum value during the period. The phase angle bisector columns give the values for the first and last date of observation.

ASTEROIDS OBSERVED FROM CS3: 2015 JULY - SEPTEMBER

Robert D. Stephens
Center for Solar System Studies (CS3)/MoreData!
11355 Mount Johnson Ct., Rancho Cucamonga, CA 91737 USA
rstephens@foxandstephens.com

(Received: 2015 October 6)

Lightcurves for 20 asteroids were obtained from the Center for Solar System Studies from 2015 July to September.

This calendar quarter the Center for Solar System Studies (CS3, MPC U81) selected targets of opportunity because of the short Northern Hemisphere summer nights, low ecliptic, and location of the Milky Way. This required selecting targets high in inclination such as Hungarias and Hildas. Some of these had previously determined rotational periods and further observations were acquired so that over time pole positions and shape models can be calculated.

All images were made with a 0.4-m or a 0.35-m SCT using an FLI-1001E or a SBIG STL-1001E CCD camera. Images were unbinned with no filter and had master flats and darks applied to the science frames prior to measurement. Measurements were made using *MPO Canopus*, which employs differential aperture photometry to produce the raw data. Period analysis was done using *MPO Canopus*, which incorporates the Fourier analysis algorithm (FALC) developed by Harris (Harris *et al*., 1989). Night-to-night calibration of the data (generally < ±0.05 mag) was done using field stars converted to approximate Cousins V magnitudes based on 2MASS J-K colors (Warner 2007). The Comp Star Selector feature in *MPO Canopus* was used to limit the comparison stars to near solar color.

1600 Vyssotsky. Vyssotsky has been well studied over the years and a pole solution has been found. Warner (Warner 2014) observed this Hungaria in 1999, 2004, 2005, 2007, 2009, 2010, and 2014; each time finding a rotational period of about 3.2 h. Observations were obtained this year to improve the pole solution model.

2253 Espinette. A rotational period for Espinette has been determined several times in the past. Wisniewski (Wisniewski *et al* 1995) reported a rotational period of 7.3 h. Behrend (Behrend 2015) and Skiff reported periods of 7.440 h and 7.442 h respectively. This result agrees with those prior period determinations.

2974 Holden. No previously reported results could be found in the Lightcurve Database (LCDB; Warner et al., 2009) for this Vestoid. Given its long rotational period of 856 h, it would expected to see it in a tumbling state since the dampening time exceeds the age of the solar system. There are some hints of tumbling in individual nightly sessions, which cannot be seen in the compressed X-axis scale. However, since it took over a month to complete one rotation, it is not likely enough data could be acquired to determine a secondary frequency.

3561 Devine. For this Hilda, rotational periods of 4.376 h and 5.354 h have nearly identical strength solutions. I have adopted the 4.376 h period here, because the extrema are 50% phase apart. However, with an amplitude of 0.08 mag., the lightcurve could be asymmetric and dominated by surface features. A period spectrum is presented to show the various aliases.

6085 Fraethi. The Lightcurve Database (LCDB; Warner et al., 2009) contains a rotational period for this Vestoid of 6.0 h reported by Behrend (Behrend 2015). However, a lightcurve plot cannot be found on that website.

6183 Viscome. Given its long rotational period, it is not usual that reported results could not be found in the Lightcurve Database (LCDB; Warner et al., 2009). The Photometric Survey for Asynchronous Binary Asteroids (Parvec *et al* 2015) reported a period on their website of 437 h using much sparser data. I was able to obtain coverage of about 110% of the phased lightcurve, which shows signs of tumbling as the magnitude at the first maximum are much greater at the start of the run than at the end of the end of the run.

Number	Name	2015 mm\dd	Pts	Phase	L_{PAB}	B_{PAB}	Period	P.E.	Amp	A.E.	Grp
1600	Vyssotsky	09/29-09/30	106	26.2,25.8	44	-15	3.204	0.003	0.21	0.02	H
2253	Espinette	08/02-08/10	165	32.2,29.7	356	-2	7.442	0.001	0.44	0.01	MC
2468	Repin	07/03-07/12	142	30.6,29.8	348	6	5.122	0.001	0.72	0.02	V
2974	Holden	08/29-10/03	176	21.5,4.1	13	4	856	2	0.7	0.05	V
3202	Graff	07/21-07/25	234	4.3,3.8	309	12	17.32	0.02	0.18	0.02	HIL
3561	Devine	07/07-07/15	127	12.8,14.1	241	8	4.376	0.002	0.08	0.01	HIL
4302	Markeev	07/09-07/13	171	20.6,19.4	329	2	5.134	0.002	0.31	0.02	V
6085	Fraethi	08/31-09/03	186	5.0,5.7	336	7	5.556	0.001	0.79	0.02	V
6183	Viscome	09/03-09/27	123	21.4,25.2	346	30	453	10	0.9	0.1	PHO
6189	Volk	08/28-09/06	438	20.9,17.4	11	7	2.896	0.001	0.18	0.02	V
6984	Lewiscarrol	07/14-07/29	587	11.0,8.8	338	15	24.65	0.05	0.16	0.02	HIL
7187	Isobe	09/29-09/30	137	31.1,31.0	49	29	4.241	0.006	0.22	0.03	H
17399	Andysanto	08/21-08/24	271	26.9,25.7	4	6	2.692	0.001	0.07	0.02	H
20037	Duke	08/03-08/06	184	28.1,28.5	301	36	5.29	0.01	0.17	0.03	H
23715	1998 FK2	08/23-08/28	187	24.9,22.6	5	6	7.434	0.002	0.36	0.03	H
27351	2000 DO73	08/11-08/17	226	28.2,25.9	356	-2	9.008	0.003	0.16	0.02	MC
37744	1996 XU14	08/08-08/22	676	24.3,18.7	351	9	35.51	0.007	0.73	0.02	H
47143	1999 LL31	07/16-07/17	77	15.0,15.1	284	22	3.312	0.004	0.36	0.03	H
53453	1999 XX135	08/18-08/20	183	20.0,19.6	344	24	3.407	0.002	0.37	0.02	H
74590	1999 OG2	07/26-08/06	600	26.6,22.8	329	26	33.409	0.005	0.86	0.02	H

6984 Lewiscarrol. No previously reported results could be found in the Lightcurve Database (LCDB; Warner et al., 2009). This is not surprising as the rotational period has gone down the rabbit hole. I have adopted a rotational period of 24.65 h, nearly commensurate with the Earth's rotation. However, as the Period Spectrum shows, there are strong aliases near 12 h and 48 h, which are possible scenarios for this low amplitude lightcurve.

7187 Isobe. This Hungaria has also been studied extensively by Warner (Warner 2013b) with observations in 2004, 2007, 2011, and 2012. Observations in 2004 and 2012 suggest that Isobe is probably a binary, with a secondary period near 33 h. The two nights of observations in 2015 did not reveal any mutual events.

20037 Duke. Warner (Warner 2011), reported that this Hungaria was a weak candidate to be a binary, with a primary period of 5.428 h. At this opposition, the lightcurve was dominated by noise and a secondary period could not be extracted. The derived rotational period of 5.29 h is in fair agreement with the Warner result.

(23715) 1998 FK2. This Hungaria was previously observed by Warner (Warner 2013) who found a rotational period of 7.436 h. This year's result is in agreement with that period.

(47143) 1999 LL31. Warner (Warner 2012) reports a rotational period of 3.32 h. Using data from the Palomar Transient Factory (PTF) Survey, Waszczak (Waszczak *et al* 2015) reports a period of 3.3262. This result agrees with those previously reported periods.

(74590) 1999 OG2. Using the PTF data, Waszczak (Waszczak *et al* 2015) reports a period of 33.3185 h. Warner (Warner 2008) previously found a similar period of 33.273 h. My result is agrees with those periods.

References

Behrend, R., (2015). Observatoire de Geneve web site, *http://obswww.unige.ch/~behrend/page_cou.html*

Chang, C.-K., Ip, W.-H., Lin, H.-W., Cheng, Y.-C., Ngeow, C.-C., Yang, T.-C., Waszczak, A., Kulkarni, S. R., Levitan, D., Sesar, B., Laher, R., Surace, J., Prince, T.A. (2015). "Asteroid Spin-rate Study Using the Intermediate Palomar Transit Factory." *Ap. J. Suppl. Ser.* **219**, A27.

Harris, A.W., Young, J.W., Bowell, E., Martin, L.J., Millis, R.L., Poutanen, M., Scaltriti, F., Zappala, V., Schober, H.J., Debehogne, H., Zeigler, K. (1989). "Photoelectric Observations of Asteroids 3, 24, 60, 261, and 863." *Icarus* 77, 171-186.

Parvec, P. (2015). Photometric Survey for Asynchronous Binary Asteroids web site.
http://www.asu.cas.cz/~asteroid/binastphotsurvey.htm

Warner, B.D. (2007). "Asteroid Lightcurve Analysis at the Palmer Divide Observatory - December 2006 - March 2007." *Minor Planet Bul*. **34**, 72-77.

Warner, B.D. (2007). "Initial Results from a Dedicated H-G Project." *Minor Planet Bul*. **37**, 57-64.

Warner, B.D. (2008). "Asteroid Lightcurve Analysis at the Palmer Divide Observatory - June - October 2007." *Minor Planet Bul*. **35**, 56-60.

Warner, B.D., Stephens, R.D., Harris, A.W. (2011). "Save the Lightcurves." *Minor Planet Bul*. **33**, 172-174.

Warner, B.D. (2011). "A Quartet of Known and Suspected Hungaria Binary Asteroids." *Minor Planet Bul*. **38**, 33-36.

Warner, B.D. (2013). "Asteroid Lightcurve Analysis at the Palmer Divide Observatory: 2012 June - September." *Minor Planet Bul*. **40**, 26-29.

Warner, B.D. (2013b). "Rounding Up the Unusual Suspects." *Minor Planet Bul*. **40**, 36-42.

Warner, B.D. (2014). "Asteroid Lightcurve Analysis at CS3-Palmer Divide Station: 2014 January-March." *Minor Planet Bul*. **41**, 144-155.

Warner, B.D., Harris, A.W., Pravec, P. (2009). *Icarus* **202**, 134-146. Updated 2015 September 1.
http://www.minorplanet.info/lightcurvedatabase.html.

Waszczak, A., Chang, C-K, Ofek, E.O., Laher, R., Masci, F., Levitan, D., Surace, J., Cheng, Y-C., Ip, W-H., Kinoshita, D., Helou, G., Prince, T.A., Kulkarni, S. (2015). "Asteroid Light Curves from the Palomar Transient Factory Survey: Rotation Periods and Phase Functions from Sparse Photometry." *Ap. J.* **150,** 75.

Wisniewski, W.Z., Michalowski, T.M., Harris, A.W., McMillan, R.S. (1995). "Photoelectric Observations of 125 Asteroids." *Abstracts of the Lunar and Planetary Science Conference.* **26**, 1511.

Acknowledgements

This research was supported by NASA grant NNX13AP56G.

The purchase of the FLI-1001E CCD camera was made possible by a 2013 Gene Shoemaker NEO Grant from the Planetary Society.

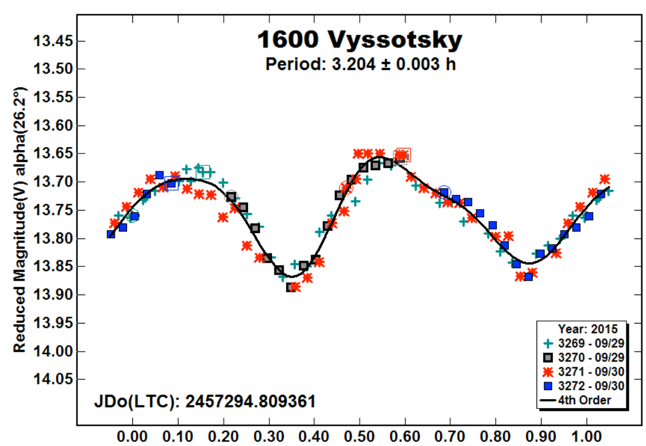

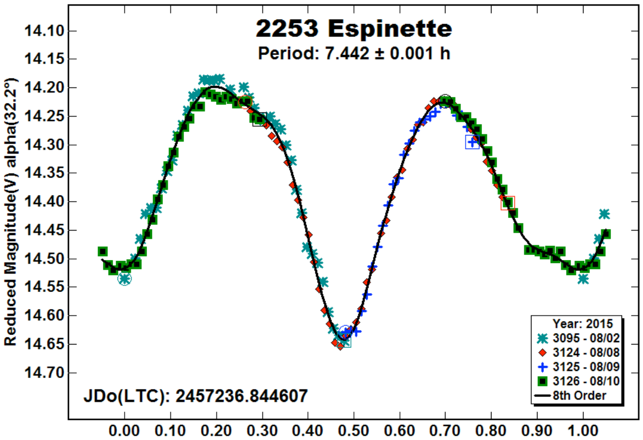
2253 Espinette
Period: 7.442 ± 0.001 h
Reduced Magnitude(V) alpha(32.2°)
Year: 2015
3095 - 08/02
3124 - 08/08
3125 - 08/09
3126 - 08/10
8th Order
JDo(LTC): 2457236.844607

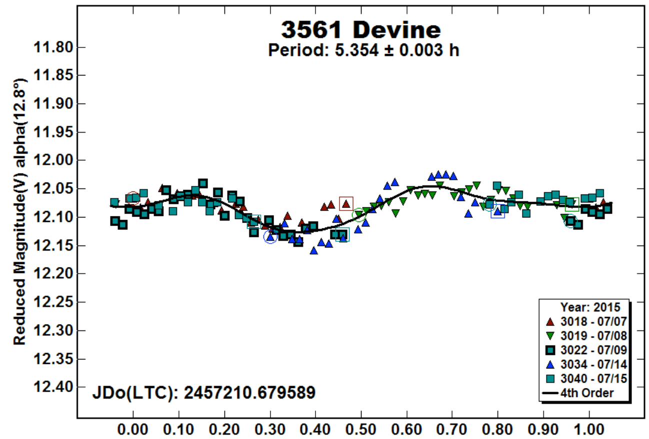
3561 Devine
Period: 5.354 ± 0.003 h
Reduced Magnitude(V) alpha(12.8°)
Year: 2015
3018 - 07/07
3019 - 07/08
3022 - 07/09
3034 - 07/14
3040 - 07/15
4th Order
JDo(LTC): 2457210.679589

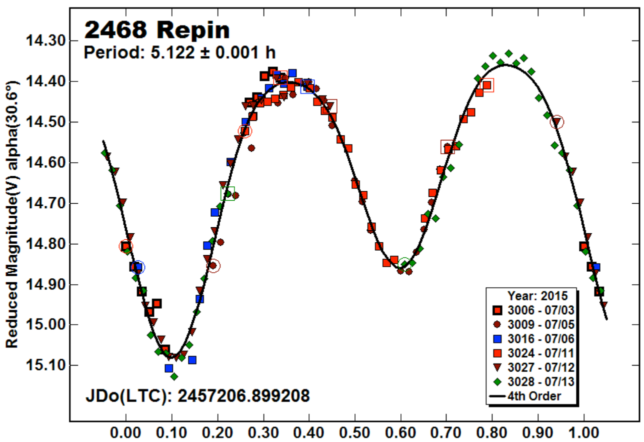
2468 Repin
Period: 5.122 ± 0.001 h
Reduced Magnitude(V) alpha(30.6°)
Year: 2015
3006 - 07/03
3009 - 07/05
3016 - 07/06
3024 - 07/11
3027 - 07/12
3028 - 07/13
4th Order
JDo(LTC): 2457206.899208

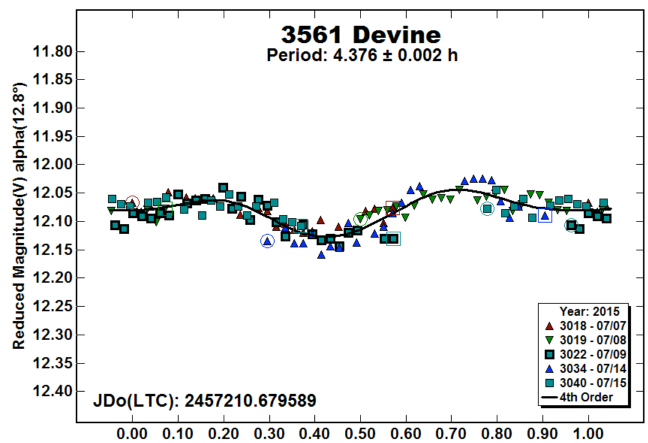
3561 Devine
Period: 4.376 ± 0.002 h
Reduced Magnitude(V) alpha(12.8°)
Year: 2015
3018 - 07/07
3019 - 07/08
3022 - 07/09
3034 - 07/14
3040 - 07/15
4th Order
JDo(LTC): 2457210.679589

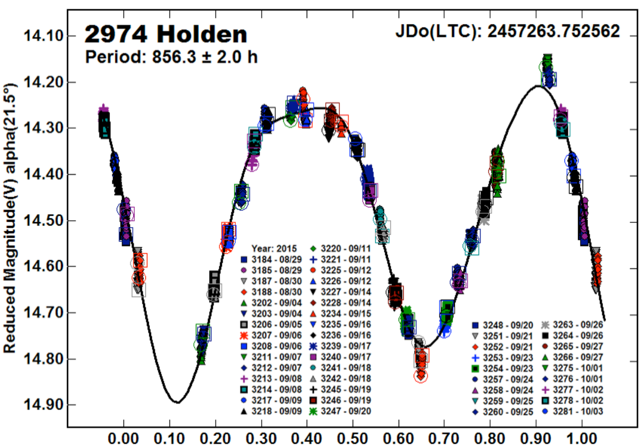
2974 Holden
Period: 856.3 ± 2.0 h
JDo(LTC): 2457263.752562
Reduced Magnitude(V) alpha(21.5°)
Year: 2015
3184 - 08/29
3185 - 08/29
3187 - 08/30
3188 - 08/30
3202 - 09/04
3203 - 09/04
3206 - 09/05
3207 - 09/06
3208 - 09/06
3211 - 09/07
3212 - 09/07
3213 - 09/08
3214 - 09/08
3217 - 09/09
3218 - 09/09
3220 - 09/11
3221 - 09/11
3225 - 09/12
3226 - 09/12
3227 - 09/14
3228 - 09/14
3234 - 09/15
3235 - 09/16
3236 - 09/16
3239 - 09/17
3240 - 09/17
3241 - 09/18
3242 - 09/18
3245 - 09/19
3246 - 09/19
3247 - 09/20
3248 - 09/20
3251 - 09/21
3252 - 09/21
3253 - 09/23
3254 - 09/23
3257 - 09/24
3258 - 09/24
3259 - 09/25
3260 - 09/25
3263 - 09/26
3264 - 09/26
3265 - 09/27
3266 - 09/27
3275 - 10/01
3276 - 10/01
3277 - 10/02
3278 - 10/02
3281 - 10/03

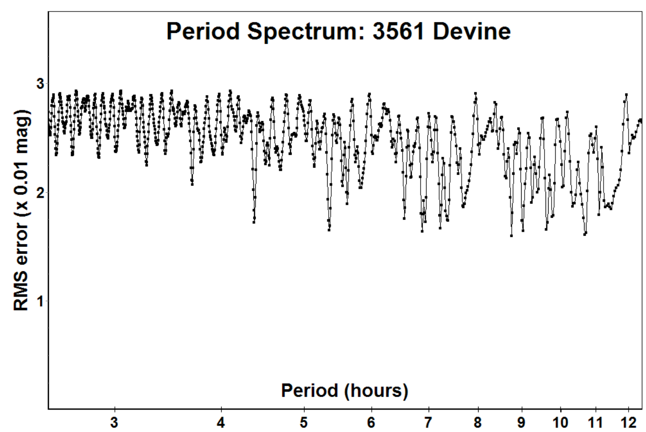
Period Spectrum: 3561 Devine
RMS error (x 0.01 mag)
Period (hours)

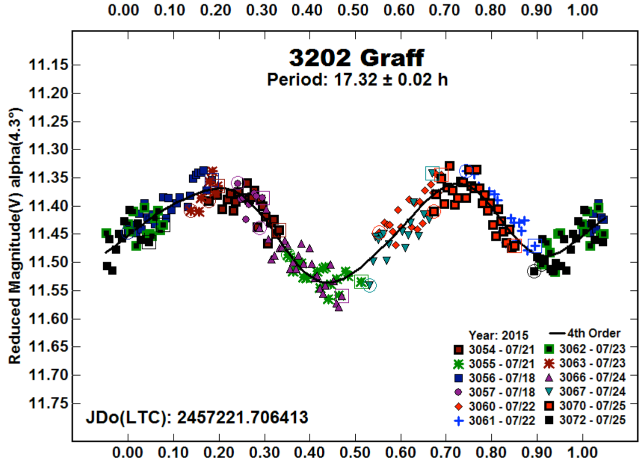
3202 Graff
Period: 17.32 ± 0.02 h
Reduced Magnitude(V) alpha(4.3°)
Year: 2015
4th Order
3054 - 07/21
3055 - 07/21
3056 - 07/18
3057 - 07/18
3060 - 07/22
3061 - 07/22
3062 - 07/23
3063 - 07/23
3066 - 07/24
3067 - 07/24
3070 - 07/25
3072 - 07/25
JDo(LTC): 2457221.706413

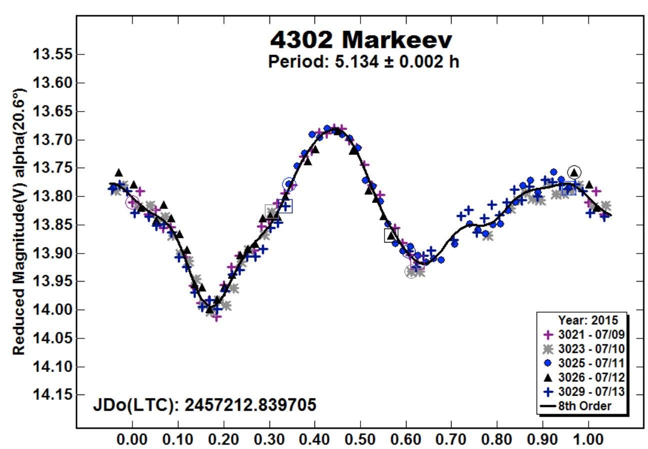
4302 Markeev
Period: 5.134 ± 0.002 h
Reduced Magnitude(V) alpha(20.6°)
Year: 2015
3021 - 07/09
3023 - 07/10
3025 - 07/11
3026 - 07/12
3029 - 07/13
8th Order
JDo(LTC): 2457212.839705

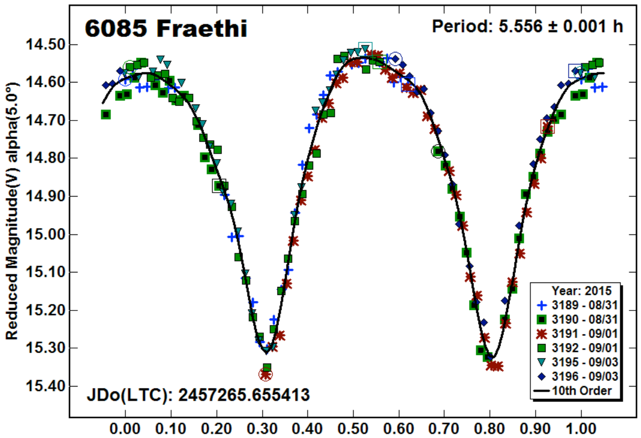
6085 Fraethi
Period: 5.556 ± 0.001 h
Reduced Magnitude(V) alpha(5.0°)
Year: 2015
3189 - 08/31
3190 - 08/31
3191 - 09/01
3192 - 09/01
3195 - 09/03
3196 - 09/03
10th Order
JDo(LTC): 2457265.655413

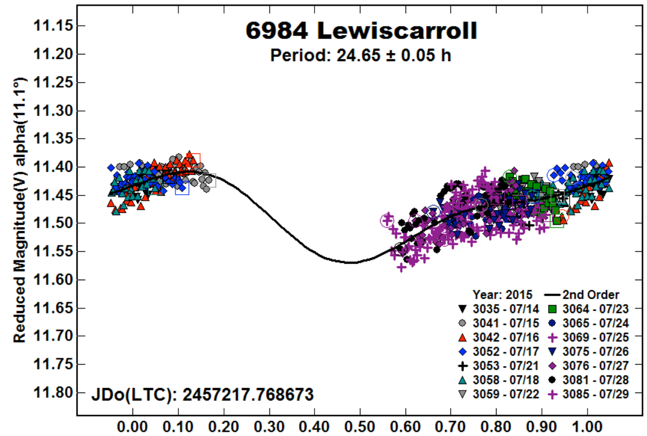
6984 Lewiscarroll
Period: 24.65 ± 0.05 h
Reduced Magnitude(V) alpha(11.1°)
Year: 2015
3035 - 07/14
3041 - 07/15
3042 - 07/16
3052 - 07/17
3053 - 07/21
3058 - 07/18
3059 - 07/22
2nd Order
3064 - 07/23
3065 - 07/24
3069 - 07/25
3075 - 07/26
3076 - 07/27
3081 - 07/28
3085 - 07/29
JDo(LTC): 2457217.768673

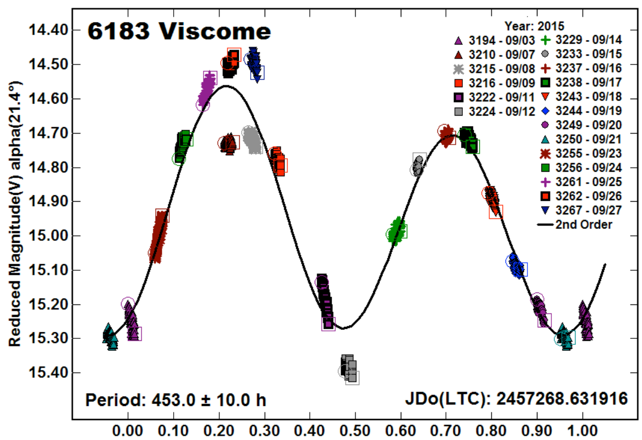
6183 Viscome
Reduced Magnitude(V) alpha(21.4°)
Year: 2015
3194 - 09/03
3210 - 09/07
3215 - 09/08
3216 - 09/09
3222 - 09/11
3224 - 09/12
3229 - 09/14
3233 - 09/15
3237 - 09/16
3238 - 09/17
3243 - 09/18
3244 - 09/19
3249 - 09/20
3250 - 09/21
3255 - 09/23
3256 - 09/24
3261 - 09/25
3262 - 09/26
3267 - 09/27
2nd Order
Period: 453.0 ± 10.0 h
JDo(LTC): 2457268.631916

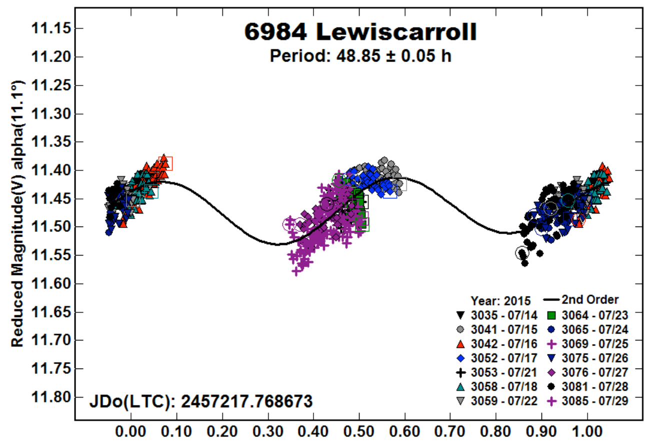
6984 Lewiscarroll
Period: 48.85 ± 0.05 h
Reduced Magnitude(V) alpha(11.1°)
Year: 2015
3035 - 07/14
3041 - 07/15
3042 - 07/16
3052 - 07/17
3053 - 07/21
3058 - 07/18
3059 - 07/22
2nd Order
3064 - 07/23
3065 - 07/24
3069 - 07/25
3075 - 07/26
3076 - 07/27
3081 - 07/28
3085 - 07/29
JDo(LTC): 2457217.768673

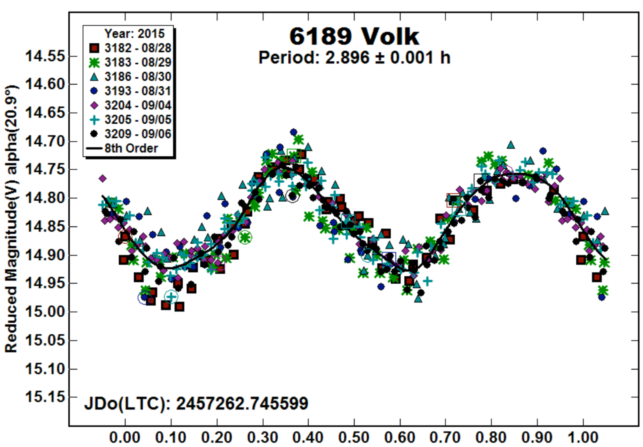
6189 Volk
Period: 2.896 ± 0.001 h
Reduced Magnitude(V) alpha(20.9°)
Year: 2015
3182 - 08/28
3183 - 08/29
3186 - 08/30
3193 - 08/31
3204 - 09/04
3205 - 09/05
3209 - 09/06
8th Order
JDo(LTC): 2457262.745599

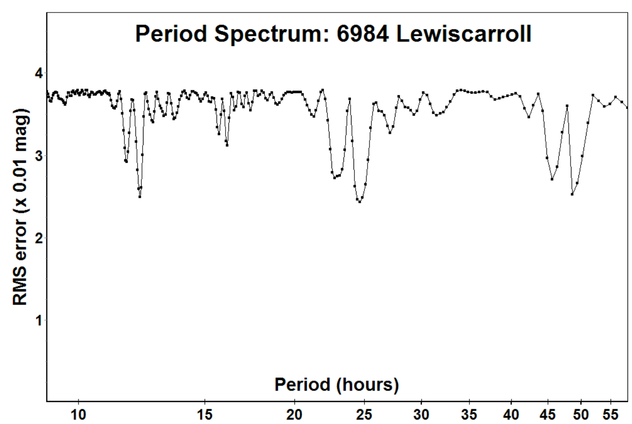
Period Spectrum: 6984 Lewiscarroll
RMS error (x 0.01 mag)
Period (hours)

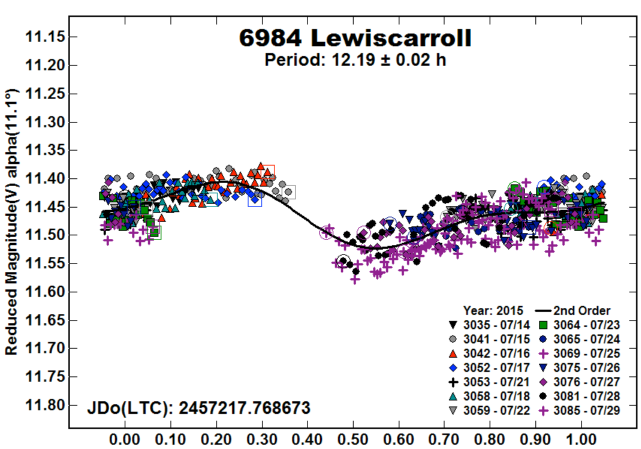
6984 Lewiscarroll
Period: 12.19 ± 0.02 h
Reduced Magnitude(V) alpha(11.1°)
Year: 2015
3035 - 07/14
3041 - 07/15
3042 - 07/16
3052 - 07/17
3053 - 07/21
3058 - 07/18
3059 - 07/22
2nd Order
3064 - 07/23
3065 - 07/24
3069 - 07/25
3075 - 07/26
3076 - 07/27
3081 - 07/28
3085 - 07/29
JDo(LTC): 2457217.768673

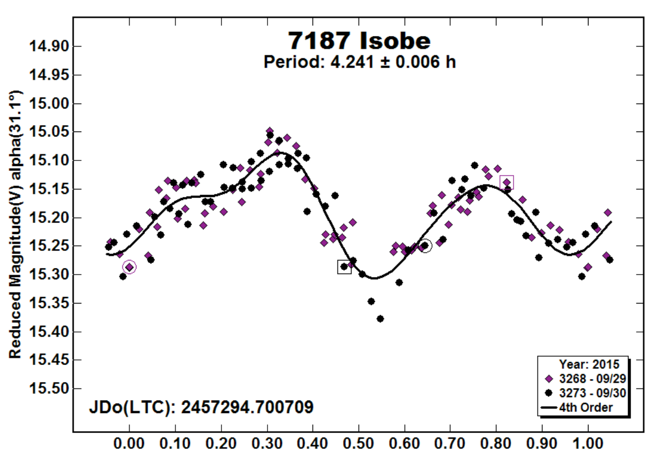
7187 Isobe
Period: 4.241 ± 0.006 h
Reduced Magnitude(V) alpha(31.1°)
Year: 2015
3268 - 09/29
3273 - 09/30
4th Order
JDo(LTC): 2457294.700709

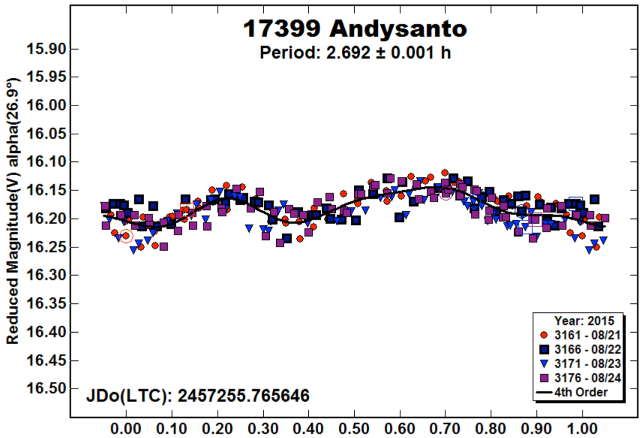
17399 Andysanto
Period: 2.692 ± 0.001 h
Reduced Magnitude(V) alpha(26.9°)
Year: 2015
3161 - 08/21
3166 - 08/22
3171 - 08/23
3176 - 08/24
4th Order
JDo(LTC): 2457255.765646

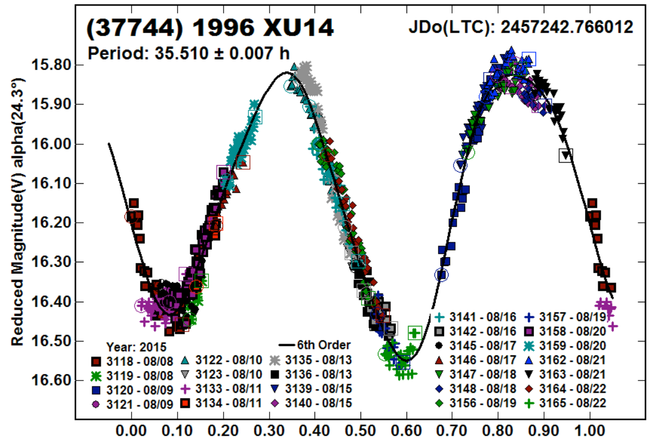
(37744) 1996 XU14
JDo(LTC): 2457242.766012
Period: 35.510 ± 0.007 h
Reduced Magnitude(V) alpha(24.3°)
Year: 2015
6th Order
3118 - 08/08
3119 - 08/08
3120 - 08/09
3121 - 08/09
3122 - 08/10
3123 - 08/10
3133 - 08/11
3134 - 08/11
3135 - 08/13
3136 - 08/13
3139 - 08/15
3140 - 08/15
3141 - 08/16
3142 - 08/16
3145 - 08/17
3146 - 08/17
3147 - 08/18
3148 - 08/18
3156 - 08/19
3157 - 08/19
3158 - 08/20
3159 - 08/20
3162 - 08/21
3163 - 08/21
3164 - 08/22
3165 - 08/22

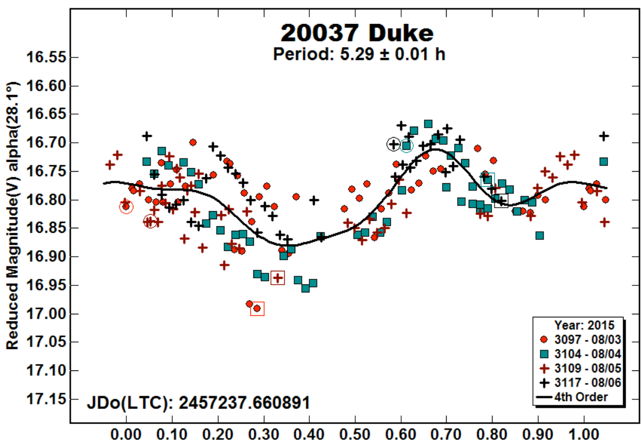
20037 Duke
Period: 5.29 ± 0.01 h
Reduced Magnitude(V) alpha(28.1°)
Year: 2015
3097 - 08/03
3104 - 08/04
3109 - 08/05
3117 - 08/06
4th Order
JDo(LTC): 2457237.660891

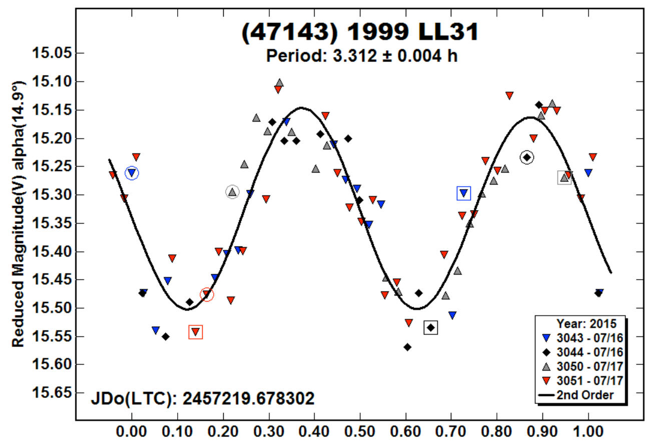
(47143) 1999 LL31
Period: 3.312 ± 0.004 h
Reduced Magnitude(V) alpha(14.9°)
Year: 2015
3043 - 07/16
3044 - 07/16
3050 - 07/17
3051 - 07/17
2nd Order
JDo(LTC): 2457219.678302

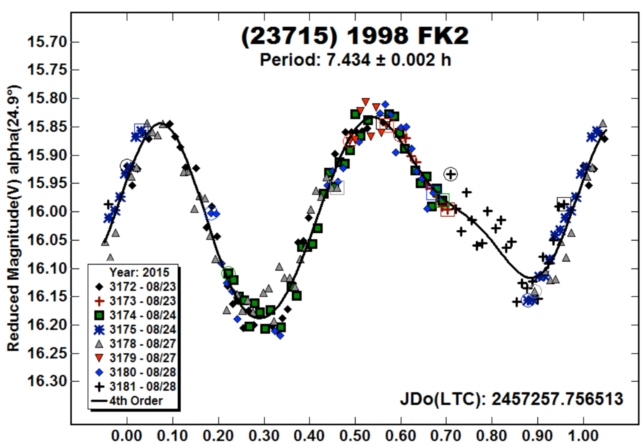
(23715) 1998 FK2
Period: 7.434 ± 0.002 h
Reduced Magnitude(V) alpha(24.9°)
Year: 2015
3172 - 08/23
3173 - 08/23
3174 - 08/24
3175 - 08/24
3178 - 08/27
3179 - 08/27
3180 - 08/28
3181 - 08/28
4th Order
JDo(LTC): 2457257.756513

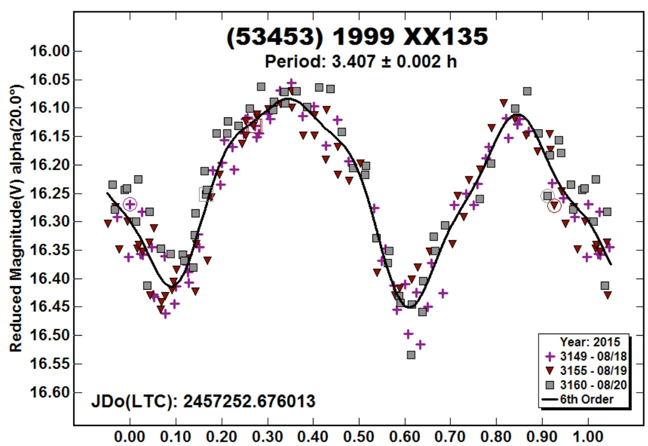
(53453) 1999 XX135
Period: 3.407 ± 0.002 h
Reduced Magnitude(V) alpha(20.0°)
Year: 2015
3149 - 08/18
3155 - 08/19
3160 - 08/20
6th Order
JDo(LTC): 2457252.676013

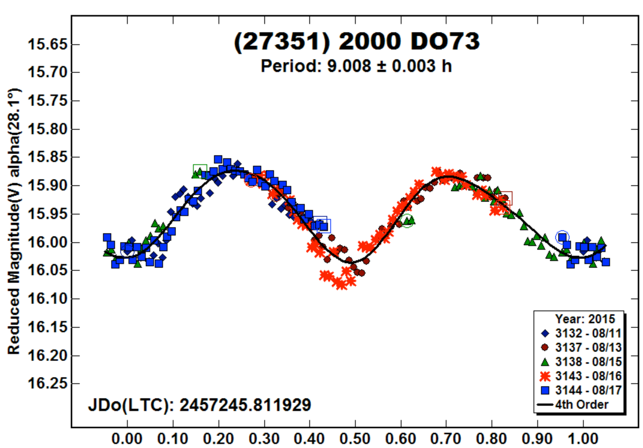
(27351) 2000 DO73
Period: 9.008 ± 0.003 h
Reduced Magnitude(V) alpha(28.1°)
Year: 2015
3132 - 08/11
3137 - 08/13
3138 - 08/15
3143 - 08/16
3144 - 08/17
4th Order
JDo(LTC): 2457245.811929

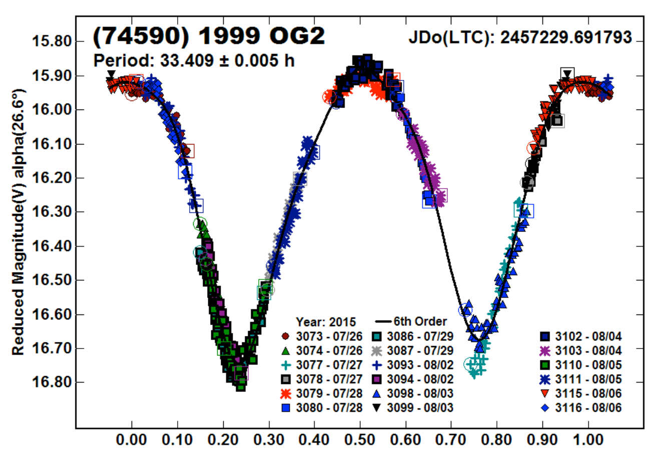
(74590) 1999 OG2
JDo(LTC): 2457229.691793
Period: 33.409 ± 0.005 h
Reduced Magnitude(V) alpha(26.6°)
Year: 2015
6th Order
3073 - 07/26
3074 - 07/26
3077 - 07/27
3078 - 07/27
3079 - 07/28
3080 - 07/28
3086 - 07/29
3087 - 07/29
3093 - 08/02
3094 - 08/02
3098 - 08/03
3099 - 08/03
3102 - 08/04
3103 - 08/04
3110 - 08/05
3111 - 08/05
3115 - 08/06
3116 - 08/06

ASTEROID LIGHTCURVE ANALYSIS AT CS3-PALMER DIVIDE STATION: 2015 JUNE-SEPTEMBER

Brian D. Warner
Center for Solar System Studies – Palmer Divide Station
446 Sycamore Ave.
Eaton, CO 80615 USA
brian@MinorPlanetObserver.com

(Received: 2015 October 6)

Lightcurves for 29 main-belt asteroids were obtained at the Center for Solar System Studies-Palmer Divide Station (CS3-PDS) from 2015 June-September. Hungaria members 1876 Napolitania and (47141) 1999 HB3 are suspected binary asteroids.

CCD photometric observations of 29 main-belt asteroids were made at the Center for Solar System Studies-Palmer Divide Station (CS3-PDS) from 2015 June-September. Table I lists the telescope/CCD camera combinations used for the observations. All the cameras use CCD chips from the KAF blue-enhanced family and so have essentially the same response. The pixel scales for the combinations range from 1.24-1.60 arcsec/pixel.

Desig	Telescope	Camera
Squirt	0.30-m f/6.3 Schmidt-Cass	ML-1001E
Borealis	0.35-m f/9.1 Schmidt-Cass	STL-1001E
Eclipticalis	0.35-m f/9.1 Schmidt-Cass	ML-1001E
Australius	0.35-m f/9.1 Schmidt-Cass	STL-1001E
Zephyr	0.50-m f/8.1 R-C	FLI-1001E

Table I. List of CS3-PDS telescope/CCD camera combinations.

All lightcurve observations were unfiltered since a clear filter can result in a 0.1-0.3 magnitude loss. The exposure duration varied depending on the asteroid's brightness and sky motion. Guiding on a field star sometimes resulted in a trailed image for the asteroid.

Measurements were made using *MPO Canopus*. If necessary, an elliptical aperture with the long axis parallel to the asteroid's path was used. The Comp Star Selector utility in *MPO Canopus* found up to five comparison stars of near solar-color for differential photometry. Catalog magnitudes were usually taken from the MPOSC3 catalog, which is based on the 2MASS catalog (*http://www.ipac.caltech.edu/2mass*) but with magnitudes converted from J-K to BVRI using formulae developed by Warner (2007). The nightly zero points have been found to be consistent to about ± 0.05 mag or better, but on occasion are as large as 0.1 mag. This consistency is critical to analysis of long period and/or tumbling asteroids. Period analysis is also done using *MPO Canopus*, which implements the FALC algorithm developed by Harris (Harris *et al.,* 1989).

In the plots below, the "Reduced Magnitude" is Johnson V as indicated in the Y-axis title. These are values that have been converted from sky magnitudes to unity distance by applying $-5*\log(r\Delta)$ to the measured sky magnitudes with r and Δ being, respectively, the Sun-asteroid and Earth-asteroid distances in AU. The magnitudes were normalized to the given phase angle, e.g., alpha(6.5°), using *G* = 0.15, unless otherwise stated. The X-axis is the rotational phase ranging from –0.05 to 1.05.

If the plot includes an amplitude, *e.g.*, "Amp: 0.65", this is the amplitude of the Fourier model curve and *not necessarily the adopted amplitude for the lightcurve*. The value is meant only to be a quick guide.

For the sake of brevity, only some of the previously reported results may be referenced in the discussions on specific asteroids. For a more complete listing, the reader is directed to the asteroid lightcurve database (LCDB; Warner *et al.,* 2009a). The on-line version at *http://www.minorplanet.info/lightcurvedatabase.html* allows direct queries that can be filtered a number of ways and the results saved to a text file. A set of text files of the main LCDB tables, including the references with bibcodes, is also available for download. Readers are strongly encouraged to obtain, when possible, the original references listed in the LCDB for their work.

1025 Riema. The apparition in 2015 was the fifth one at which a member of CS3 observed this Hungaria asteroid (*e.g.*, Stephens, 2003; Warner, 2014b). The period of 3.581 h reported here agrees well with earlier results.

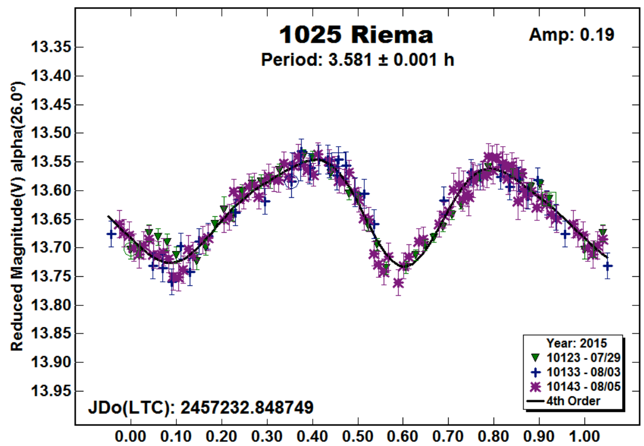

1656 Suomi. This Hungaria was last observed by the author in 2014 (Warner, 2014b). The period found from the 2015 data agrees with earlier results. There was one session (not shown) that appeared to show a large, prolonged deviation. No period could be determined nor can its cause be explained.

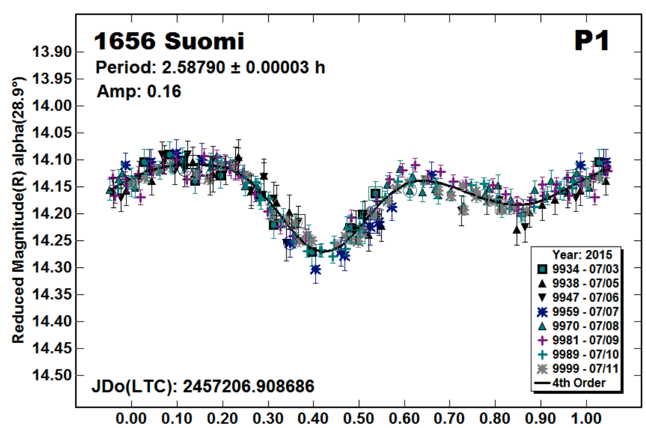

1876 Napolitania. These appear to be the first reported observations for this Hungaria and also that it might be a member of a select group of so-called "wide binary" asteroids. These are where the primary period is long and has a large amplitude and the secondary period is short and has a low amplitude. Assuming that this asteroid is a binary of this class, it has the shortest primary period by at least a factor of 3. The two lightcurves are based on the data set after subtracting the other period.

Number	Name	2015 mm/dd	Pts	Phase	L_{PAB}	B_{PAB}	Period	P.E.	Amp	A.E.	Group
1025	Riema	07/29-08/05	165	26.0,24.2	356	0	3.581	0.001	0.19	0.02	H
1656	Suomi	07/03-07/11	223	28.9,28.0	342	15	2.5879	0.0003	0.16	0.02	H
1876	Napolitania	07/23-08/09	420	18.2,11.4	329	10	45.63	0.05	0.39	0.03	H
2074	Shoemaker	06/16-07/05	159	34.2,34.6	341	33	2.809	0.001	0.13	0.02	H
2204	Lyyli	07/05-07/11	194	11.3,12.3	251	23	11.09	0.01	0.39	0.03	MC
3101	Goldberger	08/18-08/21	127	21.2,19.9	356	-9	5.270	0.005	1.05	0.03	H
3873	Roddy	07/06-07/13	187	27.9,28.3	12	24	2.486	0.001	0.10	0.02	H
4464	Vulcano	08/21-08/23	135	24.5,23.7	3	-11	3.202	0.005	0.10	0.01	H
7029	1993 XT2	10/01-10/01	70	2.1	9	-6	10	1	0.47	0.03	MB-O
7579	1990 TN1	08/09-08/17	325	24.5,22.5	3	12	18.319	0.003	1.15	0.03	H
10737	Bruck	08/22-08/28	161	20.1,16.4	355	5	3.22	0.01	0.08	0.01	H
11279	1989 TC	08/30-09/04	109	32.8,32.1	35	9	3.992	0.002	0.16	0.02	H
13186	1996 UM	07/24-07/26	92	33.0,32.8	3	12	4.297	0.002	0.53	0.03	H
16953	Besicovitch	07/27-07/27	54	13.0,13.0	330	10	-	-	-	-	MB-O
21149	Kenmitchell	07/12-07/17	202	27.9,26.4	332	18	7.22	0.02	0.14	0.02	H
23482	1991 LV	[12]06/26-07/13	108	20.5,17.0	300	22	3.126	0.001	0.17	0.01	H
23482	1991 LV	08/30-09/05	108	34.1,33.5	37	16	3.358	0.002	0.35	0.03	H
30311	2000 JS10	08/24-08/29	110	23.8,22.9	18	21	2.270	0.002	0.16	0.02	H
31450	1999 CU9	09/28-10/01	308	14.1,15.4	349	9	3.412	0.005	0.30	0.02	MB-I
31813	1999 RF41	07/23-07/28	268	20.4,18.3	327	15	18.097	0.007	1.20	0.05	H
45176	1999 XQ140	09/18-09/19	113	10.8,10.3	9	-9	3.44	0.02	0.20	0.02	MB-M
47141	1999 HB3	06/18-07/09	305	29.2,25.0	308	26	2.8614[P]	0.0002	0.14	0.02	H
48601	1995 BL	07/26-07/27	139	20.1,19.8	336	7	4.598	0.002	0.45	0.03	H
49667	1999 OM2	07/18-07/23	3	23.5,21.9	332	16	3.487	0.001	0.51	0.02	H
65597	3047 T-3	10/01-10/01	56	3.3	9	-5	7.6	0.5	0.14	0.02	V
69406	1995 SX48	09/27-10/03	201	21.1,21.0	10	31	4.468	0.005	0.12	0.02	H
77010	2001 CB9	09/16-09/16	87	16.1,16.1	10	17	3.61	0.03	0.36	0.02	MB-I
86192	1999 SV1	07/17-07/22	142	24.1,22.8	329	23	7.157	0.002	0.28	0.02	H
132597	2002 JM141	09/26-09/27	83	5.3,4.9	9	-7	7.10	0.05	0.26	0.04	EUN
189296	2005 UT407	09/24-09/30	213	8.2,5.6	9	-7	15.54	0.05	0.89	0.05	MB-I

Table II. Observing circumstances. [A] preferred period of an ambiguous solution. [P] period of the primary in a binary system. [12]Data are from 2012. The phase angle (α) is given at the start and end of each date range, unless it reached a minimum, which is then the second of three values. If a single value is given, the phase angle did not change significantly and the average value is given. L_{PAB} and B_{PAB} are each the average phase angle bisector longitude and latitude, unless two values are given (first/last date in range). The Group column gives the orbital group to which the asteroid belongs. The definitions and values are those used in the LCDB (Warner *et al.*, 2009a). EUN = Eunomia; H = Hungaria; MC = Mars-crosser; MB-I = Inner main-belt; MB-M = middle main-belt; MB-O = Outer main-belt; V = Vestoid.

Number	Name	P_1	P_2	Ref
1876	Napolitania	45	2.825	**This work**
8026	Johnmckay	372	2.2981	MPB 38, 33-36
15778	1993 NH	113	3.320	MPB 42, 60-66
23615	1996 FK12	368	3.6456	MPB 42, 183-186
67175	2000 BA19	275	2.7157	MPB 40, 36-42
119744	2001 YN42	624	7.24	MPB 41, 102-112
190208	2006 AQ	182	2.621	MPB 42, 79-83
218144	2002 RL66	588	2.49	MPB 37, 109-111
	2014 PL51	205	5.384	MPB 42, 134-136

Table III. List of suspected wide binary asteroids. P_1 is the primary's period (hours). P_2 is the satellite's, which is not tidally-locked to its orbital period. All references are Warner (*et al.*).

The chances of observing *mutual events* (occultations and/or eclipses) are extremely remote. The only way to validate these types of binaries is to observe them at future apparitions and look for positive proof of the dual period analysis.

Table III gives the current list of these suspected objects. Among these are four Hungarias, two NEAs, two Mars-crossers, and one inner main-belt objects. Since the CS3 program concentrates on NEAs and Hungarias, no statistical inference regarding families or orbital groups should be made from this tabulation. However, the results beg the question if other groups have binaries of this type.

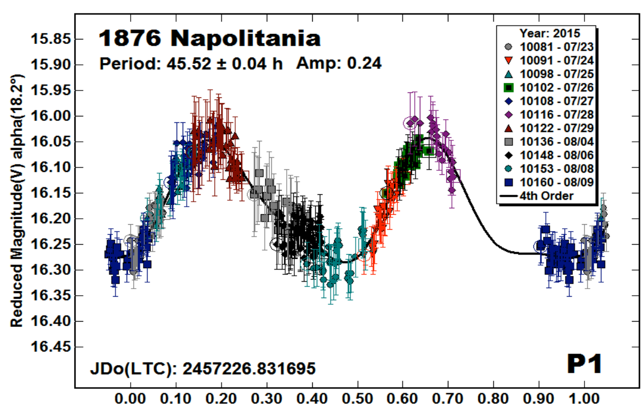

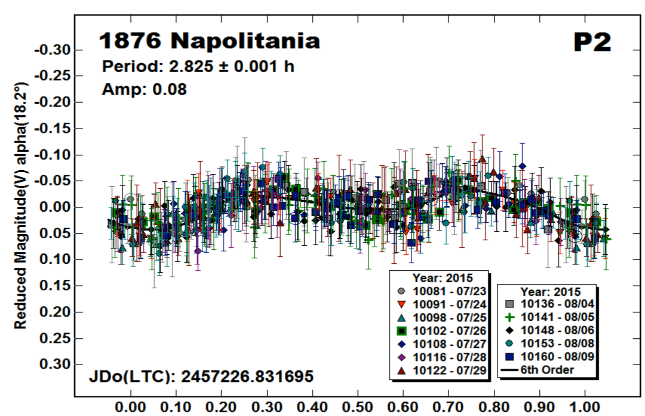

2074 Shoemaker. It has been a long and difficult task to find a definitive period for this Hungaria. Observations by Stephens (2004) that found a period of 57.02 h were reanalyzed by Warner *et al.* (2009b), who found a primary period of a suspected binary system of 2.5328 h and an orbital period of about 55 h. Analysis of observations by the author in 2010 (Warner, 2011a) found a very similar primary period but an orbital period of about 27.5 h. No signs of a binary were seen at the 2012 apparition (Warner, 2012a) but the primary period solution was ambiguous, being either 2.82 h or 2.535 h. The observations in 2015 were made in the hopes of resolving the primary ambiguity and finding more definitive proof of the satellite. Neither objective was realized.

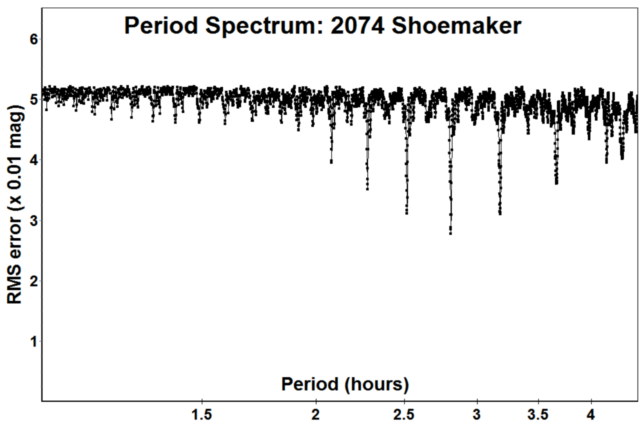

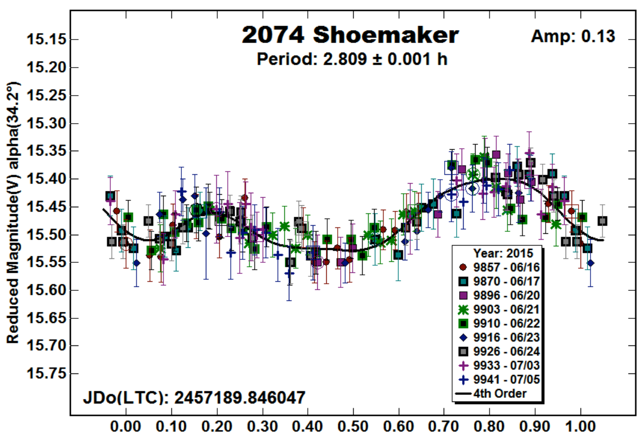

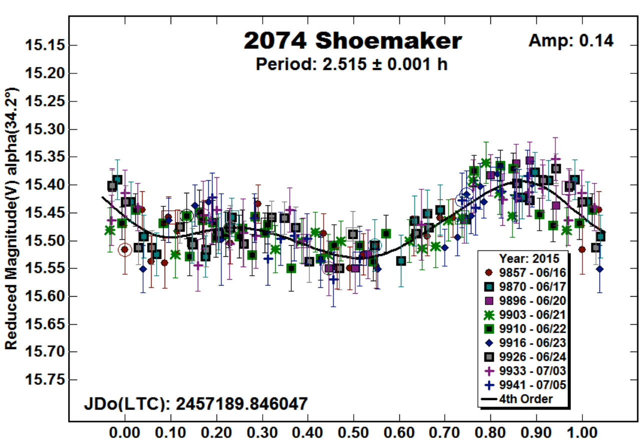

First, there were no indications of the satellite as seen by attenuations in the primary lightcurve. If there were any, they were below the limit of detection. Absence of proof is not proof of absence. The phase angle bisector longitude in 2015 was 30° removed from the 2011 apparition. It's possible the viewing aspect was not quite right to see events.

The period spectrum shows a preference for a period of 2.809 h, the period adopted for this paper, but one at 2.515 h, which is in closer agreement with the results from 2009 and 2011 apparitions, cannot be formally excluded.

2204 Lyyli. Gil-Hutton and Canada (2003) found a period of 9.51 h. The author observed this Mars-crosser in 2010 (Warner, 2010) and found a period of 11.063 h. The data from the 2015 apparition cannot be fit to the shorter period. They do yield a solution similar to the earlier result by the author.

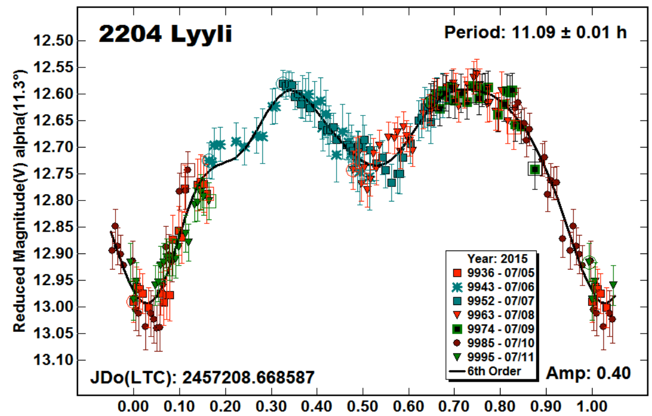

3101 Goldberger. The period of 5.270 h found from the 2015 data is in good agreement with that found at the previous apparition (Warner, 2014b).

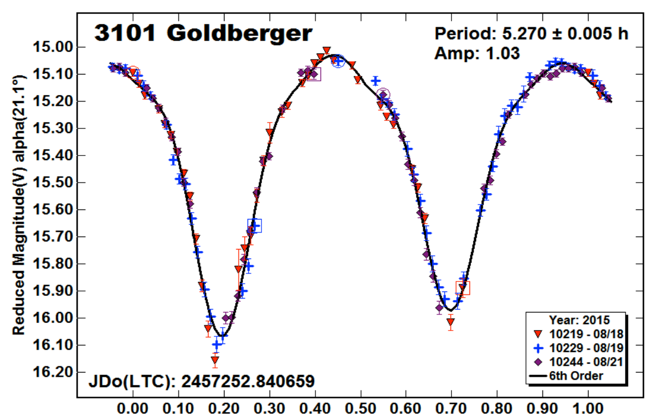

3873 Roddy. This is a suspected binary. Analysis of the data obtained by the author from the 2007 and 2012 apparitions showed indications of a satellite. Both data sets gave a primary period of about 2.48 h (Warner, 2013b). However, the 2007 data set led to an orbital period of 23.789 h while the 2012 data set led to a period of 19.24 h. The 2015 data set not only failed to solve the mystery but added to it.

The primary period lightcurve shows a low amplitude (A = 0.10 mag) monomodal solution. There seemed to be traces of a secondary period, but a dual-period search in *MPO Canopus* was not successful. It did find a period of about 23.98 h, but the data set was far too incomplete, covering only 15% of the period.

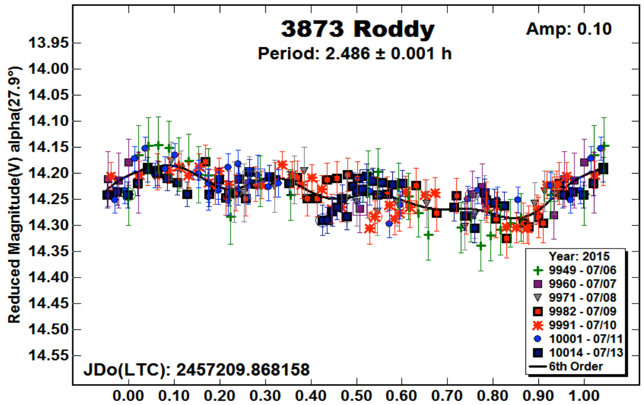

4464 Vulcano. The 2015 apparition was the fourth one at which the author observed this Hungaria. Previous results (Warner, 2014b, and references therein) and those from 2015 are in good agreement at about 3.20 h.

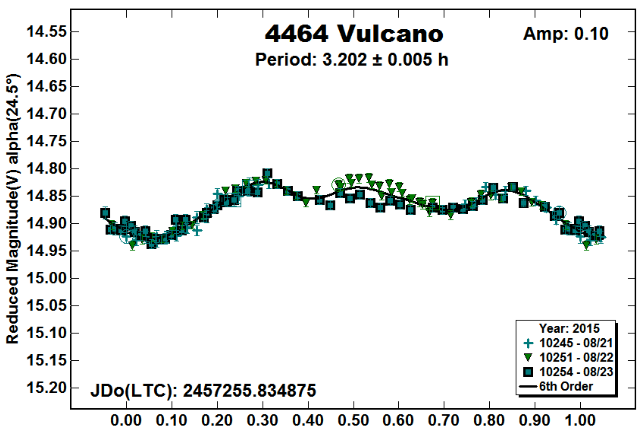

(7029) 1993 XT2. This outer main-belt asteroid was in the field of a planned target for one night. Fortunately, the observing run was long enough to capture more than half the presumed bimodal lightcurve with a period of 10 ± 1 h. The first lightcurve shows the half-period solution, which allowed finding a reasonable amplitude if assuming a symmetrical bimodal lightcurve for the longer period. The second lightcurve mainly shows that the maximums and minimums are reasonably spaced for the presumed full period of about 10 hours.

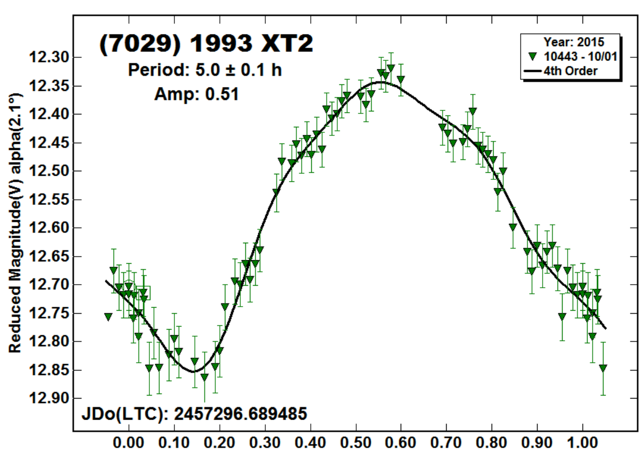

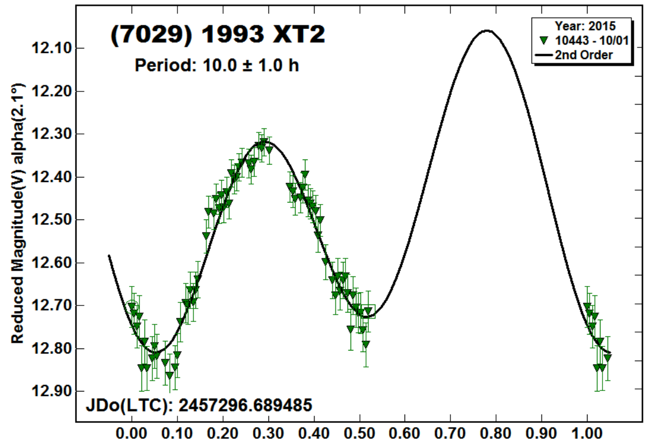

(7579) 1990 TN1. This Hungaria was observed twice before by the author (Warner, 2008; 2011c). The period found in 2015 agrees with the earlier works.

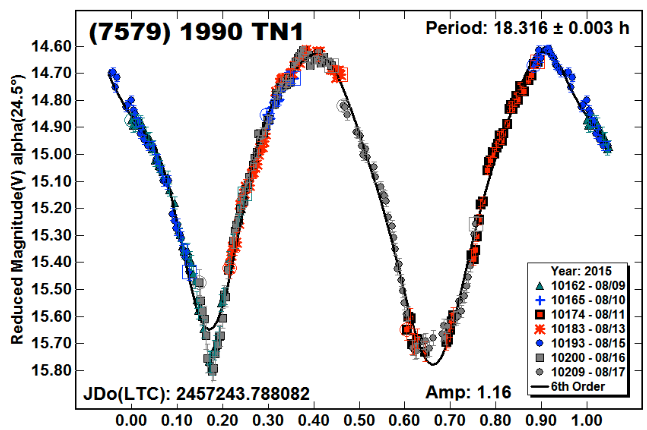

10737 Bruck. This appears to be the first published lightcurve for Bruck, a member of the Hungaria asteroids.

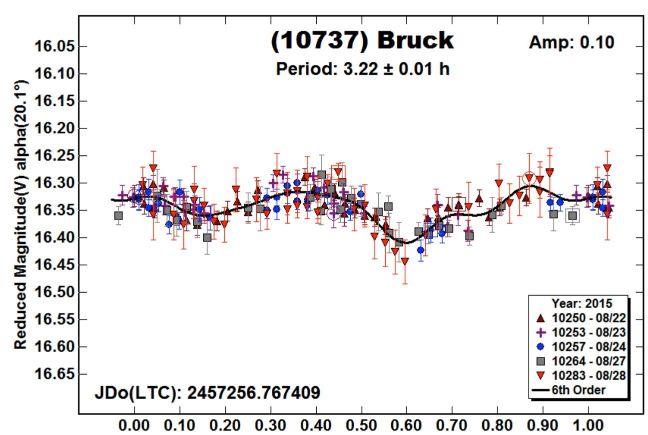

(11279) 1989 TC. Previous results include Warner (2011b, 4.020 h; 2014c, 4.003 h). The phase angle bisector longitudes (L_{PAB}; see Harris *et al.*, 1984) occur at sufficiently different values to give an idea of the pole axis orientation and/or shape based on the amplitude at each apparition. The range of amplitudes was only 0.03 mag and $A \leq 0.16$ mag, which can be interpreted as the asteroid having a nearly spheroidal shape. This will make it more difficult to find an unambiguous spin axis.

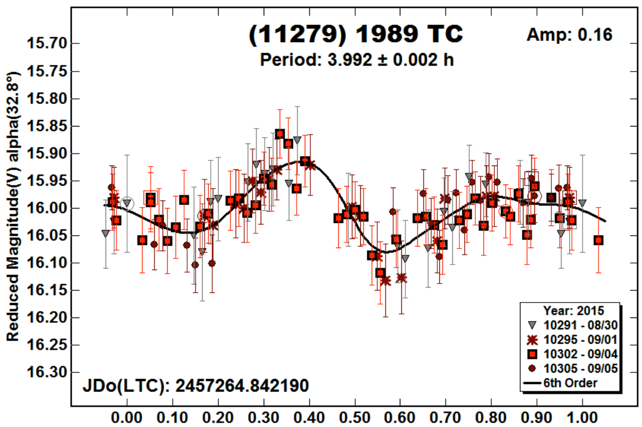

(13186) 1996 UM. This is the third apparition for this Hungaria by the author (Warner, 2013a, 4.304 h; 2014c, 4.293 h). The 2015 results are in good agreement with those works.

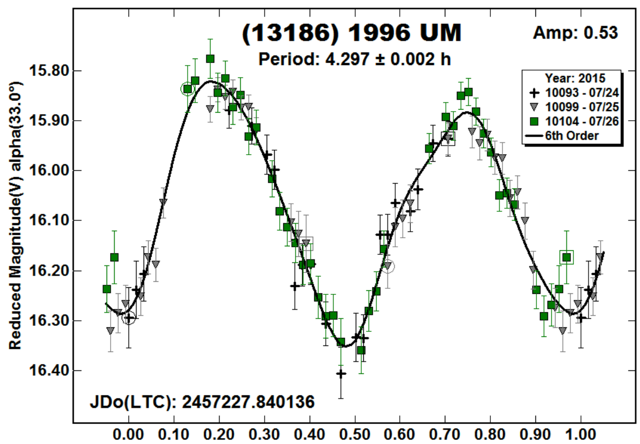

16953 Besicovitch. This outer main-belt asteroid was found wandering in the same field as a planned target. What variations are seen in the single night of data may be systematic or real. Without a second night to see if there is a longer period trend, there was no justification for trying to find a period. The asteroid is included here to let future observers know that the data exist and will be available in the ALCDEF database (Warner, 2015).

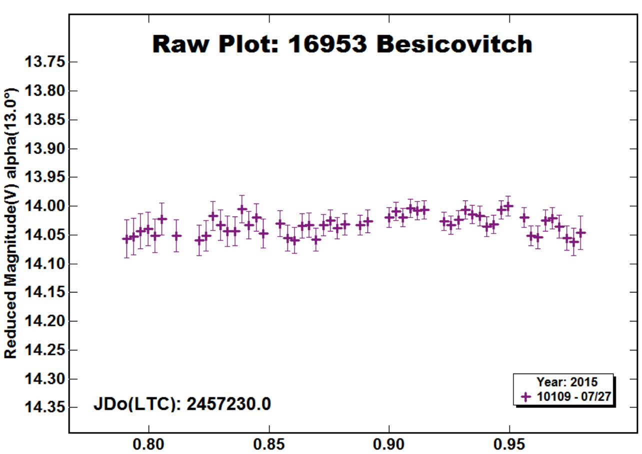

21149 Kenmitchell. This is apparently the first time that a lightcurve has been published for this Hungaria member.

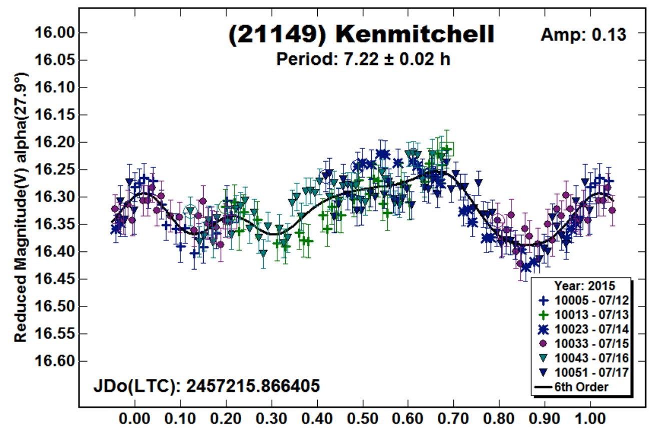

(23482) 1991 LV. Warner (2012b) found a period of 3.1388 h based on data obtained in mid-20112. The 2015 data could not be fit to that earlier result. This prompted a second look at the 2012 data and further analysis. In the plots below the 'S' and 'P' after the year refer to the shorter and longer period, respectively.

Looking at 2012 first, the period spectrum shows two groups of possible periods with the best-fit of the first group representing an additional one-half rotation over a 24-hour period versus the best-fit of the second group.

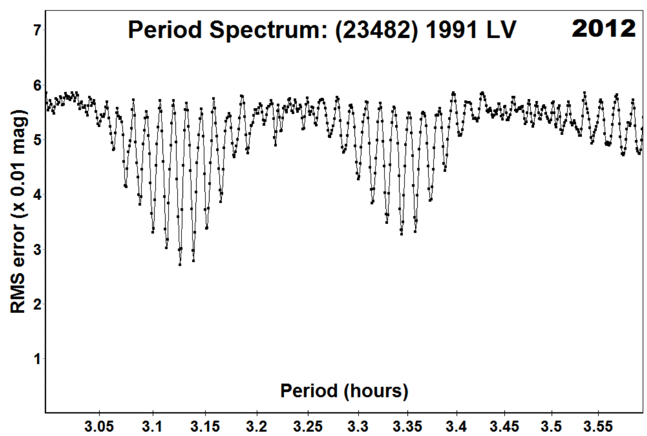

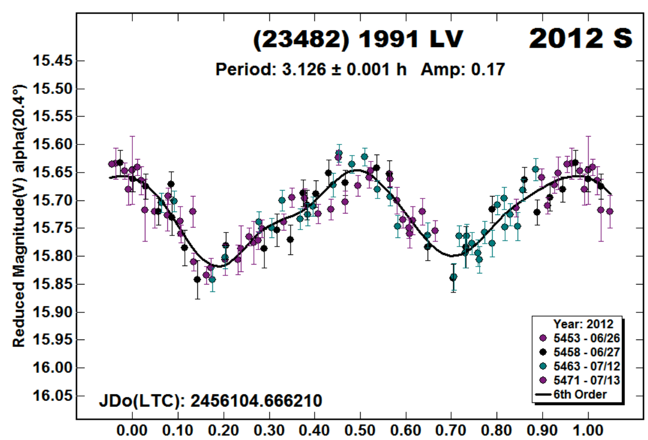

The large number of similar solutions in each group is the result of the large gap between the two sets of consecutive nights of observations. They represent an uncertainty in the number of rotations over the total span of observations. For example, there is about a 16-day (384 h) span between the first session of each set. The best-fit period of the first group is 3.126 h, while the minimum to its left is at 3.113 h. The difference between these two periods amounts to one-half rotation over the 16 days. This is what I call *rotational aliasing*, *i.e.*, the data do not allow finding a unique number of rotations over the span of observations.

Usually the solution to eliminate rotational aliasing is to obtain data on as many consecutive nights as possible over as long a span as needed to resolve the ambiguities. This example shows the need for an additional condition: there can be no gaps between groups of sessions that represent a significant number of rotations. The 16-day gap represented about 123 rotations at the average of the two periods above.

Adding one more condition will greatly reduce rotational aliasing: each observing run should cover well more than half a cycle and, even better, completely cover one or more cycles

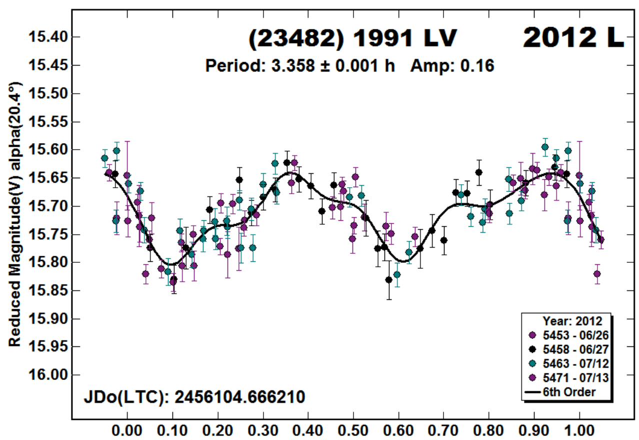

Looking at the lightcurve for the longer period from the 2012 data, the result is plausible but not nearly as good as for 3.126 h. This period is adopted by this paper to replace the earlier result of 3.1388 h, which is the minimum immediately to the right of the one for the best-fit solution at 3.126 h. Even so, the new result cannot be considered definitive.

Moving to the new results in 2015, the period spectrum again shows two likely minimums. Absent from this period spectrum are the numerous solutions on either side of each minimum. This is because the span of observations was only seven days and the gaps between individual runs were shorter. Here as well, there were only two consecutive nights of observations in the data set.

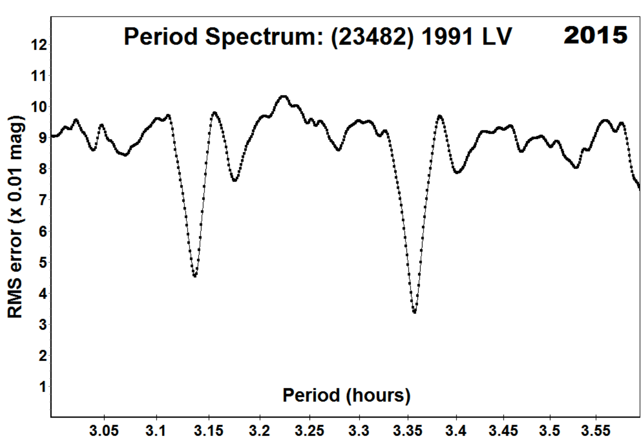

The difference between the lightcurves for the shorter and longer period is subtle given the large error bars due to the asteroid being significantly fainter in 2015. The deviation at 0.6-0.7 rotation phase in the shorter period lightcurve lends favor to the longer period.

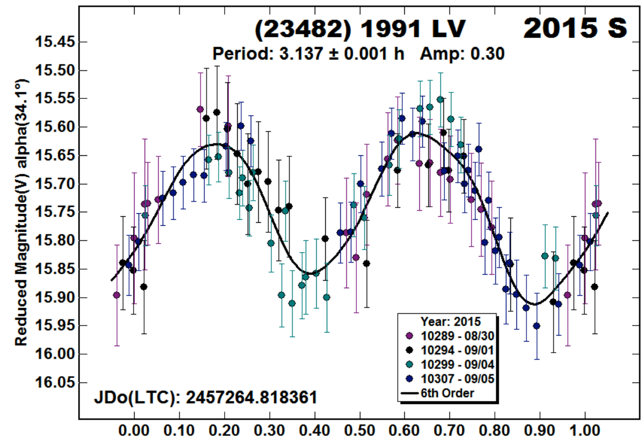

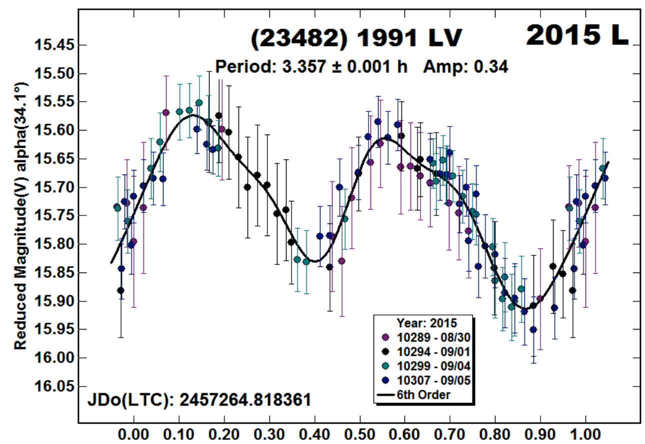

Based on the analysis of both data sets, the solution of $P = 3.357$ h using 2015 data is considered the one most likely correct, partly because of the larger amplitude of the lightcurve. However, this is not a final answer. Additional observations are required to resolve the ambiguities once and for all.

<u>(30311) 2000 JS10</u>. The period of 2.270 h found in 2015 is in good agreement with earlier results from apparitions in 2005 and 2012 (Warner, 2013b).

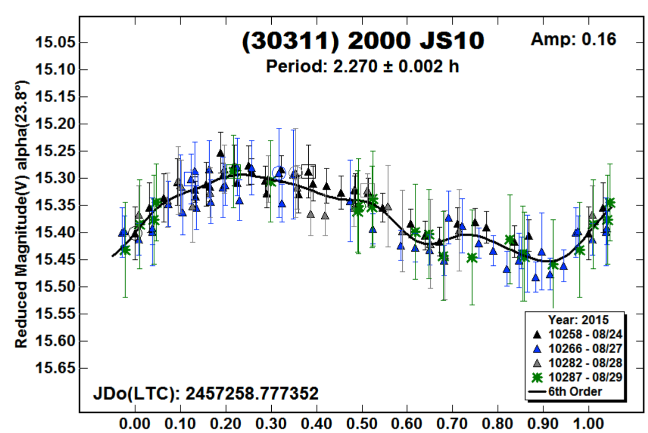

(31450) 1999 CU9. This is known binary (Petr Pravec, *private communications*). No obvious indications of *mutual events* (occultations and/or eclipses) were seen in the CS3 data.

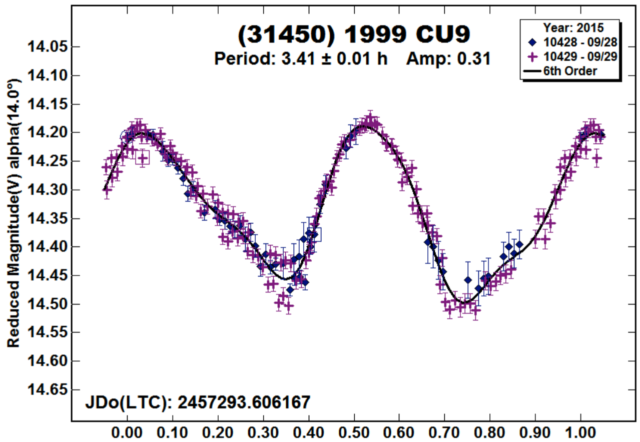

(31813) 1999 RF41, (45176) 1999 XQ140. These appear to be first-time results for these asteroids. 1999 RF41 is a Hungaria member while 1999 XQ140 is a member of the inner main-belt that was in the field of a planned target for two nights.

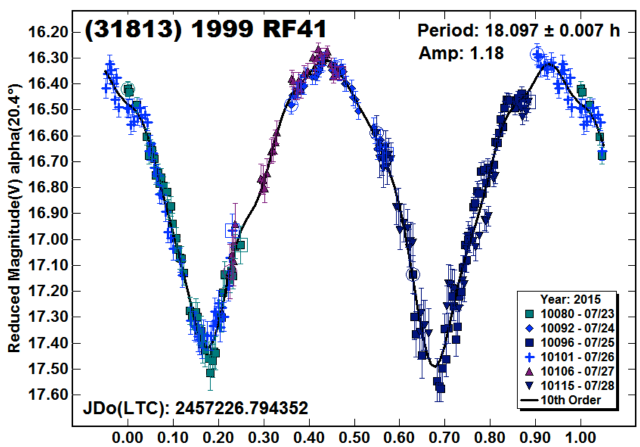

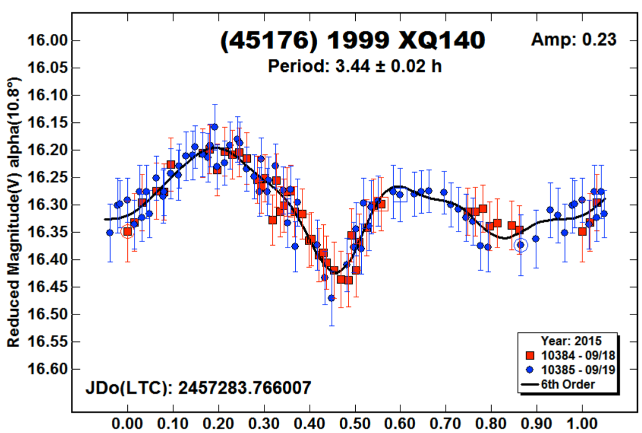

(47141) 1999 HB3. The 2015 apparition was the first time this Hungaria was observed by the author. While the concentration in recent years has been on NEAs and re-observing Hungarias for shape and spin axis modeling, occasionally "new" Hungarias are included to check on existing statistics for rotation rates and binary population. In this case, 1999 HB3 appears to be a new binary.

Initial analysis in *MPO Canopus* found a period of about 2.861 h that, despite the large error bars, seemed to have indications of a second period ("P1 – No Sub"). The dual period analysis in *MPO Canopus* was employed to find periods of P_1 = 2.86140 ± 0.00002 h, A_1 = 0.14 ± 0.02 mag and P_2 = 10.56 ± 0.01 mag, A_2 = 0.08-0.13 mag. Assuming the second lightcurve shows mutual events, then using the shallower amplitude of A_2 gives an effective diameter ratio between satellite and primary of Ds/Dp = 0.27 ± 0.02. The combination of primary period and size ratio just fits within the envelope of the model for binaries proposed by Pravec *et al.* (2010). This should be taken with a bit of caution and, maybe more so, that a satellite actually exists at all since the size of the error bars is significant in comparison to the amplitude of the P_2 lightcurve and the improvement in the P_1 lightcurve is also rivaled by the noise in the data.

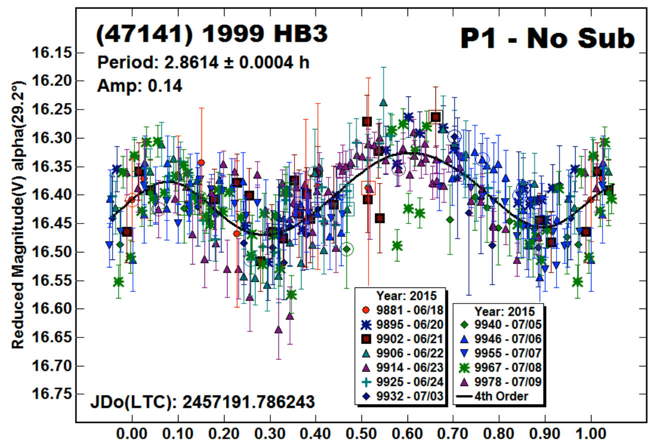

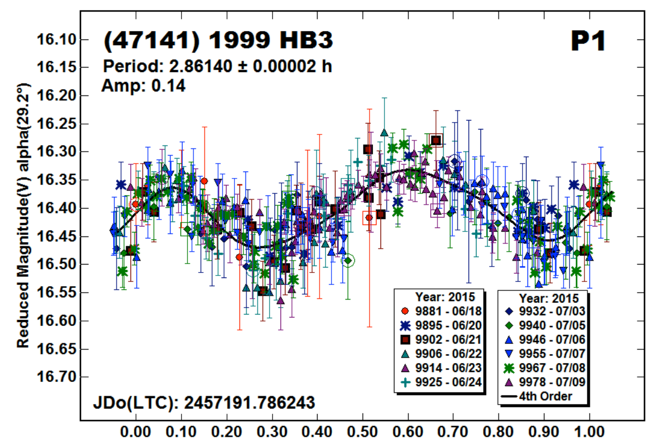

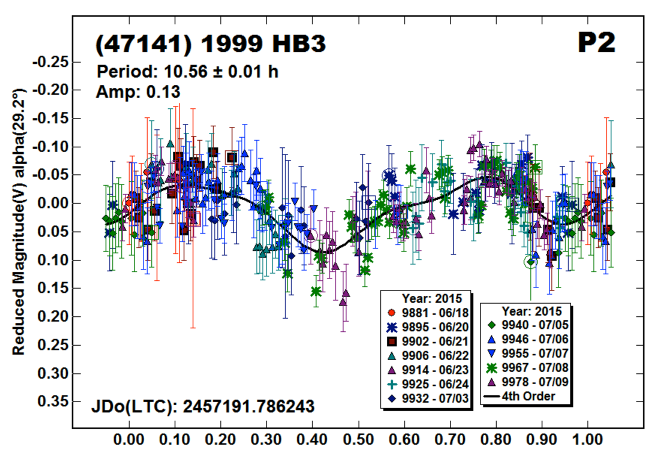

(48601) 1995 BL. The period of 4.598 h found in 2015 for this Hungaria agrees well with past results (Warner, 2011b; 2014b).

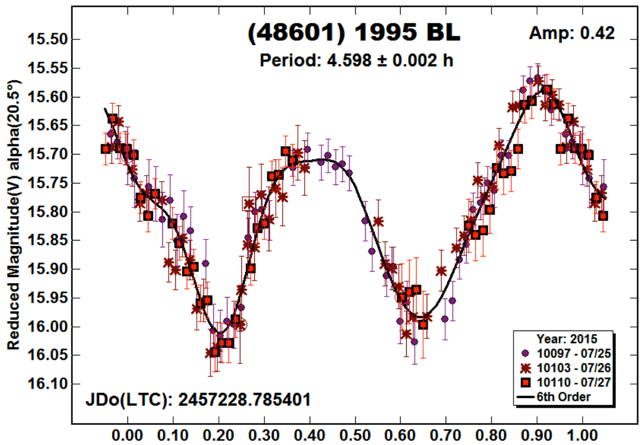

(49667) 1999 OM2. Earlier results from 2010-2014 (Warner, 2014b and references therein) match the period of 3.487 h found here.

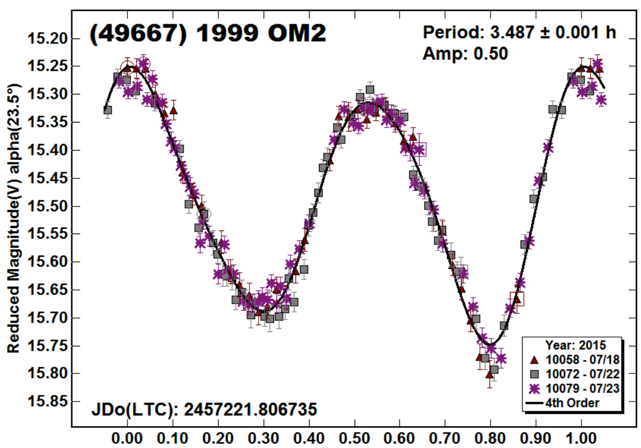

(77010) 2001 CB9. This inner main-belt object was in the same field as a planned target. Despite having only one night of data, the run covered just more than a complete cycle and so a period could be found, although the precision is limited because of short time span covered in the data set.

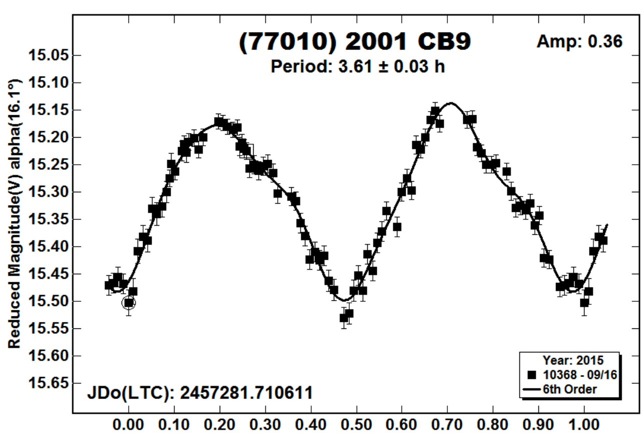

(86192) 1999 SV1. Using sparse data from 2010 obtained by the Palomar Transient Factory, Waszczak *et al.* (2015) found a period of 7.1604 h for 1999 SV1. The author (Warner, 2011b) found a period of 7.164 h from data taken about a month earlier. Results from 2014 (Warner, 2014a) and the 2015 apparition are in close agreement at 7.157 h.

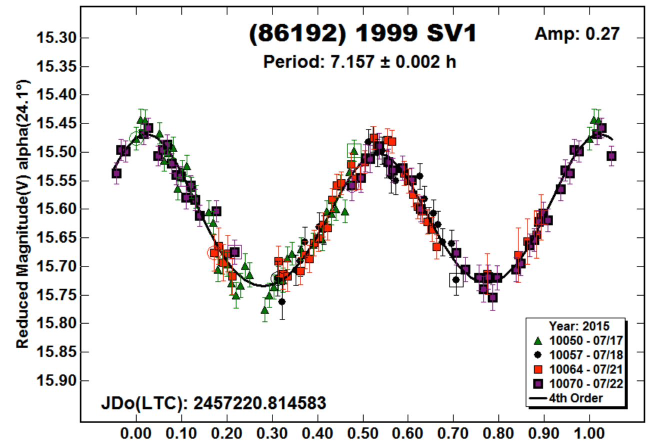

(132597) 2002 JM141, (189296) 2005 UT407. These two main-belt asteroids were initially in the field of a planned target. For 2002 JM141, the data are limited and noisy, so the period of 7.10 h reported here is far from secure. Because it showed promise of yielding a secure period, 2005 UT407 was followed after it left the field of the planned asteroid. The period of 15.54 h is reasonably secure.

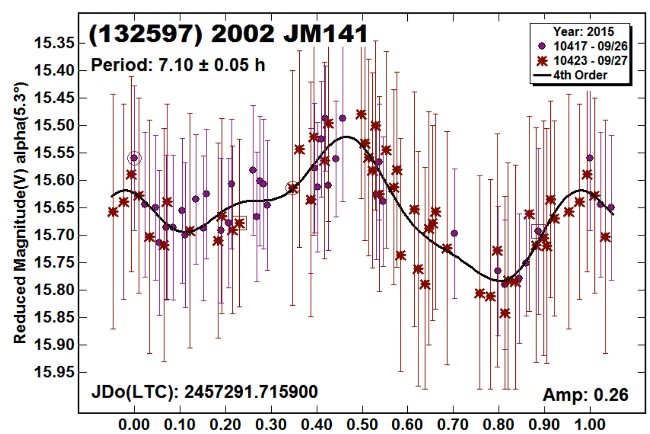

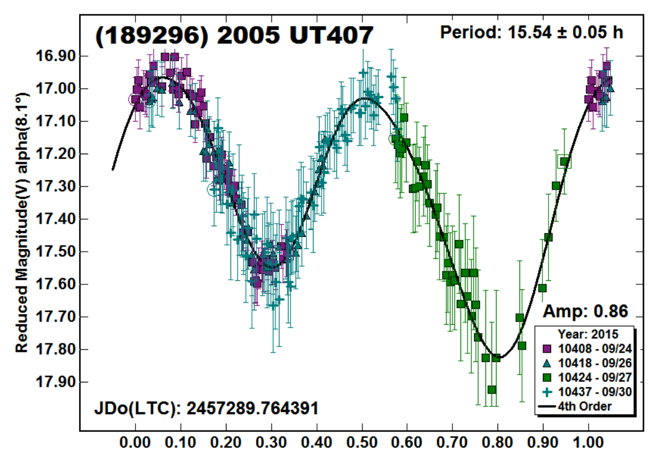

Acknowledgements

Funding for PDS observations, analysis, and publication was provided by NASA grant NNX13AP56G. Work on the asteroid lightcurve database (LCDB) was also funded in part by National Science Foundation grants AST-1210099 and AST-1507535. This research was made possible in part based on data from CMC15 Data Access Service at CAB (INTA-CSIC) and the AAVSO Photometric All-Sky Survey (APASS), funded by the Robert Martin Ayers Sciences Fund. (*http://svo2.cab.inta-csic.es/vocats/cmc15/).*

This publication makes use of data products from the Two Micron All Sky Survey, which is a joint project of the University of Massachusetts and the Infrared Processing and Analysis Center/California Institute of Technology, funded by the National Aeronautics and Space Administration and the National Science Foundation. (http://www.ipac.caltech.edu/2mass/)

References

Behrend, R. (2007). Observatoire de Geneve web site. *http://obswww.unige.ch/~behrend/page_cou.html*

Gil-Hutton, R., Canada, M. (2003). "Photometry of Fourteen Main Belt Asteroids." *Revista Mexicana de Astronomica y Astrofisica* **39**, 69-76.

Harris, A.W., Young, J.W., Scaltriti, F., Zappala, V. (1984). "Lightcurves and phase relations of the asteroids 82 Alkmene and 444 Gyptis." *Icarus* **57**, 251-258.

Harris, A.W., Pravec, P., Galad, A., Skiff, B.A., Warner, B.D., Vilagi, J., Gajdos, S., Carbognani, A., Hornoch, K., Kusnirak, P., Cooney, W.R., Gross, J., Terrell, D., Higgins, D., Bowell, E., Koehn, B.W. (2014). "On the maximum amplitude of harmonics on an asteroid lightcurve." *Icarus* **235**, 55-59.

Henden, A.A., Terrell, D., Levine, S.E., Templeton, M., Smith, T.C., Welch, D.L. (2009). *http://www.aavso.org/apass*

Pravec, P., Vokrouhlicky, D., Polishook, D., Scheeres, D.J., Harris, A.W., Galad, A., Vaduvescu, O., Pozo, F., Barr, A., Longa, P., *and 16 coauthors*. (2010). "Formation of asteroid pairs by rotational fission." *Nature* **466**, 1085-1088.

Stephens, R.D. (2003). "Photometry of 628 Christine, 754 Malabar, 815 Coppelia, and 1025 Riema." *Minor Planet Bull.* **30**, 69-70.

Stephens, R.D. (2004). "Photometry of 804 Hispania, 899 Jokaste, 1306 Scythia, and 2074 Shoemaker." *Minor Planet Bull*. **31**, 40-41.

Warner, B.D. (2007). "Initial Results of a Dedicated H-G Program." *Minor Planet Bull.* **34**, 113-119.

Warner, B.D. (2008). "Asteroid Lightcurve Analysis at the Palmer Divide Observatory: December 2007 - March 2008." *Minor Planet Bull*. **35**, 95-98.

Warner, B.D., Harris, A.W., Pravec, P. (2009a). "The Asteroid Lightcurve Database." *Icarus* **202**, 134-146. Updated 2015 Sept. *http://www.minorplanet.info/lightcurvedatabase.html*

Warner, B.D., Stephens, R.D., Harris, A.W., Pravec, P. (2009b). "A Re-examination of the Lightcurves for Seven Hungaria Asteroids." *Minor Planet Bull*. **36**, 176-178.

Warner, B.D. (2010). "Asteroid Lightcurve Analysis at the Palmer Divide Observatory: 2010 March - June." *Minor Planet Bull*. **37**, 161-165.

Warner, B.D. (2011a). "A Quartet of Known and Suspected Hungaria Binary Asteroids." *Minor Planet Bull*. **38**, 33-36.

Warner, B.D. (2011b). "Asteroid Lightcurve Analysis at the Palmer Divide Observatory: 2010 September-December." *Minor Planet Bull.* **38**, 82-86.

Warner, B.D. (2011c). "Asteroid Lightcurve Analysis at the Palmer Divide Observatory: 2010 December- 2011 March." *Minor Planet Bull*. **38**, 142-149.

Warner, B.D., Stephens R. (2012a). "Lightcurve for 2074 Shoemaker." *Minor Planet Bull*. **39**, 225.

Warner, B.D. (2012b). "Asteroid Lightcurve Analysis at the Palmer Divide Observatory: 2012 March - June." *Minor Planet Bull*. **39**, 245-252.

Warner, B.D. (2013a). "Asteroid Lightcurve Analysis at the Palmer Divide Observatory: 2012 June - September." *Minor Planet Bull*. **40**, 26-29.

Warner, B.D. (2013b). "Rounding Up the Unusual Suspects." *Minor Planet Bull*. **40**, 36-42.

Warner, B.D. (2014a). "Asteroid Lightcurve Analysis at CS3-Palmer Divide Station: 2013 September-December." *Minor Planet Bull.* **41**, 102-112.

Warner, B.D. (2014b). "Asteroid Lightcurve Analysis at CS3-Palmer Divide Station: 2014 January-March." *Minor Planet Bull.* **41**, 144-155.

Warner, B.D. (2014c). "Asteroid Lightcurve Analysis at CS3-Palmer Divide Station: 2014 March-June." *Minor Planet Bull*. **41**, 235-241.

Warner, B.D. (2015). "The ALCDEF database." *http://www.minorplanetcenter.net/light_curve*

Waszczak, A., Chang, C.-K., Ofek, E.O., Laher, R., Masci, F., Levitan, D., Surace, J., Cheng, Y.-C., Ip, W.-H., Kinoshita, D., Helou, G., Prince, T.A., Kulkarni, S. (2015). "Asteroid Light Curves from the Palomar Transient Factory Survey: Rotation Periods and Phase Functions from Sparse Photometry." *Astron. J.* **150**, A75.

Wisniewski, W.Z., Michalowski, T.M., Harris, A.W., McMillan, R.S. (1997). "Photometric Observations of 125 Asteroids." *Icarus* **126**, 395-449.

NEAR-EARTH ASTEROID LIGHTCURVE ANALYSIS AT CS3-PALMER DIVIDE STATION: 2015 JUNE-SEPTEMBER

Brian D. Warner
Center for Solar System Studies / MoreData!
446 Sycamore Ave.
Eaton, CO 80615 USA
brian@MinorPlanetObserver.com

(Received: 2015 October 6)

Lightcurves for 46 near-Earth asteroids (NEAs) were obtained at the Center for Solar System Studies-Palmer Divide Station (CS3-PDS) from 2015 June-September. Four of the asteroids showed indications of non-principal axis rotation (NPAR), or tumbling, (9400) 1994 TW1, (86666) 2000 FL10, (154807) 2004 PP97, and (206378) 2003 RB, but there were insufficient data for full analysis. On the other hand, 2015 JY1 is a confirmed tumbler with a dominate period of 6.442 h and a likely second period of 11.42 h. Evidence of the satellite for the known binary system (385186) 1994 AW1 was found. The estimated size ratio of Ds/Dp ≥ 0.25 is in good agreement with earlier results. A third period was also found but its origin is not confirmed.

CCD photometric observations of 46 near-Earth asteroids (NEAs) were made at the Center for Solar System Studies-Palmer Divide Station (CS3-PDS) from 2015 June-September. Table I lists the telescope/CCD camera combinations used for the observations. All the cameras use CCD chips from the KAF blue-enhanced family and so have essentially the same response. The pixel scales for the combinations range from 1.24-1.60 arcsec/pixel.

Desig	Telescope	Camera
Squirt	0.30-m f/6.3 Schmidt-Cass	ML-1001E
Borealis	0.35-m f/9.1 Schmidt-Cass	STL-1001E
Eclipticalis	0.35-m f/9.1 Schmidt-Cass	ML-1001E
Australius	0.35-m f/9.1 Schmidt-Cass	STL-1001E
Zephyr	0.50-m f/8.1 R-C	FLI-1001E

Table I. List of CS3-PDS telescope/CCD camera combinations.

All lightcurve observations were unfiltered since a clear filter can result in a 0.1-0.3 magnitude loss. The exposure duration varied depending on the asteroid's brightness and sky motion. Guiding on a field star sometimes resulted in a trailed image for the asteroid.

Measurements were done using *MPO Canopus*. If necessary, an elliptical aperture with the long axis parallel to the asteroid's path was used. The Comp Star Selector utility in *MPO Canopus* found up to five comparison stars of near solar-color for differential photometry. Catalog magnitudes were usually taken from the MPOSC3 catalog, which is based on the 2MASS catalog (*http://www.ipac.caltech.edu/2mass*) but with magnitudes converted from J-K to BVRI using formulae developed by Warner (2007). The nightly zero points have been found to be consistent to about ± 0.05 mag or better, but on occasion are as large as 0.1 mag. Period analysis is also done using *MPO Canopus*, which implements the FALC algorithm developed by Harris (Harris *et al.,* 1989).

In the plots below, the "Reduced Magnitude" is Johnson V as indicated in the Y-axis title. These are values that have been converted from sky magnitudes to unity distance by applying –5*log (rΔ) to the measured sky magnitudes with r and Δ being, respectively, the Sun-asteroid and Earth-asteroid distances in AU. The magnitudes were normalized to the given phase angle, e.g., alpha(6.5°), using $G = 0.15$, unless otherwise stated. The X-axis is the rotational phase, ranging from –0.05 to 1.05.

For the sake of brevity, only some of the previously reported results may be referenced in the discussions on specific asteroids. For a more complete listing, the reader is directed to the asteroid lightcurve database (LCDB; Warner *et al.,* 2009). The on-line version at *http://www.minorplanet.info/lightcurvedatabase.html* allows direct queries that can be filtered a number of ways and the results saved to a text file. A set of text files of the main LCDB tables, including the references with bibcodes, is also available for download. Readers are strongly encouraged to obtain, when possible, the original references listed in the LCDB for their work.

If the plot includes an amplitude, *e.g.*, "Amp: 0.65", this is the amplitude of the Fourier model curve and *not necessarily the adopted amplitude for the lightcurve*. The value is provided as a matter of convenience.

6239 Minos. Pravec *et al*. (2004w) found a period of 3.5558 h for Minos. The closest solution using the 2015 CS3 data is about 0.04 h longer.

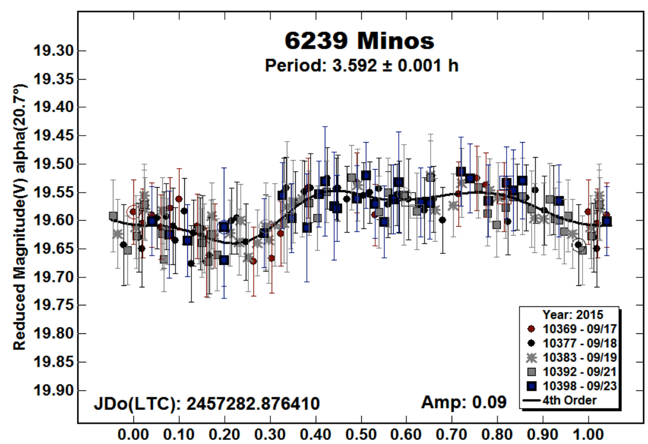

(7822) 1991 CS. Earlier results for this NEA include Pravec *et al*. (1998; 2.389 h) and Krugly *et al*. (2002; 2.3987 h). The period reported here is in good agreement. Among the three apparitions, 2015 showed the largest amplitude: 0.39 mag.

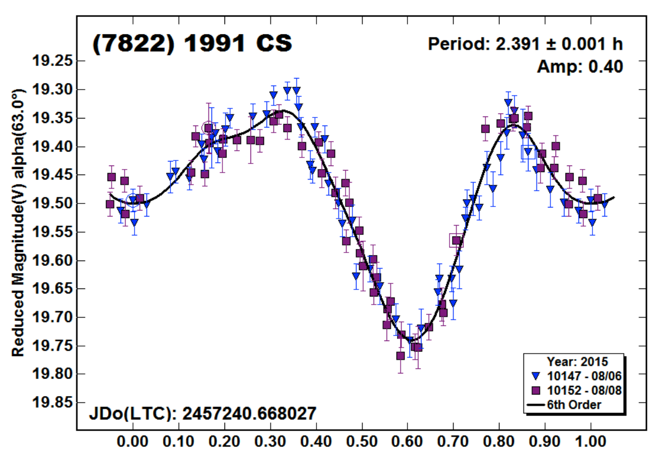

(7889) 1994 LX. Previously reported periods (Pravec *et al.*, 1996, 1998w; Behrend, 2005) found periods of about 2.74 h. Warner (2015) found a period of 2.741 h with an amplitude of 0.39 mag at solar phase angle α ≅ 51° from data obtained in 2015 March. Four months later, the same period was found but the amplitude was 0.27 mag at α ≅ 33°. This is expected since there is a known amplitude-phase angle relation that gives lower amplitudes with lower phase angles (Zappala *et al.*, 1990).

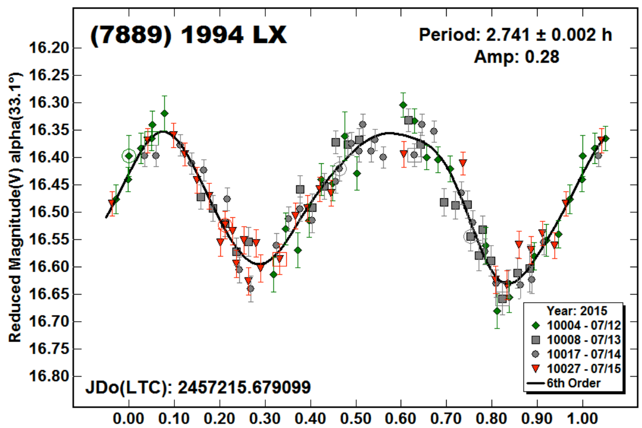

(9400) 1994 TW1. The best-fit period of 82.8 h is based on a presumed bimodal lightcurve. Given that the slopes of individual nights do not follow the slope of the Fourier model curve, it's probable that the asteroid is tumbling, *i.e.*, in non-principal axis rotation (NPAR; see Pravec *et al.*, 2005).

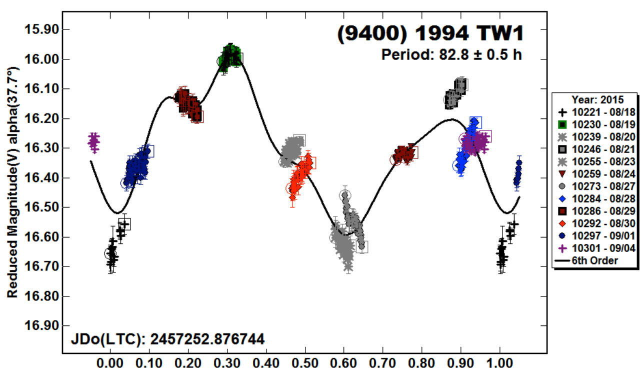

(66008) 1998 QH2. No previous results could be found in the literature for 1998 QH2.

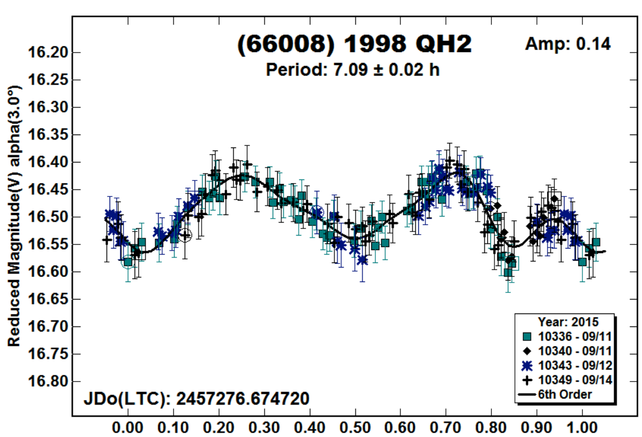

(86666) 2000 FL10. This is another suspected tumbler. There were several possible solutions in the range of 35 to 250 h. The period of 206 h produces the closest fit to a bimodal lightcurve, which – given the amplitude – is a likely solution.

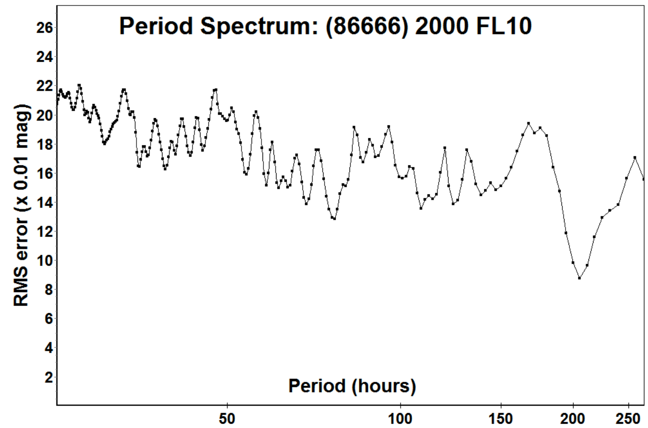

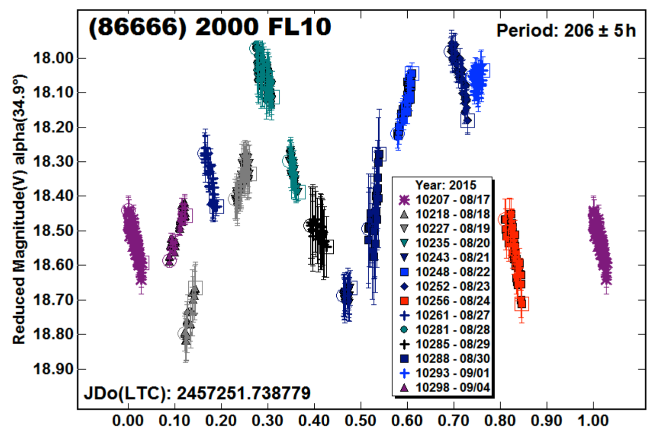

(112985) 2002 RS28. The author (Warner, 2015r) found a period of 5.94 h based on data from 2015 April, when the amplitude was only 0.06 mag. The July data produced a lightcurve with an amplitude of 0.24 mag. Even with this advantage, a definitive period was not found. Other solutions at about 4.59 h and 5.74 h are almost equally possible.

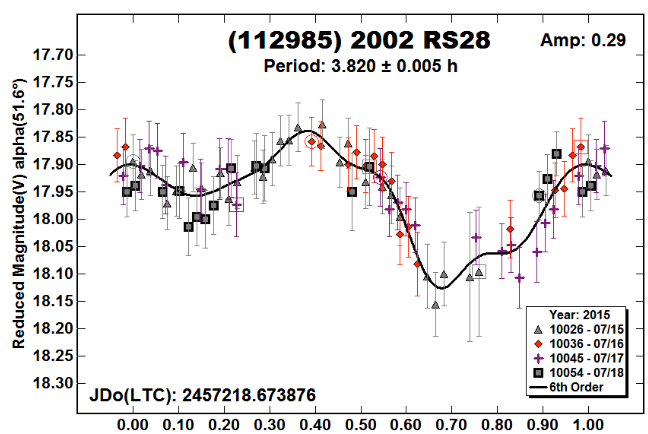

(142040) 2002 QE15. Pravec *et al.* (2002w) reported a period of 2.5811 h based on data obtained in 2002, but also found a period of ~3.87 h as a possible solution. The data from initial observations of the asteroid in 2015 July could not be fit to the shorter period. However, they did fit a monomodal lightcurve with a period of

3.66 h. A bimodal solution at 7.33 h also fits the data but this may be due to a *fit by exclusion*, where Fourier modeling minimizes overlapping data points to reduce the RMS fit.

The asteroid was worked again in 2015 October to see if it was possible to find a more definitive solution. The result was a period of 3.884 h with an amplitude of 0.17 mag. This period is closer to the alternate period reported by Pravec *et al.* (2002w).

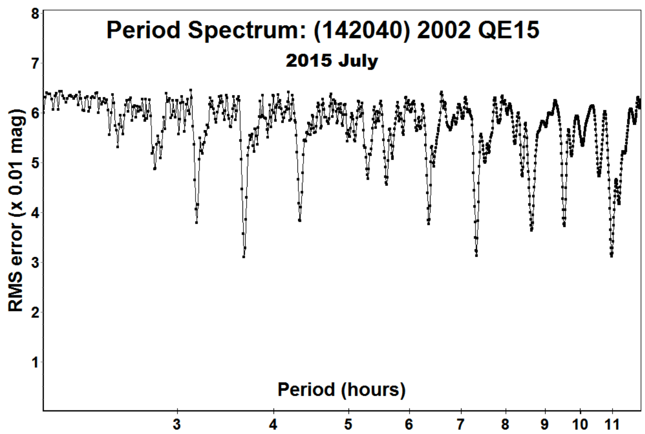

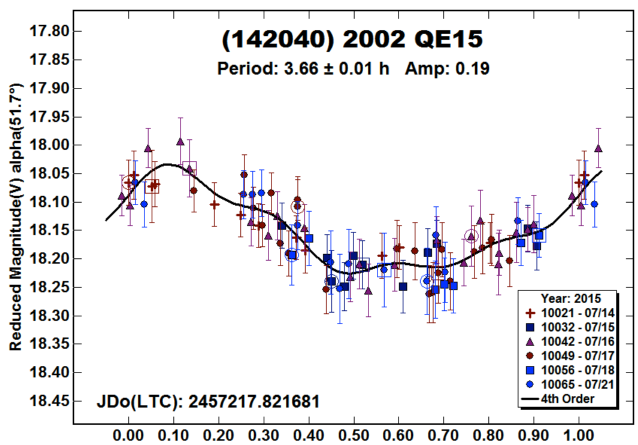

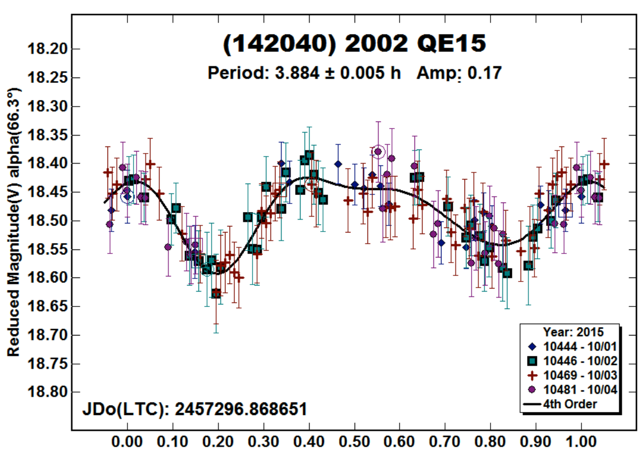

(154807) 2004 PP97. There are small indications of tumbling in the lightcurve for 2004 PP97, specifically the sessions on 2015 Sept 21 and 24 show slopes contrary to the Fourier model curve. The very long period makes it a candidate for NPAR, the longest predicted damping time being about 44 h (see Pravec *et al.*, 2014, and references therein).

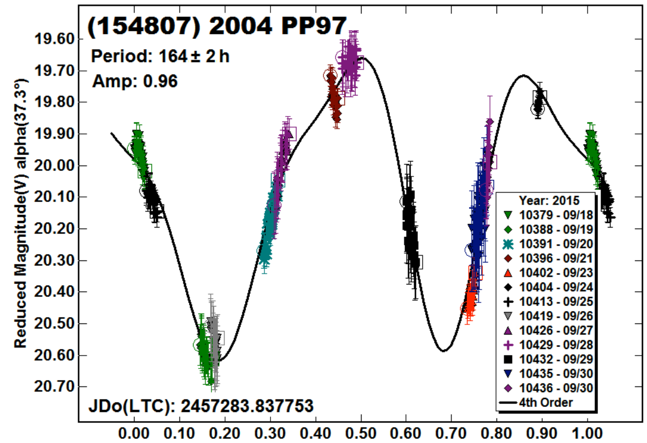

(155334) 2006 DZ169. No previously reported periods were found in the LCDB (Warner *et al.,* 2009).

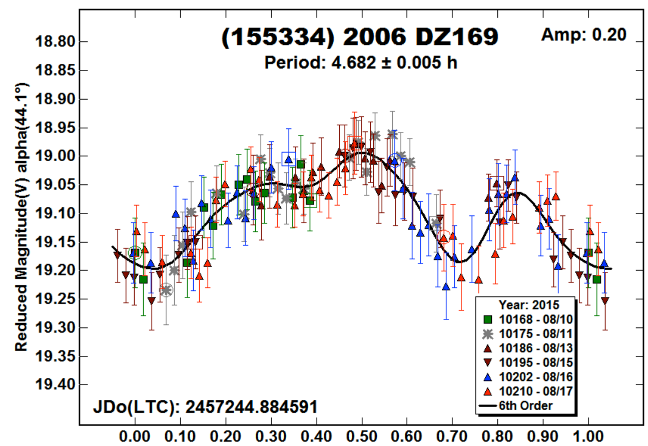

(206378) 2003 RB. This asteroid is another likely tumbler. No combination of adjusting zero points produced a reasonable fit, *i.e.*, one where all the slopes of the individual sessions matched the Fourier curve. Radar observations were made of the asteroid at Arecibo and Goldstone in mid-August. Initial indications were that the period of 37.5 h fit those data but they could not confirm whether or not the asteroid was tumbling (James Richardson; Marina Brozovic, *private communications*).

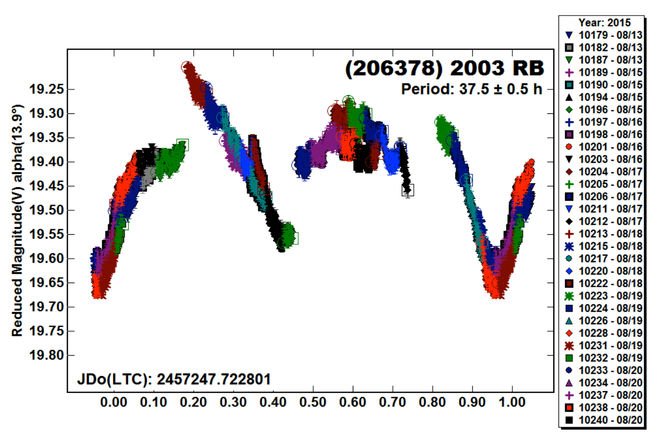

(242191) 2003 NZ6. Polishook and Brosch (2008) reported P = 13.51 h, A = 1.5 mag at $\alpha \cong 59.5°$ for data with an average date of 2005 June 5. A week later, June 12, the amplitude had dropped to

1.4 mag at α ≅ 58.2°. The CS3 data were taken at α ≅ 84.6° and found A = 1.19 mag. The lower amplitude at higher phase angle for the CS3 data can be explained by the difference of about 50° in the phase angle bisector longitude (L_{PAB}, see Harris *et al.*, 1984) between the two apparitions. Radar observations at Arecibo in mid-July suggested a double-lobed object with a period compatible to what's reported here (Patrick Taylor, *private communications*).

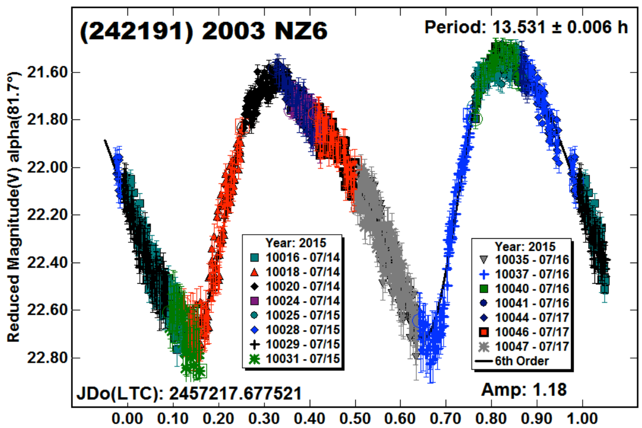

<u>(281375) 2008 JV19, (293054) 2006 WP127, (297274) 1996 SK</u>. No previously reported periods were found in the LCDB for these three asteroids.

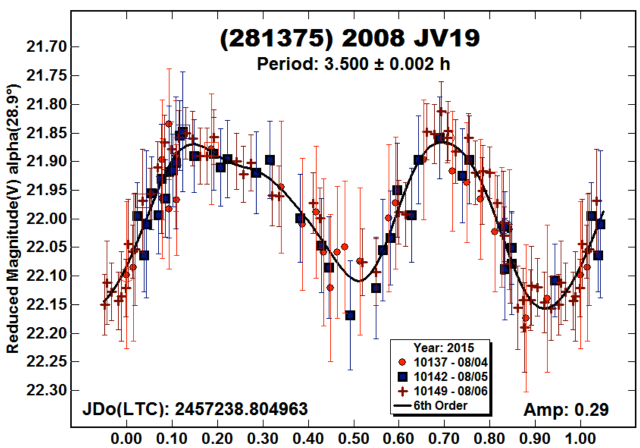

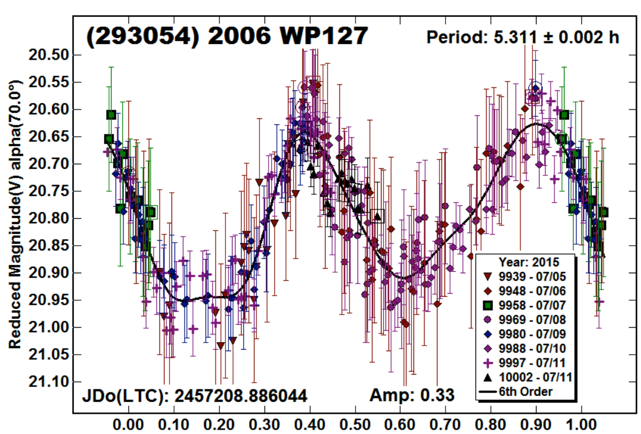

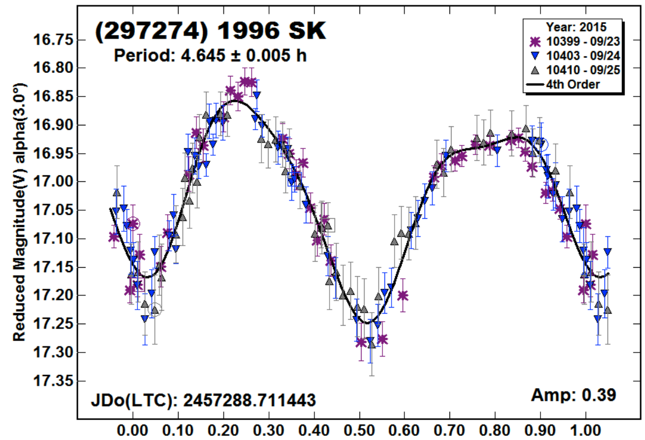

<u>(385186) 1994 AW1</u>. Mottola *et al.* (1995a) first reported that this asteroid was a binary. Pravec and Hahn (1997) confirmed the existence of a satellite and found an orbital period of P_{ORB} = 22.3 h. This was later improved to 22.38 h (Birlan *et al.*, 2010). The primary period (P_1) was found to be ~2.519 h in both cases.

The CS3 data led to P_1 = 2.5182 h and orbital period (P_2 from here on) of 22.34 h. Even after subtracting these two periods from the Fourier analysis, a third period remained, P_3 = 4.509, A = 0.07 mag. The lightcurves below show P_1 and P_2 with and without subtracting P_3 and then P_3 alone. P_1 and P_3 do not appear to be harmonically related. However, P_2/P_3 ≅ 5, or very close to an integral ratio. This could indicate that P_3 is residual noise in the solution for P_2. Neither Pravec and Hahn (1997) or Birlan *et al.* (2010) reported a third period.

The depth of the secondary (shallower) minimum of A ~ 0.07 mag for P_2 was used to find the size ratio of Ds/Dp ≥ 0.25 ± 0.02. This is close to the value of 0.28 found by Pravec and Hahn (1997).

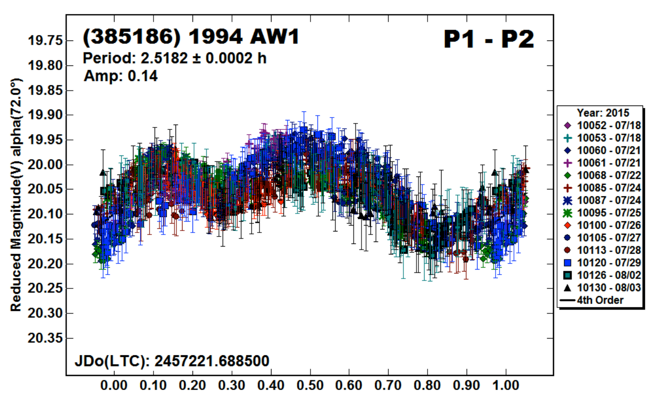

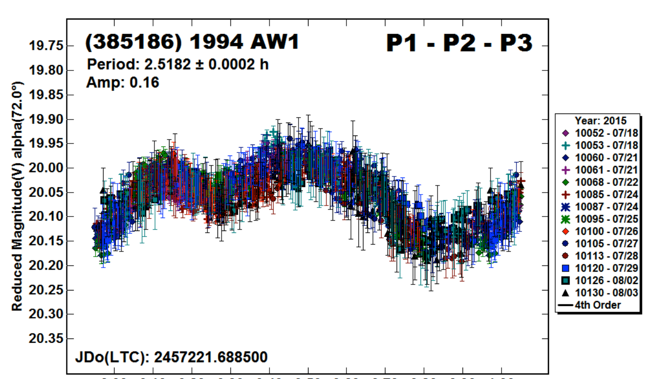

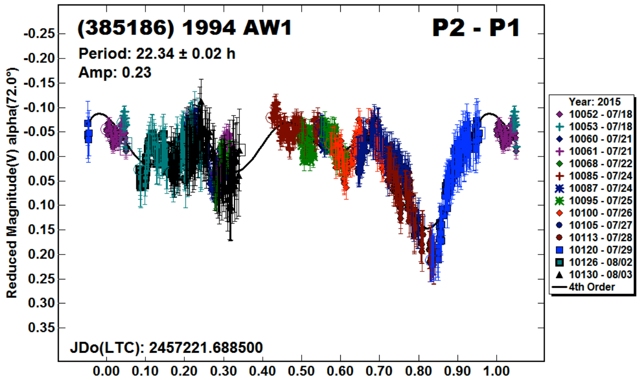

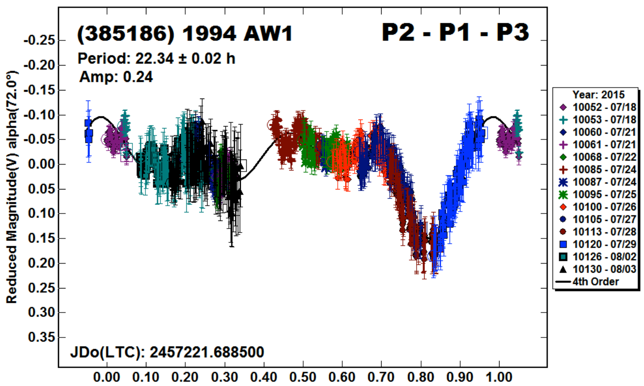

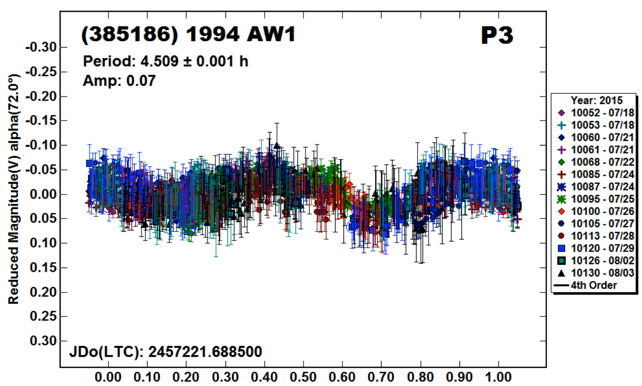

(389694) 2011 QD48. This appears to be the first reported lightcurve for 2011 QD48.

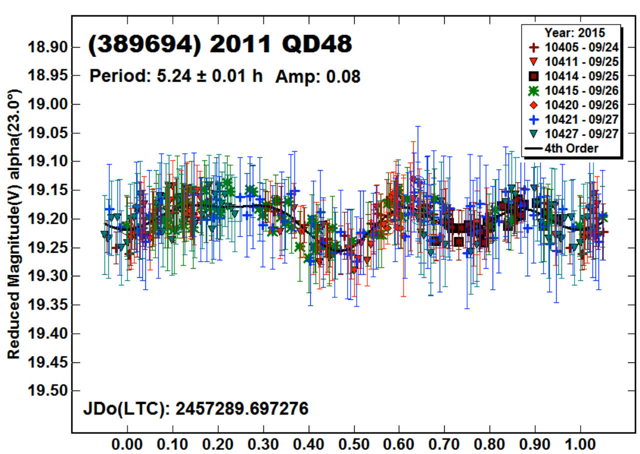

(436724) 2011 UW158. Data were obtained of 2011 UW158 in support of radar observations which confirmed the short rotation period of only 36.64 minutes (Patrick Taylor, *private comm.*).

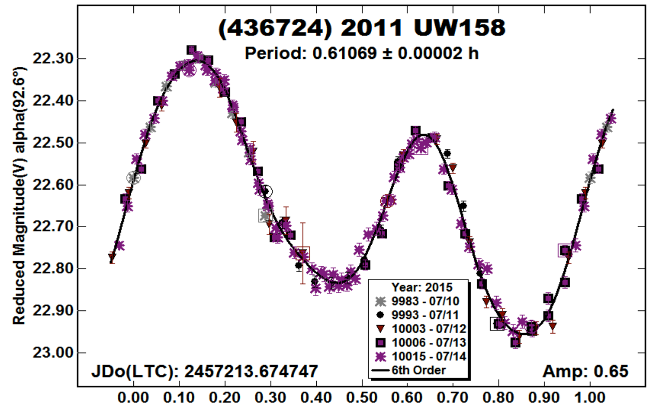

(438105) 2005 GO22, (438429) 2006 WN1, (441825) 2009 SK1. The LCDB did not have any entries for these three NEAs. Radar observations at Arecibo on August 11 (Patrick Taylor, *private communications*) confirm a rapid rotation for 2005 GO22. However, for the reported period of 4.1 hours, this requires that the absolute magnitude of H = 18.6 is too large (faint) and/or the albedo be on the order of $p_V \sim 0.02$.

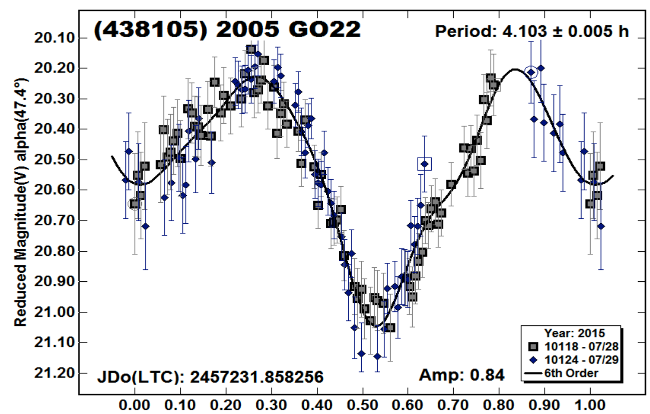

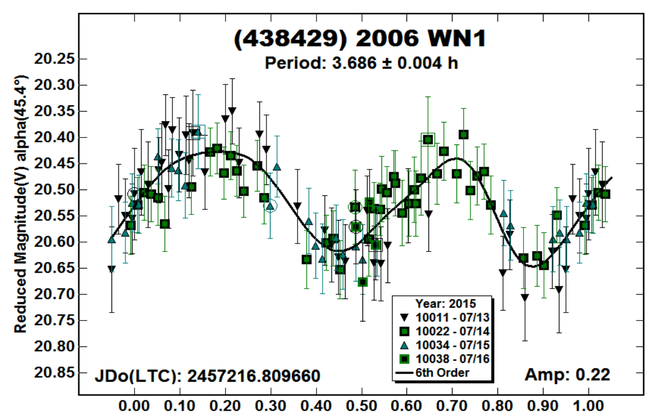

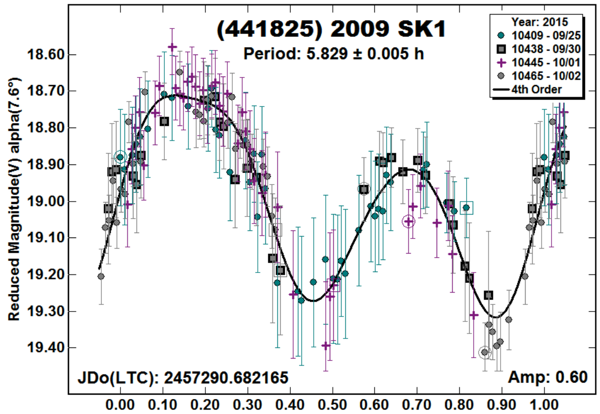

(443880) 2001 UZ16. The period spectrum for this asteroid showed several possible solutions. The one near 7 hours was rejected because its lightcurve was monomodal. Given the amplitude of 0.97 mag, a bimodal solution was presumed, despite the phase angle of 85°, where presumptions about lightcurve shape do not always hold. Radar observations at Arecibo on September 13 (Patrick Taylor, *private communications)* are consistent with the lightcurve-derived period.

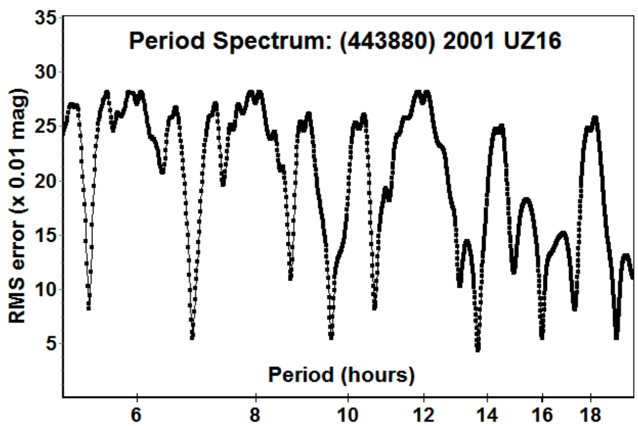

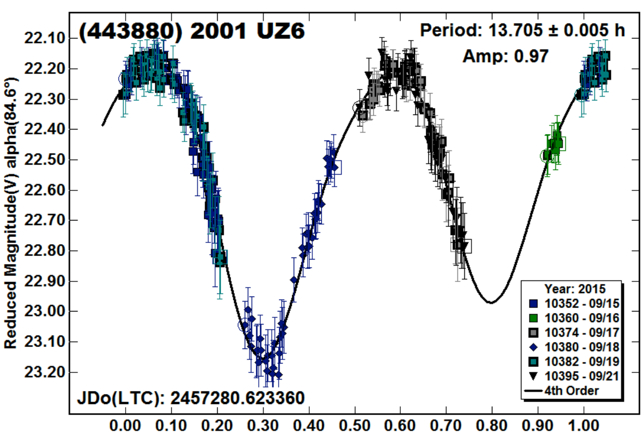

2004 MW2. The period spectrum demonstrates the oft-stated requirement of obtaining data on consecutive nights. With a gap of nine days, the uncertainty about the number of rotations is enormous. The adopted period is based on the assumption that, because of the amplitude of 0.41 mag, the shortest bimodal solution is more likely correct. It remains to be seen if that assumption is valid.

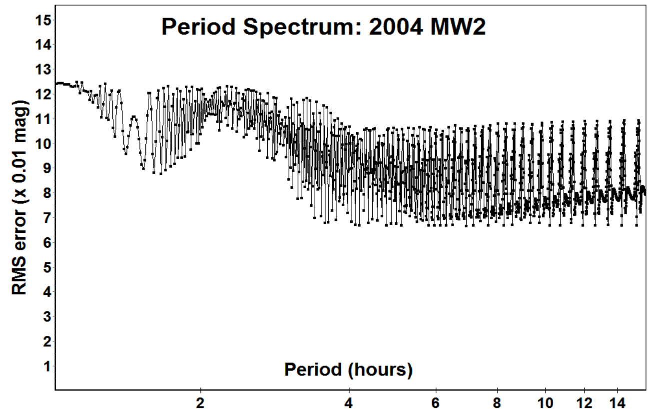

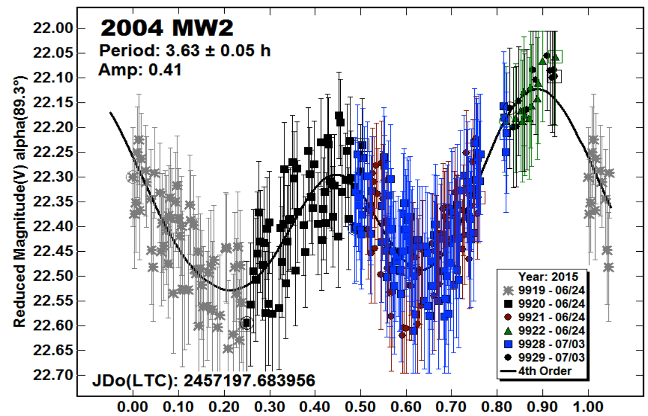

2006 AW, 2007 RU9. These appear to be the first reported lightcurves for these two NEAs.

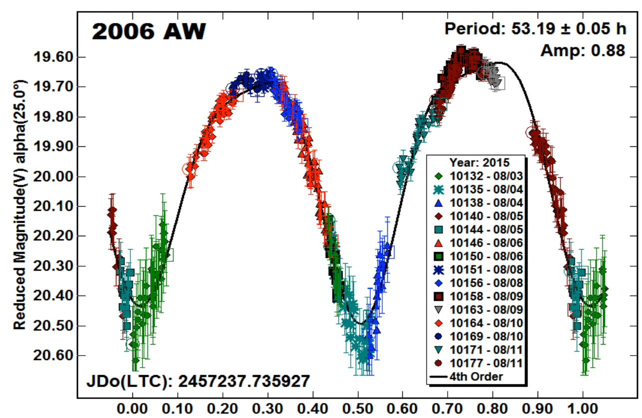

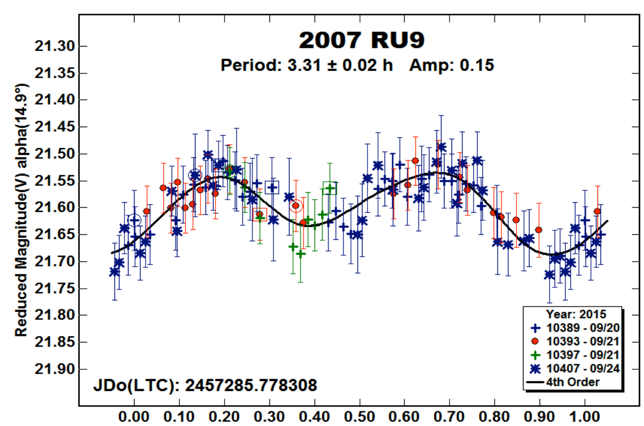

(442037) 2010 PR66. The period for 2010 PR66 is just slightly above the so-called *spin barrier*, which is used to separate *rubble pile* asteroids, those held together by mutual gravitation, and *strength-bound* asteroids, those that are held together by cohesive and other forces. However, the barrier is not a hard-fast line since it depends on density as well as rotation period. Until and unless other data, *e.g.*, spectroscopic or thermal, are available, this will remain a border-line object that could be either type. Analysis of radar observations at Arecibo in late July (Patrick Taylor, *private communications*) is consistent with the lightcurve-derived period.

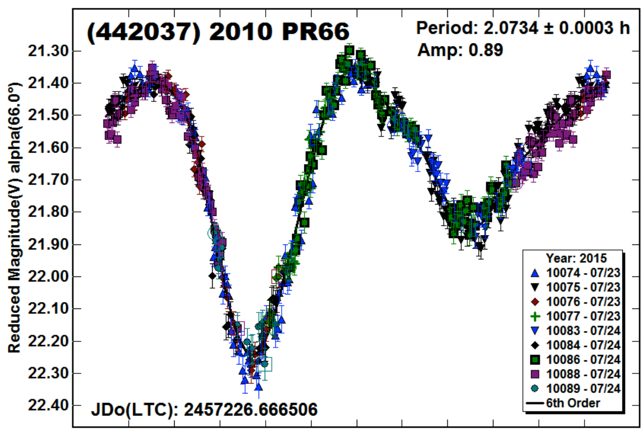

2012 NP. There were no previously reported periods found. The amplitude and phase angle make a bimodal solution likely (Harris *et al.*, 2014).

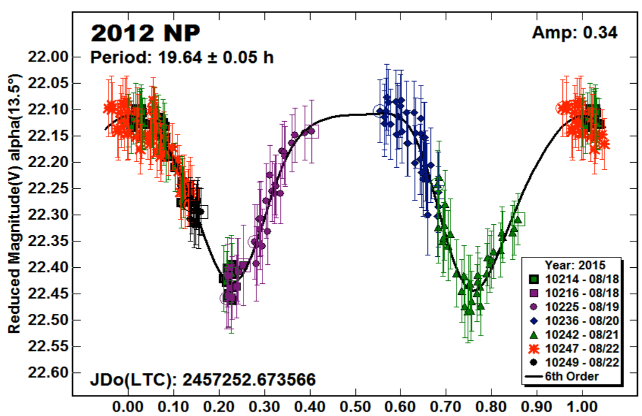

2012 TM139. The period spectrum shows more than one likely period. The one at 2.68 h is adopted for this paper although the double period at 5.37 h cannot be formally excluded.

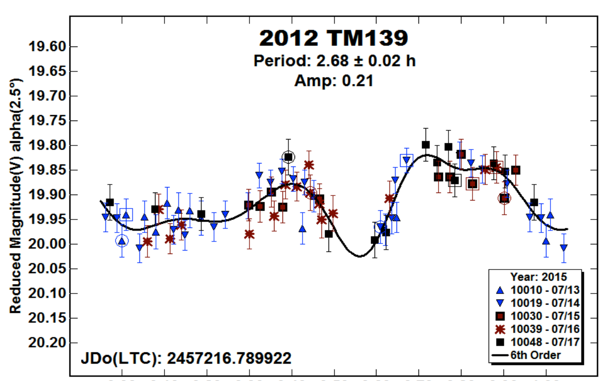

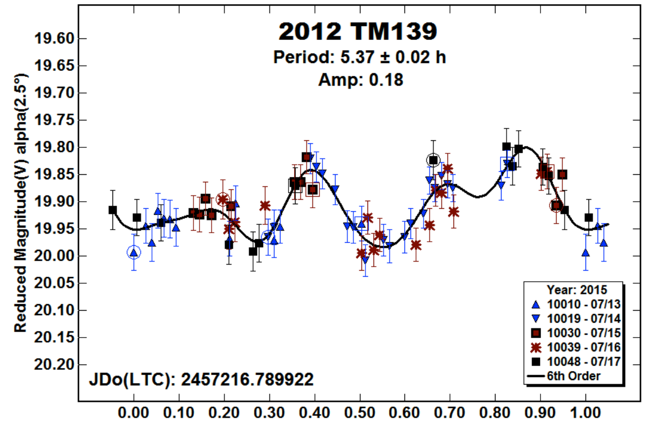

2015 OH. While the period spectrum for 2015 OH shows a preference for a period of 4.729 hours, this results in a somewhat unusual shape. However, this is not improbable given the large phase angle (Harris *et al.*, 2014). The alternate solution of 2.630 h is a more typical bimodal shape though, here again, that assumption is not always valid for asteroids with a lightcurve amplitude of 0.20 mag (Harris *et al.*, 2014). Radar observations at Arecibo on July 23 (Patrick Taylor, *private communications*) were too marginal to estimate a rotation period.

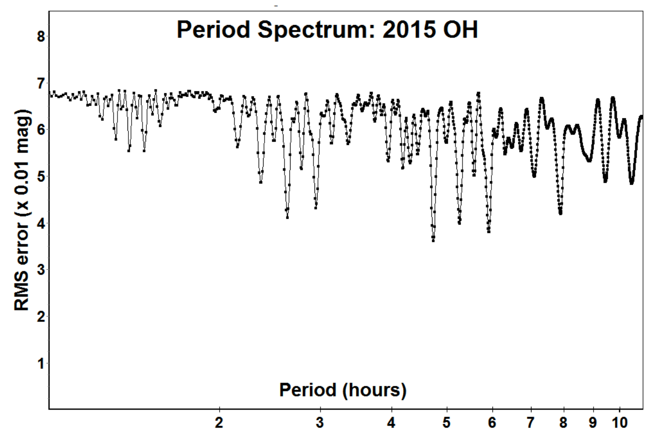

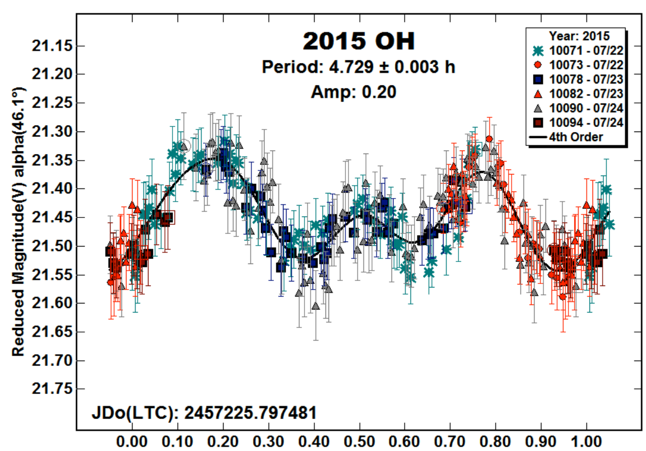

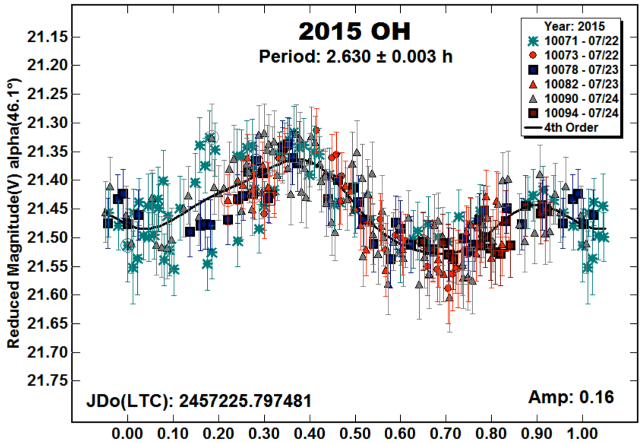

2015 NF. The combination of a short observing window, data from a single station, and a period closely commensurate with an Earth day often makes for an ambiguous solution. In this case, the situation was more difficult because adjustments of only 0.05 mag in the nightly zero points changed which of the two more likely periods, 12.06 h or 9.63 h, was favored. The lightcurves for each period make a compelling case. Fortunately, the raw plot of the data from 2015 July 8 shows that the session appears to have covered a minimum and succeeding maximum. Assuming a nearly symmetrical bimodal lightcurve, this led to a period of about 11 hours. Furthermore a search for the half-period in the range of 3-7 hours showed a strong preference for 6 hours, not 4.8, and so the longer period of 12.06 h is adopted for this paper.

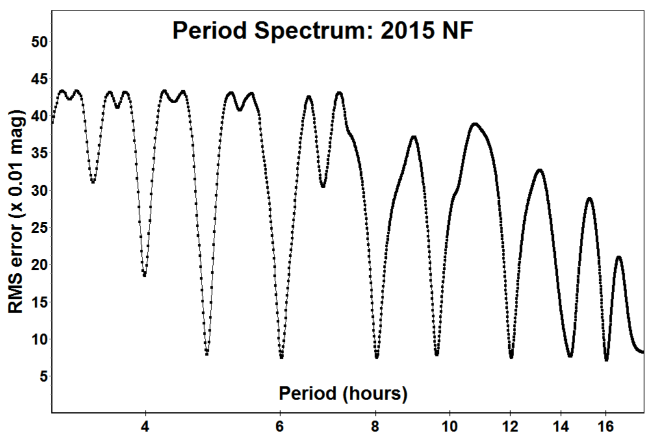

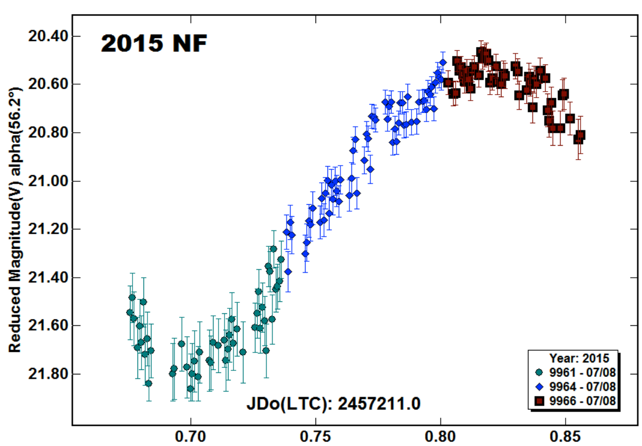

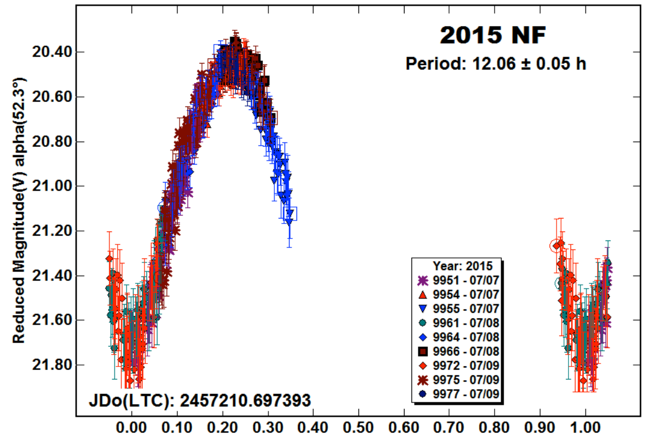

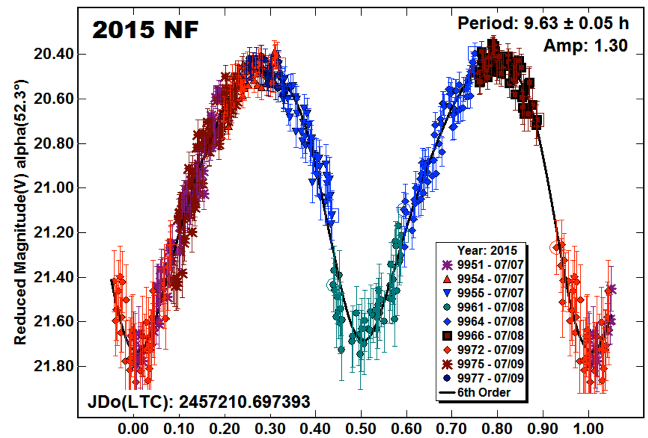

2015 PR. This appears to be the first reported period for 2015 PR. It not considered secure, however.

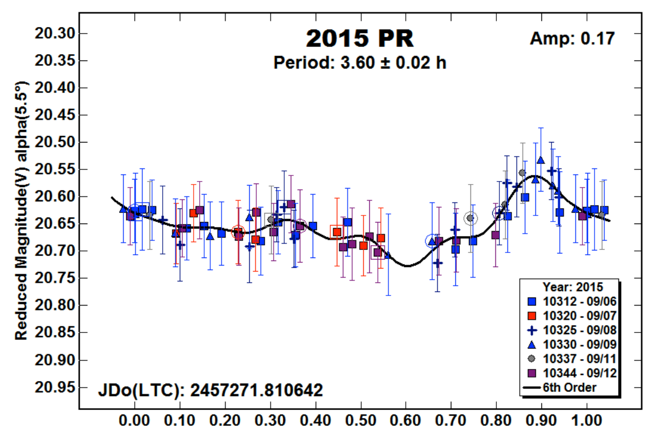

2015 JY1. The two lightcurves for this tumbling asteroid presented here are forced to the periods found by Petr Pravec (*private communications*). The solution for the shorter period of 6.442 h is stronger than for the longer period of 11.417 h. It is not certain which is the period of rotation and that of precession. It is also not certain that these are the true periods but those found as a result of a linear combination of two frequencies, *i.e.*,

$$1/mf_1 + 1/nf_2$$

where m and n are integer values (see Pravec *et al.*, 2005). Radar observation on July 5 (Patrick Taylor, *private communications*) indicated a period of about 5 hours, not far removed from the dominant period reported from the lightcurve data. The difference might be explained by the asteroid being a little larger than the radar data indicated.

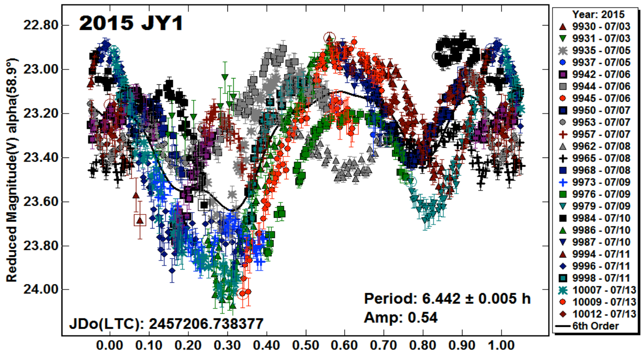

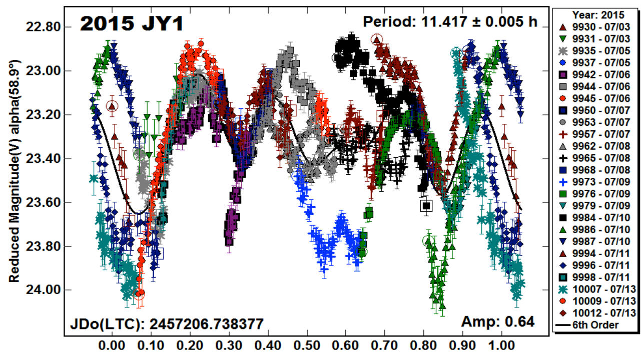

2015 RS1. No earlier results on this asteroid were reported in the LCDB.

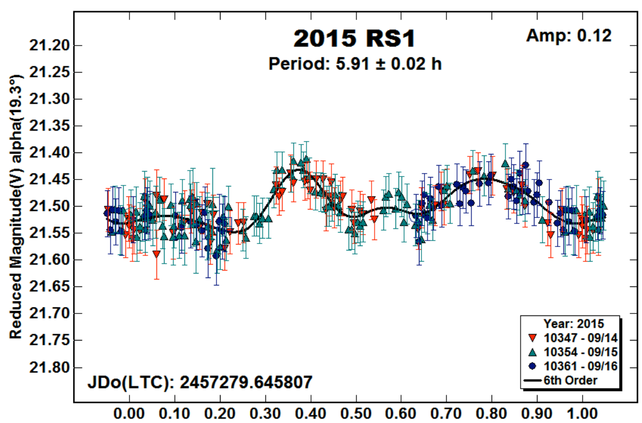

2015 LG2. The original period spectrum only slightly favored a period of 16.31 h. However, radar observations on July 31 (Patrick Taylor, *private communications*) suggested a period of a few hours rather than 16 hours, unless the asteroid was much larger than expected. Assuming that the radar period was closer to the actual period, the lightcurve data were re-analyzed.

As seen in the revised period spectrum, there are five solutions that are equally likely. The solution near 8 hours is simply the half-period of the 16-hour solution. The second lightcurve shown here is for 6.12 hours, which had the second lowest RMS fit to the Fourier model curve. A plausible case can also be made for the double-period of about 12 hours. However, given the large phase angle, the usual assumptions about a bimodal solution, even with an amplitude of at least 0.3 mag, do not always hold.

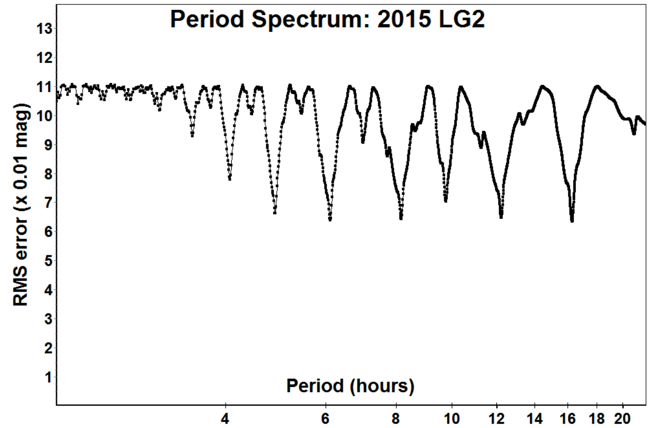

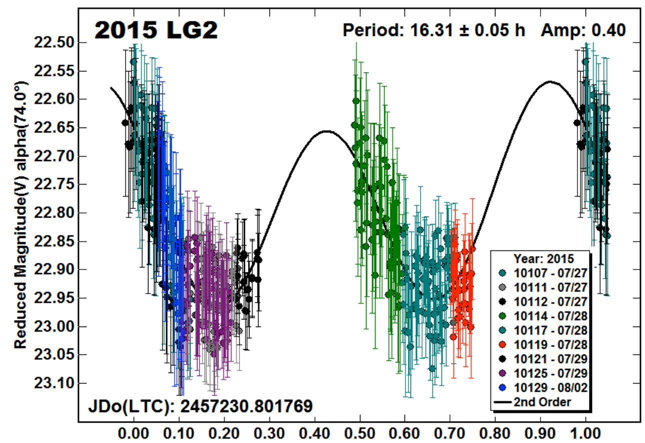

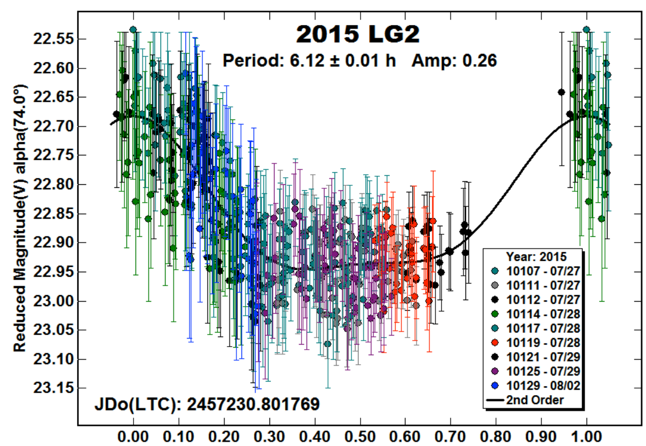

2015 PK9. This asteroid was not originally a target for radar observations at Arecibo or Goldstone. When initial lightcurve results were sent to the radar team, it was put on the list for Arecibo. The radar data had a low SNR but did support the period of 3.298 h and apparently elongated body (large amplitude) reported here (James Richardson, *private communications*). This is another example where open communications between optical and radar observers proved fruitful.

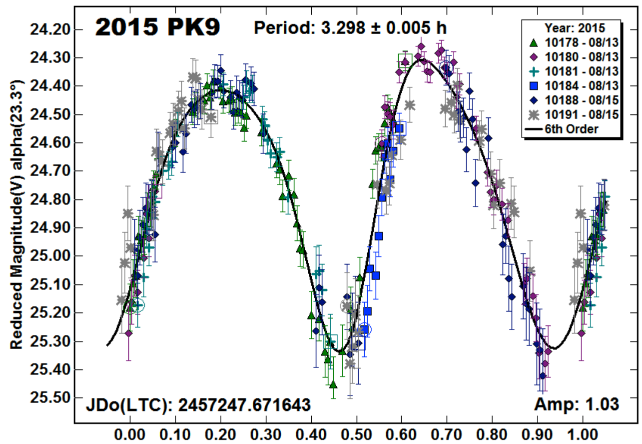

2015 QT9. The period spectrum showed a number of possibilities. A search on the half-period for some of those led to the adoption a period of 7.74 h for the asteroid.

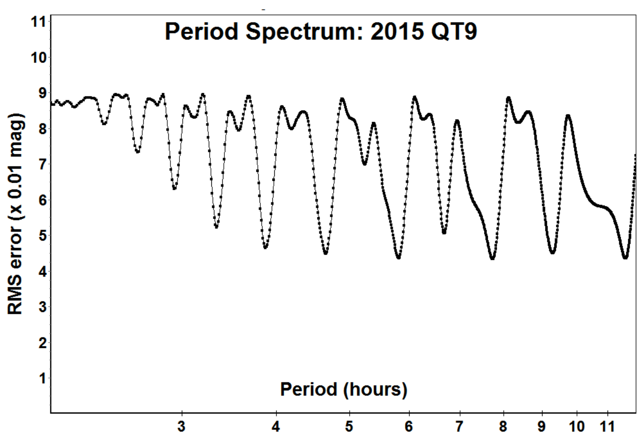

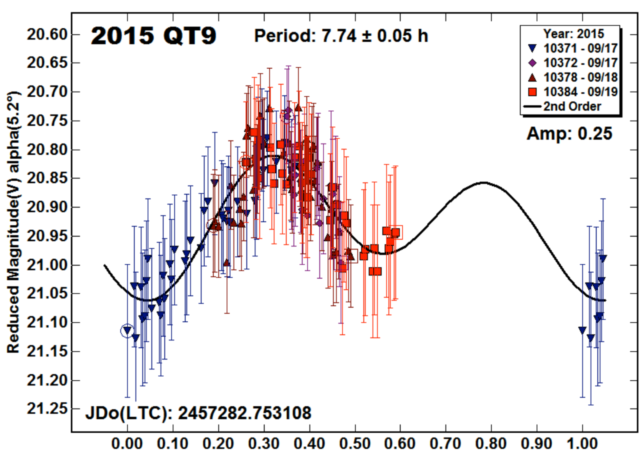

2015 NK13, 2015 NS13. No previously reported periods were found in the literature for either asteroid. Due to the very large error bars, the solution for 2015 NK13 should be considered suspect. On the other hand, the solution of 2015 NS13 is fairly secure given the relatively low phase angle and amplitude (see Harris *et al.*, 2014).

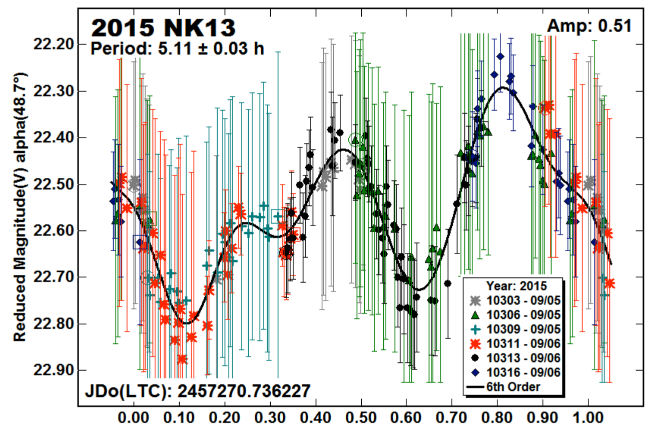

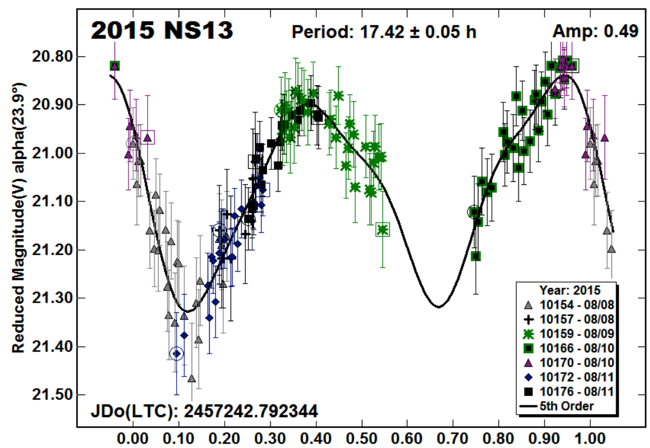

2015 NZ13. Several possible solutions were seen in the period spectrum. The lightcurve for a period at 3.42 h managed to fit the best, but the solution could be entirely wrong. Radar observations at Arecibo on July 27 (Patrick Taylor, *private communications*) were suggestive of a "long-ish" period, but this is subject to the viewing geometry, *i.e.*, an assumed equatorial view results in the slowest possible speed. If the radar observations were pole-on, then the period derived from those data could be faster.

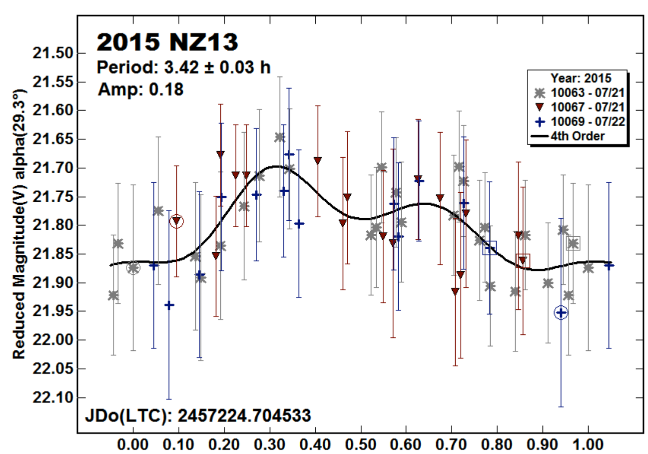

2015 A14. Radar observations (Patrick Taylor, *private communications*) about the same time as the data were obtained at CS3 support the period of 6.91 h.

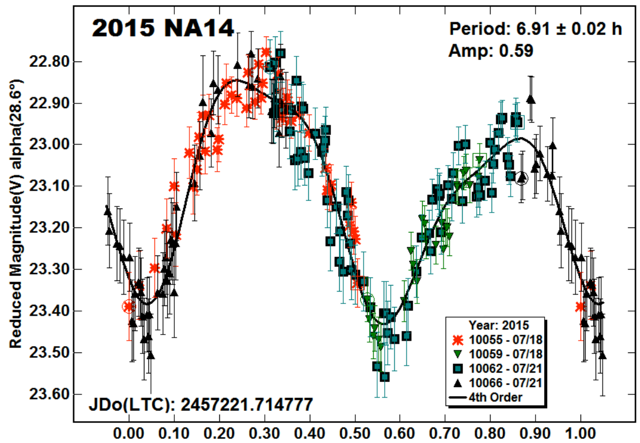

2015 SA17. This appears to be the first reported lightcurve for this NEA.

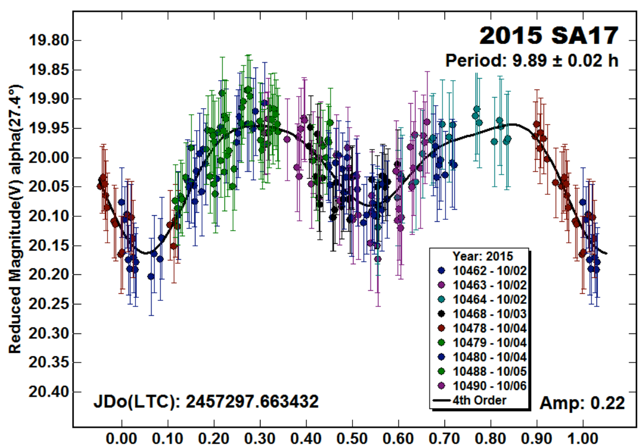

2015 OL35. Despite the unusual shape of the lightcurve with a period of 5.349 h, no other solution had a reasonably good fit. The unusual shape may be due to shadowing at the relatively high phase angle.

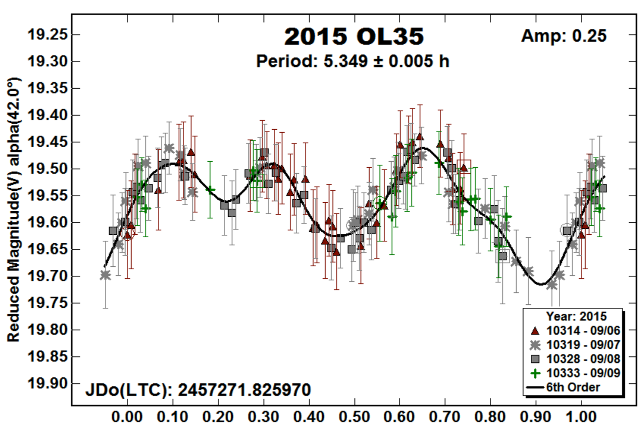

2015 MU59. There are two distinctly favored results in the period spectrum for 2015 MU59. Neither lightcurve is overly convincing. A search covering the range of the half periods favored full periods of 16 and 19 hours and, therefore, did not help resolve the ambiguity. The shorter period of 14.31 h is adopted for this paper.

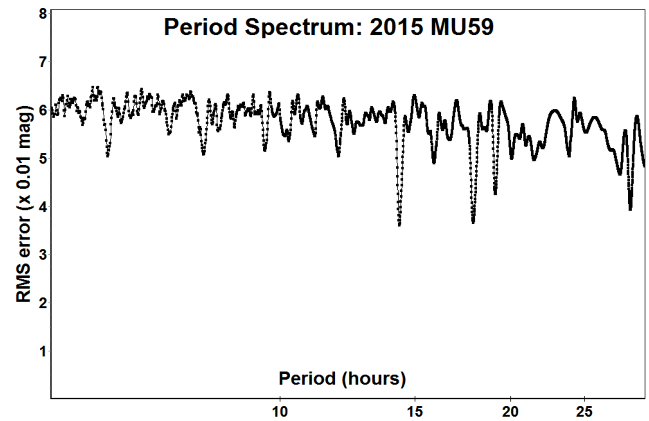

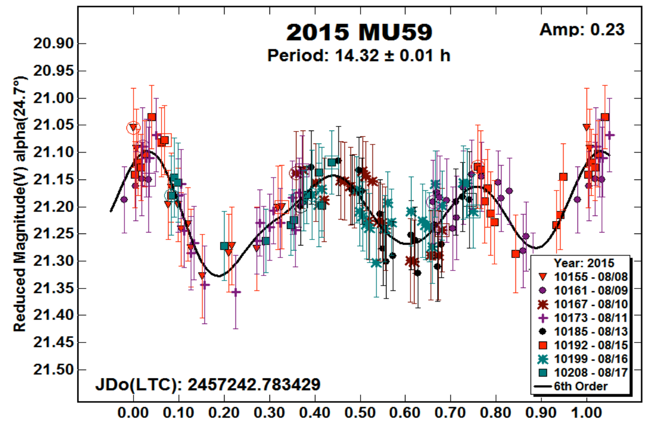

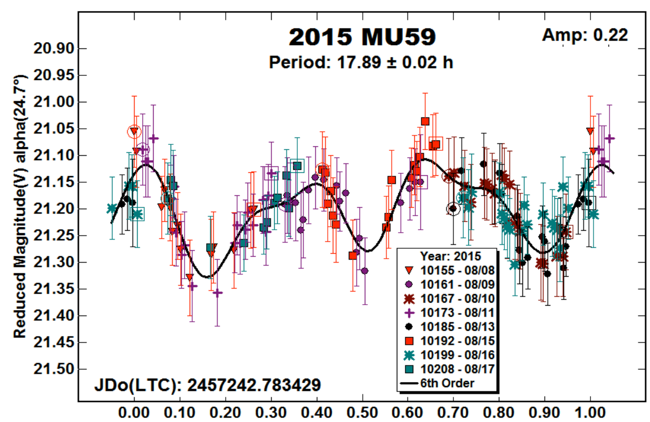

2015 OZ78. There were no entries in the LCDB for this asteroid.

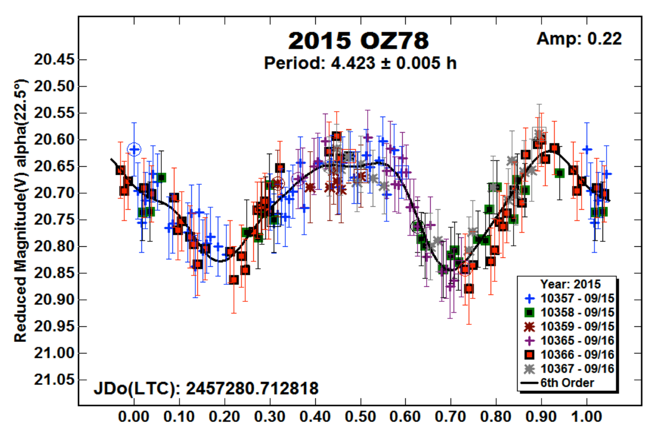

2015 RF36. The results derived from the photometry at CS3 proved to be entirely wrong. However, this serves as a good lesson in data acquisition and lightcurve analysis. As seen in the "Long" period spectrum, there were some periods that stood out and, after further analysis, the period of 4.407 h was adopted in preparation for this paper. Then the radar data came. Based on analysis of data obtained at Arecibo on 2015 July 23, the period for the asteroid was 1 to 2 *minutes*, not several hours (Patrick Taylor, *private communications*). The Doppler spread allowed no possibility of a much longer period.

The reason the optical data analysis failed was the length of the exposures used. The asteroid was faint and had a large sky motion: a bad combination for good photometry. To keep the signal-to-noise ratio as high as possible but keeping trailing to a minimum (guiding was on field stars, not the asteroid), exposures of 2 minutes were used. The net effect was that *one exposure was capturing an entire rotation of the asteroid*, smearing out any details within the lightcurve that would allow finding the true period.

Pravec *et al*. (2000) showed that to avoid this *rotational smearing*, exposures need to about 0.187 times the rotation period. For example, the two-minute exposures would have been good for a rotation period of about 10 minutes but not much shorter. They were able to recover data from sets with too long of exposures but the process can be difficult and there is eventually a limit to how much can be done.

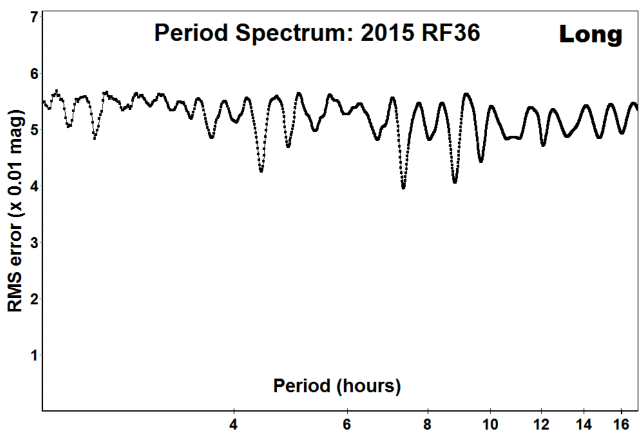

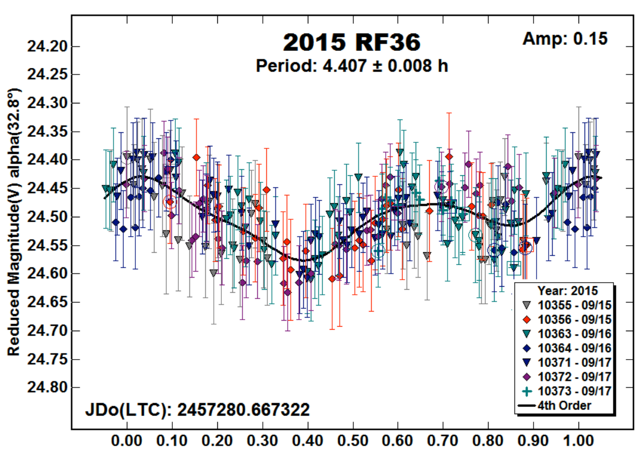

The "Short" period spectrum shows analysis that ranged from 0.01 to 0.1 hours (36 seconds to 6 minutes). The two following lightcurves show the data from CS3 on two nights forced to the solution of about 0.037 h (2.4 minutes), which happens to be close to the estimate based on the radar data. However, the plots are unconvincing. The bunching of the data points is probably tied to the fixed and regular observing cadence, which shows a good reason why irregular cadences are preferable, especially when the period of the asteroid may be very short.

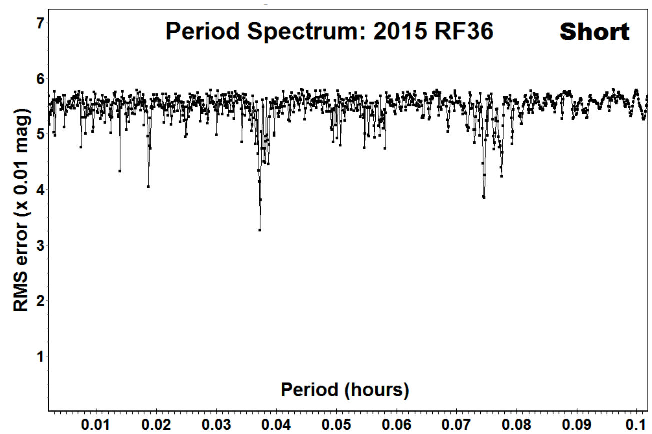

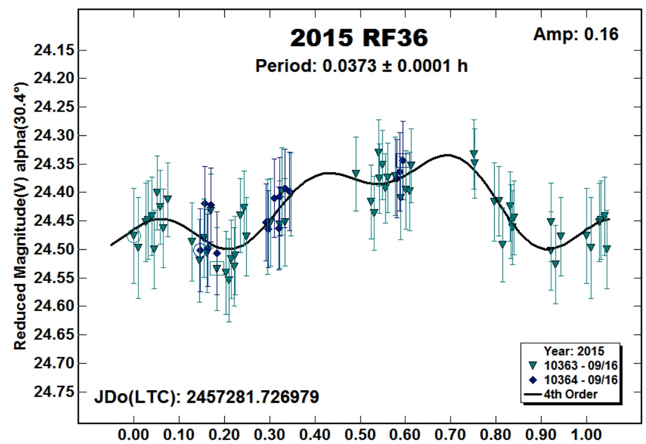

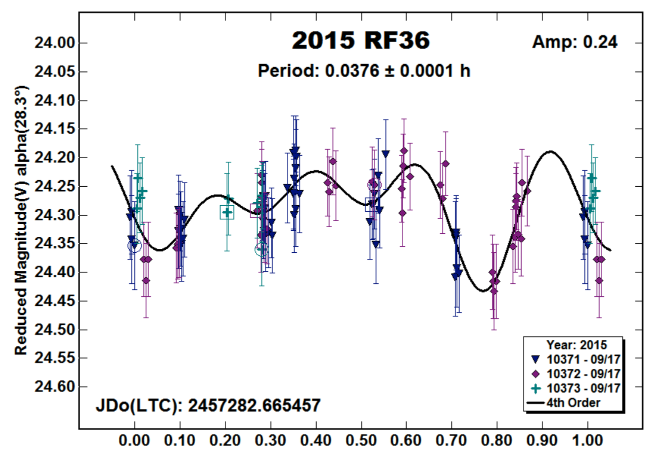

The primary lesson is that when the diameter of the asteroid is on the order of $D < 200$ m ($H \sim 21.2$, assuming an albedo of 0.2), exposures should be kept to an absolute minimum, even at the cost of low signal-to-noise. This can be overcome by increasing the number of exposures, what's sometimes called "beating down the noise." For example, instead of 10 two-minute exposures, it would have been better to have 50 to 75 ten- to fifteen-second exposures. After the first 50-200 images are taken, a quick review can determine if the asteroid appears to have a short period. If not, then it may be possible to increase the exposures to improve the SNR, as long as trailing does not become too severe.

2015 FS332. This appears to be the first published lightcurve for this asteroid.

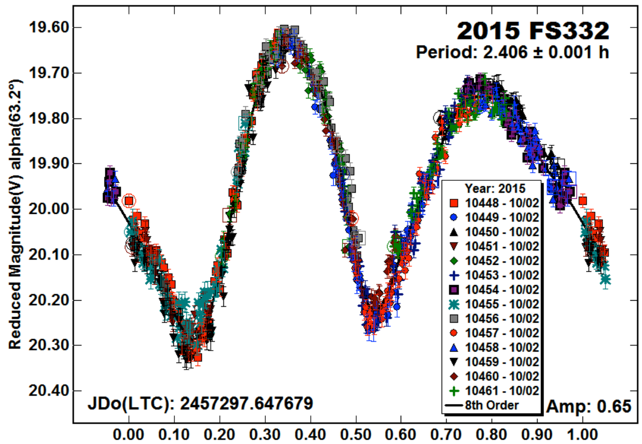

Acknowledgements

Funding for PDS observations, analysis, and publication was provided by NASA grant NNX13AP56G. Work on the asteroid lightcurve database (LCDB) was also funded in part by National Science Foundation grants AST-1210099 and AST-1507535.

This research was made possible in part based on data from CMC15 Data Access Service at CAB (INTA-CSIC) and the AAVSO Photometric All-Sky Survey (APASS), funded by the Robert Martin Ayers Sciences Fund. (*http://svo2.cab.inta-csic.es/vocats/cmc15/*).

This publication makes use of data products from the Two Micron All Sky Survey, which is a joint project of the University of Massachusetts and the Infrared Processing and Analysis Center/California Institute of Technology, funded by the National Aeronautics and Space Administration and the National Science Foundation. (*http://www.ipac.caltech.edu/2mass/*).

References

Behrend, R. (2005) Observatoire de Geneve web site. *http://obswww.unige.ch/~behrend/page_cou.html*

Birlan, M., Vaduvescu, O., Tudorica, A., Sonka, A., Nedelcu, A., Galad, A., Colas, F., Pozo N.F., Barr D.A., Toma, R., Comsa, I., Rocher, P., Lainey, V., Vidican, D., Asher, D., Opriseanu, C., Vancea, C., Colque, J.P., Soto, C.P., Rekola, R., Unda-Sanzana, E. (2010). “More than 160 near Earth asteroids observed in the EURONEAR network.” *Astron. Astrophys*. **511**, A40.

Harris, A.W., Young, J.W., Scaltriti, F., Zappala, V. (1984). “Lightcurves and phase relations of the asteroids 82 Alkmene and 444 Gyptis.” *Icarus* **57**, 251-258.

Harris, A.W., Young, J.W., Bowell, E., Martin, L.J., Millis, R.L., Poutanen, M., Scaltriti, F., Zappala, V., Schober, H.J., Debehogne, H., Zeigler, K.W. (1989). “Photoelectric Observations of Asteroids 3, 24, 60, 261, and 863.” *Icarus* **77**, 171-186.

Harris, A.W., Pravec, P., Warner, B.D. (2012). “Looking a gift horse in the mouth: Evaluation of wide-field asteroid photometric surveys.” *Icarus* **221**, 226-235.

Harris, A.W., Pravec, P., Galad, A., Skiff, B.A., Warner, B.D., Vilagi, J., Gajdos, S., Carbognani, A., Hornoch, K., Kusnirak, P., Cooney, W.R., Gross, J., Terrell, D., Higgins, D., Bowell, E., Koehn, B.W. (2014). “On the maximum amplitude of harmonics on an asteroid lightcurve.” *Icarus* **235**, 55-59.

Krugly, Yu.N., Belskaya, I.N., Shevchenko, V.G., Chiorny, V.G., Velichko, F.P., Mottola, S., Erikson, A., Hahn, G., Nathues, A., Neukum, G., Gaftonyuk, N.M., Dotto, E. (2002). “The Near-Earth Objects Follow-up Program. IV. CCD Photometry in 1996-1999.” *Icarus* **158**, 294-304.

Mottola, S., De Angelis, G., Di Martino, M., Erikson, A., Hahn, G., Neukum, G. (1995). “The near-earth objects follow-up program: First results.” *Icarus* **117**, 62-70.

MPC (2015). Asteroid Lightcurve Data Exchange Format (ALCDEF) web site. *http://www.minorplanetcenter.net/light_curve2/light_curve.php*

Polishook, D., Brosch, N. (2008). “Photometry of Aten asteroids—More than a handful of binaries.” *Icarus* **194**, 111-124.

Pravec, P., Sarounova, L., Wolf, M. (1996). “Lightcurves of 7 Near-Earth Asteroids.” *Icarus* **124**, 471-482.

Pravec, P., Hahn, G. (1997). “Two-Period Lightcurve of 1994 AW1: Indication of a Binary Asteroid?” *Icarus* **127**, 431-440.

Pravec, P., Wolf, M., Sarounova, L. (1998). “Lightcurves of 26 Near-Earth Asteroids.” *Icarus* **136**, 124-153.

Pravec, P., Hergenrother, C., Whiteley, R., Sarounova, L., Kusnirak, P. (2000). “Fast Rotating Asteroids 1999 TY2, 1999 SF10, and 1998 WB2.” *Icarus* **147**, 477-486.

Pravec, P., Harris, A.W., Scheirich, P., Kušnirák, P., Šarounová, L., Hergenrother, C.W., Mottola, S., Hicks, M.D., Masi, G., Krugly, Yu.N., Shevchenko, V.G., Nolan, M.C., Howell, E.S., Kaasalainen, M., Galád, A., Brown, P., Degraff, D.R., Lambert, J.V., Cooney, W.R., Foglia, S. (2005). “Tumbling asteroids.” *Icarus* **173**, 108-131.

Pravec, P., Scheirich, P., Durech, J., Pollock, J., Kusnirak, P., Hornoch, K., Galad, A., Vokrouhlicky, D., Harris, A.W., Jehin, E., Manfroid, J., Opitom, C., Gillon, M., Colas, F., Oey, J., Vrastil, J., Reichart, D., Ivarsen, K., Haislip, J., LaCluyze, A. (2014). “The tumbling state of (99942) Apophis.” *Icarus* **233**, 48-60.

Pravec, P., Wolf, M., Sarounova, L. (1998w, 2002w, 2004w). *http://www.asu.cas.cz/~ppravec/neo.htm*

Warner, B.D. (2007). “Initial Results of a Dedicated H-G Program.” *Minor Planet Bull.* **34**, 113-119.

Warner, B.D., Harris, A.W., Pravec, P. (2009). “The Asteroid Lightcurve Database.” *Icarus* **202**, 134-146. Last update: 2015 Sept. *http://www.minorplanet.info/lightcurvedatabase.html*

Warner, B.D. (2015). “Near-Earth Asteroid Lightcurve Analysis at CS3-Palmer Divide Station: 2015 March-June” *Minor Planet Bull.* **42**, 256-266.

Zappala, V., Cellini, A., Barucci, A.M., Fulchignoni, M., Lupishko, D.E. (1990). “An analysis of the amplitude-phase relationship among asteroids.” *Astron. Astrophys*. **231**, 548-560.

Number	Name	2015 mm/dd	Pts	Phase	L_{PAB}	B_{PAB}	Period	P.E.	Amp	A.E.	Grp
6239	Minos	09/17-09/23	153	20.8,13.4	12	3	3.592	0.005	0.10	0.02	NEA
7822	1991 CS	08/06-08/07	108	63.0,63.2	308	49	2.391	0.001	0.39	0.03	NEA
7889	1994 LX	07/12-07/15	107	33.1,33.5	251	26	2.741	0.002	0.27	0.02	NEA
9400	1994 TW1	08/18-09/04	377	37.7,37.4	15	-9	82.8[T]	0.5	0.80	0.05	NEA
66008	1998 QH2	09/12-09/14	169	3.0,3.9	347	3	7.09	0.02	0.13	0.02	NEA
86666	2000 FL10	08/17-09/04	511	34.9,32.0	349	29	206[T]	5	0.85	0.05	NEA
112985	2002 RS28	07/15-07/18	70	51.6,52.0	227	51	3.820	0.005	0.24	0.03	NEA
142040	2002 QE15	07/14-07/21	92	51.7,53.4	349	43	7.332	0.005	0.19	0.03	NEA
142040	2002 QE15	10/01-10/04	131	66.3,66.1	66	14	3.884	0.005	0.17	0.03	NEA
154807	2004 PP97	09/18-09/30	265	37.3,35.6	29	-3	164	2	0.90	0.05	NEA
155334	2006 DZ169	08/10-08/17	129	44.2,40.4	2	-7	4.682	0.005	0.21	0.03	NEA
206378	2003 RB	08/13-08/20	800	14.0,37.5	335	9	37.5	0.5	0.43	0.05	NEA
242191	2003 NZ6	07/14-07/17	1234	82.2,0.0,94.3	202	33	13.531	0.006	1.19	0.04	NEA
281375	2008 JV19	08/04-08/05	119	28.9,28.0	329	4	3.500	0.002	0.30	0.03	NEA
293054	2006 WP127	07/05-07/11	278	70.4,52.6	324	18	5.311	0.002	0.35	0.05	NEA
297274	1996 SK	09/23-09/25	140	3.1,5.2	356	1	4.645	0.005	0.39	0.03	NEA
385186	1994 AW1	07/18-08/03	1246	72.2,20.5,81.6	267	22	2.5182[P]	0.0001	0.16	0.02	NEA
389694	2011 QD48	09/24-09/27	352	23.0,22.9,23.0	18	8	5.24	0.01	0.08	0.02	NEA
436724	2011 UW158	07/10-07/14	142	92.6,100.9	239	3	0.61069	0.00002	0.68	0.02	NEA
438105	2005 GO22	07/28-07/29	141	47.3,49.0	340	-5	4.103	0.005	0.76	0.05	NEA
438429	2006 WN1	07/13-07/16	110	45.4,46.4	326	10	3.686	0.004	0.22	0.03	NEA
441825	2009 SK1	09/25-10/02	148	7.6,11.3	358	3	5.829	0.005	0.61	0.05	NEA
442037	2010 PR66	07/23-07/24	489	65.2,60.7	268	14	2.0734	0.0003	0.90	0.03	NEA
443880	2001 UZ16	09/15-09/23	232	84.6,83.5	319	36	13.719	0.005	0.97	0.05	NEA
	2004 MW2	06/24-07/03	307	88.5,48.8	245	23	3.63	0.05	0.44	0.05	NEA
	2006 AW	08/03-08/11	448	25.0,31.1	325	18	53.19	0.05	0.95	0.05	NEA
	2007 RU9	09/20-09/24	103	14.9,16.6	6	-7	3.31	0.02	0.15	0.02	NEA
	2012 NP	08/18-08/22	204	13.5,9.6	320	3	19.64	0.05	0.39	0.05	NEA
	2012 TM139	07/13-07/17	75	2.5,3.6	292	2	2.68[A]	0.02	0.18	0.03	NEA
	2015 OH	07/22-07/24	275	46.2,44.9	328	8	4.729	0.003	0.20	0.03	NEA
	2015 NF	07/07-07/09	451	52.7,61.3	257	25	12.06[A]	0.05	1.30	0.04	NEA
	2015 PR	09/06-09/12	67	5.6,4.1	349	-2	3.60	0.02	0.12	0.02	NEA
	2015 JY1	07/03-07/13	1300	58.9,60.6	263	24	6.442[T]	0.005	1.16	0.05	NEA
	2015 RS1	09/14-09/16	212	19.3,19.5	344	9	5.91	0.02	0.10	0.02	NEA
	2015 LG2	07/27-08/02	437	74.0,74.6	346	10	16.31[A]	0.05	0.40	0.05	NEA
	2015 PK9	08/13-08/15	235	23.5,27.0	160	13	3.298	0.005	1.03	0.05	NEA
	2015 QT9	09/17-09/19	150	5.3,8.4	355	-5	7.74	0.05	0.27	0.03	NEA
	2015 NK13	09/05-09/06	199	48.7,50.2	5	21	5.11	0.03	0.51	0.05	NEA
	2015 NS13	08/08-08/11	148	23.9,24.2	332	11	17.42	0.05	0.60	0.05	NEA
	2015 NZ13	07/21-07/22	57	29.3,30.8	304	20	3.42[A]	0.03	0.18	0.04	NEA
	2015 NA14	07/18-07/21	207	28.6,31.2	305	14	6.91	0.02	0.63	0.04	NEA
	2015 SA17	10/02-10/06	231	27.4,28.2	24	16	9.89	0.02	0.22	0.03	NEA
	2015 OL35	09/06-09/09	124	42.0,43.6	21	-7	5.349	0.005	0.21	0.02	NEA
	2015 MU59	08/08-08/16	132	24.7,21.8	337	1	14.31[A]	0.02	0.23	0.03	NEA
	2015 OZ78	09/15-09/16	155	22.6,23.6	2	14	4.423	0.005	0.20	0.03	NEA
	2015 RF36	09/15-09/17	247	32.6,28.1	5	12	7.34	0.02	0.19	0.03	NEA
	2015 FS332	10/02-10/02	765	61.8,61.8	31	26	2.406	0.001	0.65	0.03	NEA

Table II. Observing circumstances. [A]preferred period for an ambiguous solution. [P]period of primary in binary. [T]dominant period of a tumbler. Pts is the number of data points used in the analysis. The phase angle (α) is given at the start and end of each date range, unless it reached a minimum, which is then the second of three values. If a single value is given, the phase angle did not change significantly and the average value is given. L_{PAB} and B_{PAB} are, respectively the average phase angle bisector longitude and latitude, unless two values are given (first/last date in range). Grp is the orbital group of the asteroid. See Warner *et al.* (LCDB; 2009; *Icarus* **202**, 134-146.).

SHAPE MODELLING OF ASTEROIDS 1708 POLIT, 2036 SHERAGUL, AND 3015 CANDY

Dr. Maurice Clark
Department of Physics
Texas Tech University
Lubbock TX 79409
maurice.clark@ttu.edu

(Received: 2015 Oct 7)

Results are presented on efforts to model the shapes of three asteroids: 1708 Polit, 2036 Sheragul, and 3015 Candy. Observations used in this study were made by the author over a number of oppositions from a variety of locations, most recently at the Preston Gott Observatory at Texas Tech University.

Asteroid shape modeling is a challenging but very useful extension to asteroid photometry. While it is not possible to determine the 3-dimensional shape of an asteroid from just one lightcurve, by using lightcurves obtained from a number of oppositions with the asteroid at different locations in its orbit, not only can a shape model be derived, but also the pole orientation and the direction of rotation can be estimated.

The results presented here are a continuation of those presented by the author at the 2012 Society for Astronomical Sciences Symposium (Clark, 2012). That paper discussed initial attempts at shape modeling and results that were preliminary since observations from only 2 or 3 oppositions were used. The results in this paper contain data from subsequent oppositions and cover a wider range of orbital locations for each asteroid. This should increase the reliability of the results obtained.

Period analysis was done using *MPO Canopus*, which implements the algorithm developed by Alan Harris (Harris *et al.*, 1989). Differential magnitudes were calculated using reference stars from the USNO-A 2.0 catalog and the UCAC2 catalog. Shape models were derived from the lightcurve data using *MPO LCInvert*.

Observations and Data Analysis

Tables I-III summarize the observations used in this study. Included in the tables are the dates over which observations were obtained, the observatory at which the observations were obtained, the number of observing sessions in which useful data were obtained, the derived period and its estimated uncertainty, and finally, the amplitude of the lightcurve and its estimated uncertainty.

<u>1708 Polit</u>. For the analysis of 1708 Polit, the lightcurve data from four years were used. Lightcurves for three of the years are shown here. The data were imported into *MPO LCInvert* to find a probable sidereal period. This was then applied in a pole search that generated 310 solutions using discrete, fixed longitude-latitude pairs but allowing the sidereal period to "float." The results of this initial search are shown in Figure 4. Dark blue indicates the lower values of log(chi-square) in the range of solutions. Colors progress towards bright red with increasing log(chi-square) with the highest value indicated by maroon (dark red).

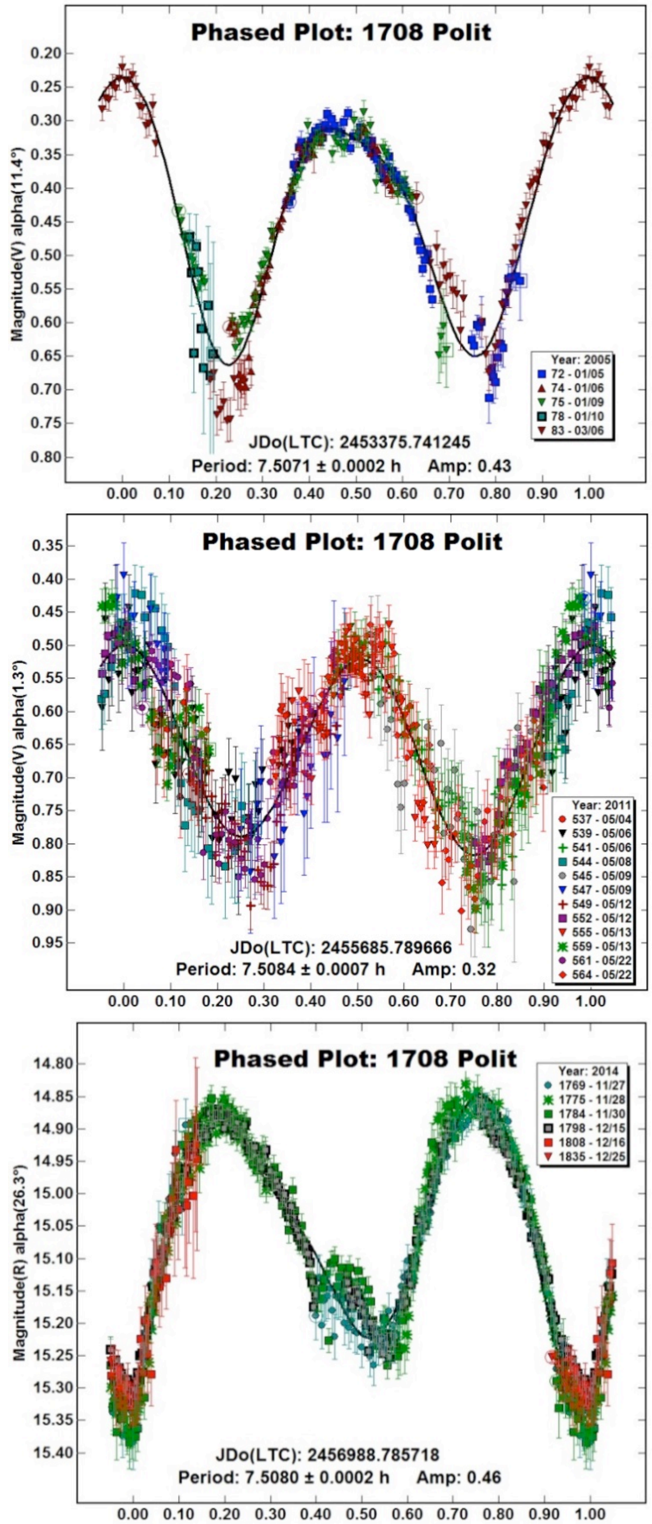

Figures 1-3. The phased lightcurves for 1708 Polit show different shapes and amplitudes at different apparitions.

From Figure 4, two general solutions in ecliptic longitude and latitude are seen, one near $\lambda = 0°$, $\beta = +45°$, and a second near $\lambda = 165°$, $\beta = +45°$. The two intermediate solutions were then refined by running the search again using one of the two solutions as a starting point and allowing the longitude and latitude as well as the sidereal period to float.

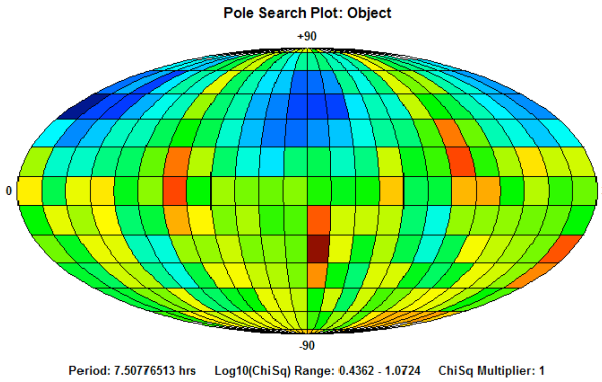

Figure 4. Plot of the log (chi-square) values for 1708 Polit. Dark blue represents the lowest chi-square value.

The final result showed a best solution at λ = 2.1°, β = 47.5°, sidereal period P = 7.50776446 h. The error for the poles is about ±15° while the period solution has an error on the order of 2-3 units in the last decimal place. This solution indicates a prograde rotation.

Figures 5 and 6 show the derived model using the above solution. In this model the spin axis is closely aligned with the shortest axis of the asteroid, which is to be expected.

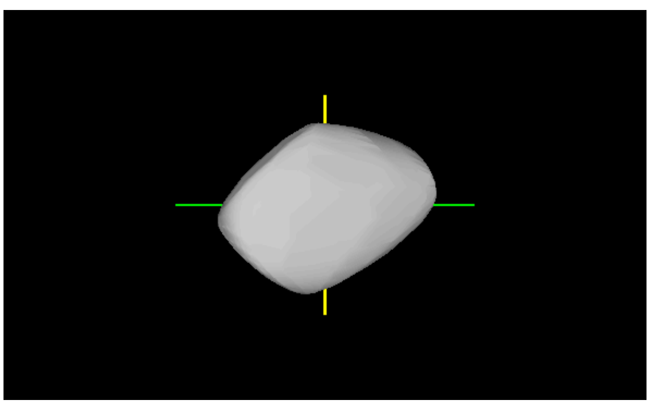

Figure 5. 3-D model of 1708 Polit for solution λ = 2.1°, β = 47.5°, P = 7.50776446h. Z-axis rotation = 0°.

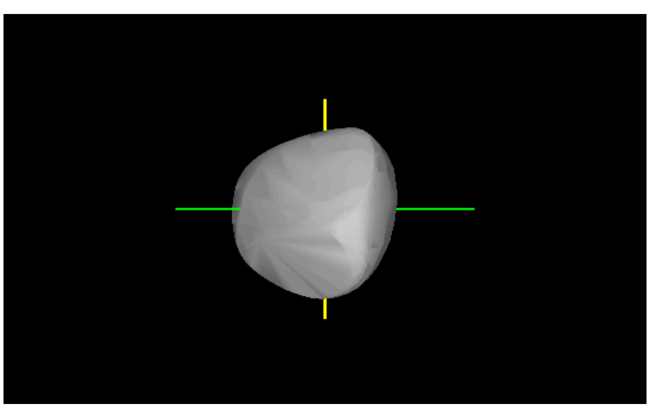

Figure 6. 3-D model of 1708 Polit for solution λ = 2.1°, β = 47.5°, P = 7.50776446h. Z-axis rotation = 90°.

Also supporting this solution is the way the model fairly closely matches the observed lightcurve. Examples of this are shown in Figures 7-9.

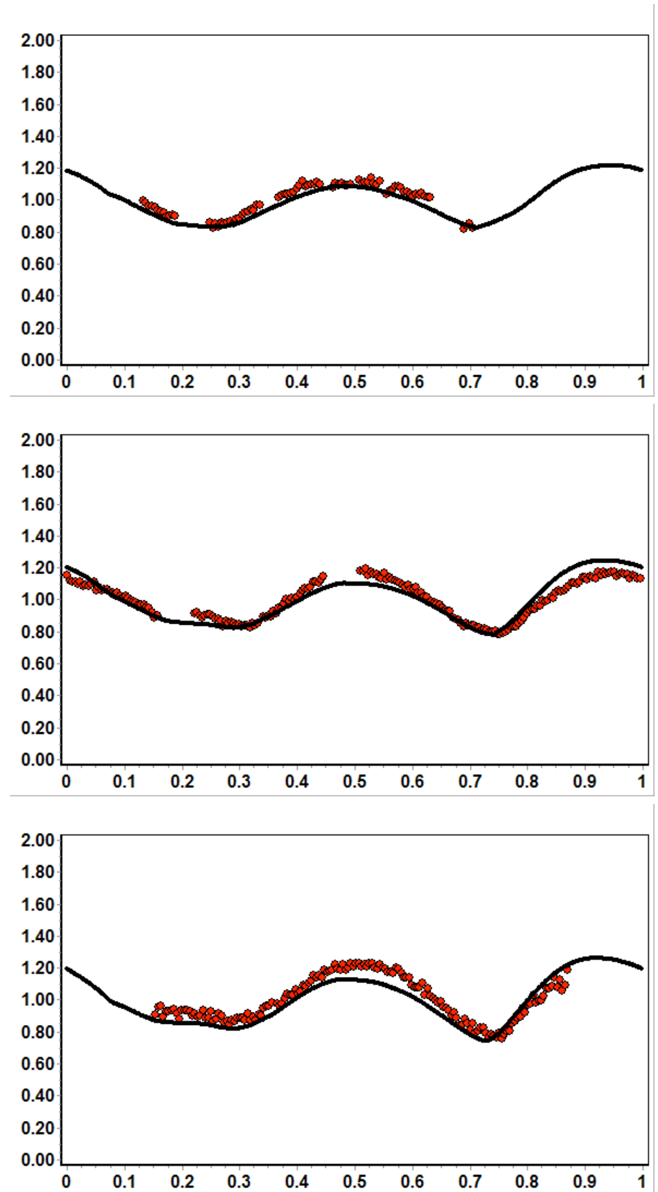

Figures 7-9. Correspondence between model and observed lightcurve of 1708 Polit for solution λ = 2.1°, β = +47.5°, P = 7.50776446 h. From top to bottom: 2005 Jan 9, 2014 Nov 30, and 2014 Dec 25.

<u>2036 Sheragul</u>. The process and analysis for Sheragul proceeded the same way as for 1708 Polit, but using the data outlined in Table II. The general shape of the lightcurves in the four years did not change significantly (see Figures 10-13), save that in two years the second minimum was slightly shallower than the first minimum. More important, the amplitudes did change, ranging from 0.58 to 0.90 mag. If nothing else, this helped confine the solutions in longitude for the spin axis, *i.e.*, the lower amplitude years indicated a more pole-on view than the other two years.

The initial pole search result is seen in Figure 14, in which two possible solutions are seen. The first one is near ecliptic longitude and latitude λ = 300°, β = –30° while the other is near λ = 120°, β = –30°. The two intermediate solutions were refined by running the search again using one of the two solutions as a starting point and allowing the longitude and latitude as well as the sidereal period to float.

The first result showed a best solution at λ = 306°, β = –35.8°, *P* = 5.4159697 h. The error for the poles is about ±15° while the period solution has an error on the order of 2-3 units in the last decimal place. This solution indicates a retrograde rotation.

The second result showed a best solution at λ = 117.3°, β = –28.9°, *P* = 5.4159686h. The error for the poles is about ±15° while the period solution has an error on the order of 2-3 units in the last decimal place. This solution also indicates a retrograde rotation.

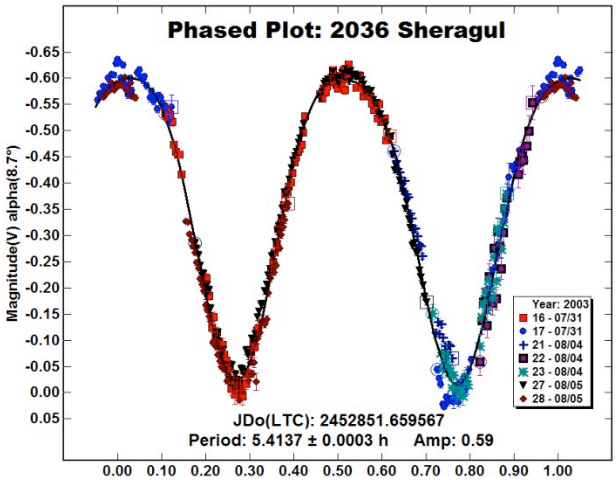

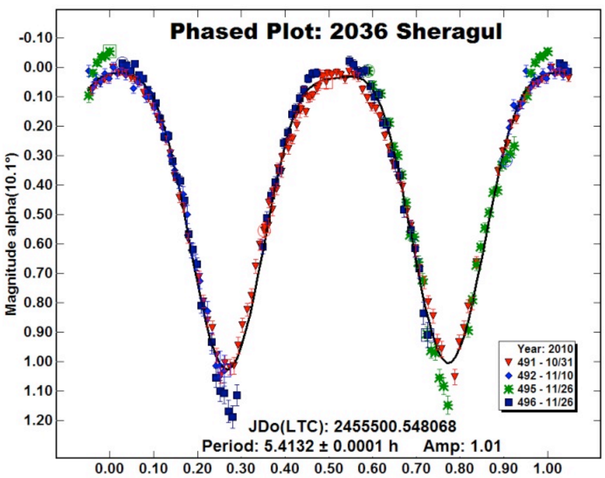

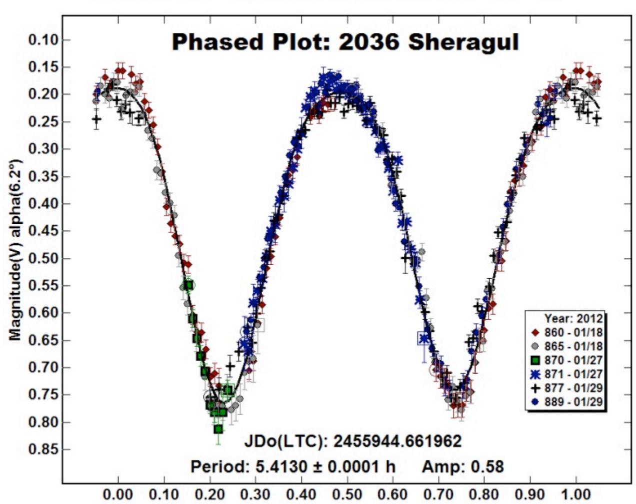

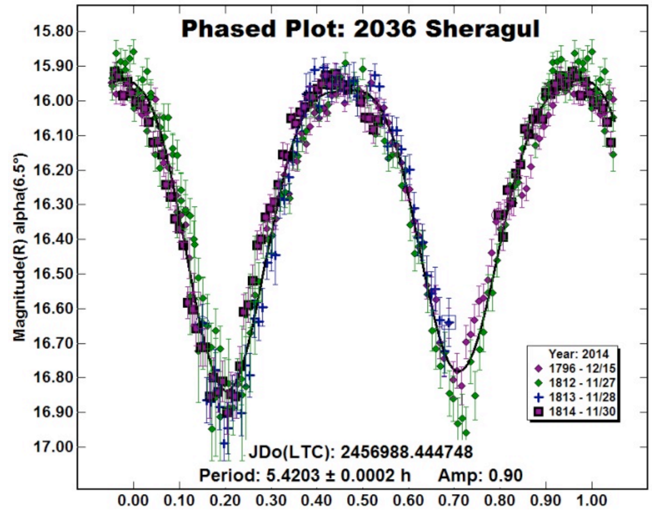

Figures 10-13 (from top to bottom) show the changing amplitude of the lightcurve for 2036 Sheragul at the four apparitions at which the asteroid was observed.

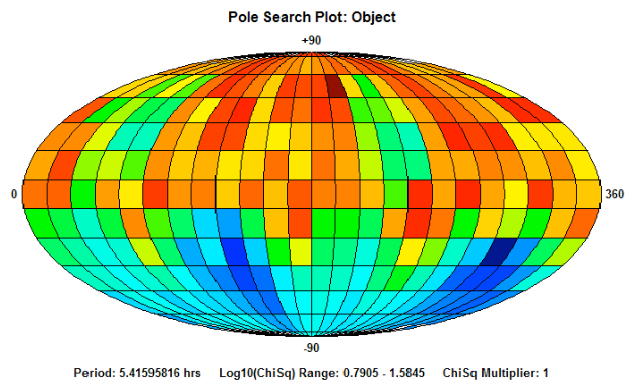

Figure 14. Plot of the log (chi-square) values for 2036 Sheragul. Dark blue represents the lowest chi-square value.

Neither of these two solutions has a high confidence. Figures 15 and 16 show the derived model using the first solution while Figures 17 and 18 show the derived model using the second solution.

As can be seen, the spin axis in the model is not aligned with the shortest axis of the asteroid as is the lowest energy rotational state; making the model not a likely physical representation in this case. The modelling difficulty arises from all available lightcurves being at a similar aspect angle, thereby not providing sufficient information for the overall shape. Also casting doubt on the shape model solution is the way both models show differences between the observed and model lightcurves. Examples of these are shown in Figures 19-22.

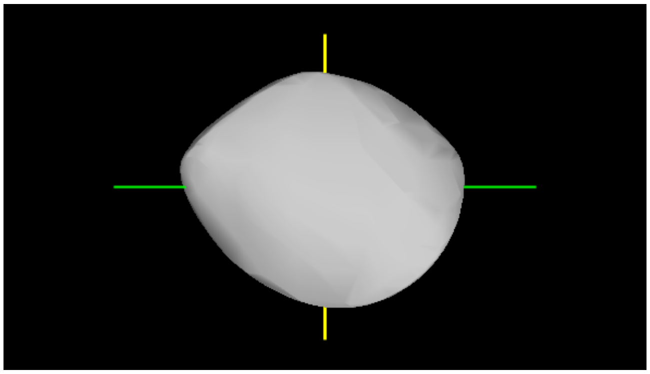

Figure 15. 3-D model of 2036 Sheragul for solution λ = 306°, β = –35.8°, P = 5.4159697 h. Z-axis rotation = 0°.

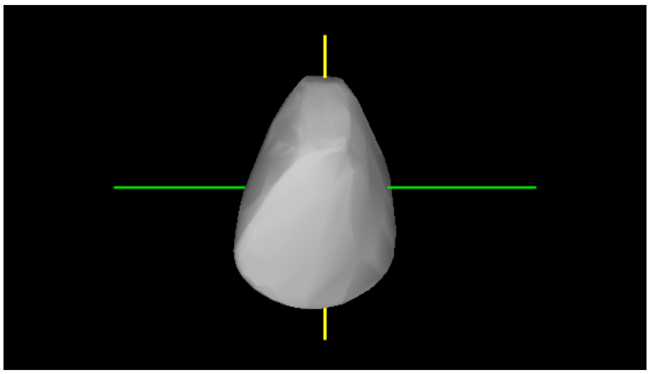

Figure 16. 3-D model of 2036 Sheragul for solution λ = 306°, β = –35.8°, P = 5.4159697 h. Z-axis rotation = 90°.

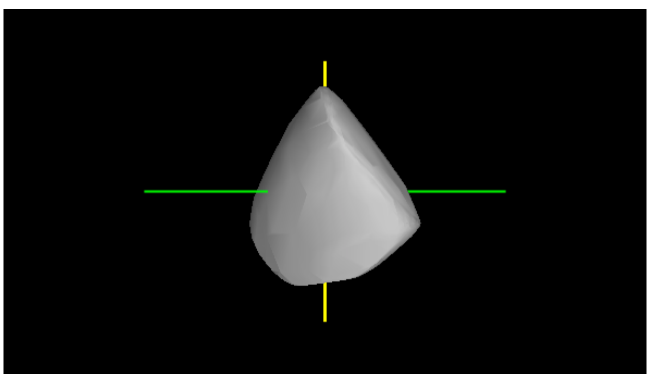

Figure 17. 3-D model of 2036 Sheragul for solution at λ = 117.3°, β = –28.9°, P = 5.4159686 h. Z-axis rotation = 0°.

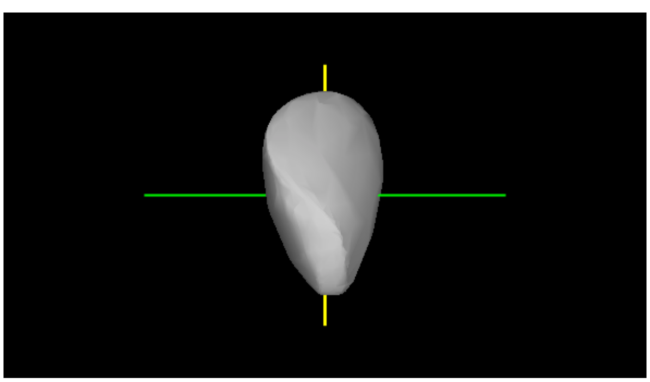

Figure 18. 3-D model of 2036 Sheragul for solution at λ = 117.3°, β = –28.9°, P = 5.4159686 h. Z-axis rotation = 90°.

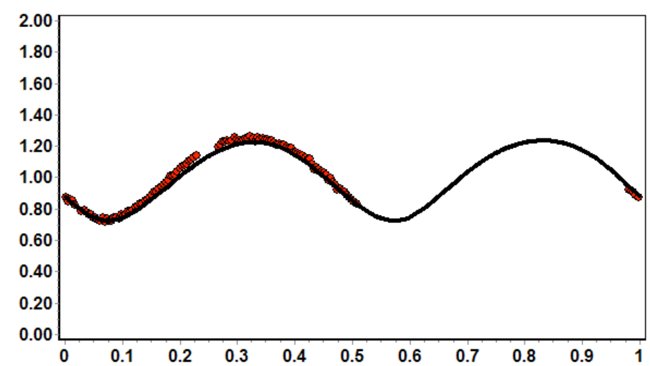

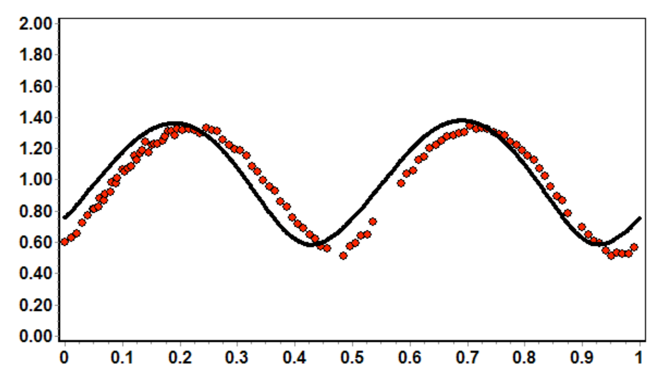

Figures 19-20. Correspondence between model (black) and observed lightcurve (red) for 2036 Sheragul for pole solution λ = 306°, β = –35.8°, *P* = 5.4159697 h. The top plot is from 2003 Aug 5 and shows a somewhat close fit to the model lightcurve. The bottom plot features data from 2010 Oct 31 and shows a significant different in phase, which may indicate an incorrect sidereal period.

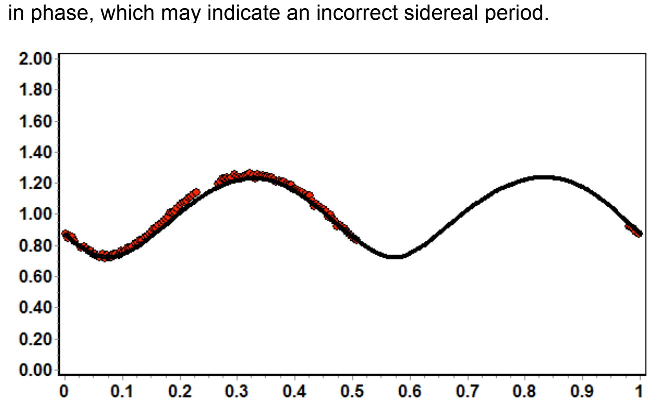

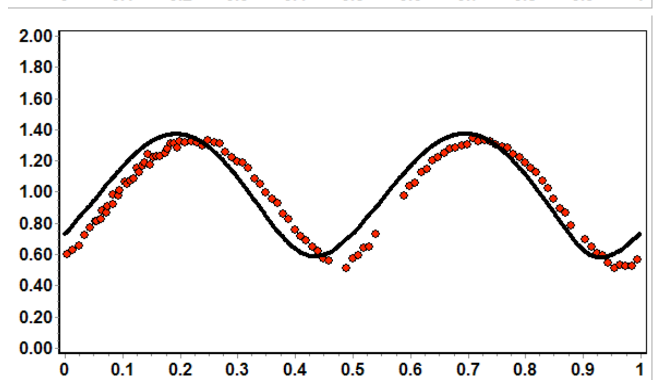

Figures 21-22. Correspondence between model (black) and observed lightcurve (red) for 2036 Sheragul for pole solution λ = 117.3°, β = –28.9°, *P* = 5.4159686h. As for the first pole solution, the fit for 2003 Aug 5 is much better than for 2010 Oct 31.

As it happens, the best fits of actual data to model lightcurve occur in the two years (2003 and 2012) when the amplitude was lowest and, presumably, when the view was more pole-on. The apparent phase shift in the larger amplitude years (2010 and 2014) may be due to a combination of incorrect sidereal period and, maybe more so, the implausible solutions that have the asteroid spinning about one of its longer axes and not the shortest.

3015 Candy. The analysis of 3015 Candy used the lightcurve data from the four years shown in Table III. Figures 23-26 show the lightcurves obtained by the author in those four years. The amplitude changed significantly over the four apparitions, ranging from 0.52 mag in 2013/2014 to 0.91 mag in 2005.

The inversion process followed the same steps as described for the previous two asteroids. The initial pole solution plot is shown in Figure 27. Two possible solutions stand out. The first is at λ = 300° β = –45° and the other is at λ = 135° β = –30°.

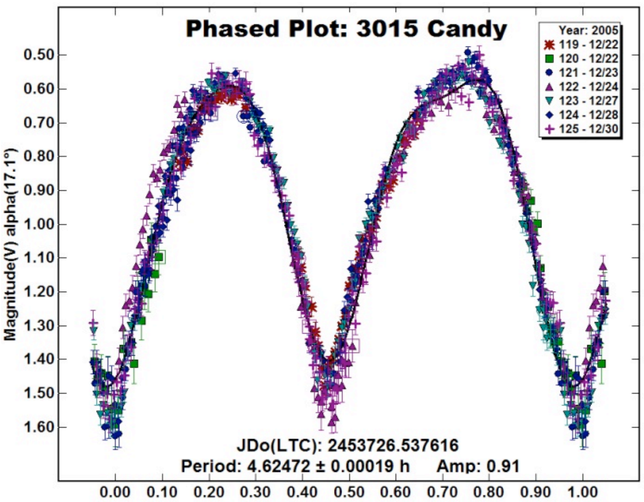

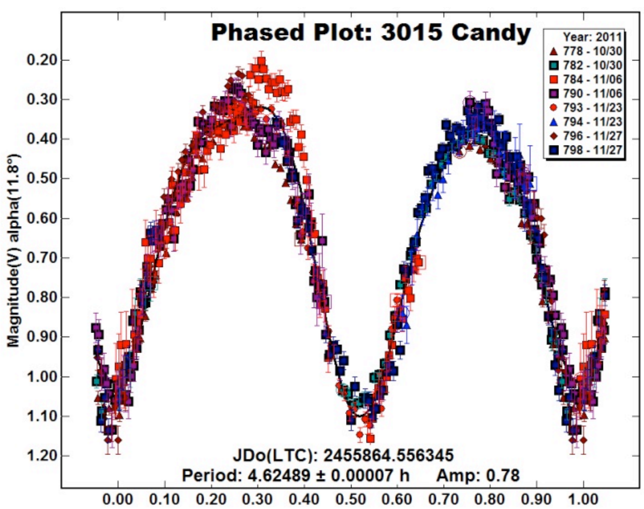

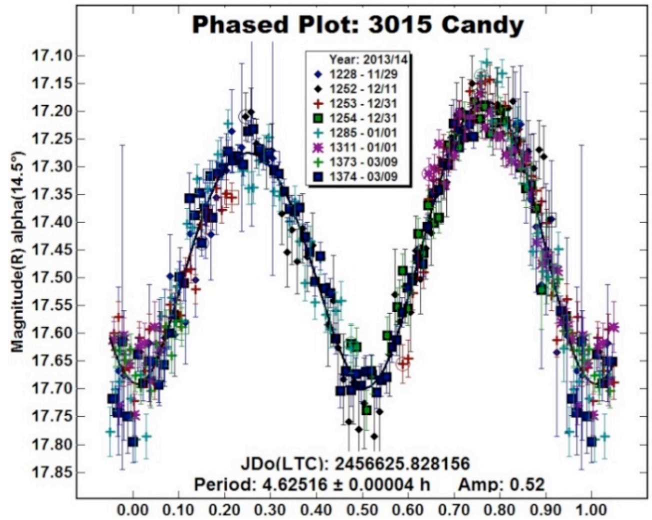

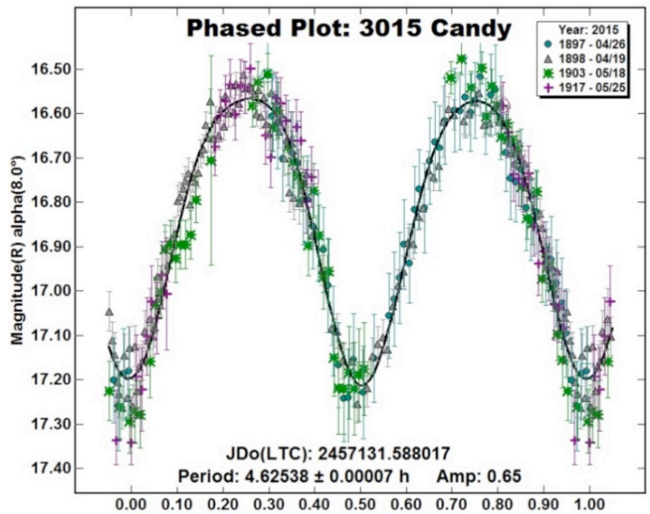

Figure 23-26. The lightcurves for 3015 Candy show some variation in shape as well as amplitude over the four apparitions at which observations were made.

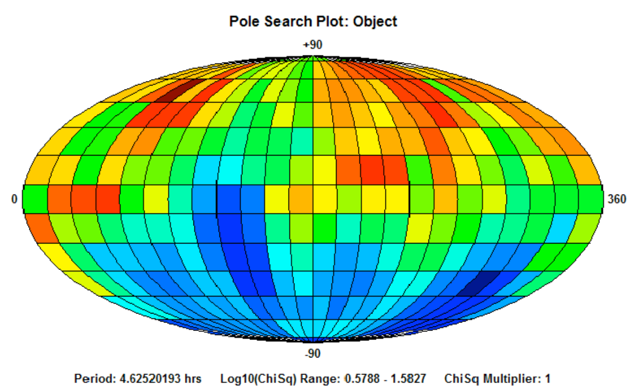

Figure 27. Plot of the log (chi-square) values for 3015 Candy. Dark blue represents the lowest chi-square value.

The two intermediate solutions were then refined by running the search again using one of the two solutions as a starting point and allowing the longitude and latitude as well as the sidereal period to float. The final result showed a best solution at λ = 306°, β = –42.8°, *P* = 4.63519895 h. The error for the poles is about ±15° while the period solution has an error on the order of 2-3 units in the last decimal place. This solution indicates a retrograde rotation.

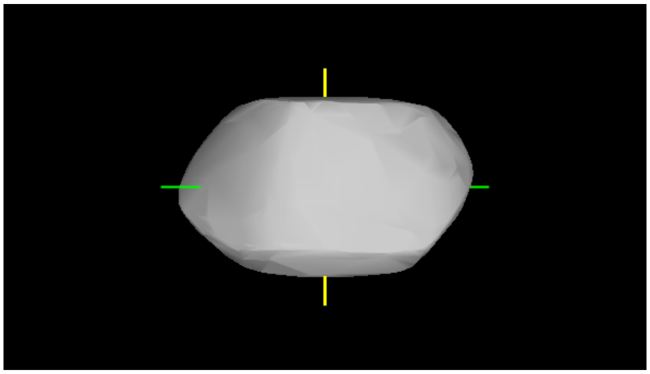

Figure 28. 3-D model of 3015 Candy for solution λ = 306°, β = –42.8°, P = 4.63519895 h. Z-axis rotation = 0°.

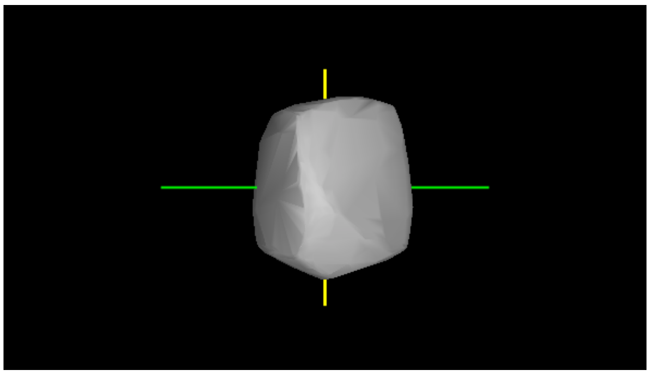

Figure 29. 3-D model of 3015 Candy for solution λ = 306°, β = –42.8°, P = 4.63519895 h. Z-axis rotation = 90°.

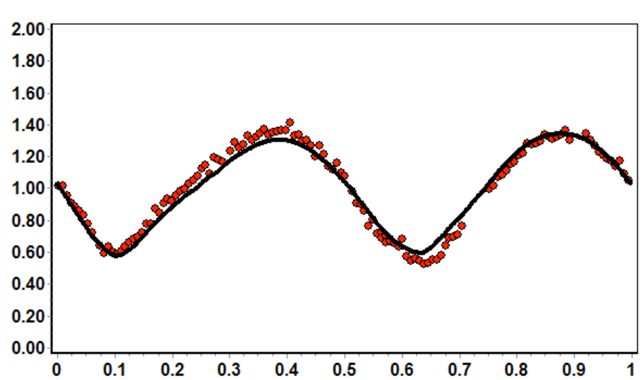

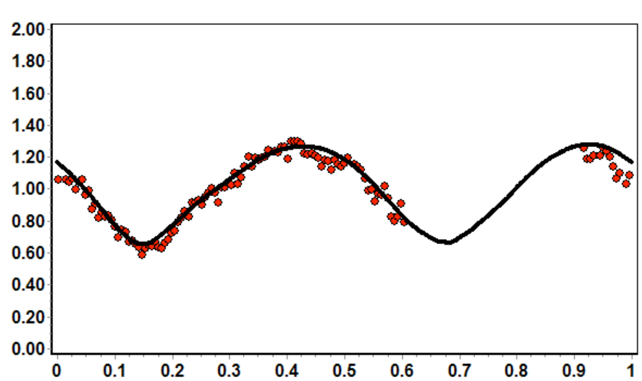

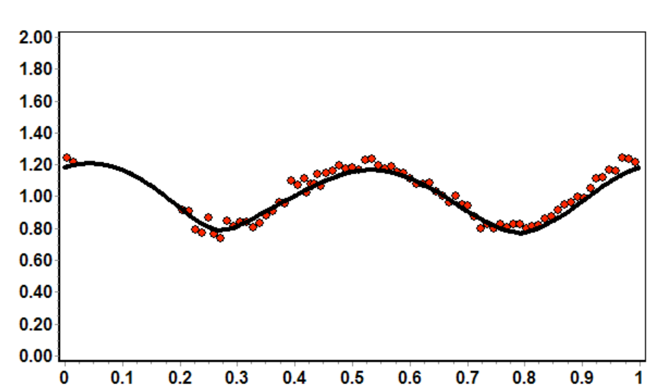

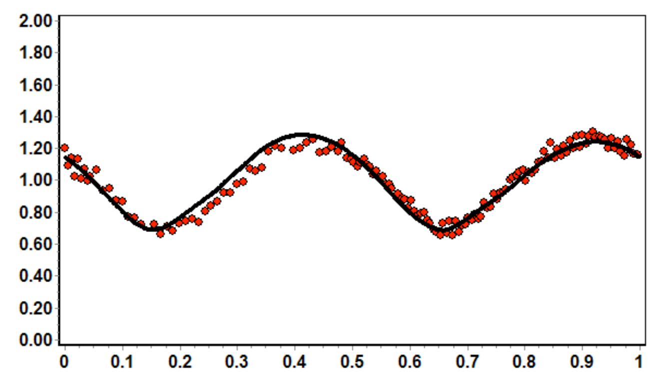

Figures 30-33. Correspondence between model and observed lightcurve of 3015 Candy for solution λ = 306°, β = -42.8°, P = 4.63519895 h. From top to bottom: 20015 Dec 21, 2011 Nov 6, 2014 Mar 9, and 2015 Apr 19.

Figures 28 and 29 show the derived model using the adopted solution. The spin axis is closely aligned with the shortest axis of the asteroid, which is to be expected. Also supporting this solution is the good agreement between the model and observed lightcurves. Examples of this are shown in Figures 30-33.

Conclusions

Converting lightcurves into 3-D models of these three asteroids has been an interesting and enjoyable experience, despite the steep learning curve. It is certainly a worthwhile endeavor and something in which I would encourage other asteroid photometrists to become involved. Of the three asteroids studied in this paper, the results for 1708 Polit and 3015 Candy have the highest confidence. The spin axes of both models for these asteroids are aligned with the shortest axis and there is a close correspondence between the observed and modeled lightcurves. The model results for 2036 Sheragul, however, are dubious. There are clear discrepancies between the observed and modeled lightcurves and the spin axis is not aligned with the shortest axis of the asteroid shape model. Further observations at future oppositions are planned for all three asteroids, but especially for 2036 Sheragul.

Acknowledgments

I would like to thank Brian Warner for all of his work with the programs *MPO Canopus, MPO LCInvert,* and for his efforts in maintaining the CALL website.

References

Clark, M.L. (2012). "First Attempts at Asteroid Shape Modelling." In Proceedings for the 31st Annual Symposium on Telescope

Science. pp 37-44. Society for Astronomical Sciences. Rancho Cucamonga, CA.

Harris, A.W., Young, J.W., Bowell, E., Martin, L.J., Millis, R.L., Poutanen, M., Scaltriti, F., Zappala, V., Schober, H.J., Debehogne, H., Zeigler, K.W. (1989). "Photoelectric Observations of Asteroids 3, 24, 60, 261, and 863." *Icarus* **77**, 171-186.

Year	Date Range	Observatory	Sess	Per (h)	P.E. (h)	Amp (mag)	A.E. (mag)
2005	Jan 5 – Mar 6	Rosemary Hill[1]	5	7.507	0.001	0.4	0.1
2011	May 6 – June 22	Preston Gott[2]	6	7.5085	0.0008	0.35	0.1
2013	Sept 7	Preston Gott[2]	1	7.50		0.3	
2014	Nov 27 – Dec 16	Preston Gott[2]	5	7.5080	0.0002	0.46	0.05

Table 1. Observational data for 1708 Polit

Year	Date Range	Observatory	Sess	Per (h)	P.E. (h)	Amp (mag)	A.E. (mag)
2003	July 29 – Aug 4	Bucknell[3]	5	5.4136	0.0002	0.58	0.02
2010	Oct 31 – Nov 28	Preston Gott[2]	4	5.4132	0.0001	0.95	0.02
2012	Jan 18 – Jan 29	Preston Gott[2]	4	5.4120	0.0002	0.60	0.02
2014	Nov 27 – Dec 16	Preston Gott[2]	5	5.42026	0.00015	0.90	0.05

Table 2. Observational data for 2036 Sheragul

Year	Date Range	Observatory	Sess	Per (h)	P.E. (h)	Amp (mag)	A.E. (mag)
2005	Dec 22 – Dec 30	Rosemary Hill[1]	6	4.62472	0.00019	0.91	0.05
2011	May 6 – June 22	Preston Gott[2]	4	4.62489	0.00007	0.78	0.05
2013/14	Nov 29 – Mar 9	Preston Gott[2] Chiro[4]	5	4.62516	0.00004	0.52	0.02
2015	April 19 – May 25	Preston Gott[2]	4	4.62538	0.00007	0.65	0.05

Table 3. Observational data for 3015 Candy

Table Footnotes

1. Rosemary Hill Observatory (MPC code 831) is owned by the University of Florida, Gainesville, and is located near Bronson in Florida at an elevation of 51 m. The main instrument at Rosemary Hill is a 0.76-m Tinsley reflector. For these observations, the instrument was used at its *f*/5 Newtonian focus with an SBIG ST-7E CCD camera.

2. The Preston Gott Observatory is the main astronomical facility of the Texas Tech University. Located about 20 km north of Lubbock, the main instrument is a 0.5-m *f*/6.8 Dall-Kirkam Cassegrain. An SBIG STL-1001E CCD was used with this telescope. Other instruments include several 30-cm *f*/10 Schmidt-Cassegrain telescopes that are used with *f*/6.3 focal reducers and SBIG ST9XE CCD's, and a 35-cm *f*/11 Celestron used with a focal reducer at *f*/7 and SBIG ST-9E CCD.

3. Bucknell Observatory is located on the campus of Bucknell University in Lewisburg, Pennsylvania. The elevation is 171 m. The telescope used for these observations was a 35-cm *f*/11 Celestron with a focal reducer at *f*/7 and an SBIG ST-9E CCD.

4. Chiro Observatory (MPC code 320) is a private observatory located near the town of Yerecoin in Western Australia, The elevation is about 250 m. The main telescope at this facility is a 30-cm *f*/18 Cassegrain that can operated as an *f*/6 Newtonian. For these observations, the *f*/6 Newtonian focus was used along with either an SBIG ST-9E CCD or STL-1001E CCD.

ASTEROID LIGHTCURVE ANALYSIS AT THE OAKLEY SOUTHERN SKY OBSERVATORY: 2015 FEBRUARY

Kylie Hess, Richard Ditteon
Rose-Hulman Institute of Technology, CM 171
5500 Wabash Avenue, Terre Haute, IN 47803, USA
ditteon@rose-hulman.edu

(Received: 2015 Oct 7)

Photometric data were taken over ten nights in 2015 February for five asteroids: 2601 Bologna, 2689 Bruxelles, 4207 Chernova, 11151 Oodaigahara, and (11512) 1991 AB2.

Five asteroids were targeted on the nights of 2015 February 6-11 and 13-16 from the Oakley Southern Sky Observatory in New South Wales, Australia. The observations were made using a 0.5-m Ritchey-Chretien telescope operating at *f*/8.1 and a STX-16803 camera, binned 3x3, with a luminance filter. The exposure time used for all images was 180 s. The image scale was 1.35 arcseconds per pixel. The raw images were calibrated in *MaxIm DL* using twilight flats, bias, and dark frames. The images were then measured and lightcurves produced using *MPO Canopus*.

Periods were measured for 2689 Bruxelles, 4207 Chernova, and (11512) 1991 AB2. We were not able to determine periods for 2601 Bologna and 11151 Oodaigahara because the data were too noisy. For these two objects, only an amplitude is reported.

A period of 10.288 ± 0.015 h had been previously reported for 4207 Chernova by Albers *et al.* (2010) with only 56 data points. That period does not agree with the new measurement within experimental error. An attempt was made to fit the new data with the previous period; however, an increase in RMS value indicated that the previously reported period did not fit the new data as well as the newly measured value.

References

Albers, K., Kragh, K., Monnier, A., Pligge, Z., Stolze, K., West, J., Yim, A., and Ditteon, R. (2010). "Asteroid Lightcurve Analysis at the Oakley Southern Sky Observatory: 2009 October Thru 2010 April." *Minor Planet Bull.* **37**, 152-158.

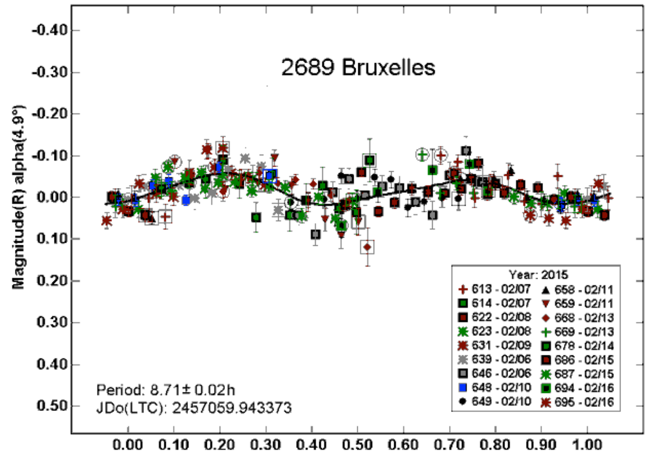

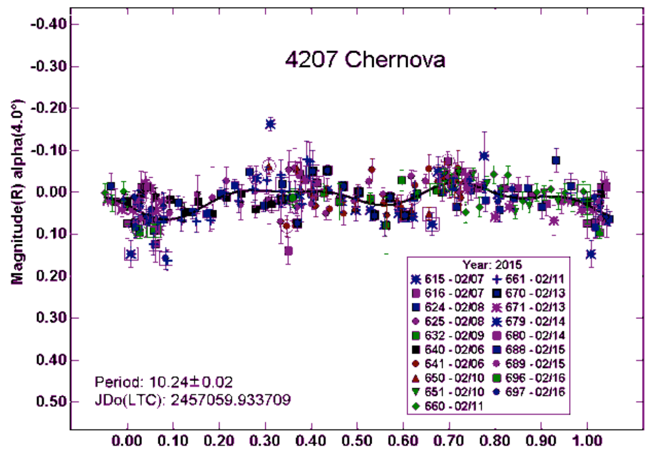

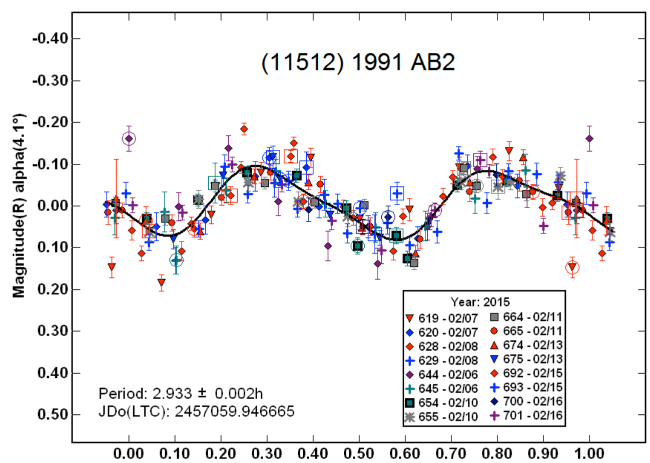

Number	Name	Dates (2015/MM/DD)	Period (h)	P. E. (h)	Amplitude (mag)	A.E. (mag)	Points
2601	Bologna	02/06-02/11, 02/13-02/16	-	-	0.10	0.05	159
2689	Bruxelles	02/06-02/11, 02/13-02/17	8.71	0.02	0.13	0.05	167
4207	Chernova	02/06-02/11, 02/13-02/18	10.24	0.02	0.13	0.05	216
11151	Oodaigahara	02/06-02/11, 02/13-02/19	-	-	0.08	0.04	193
11512	1991 AB2	02/06-02/11, 02/13-02/20	2.933	0.002	0.20	0.06	159

ROTATIONAL PERIOD DETERMINATION FOR (8563) 1995 US

Riccardo Papini
Carpione Observatory (K49)
via Potente 52, 50026 San Casciano in val di Pesa (FI), ITALY
riccardo.papini@yahoo.it

Alessandro Marchini, Sara Marullo
Astronomical Observatory, DSFTA - University of Siena (K54)
Via Roma 56, 53100 – Siena, ITALY

Fabio Salvaggio
21047 – Saronno, ITALY

(Received: 2015 October 13)

Analysis of photometric observations in 2015 August of the main-belt asteroid (8563) 1995 US found the most likely synodic period to be 3.197 ± 0.001 hours with a lightcurve amplitude of 0.56 ± 0.03 mag.

(8563) 1995 US is a main-belt asteroid discovered on 1995 October 19 by T.B. Spahr at Catalina Station. It orbits with a semi-major axis of about 2.97 AU, eccentricity 0.12, and a period of 5.12 years (JPL, 2014). According to the WISE satellite infrared radiometry, the diameter is 14.5 ± 0.2 km and its absolute magnitude *H* = 11.9 (Masiero *et al.*, 2012). The asteroid was chosen from a list of asteroid photometry opportunities in the *Minor Planet Bulletin* (Warner *et al.*, 2015).

Observations were made on four nights from 2015 August 22-27 with a total of 248 useful data points collected over the interval of about six days. During that time, the phase angle ranged from 5.4° to 3.5° before opposition. Images were taken at the Astronomical Observatory of the University of Siena (K54) using a 0.30-m *f*/5.6 Maksutov-Cassegrain telescope, SBIG STL-6303E NABG CCD camera, and clear filter; the pixel scale was 2.26 arc-seconds (2x2 binning). Exposures were 300 seconds.

Images were calibrated with dark and flat-field frames while photometric processing was performed with *MPO Canopus* v10.4.7. Differential photometry measurements were performed using the Comp Star Selector (CSS) procedure in *MPO Canopus* that allows selecting of up to five comparison stars of near solar color. Minor adjustments to the magnitude zero-points for the particular data sets were carried out to minimize the RMS error in the Fourier analysis.

The period analysis yielded several solutions with similar lower RMS errors (Fig. 1). We suggest that the most likely solution is a bimodal lightcurve with a synodic period of 3.197 ± 0.001 hours and amplitude of 0.56 ± 0.03 mag (Fig. 2) because large amplitudes would be improbable for monomodal, or trimodal lightcurves (Harris *et al.*, 2014). A search of the Asteroid Lightcurve Database (LCDB; Warner *et al.*, 2009) indicates that this lightcurve and results might be the first ones for this asteroid.

Acknowledgments

The authors particularly note here the role of co-author Sara Marullo, a student of the course in Physics and Advanced Technologies, who looked after the collection and analysis of data during her internship activities at the Astronomical Observatory of the University of Siena.

References

Harris, A.W., Pravec, P., Galad, A., Skiff, B.A., Warner, B.D., Vilagi, J., Gajdos, S., Carbognani, A., Hornoch, K., Kusnirak, P., Cooney, W.R., Gross, J., Terrell, D., Higgins, D., Bowell, E., Koehn, B.W. (2014). "On the maximum amplitude of harmonics on an asteroid lightcurve." *Icarus* **235**, 55-59.

JPL (2014). Small-Body Database Browser. *http://ssd.jpl.nasa.gov/sbdb.cgi#top*

Masiero, J.R., Mainzer, A.K., Grav, T., Bauer, J.M., Cutri, R.M., Dailey, J., Eisenhardt, P.R.M., McMillan, R.S., Spahr, T.B., Skrutskie, M.F., Tholen, D., Walker, R.G., Wright, E.L., DeBaun, E., Elsbury, D., Gautier, T., IV, Gomillion, S., Wilkins, A. (2011). "Main Belt Asteroids with WISE/NEOWISE. I. Preliminary Albedos and Diameters." *Ap. J.* **741**, A68.

Warner, B.D., Harris, A.W., Durech, J., Benner, L.A.M. (2015). "Lightcurve photometry opportunities: 2015 January-March." *Minor Planet Bulletin* **42**, 83-86.

Warner, B.D., Harris, A.W., Pravec, P. (2009). "The asteroid lightcurve database." *Icarus* **202**, 134-146. Updated 2015 February 7. *http://www.minorplanet.info/lightcurvedatabase.html*

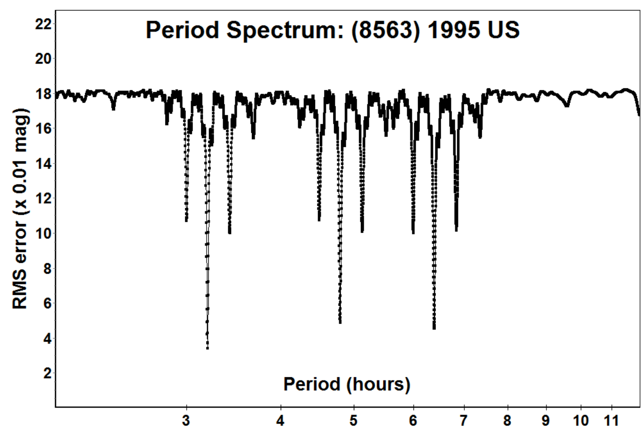

Figure 1. The period spectrum for (8563) 1995 US shows several possible solutions with nearly the same error.

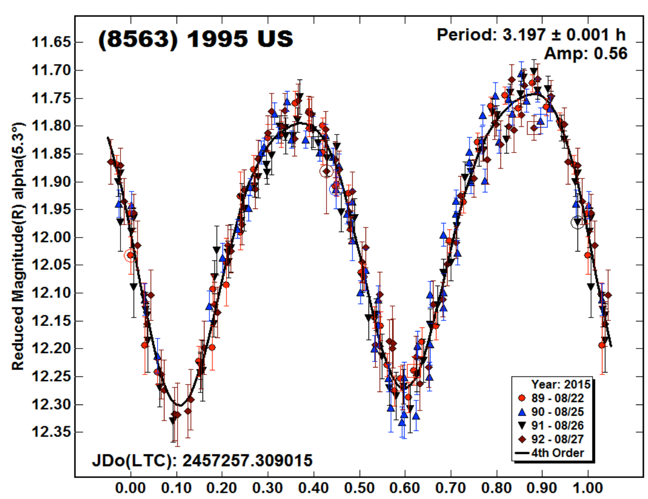

Figure 2. The lightcurve for (8563) 1995 US phased to the adopted period of 3.197 ± 0.001 hours.

ROTATION PERIODS OF 1831 NICHOLSON, 2929 HARRIS, 8463 NAOMIMURDOCH, AND (34173) 2000 QY37

Vladimir Benishek
Belgrade Astronomical Observatory
Volgina 7, 11060 Belgrade 38, SERBIA
vlaben@yahoo.com

(Received: 2015 Oct 15)

Photometric observations of four main-belt asteroids were conducted from 2015 February-May. Lightcurves and synodic rotation periods for 1831 Nicholson, 2929 Harris, 8463 Naomimurdoch, and (34173) 2000 QY37 are reported.

Photometric observations of four main-belt asteroids were conducted at Sopot Astronomical Observatory in the interval 2015 February-May in order to determine their synodic rotation periods. For this purpose a 0.35-m Meade LX200GPS Schmidt-Cassegrain telescope with an *f*/6.3 focal reducer and SBIG ST-8 XME CCD camera was employed. The exposures were unfiltered and unguided. The camera was operated in a 2x2 binning mode providing an image scale of 1.66 arcsec/pixel.

Photometric reductions and period analysis were performed in *MPO Canopus* software by BDW Publishing. Differential aperture photometry with up to five comparison stars of near solar color (0.5 ≤ B-V ≤ 0.9) was carried out using the Comparison Star Selector (CSS) feature of *MPO Canopus* by selecting the V-band comparison star magnitudes taken from the hybrid MPOSC3 catalog provided with the program. The MPOSC3 catalog contains BVRI magnitudes derived from J and K 2MASS catalog magnitudes by the formulae developed by Warner (2007). In order to achieve minimum RMS residual of a Fourier fit, adjustments of the magnitude zero-points for individual sessions were necessary due to the existence of more significant misfits between particular data sets that reached up to several tenths of magnitude. Such discrepancies are likely attributed to the catalog magnitude errors.

<u>1831 Nicholson</u>. This asteroid was observed from 2015 April 4 to May 17 resulting in 3 individual data sets. Analysis of the data found a bimodal lightcurve with a period of $P = 3.25510 \pm 0.00003$ h and a fairly large amplitude (0.29 ± 0.02 mag.). The data were obtained over a range of relatively low solar phase angles. This and the amplitude suggest a secure solution. A recently published rotation period by Garceran *et al.* (3.228 h) slightly differs from the result reported here.

<u>2929 Harris</u>. This "off-schedule" main-belt target was observed on only one night (2015 February 17-18) for more than 7 hours. There were no published rotation period results at that time. As it turned out, the photometric run encompassed more than two full rotational cycles. Since the amplitude of the obtained lightcurve amounts to 0.35 mag at the low average phase angle of only 2.4 degrees, the bimodal solution of $P = 3.13 \pm 0.02$ h is considered secure. In 2015 September, Waszczak *et al.* (2015) published a value of 3.1136 h for the rotation period, which is consistent with the result presented here.

<u>8463 Naomimurdoch</u>. No previous rotation period determinations were found. Two photometric data sets were obtained for this target in 2015 February. This main-belt asteroid was quite faint at the time of observations. It was at low phase angles of 2.73 and 3.18 degrees. The amplitude of 0.17 mag makes a monomodal solution of 3.74 h possible, especially given the close match of the two halves of the bimodal lightcurve when phased to 7.50 h (see the relevant split halves plot). The high noise level may conceal subtle differences between the two halves of the lightcurve and so the bimodal period should not be formally ruled out.

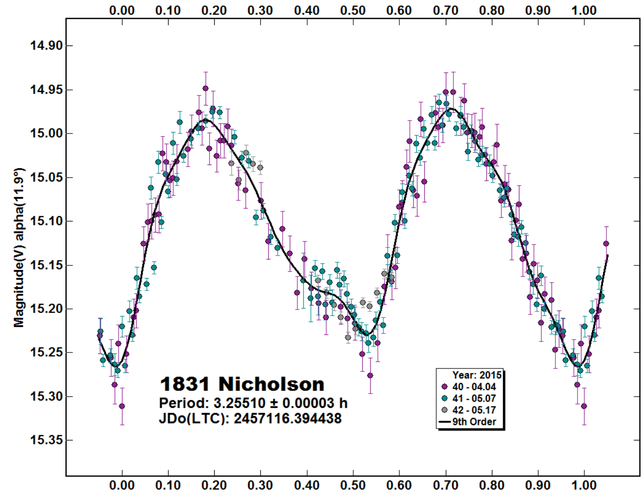

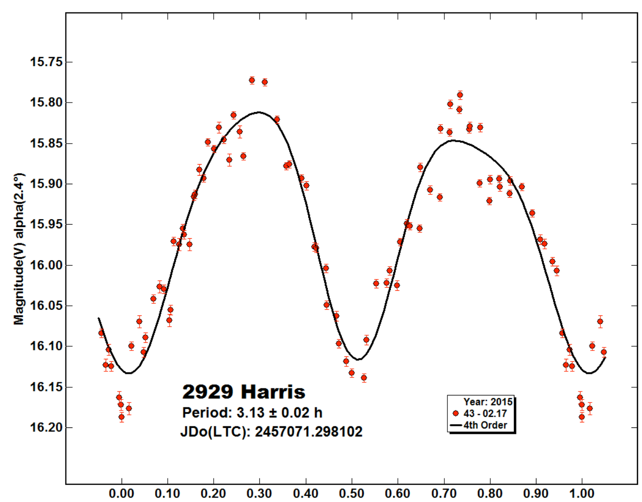

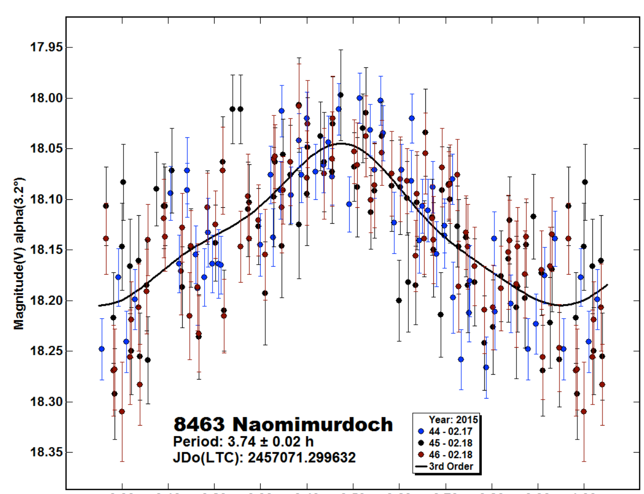

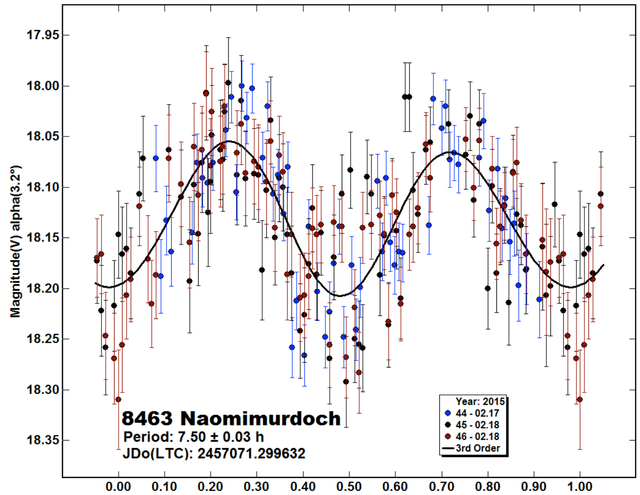

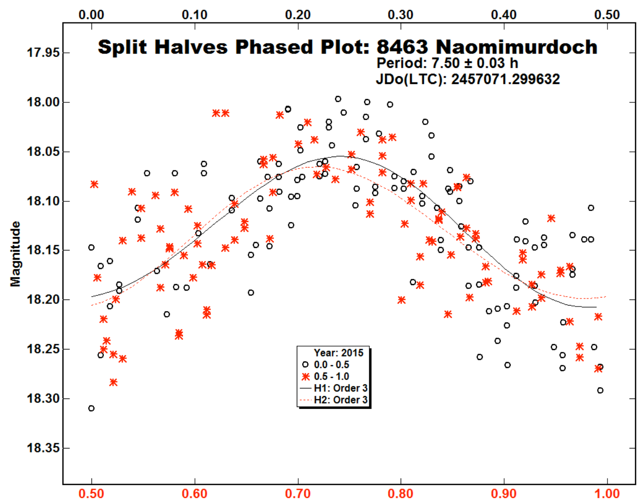

<u>(34173) 2000 QY37</u>. No previously determined rotation period was found for this asteroid. The target was observed over two nights on 2015 February 11 and 15. The period was found to be P = 3.521 ± 0.002 h. The fairly large amplitude, A = 0.33 mag, almost assures the bimodal lightcurve is the correct solution.

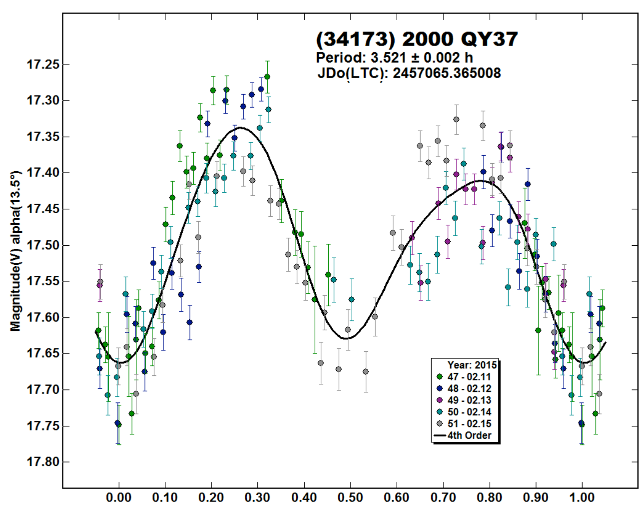

References

Garceran, A.C., Macias, A.A., Mansego, E.A., Rodriguez, P.B., De Haro, J.L. (2015). "Lightcurve Analysis of Six Asteroids." *Minor Planet Bul.* **42**, 235-237.

Warner, B.D. (2007). "Initial Results from a Dedicated H-G Project." *Minor Planet Bull*. **34**, 113-119.

Waszczak, A., Chang, C.-K., Ofek, E.O., Laher, R., Masci, F., Levitan, D., Surace, J., Cheng, Y.-C., Ip, W.-H., Kinoshita, D., Helou, G., Prince, T.A., Kulkarni, S. (2015). "Asteroid lightcurves from the Palomar Transient Factory survey: Rotation periods and phase functions from sparse photometry." *Astron. J.* **150**, 3.

ROTATION PERIOD DETERMINATION FOR (9773) 1993 MG1

Vladimir Benishek
Belgrade Astronomical Observatory
Volgina 7, 11060 Belgrade 38, SERBIA
vlaben@yahoo.com

Stephen M. Brincat
Flarestar Observatory
San Gwann SGN 3160, MALTA

(Received: 2015 Oct 15)

Photometric observations of the Mars-crossing asteroid (9773) 1993 MG1 were conducted over seven nights in 2015 July from Malta and Serbia. A synodic rotation period of 2.74595 ± 0.00006 h and lightcurve amplitude of 0.29 ± 0.02 mag were determined from the data.

Mars-crossing asteroid (9773) 1993 MG1 was discovered on 1993 June 23 by E.F. Helin at Palomar. In order to establish a secure synodic rotation period, Benishek began photometric observations on 2015 July 6 at Sopot Astronomical Observatory in Serbia. Brincat started photometric observations independently on 2015 July 13 at Flarestar Observatory in Malta with the same objective. An observing notification on the CALL website led to us forming a collaboration and pooling our data sets.

The Flarestar observations were conducted using a 0.25-m Meade SSC-10 Schmidt-Cassegrain telescope (SCT) operating at *f*/6.3 and a Moravian Instruments G2-1600 CCD camera. Sopot Observatory was equipped with a 0.35-m Meade LX200GPS SCT with an *f*/6.3 focal reducer and SBIG ST-8 XME CCD camera. All exposures were unfiltered. Brincat used autoguiding employing an Orion ST-80 Guidescope and a QHY 5 II camera with a monochrome CMOS chip, while all images obtained by Benishek were unguided.

The collaborative observations that spanned 2015 July 6-22 resulted in seven sessions with a total of 363 data points. Four of the sessions were obtained by Benishek and three by Brincat. Almost all observations were carried out before the opposition on 2015 July 21, when the lowest phase angle was 9.0 degrees. The phase angle ranged between 12.6 degrees before opposition to 9.2 degrees after opposition.

MPO Canopus by BDW Publishing (2015) was used by both authors to perform differential aperture photometry as well as for period analysis. Benishek used the Comparison Star Selector (CSS) procedure within *MPO Canopus* to provide a satisfactory correlation of the measurements with the standard magnitude framework. APASS V magnitudes were taken from the UCAC4 catalog available on the VizieR website (2015) to calibrate near solar color field comparison stars. Brincat provided CSS derived instrumental magnitudes. To combine the individual data sets obtained by both observers, gradual adjustments of the magnitude zero-points for each session were made in order to minimize the RMS error in the Fourier analysis.

Although a number of period solutions stand out in the period spectrum (Fig. 1), a bimodal solution of $P = 2.746$ hours (Fig. 2) is strongly favored over the others. This is based on the lightcurve amplitude of 0.29 mag as well as the relatively low phase angles over which the observations were made. Harris *et al.* (2014) asserted that only the second harmonic of a lightcurve can exceed a peak-to-peak amplitude of ~0.3 magnitude. For this reason, we believe that the amplitude of 0.29 mag, even though at the boundary for such a conclusion, represents a strong argument for a bimodal solution. To be sure of this, we considered other solutions and whether or not they were reasonable alternatives.

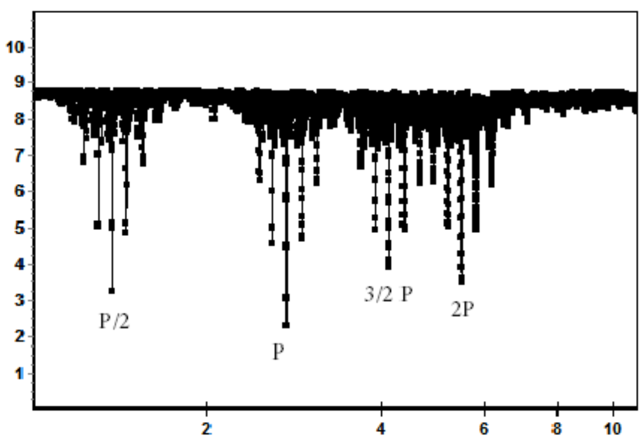

Fig.1 Period Spectrum for (9773) MG1

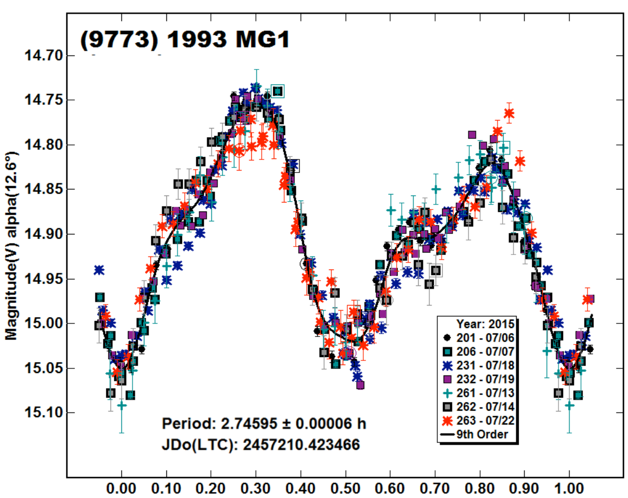

Fig.2 Composite Lightcurve Plot

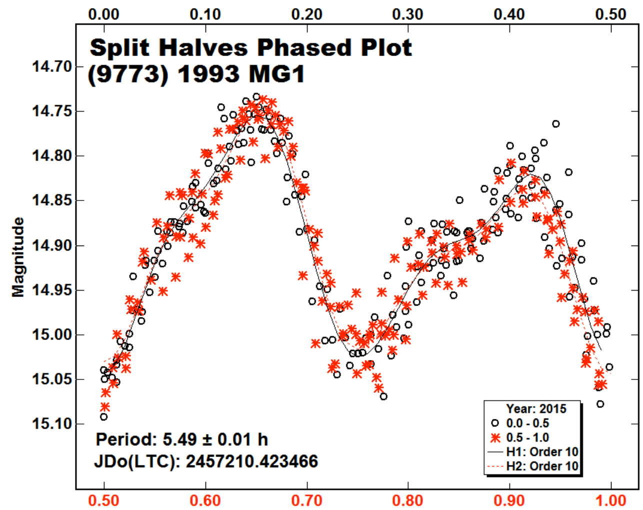

Fig. 3 Split Halves Plot

For example, the monomodal solution of 1.373 hours ($P/2$) is also characterized by a fairly low RMS error. Nevertheless, a larger data scatter and considerable mismatch between particular data sets make this unlikely. More so, the period would make the object go above the so-called "spin barrier" at about 2.2 hours. With a size of about 5 km, this was very unlikely. The solution at 4.119 hours ($3/2\ P$) produced a lightcurve with three minima and three maxima per cycle. This was rejected by taking into account that a triangular shape cannot provide an amplitude larger than 0.156 magnitudes (Harris *et al.*, 2014). The period value of 5.492 hours ($2P$) corresponds to a quadramodal lightcurve composed of two almost identical halves. The two halves of the lightcurve closely overlap each other without substantial discrepancies that rise above the noise levels of the both halves (Fig. 3). Furthermore, the RMS error was significantly higher than for a bimodal lightcurve and so the double period was rejected.

Based on the foregoing considerations, we conclude that a bimodal lightcurve with a synodic period of $P = 2.74595 \pm 0.00006$ hours and amplitude $A = 0.29 \pm 0.02$ mag is the most likely correct.

Near the completion of our photometric observations, Salvaggio *et al.* (2015) published a rotation period 2.746 hours, which is consistent with our results. The larger amplitude presented in their article (0.35 mag) could be attributed to the higher pre-opposition phase angles of their observations, which were made mainly in late June of 2015.

References

Harris, A.W., Pravec, P., Galad, A., Skiff, B.A., Warner, B.D., Vilagi, J., Gajdos, S., Carbognani, A., Hornoch, K., Kusnirak, P., Cooney, W.R., Gross, J., Terrell, D., Higgins, D., Bowell, E., Koehn, B.W. (2014). "On the maximum amplitude of harmonics on an asteroid lightcurve." *Icarus* **235**, 55-59.

Salvaggio, F., Franco, L., Marchini, A., Papini, R. (2015). "Lightcurve and Rotation Period Determination for 1492 Oppolzer and (9773) 1993 MG1." *Minor Planet Bul.* **42**, 283-284.

VizieR (2015). *http://vizier.u-strasbg.fr/viz-bin/VizieR*

Warner, B.D. (2015). MPO Canopus software.
http://www.minorplanetobserver.com/MPOSoftware/MPOCanopus.htm

NINETEEN ASTEROIDS LIGHTCURVES AT ASTEROIDS OBSERVERS (OBAS) - MPPD: 2015 APRIL - SEPTEMBER

Alfonso Carreño Garcerán
Zonalunar Observatory,Valencia, SPAIN
obas@minorplanet.es

Amadeo Aznar
Isaac Aznar Observatory, Valencia, SPAIN

Enrique Arce Mansego
Vallbona Observatory, Valencia, SPAIN

Pedro Brines Rodriguez
TRZ Observatory, Valencia, SPAIN

Juan Lozano de Haro
Elche Observatory, Alicante, SPAIN

Alvaro Fornas Silva
Oropesa Observatory, Valencia, SPAIN

Gonzalo Fornas Silva, Vicente Mas Martinez
CAAT, Centro Astronómico del Alto Turia, SPAIN

Onofre Rodrigo Chiner
Bétera Observatory, Valencia, SPAIN

(Received: 2015 Oct 12)

Photometric observations of 19 asteroids were made from 2015 April to September. We report the results of our lightcurve analysis for 392 Wilhelmina, 631 Philippina, 738 Alagasta, 758 Mancunia, 863 Benkoela, 873 Mechthild, 891 Gunhild, 900 Rosalinde, 1166 Sakuntala, 1232 Cortusa, 1243 Pamela, 1284 Latvia, 1331 Solvejg, 1353 Maartje, 1795 Woltjer, 2166 Handahl, 2379 Heiskanen, 2692 Chkalov, and 4875 Ingalls.

This paper contains lightcurve analysis for 19 asteroids obtained from the Spanish photometric asteroid analysis group (OBAS). The observatories coordinated their efforts as a network of telescopes working around weather and equipment issues. All lightcurves will be uploaded to Minor Planet Photometric Database (*http://www.minorplanet.es*) in order to get a visual database of asteroid lightcurves. The data have been sent to Collaborate Asteroid Lightcurve, as were previous works.

The data for our analysis were obtained from 2015 April to September. These asteroids were selected from the Collaborative Asteroid Lightcurve Link (CALL): 392 Wilhelmina, 631 Philippina, 738 Alagasta, 758 Mancunia, 863 Benkoela, 873 Mechthild, 891 Gunhild, 900 Rosalinde, 1166 Sakuntala, 1232 Cortusa, 1243 Pamela, 1284 Latvia, 1331 Solvejg, 1353 Maartje, 1795 Woltjer, 2166 Handahl, 2379 Heiskanen, 2692 Chkalov and 4875 Ingalls.

Nine observers: Alfonso Carreño, Amadeo Aznar, Enrique Arce, Pedro brines, Juan Lozano, Alvaro Fornas, Gonzalo Fornas, Onofre Rodrigo, and Vicente Mas contributed lightcurves. All exposures were made with clear filters (see Table I for equipment details) and all images were dark and flat-field corrected.

Telescope	Observatory	CCD
Refractor 10cm	Zonalunar	Atik 383L+
Cassegrain 35cm	Isaac Aznar	SBIG STL1001E
Cassegrain 25cm	Vallbona	SBIG ST7-XME
R-Chretien 20cm	TRZ	QHY8
D-Kirkham 25cm	Elche	SBIG ST8-XME
Cassegrain 20cm	Oropesa	Atik 16I
Cassegrain 23cm	Bétera	Atik 314L+
D-Kirkham 43cm	CAAT	SBIG STX-11K

Table I. List of instruments used for the observations.

<u>392 Wilhelmina</u> is a main-belt asteroid (D = 62.9 km) discovered by Max Wolf in 1894. A total of 431 data points were obtained over 8 nights from 2015 May 16 to Jun 5. The solar phase angle was –6.0° and +5° at the start and end of the period. Its magnitude was V ~ 14.3. The lightcurve shows a period of 16.98 ± 0.01 h and amplitude of 0.26 mag. The LCDB (Warner *et al.*, 2009) shows a period of 17.96 h and amplitude between 0.04-0.70.

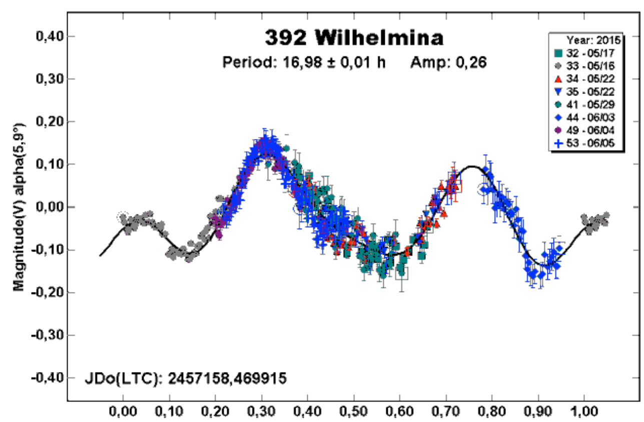

<u>631 Philippina</u> is a main-belt asteroid (D = 57.65 km) discovered by August Kopff in 1907. 300 points were obtained over 4 nights from 2015 July 12-14. The solar phase angle was 9º during span of observations. The asteroid's magnitude was V ~ 13.2. The lightcurve shows a period of 5.90 ± 0.01 h and amplitude of 0.63 mag. The LCDB shows several periods, *e.g.,* Behrend (2011, 5.899 h) and Hanus *et al.* (2011, 5.902 h).

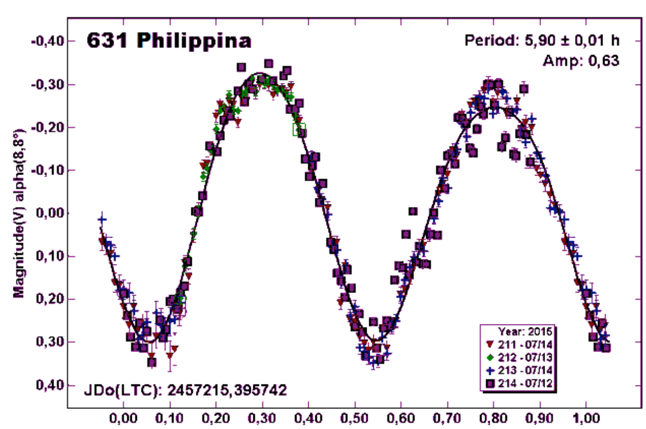

#	Name	Date Range	Nights	Period (h)	Error (h)	Amp (mag)	Points	LCD B
392	Wilhelmina	May 16 - Jun 05 2015	8	16.98	0.01	0.26	431	2
631	Philippina	Jul 12 - Jun 14 2015	4	5.90	0.01	0.63	300	3
738	Alagasta	May 27 - Jun 06 2015	6	18.86	0.01	0.11	338	2
758	Mancunia	May 27 - Jun 06 2015	6	12.71	0.01	0.22	349	3
863	Benkoela	Apr 04 - Apr 08 2015	3	8.20	0.01	0.27	176	2+
873	Mechthild	May 12 - May 16 2015	6	10.99	0.01	0.18	519	3
891	Gunhild	Jun 14 - Jul 17 2015	14	11.892	0.001	0.36	679	2
900	Rosalinde	Jun 19 - Jul 19 2015	5	16.70	0.01	0.28	297	2
1166	Sakuntala	Jun 28 - Jul 08 2015	4	6.29	0.01	0.38	210	2
1232	Cortusa	Jun 18 - Jun 27 2015	4	22.05	0.01	0.17	292	2
1243	Pamela	Aug 27 - Sep 22 2015	6	26.00	0.01	0.51	350	2
1284	Latvia	Sep 22 - Sep 30 2015	4	9.55	0.01	0.23	347	2
1331	Solvejg	Aug 23 - Sep 21 2015	6	19.30	0.01	0.44	309	2
1353	Maartje	Jun 30 - Jul 20 2015	18	22.930	0.001	0.46	724	2
1795	Woltjer	Jun 07 - Jun 16 2015	5	12.102	0.001	0.36	298	
2166	Handahl	Jul 23 - Jul 28 2015	4	7.21	0.01	0.11	269	3
2379	Heiskanen	Sep 21 - Sep 24 2015	3	3.76	0.01	0.17	271	
2692	Chkalov	Apr 30 - May 08 2015	3	6.11	0.01	0.13	184	
4875	Ingalls	May 28 - Jun 04 2015	3	3.78	0.01	0.13	360	

Table 2: Dates of observation, number of nights, and derived periods/amplitudes. The LCDB column gives the U rating (quality) listed in the in the asteroid lightcurve database (Warner *et al.,* 2009). A rating in the 2's indicates some uncertainty, *e.g.*, by up to 30% or being the double or half period of the "true" period. A rating of U=3 indicates a secure result.

<u>738 Alagasta</u> is a main-belt asteroid (*D* = 62.79 km) discovered by Franz Heinrich in 1913. 338 points were obtained over 6 nights, from 2015 May 27 to Jun 6. The solar phase angle was +2° and +4° at the start and end of the period. The asteroid was V ~ 14.2. The lightcurve shows a period of 18.86 ± 0.01 h and amplitude of 0.11 mag. Sada *et al.* (2005) found a period of 17.83 h.

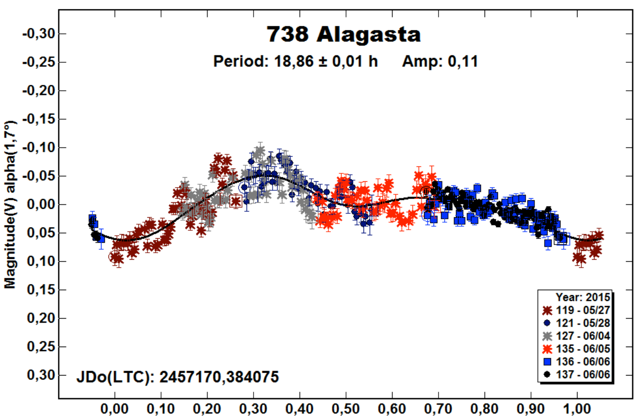

<u>758 Mancunia</u> is a main-belt asteroid (*D* = 85.48 km) discovered by Harry Edwin in 1912. 349 points were obtained over 6 nights in the period 2015 May 27 to Jun 6. The solar phase angle was +1° and +3° at the start and end of the period. The asteroid was V ~ 13.4. The lightcurve shows a period of 12.71 ± 0.01 h and amplitude of 0.22 mag. Due to weather problems, we could not get a complete lightcurve. Nevertheless, the Fourier analysis provides a consistent result. The LCDB shows a period of 12.73 h (Warner, 2008), 12.72 h (Behrend, 2007), and 12.8 h (Chang, 2014).

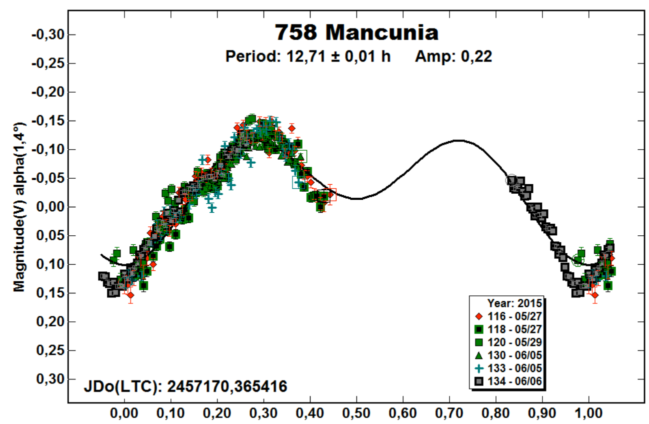

<u>863 Benkoela</u> is a main-belt asteroid (D = 27.06 km) discovered by Max Wolf in 1917. 176 points were obtained over 3 nights from 2015 April 4-8. The solar phase angle was +12°. The asteroid was V ~ 14 at the time. The lightcurve shows a period of 8.20 ± 0.01 h and amplitude of 0.27 mag. The LCDB shows a period of 7.03 h (Behrend, 2003) and Warner (2004), the latter having the better LCDB U rating of 2+.

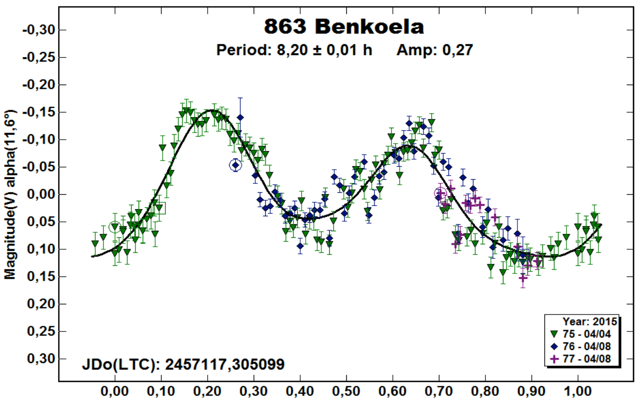

873 Mechthild is a main-belt asteroid (D = 29.04 km) discovered by Max Wolf in 1917. 519 points were obtained over 6 nights from 2015 May 12-16. The solar phase angle was +5°. The asteroid was V ~ 14.2 at the time. The lightcurve shows a period of 10.99 ± 0.01 h and amplitude of 0.18 mag. The LCDB shows periods of 10.6 h (Lagerkvist, 1978), 11.007 h (Warner, 2009), and 11.006 h (Wakszczak, 2015).

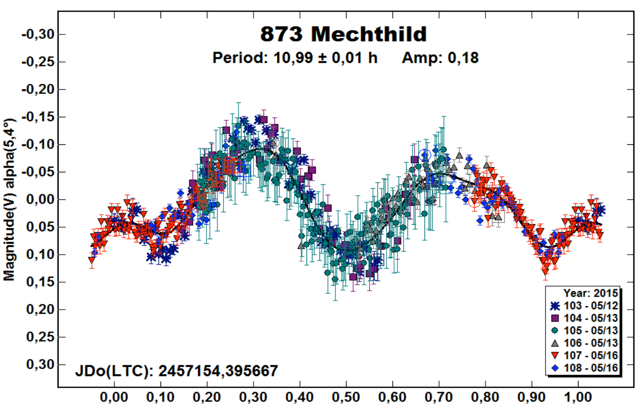

891 Gunhild is a main-belt asteroid (D = 51.95 km) discovered by Max Wolf in 1918. 679 points were obtained over 14 nights from 2015 June 14 to July 17. The solar phase angle was +4° and +14° at the start and end of the period. The asteroid was V ~ 14.0-14.6 over the period. The lightcurve shows a period of 11.892 ± 0.001 h and amplitude of 0.36 mag. The deformation near first minimum is likely due to a shape feature of the asteroid. Stephens (2000) reported a period of 7.93 h while Behrend (2005) reported P = 11.853.

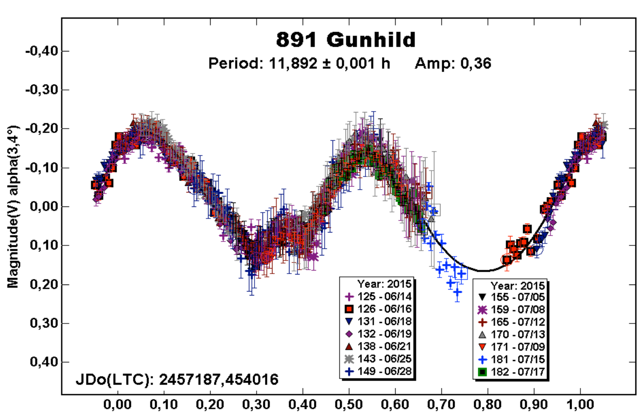

900 Rosalinde is a main-belt asteroid (D = 18.78 km) discovered by Max Wolf in 1918. 297 points were obtained over 5 nights from 2015 June 19 to July 19. The solar phase angle was +10° and +17° at the start and end of the period. The asteroid was V ~ 14.3 at the time. The lightcurve shows a period of 16.70 ± 0.01 h and amplitude of 0.28 mag. The LCDB shows a period of 16.5 h (Binzel, 1987) rated U = 2. There is another provisional lightcurve obtained by Behrend (2007), which has a period of 23.0 hours. Although it clearly shows a slope form, it covers less than 25% of a full rotation and so the lightcurve amplitude, and even period, can't be reliably determined.

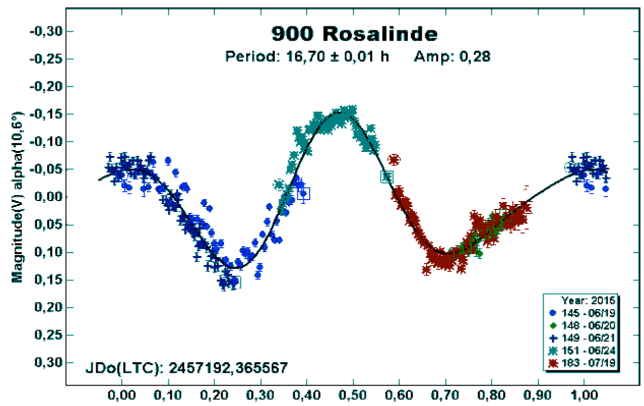

1166 Sakuntala is a main-belt asteroid (D = 28.74 km) discovered by Serguéi Beliavski in 1930. 210 points were obtained over 4 nights from 2015 Jun 28 to July 08. The solar phase angle was +8° and +12° at the start and end of the period. The asteroid was V ~ 12.6 at the time. The lightcurve shows a period of 6.29 ± 0.01 h and amplitude of 0.38 mag. Malcolm (2001) found a period of 6.30 h (U = 2). The LCDB contains other periods reported only as $P > 20$ h; those are rated U = 1.

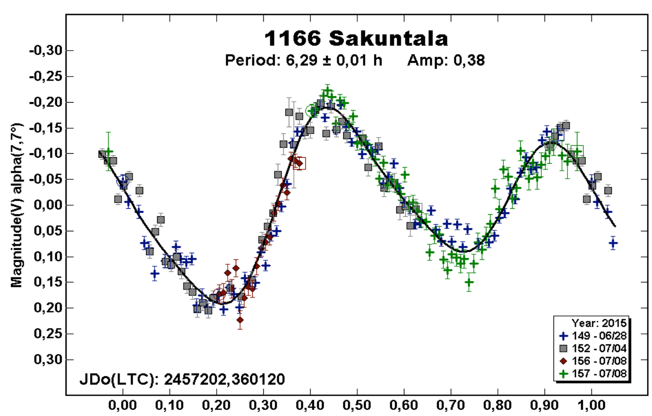

1232 Cortusa is a main-belt asteroid (D = 33.13 km) discovered by Karl Reinmuth in 1931. 292 points were obtained over 4 nights from 2015 Jul 18-27. The solar phase angle was +3° and +6° at the start and end of the period. The asteroid was V ~ 14.2 at the time. The lightcurve shows a period of 22.05 ± 0.01 h and amplitude of 0.17 mag. The LCDB shows a period of 25.16 h attributed to Behrend (2004; U = 2).

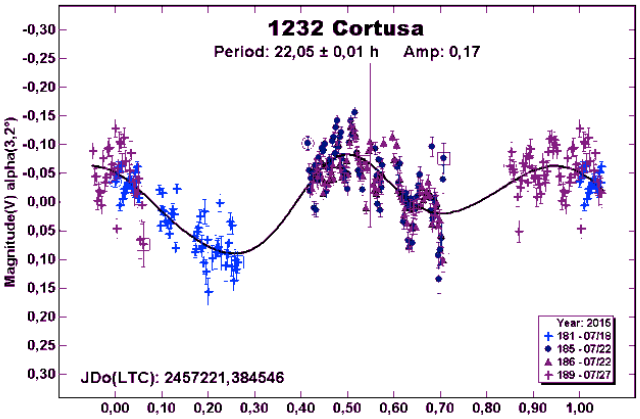

1243 Pamela is a main-belt asteroid of 70.07 km discovered by Cyril Jackson in 1932. 350 points were obtained over 6 nights from 2015 Aug 27 to Sep 22. The solar phase angle was +7° and +10° at the start and end of the period. The asteroid was V ~ 14.2 at the time. The lightcurve shows a period of 26.00 ± 0.01 h and amplitude of 0.51 mag. Warner (2000) reported a period of 26.017 h based on less than full coverage, the same us our curve.

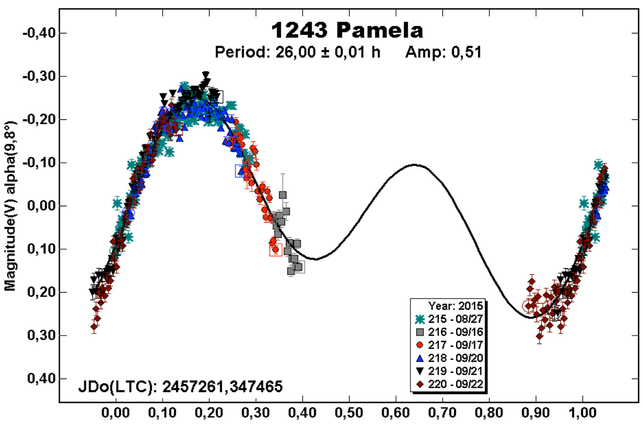

1284 Latvia is a main-belt asteroid (D = 36.81 km) discovered by Karl Reinmuth in 1933. 347 points were obtained over 4 nights from 2015 Sep 22-30. The solar phase angle was +7° at the start and end of the period. The asteroid was V ~ 13.2 at the time. The lightcurve shows a period of 9.55 ± 0.01 h and amplitude of 0.23 mag. Previously reported periods include Behrend (2004; 9.644 h) and Brinsfield (2008; 9.552 h). Both are rated U = 2.

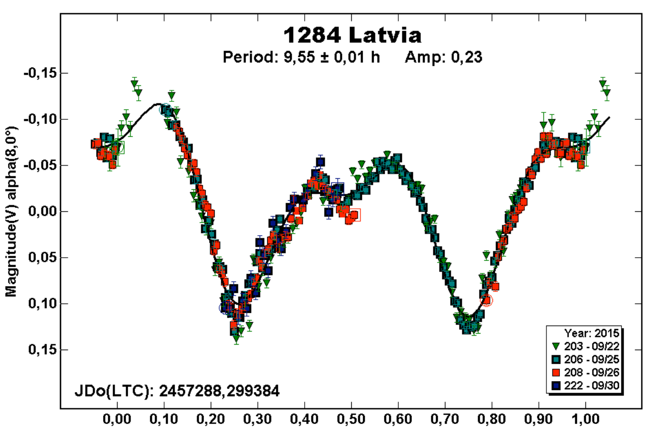

1331 Solvejg is a main-belt asteroid (D = 32.08 km) discovered by Grigori Neúimin in 1933. 309 points were obtained over 6 nights from 2015 Aug 23 to Sep 21. The solar phase angle was +4° and –15° at the start and end of the period. The asteroid was V ~ 13.5-14.2 at the time. The lightcurve shows a period of 19.3 ± 0.01 h and amplitude of 0.44 mag. Waszczak *et al.* (2015) found a period of 19.2885 h. This was a wide-field survey from which the results were imported into the LCDB *en masse* and given only a pass/fail rating, *i.e.,* U = 2 or U = 1, respectively. Many of the Waszczak *et al.* lightcurves are worthy of higher ratings, even U = 3.

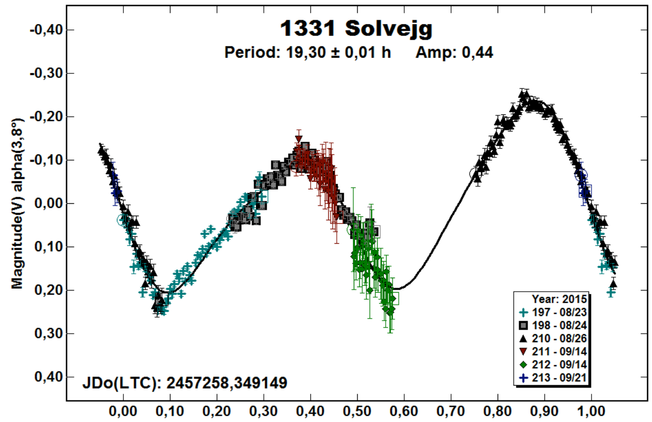

1353 Maartje is a main-belt asteroid (D = 33.75 km) discovered by Hendrik van Gent in 1935. 724 points were obtained over 18 nights from 2015 Jun 30 to Jul 20. The solar phase angle was –9° and +5° at the start and end of the period. The asteroid was V ~ 13.5 at the time. The lightcurve shows a period of 22.93 ± 0.001 h and amplitude of 0.46 mag. Behrend (2005) found a period of 22.98 h. Using the Behrend data along with those from other observers, Hanus *et al.* (2013) derived two possible spin axis orientations and shape. They reported a *sidereal* rotation period of 22.9926 h.

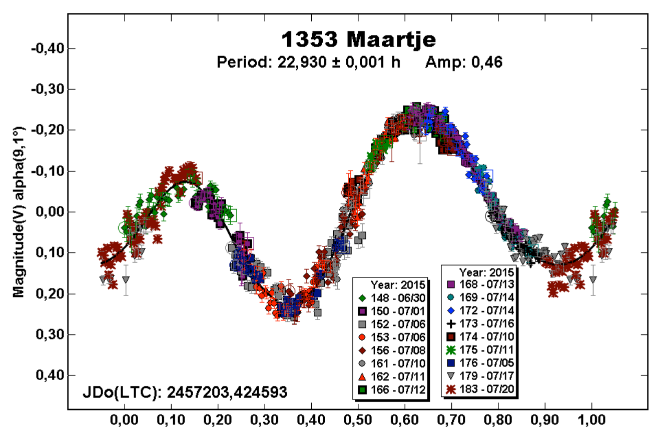

1795 Woltjer is a main-belt asteroid (D = 27.09 km) discovered by The P-L Survey at Palomar in 1960. 298 points were obtained over 5 nights from 2015 Jun 7-16. The solar phase angle was +6° and +10° at the start and end of the period. The asteroid was V ~ 14.7 at the time. The lightcurve shows a period of 12.102 ± 0.001 h and amplitude of 0.36 mag. The LCDB doesn't show a period for this asteroid.

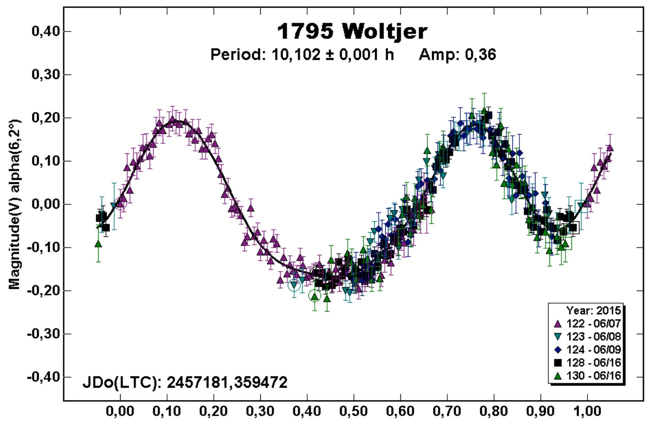

2166 Handahl is a main-belt asteroid (*D* ~ 5.5 km) discovered by Nikoláievich Neúimin in 1936. 269 points were obtained over 4 nights from 2015 Jul 23-28. The solar phase angle was –7° and +4° at the start and end of the period. The asteroid was V ~ 14.2 at the time. The lightcurve shows a period of 7.21 ± 0.01 h and amplitude of 0.11 mag. Chang *et al.* (2015) found a period of 7.330 h. Pravec *et al.* (2015) found a secure period of 7.2263 h based on observations in mid-2015.

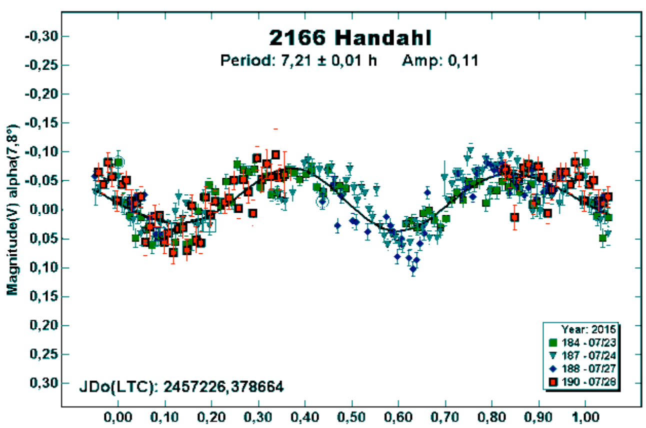

2379 Heiskanen is a main-belt asteroid (*D* = 31.6 km) discovered by Y. Vaisala in 1941. 271 points were obtained over 3 nights from 2015 Sep 21-24. The solar phase angle was +8°. The asteroid was V ~ 13.9 at the time. The lightcurve shows a period of 3.76 ± 0.01 h and amplitude of 0.17 mag. The LCDB doesn't show a period for this asteroid.

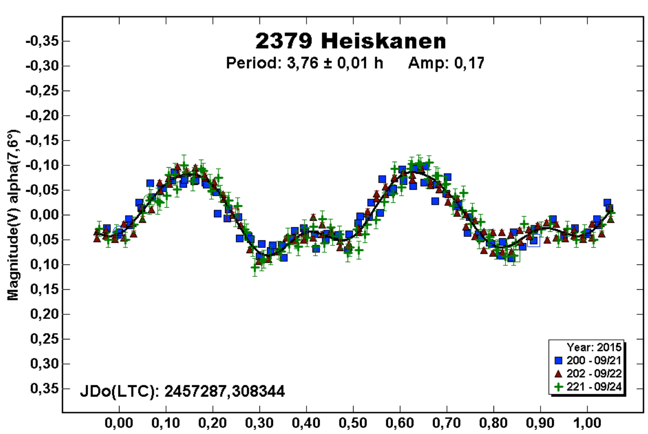

2692 Chkalov is a main-belt asteroid (*D* ~ 12 km) discovered by L. Chernykh in 1976. 184 points were obtained over 3 nights from 2015 April 30 to May 8. The solar phase angle was +7° and +14° at the start and end of the period. The asteroid was V ~ 14.5 at the time. The lightcurve shows a period of 6.11 ± 0.01 h and amplitude of 0.13 mag. The LCDB doesn't show a period for this asteroid.

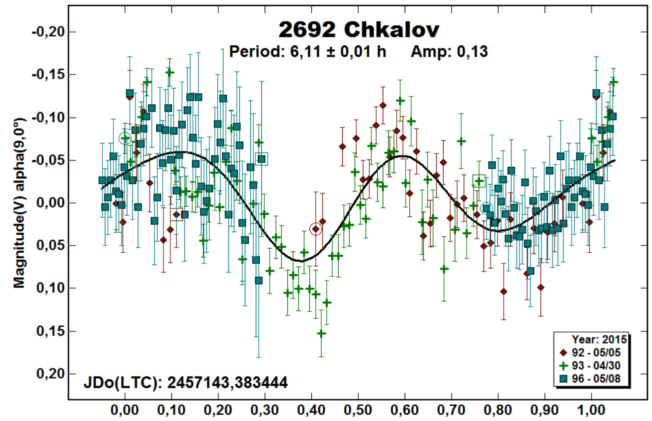

4875 Ingalls is a main-belt asteroid. The WISE survey (Mainzer *et al.*, 2011) gives an estimated diameter of 5.5 km based on an albedo of p_V = 0.3679 and *H* = 13.0. The asteroid was discovered by Y. Kushida and R. Kushida at Yatsugatake in 1991. 360 points were obtained over 3 nights from 2015 May 28 to Jun 4. The solar phase angle was +5° and +7° at the start and end of the period. The asteroid was V ~ 14.6 at the time. The lightcurve shows a period of 3.78 ± 0.01 h and amplitude of 0.13 mag. The LCDB doesn't show a period for this asteroid.

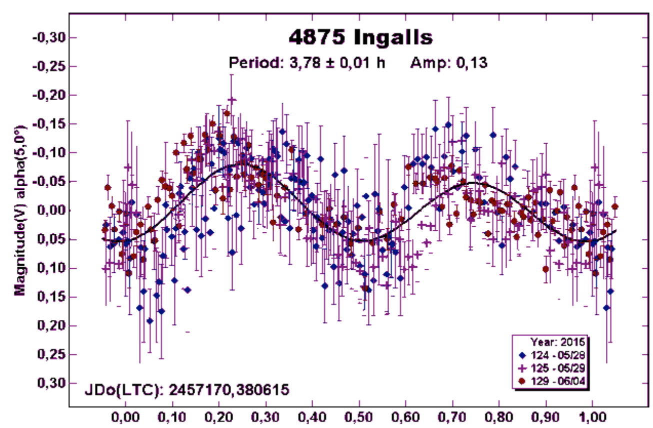

Acknowledgments

We would like to thank Brian Warner for all of his work with the program *MPO Canopus*, his efforts in maintaining the CALL website, and advice on asteroid lightcurve analysis.

References

Behrend, R. (2003 2004, 2005, 2007, 2011). Observatoire de Geneve web site. *http://obswww.unige.ch/~behrend/page_cou.html*

Binzel, R.P. (1987). "A photoelectric survey of 130 asteroids". *Icarus* **72**, 135-208.

Brinsfield, J. (2008). "Asteroid Lightcurve Analysis at the Via Capote Observatory: First Quarter 2008." *Minor Planet Bull.* **35**, 119-122.

Chang, C.-K., Ip, W.-H., Lin, H.-W., Cheng, Y.-C., Ngeow, C.-C., Yang, T.-C., Waszczak, A., Kulkarni, S.R., Levitan, D., Sesar, B., Laher, R., Surace, J., Prince, T.A. (2014). "313 New Asteroid Rotation Periods from Palomar Transient Factory Observations." *Ap. J.* **788**, A17.

Gil-Hutton, R., Canada, M. (2003). "Photometry of Fourteen Main-Belt Asteroids." *Revista Mexicana de Astronomica y Astrofisica* **39**, 69-76.

Hanuš, J., Ďurech, J., Brož, M., Warner, B.D., Pilcher, F., Stephens, R., Oey, J., Bernasconi, L., Casulli, S., Behrend, R., Polishook, D., Henych, T., Lehký, M., Yoshida, F., Ito, T. (2011). "A study of asteroid pole-latitude distribution based on an extended set of shape models derived by the lightcurve inversion method." *Astron. Astrophys*. **530**, A134.

Hanuš, J., Brož, M., Durech, J., Warner, B.D., Brinsfield, J., Durkee, R., Higgins, D., Koff, R.A., Oey, J., Pilcher, F., Stephens, R., Strabla, L.P., Ulisse, Q., Girelli, R. (2013). "An anisotropic distribution of spin vectors in asteroid families." *Astron. Astrophys.* **559**, A134.

Lagerkvist, C.-I. (1978). "Photographic photometry of 110 main-belt asteroids." *Astron. Astrophys. Suppl. Ser*. **31**, 361-381.

Mainzer, A., Grav, T., Masiero, J., Hand, E., Bauer, J., Tholen, D., McMillan, R.S., Spahr, T., Cutri, R.M., Wright, E., Watkins, J., Mo, W., Maleszewski, C. (2011). "NEOWISE Studies of Spectrophotometrically Classified Asteroids: Preliminary Results." *Ap. J.* **741**, A90.

Pravec, P., Wolf, M., Sarounova, L. (2015). *http://www.asu.cas.cz/~ppravec/neo.htm*

Stephens, R.D. (2000). "Rotational Periods and Lightcurves of 891 Gunhild and 1017 Jacqueline." *Minor Planet Bulletin* **27,** 54-55.

Sada, P.V., Canizales, E.D., Armada, E.M. (2005). "CCD photometry of asteroids 651 Antikleia, 738 Alagasta, and 2151 Hadwiger using a remote commercial telescope." *Minor Planet Bull*. **32**, 73-75.

Warner, B.D. (2000). "Asteroid Photometry at the Palmer Divide Observatory." *Minor Planet Bull.* **27**, 4-6.

Warner, B.D. (2004). "Lightcurve analysis for numbered asteroids 863, 903, 907, 928, 977, 1386 2841, and 75747." *Minor Planet Bull*. **31**, 85-88.

Warner, B.D., Behrend, R., Poncy, R., Coliac, J.F. (2008). "Lightcurve Analysis of 758 Mancunia." *Minor Planet Bull.* **35**, 25.

Warner, B.D. (2009). "Asteroid Lightcurve Analysis at the Palmer Divide Observatory: 2009 March-June." *Minor Planet Bull.* **36**, 172-176.

Warner, B.D., Harris, A.W., Pravec, P. (2009). "The asteroid lightcurve database." *Icarus* **202**, 134-146. Updates available at *http://www.minorplanet.info/lightcurvedatabase.html*.

Warner, B.D. (2012). MPO Software, *MPO Canopus* v10.4.1.12.

Waszczak, A., Chang, C.-K., Ofek, E.O., Laher, R., Masci, F., Levitan, D., Surace, J., Cheng, Y.-C., Ip, W.-H., Kinoshita, D., Helou, G., Prince, T.A., Kulkarni, S. (2015). "Asteroid Light Curves from the Palomar Transient Factory Survey: Rotation Periods and Phase Functions from Sparse Photometry." *Astron. J.* **150**, A75.

LIGHTCURVE AND ROTATION PERIOD DETERMINATION FOR MINOR PLANET 5236 YOKO

Mike Foylan
Cherryvalley Observatory (I83)
Cherryvalley, Rathmolyon, County Meath, IRELAND
mfoylan@yahoo.co.uk

(Received: 2015 Oct 15)

CCD photometric observations of minor planet 5236 Yoko (1990 TG3) were undertaken in 2015 October. Analysis of the data from four nights found a synodic rotation period of $P = 2.6175 \pm 0.0004$ h and lightcurve amplitude $A = 0.39 \pm 0.05$ mag.

Cherryvalley Observatory (MPC Code I83) is an amateur observatory located in Ireland. Observations were conducted with a 0.2-m Schmidt-Cassegrain Telescope (SCT) operating at *f*/7.6. The camera was an SBIG STL-1301E CCD with a 1280x1024 array of 16-micron pixels fitted with an R-band Bessel filter. The resulting image scale was 2.17 arcseconds per pixel at 1x1 binning. Image acquisition was undertaken with Software Bisque's *TheSky6 Professional* and *CCDSoft v5* (Software Bisque, 2011). All science images were aligned, dark, and flat-field corrected using *CCDSoft* v5 with mid-exposure times light corrected using *MPO Canopus v10.7.0.1* (Warner, 2015).

Data were reduced in *MPO Canopus* using differential photometry to facilitate easy exportation. The Comp Star Selector (CSS) utility in *MPO Canopus* allows selecting up to five near solar colour stars within the field of view for differential photometry. This also helped with night-to-night zero point calibrations. The Cousins R Magnitudes for the comparisons were derived using the 2MASS to BVRI formulae developed by Warner (2007). Period analysis was completed using *MPO Canopus*, which incorporates the Fourier analysis algorithm (FALC) developed by Harris (Harris *et al*., 1989).

5236 Yoko is a main-belt asteroid constrained by a defined orbit (JPL, 2015) of $2.0 < a < 3.2$ AU; $q > 1.666$ AU, where a is the orbital semi-major axis and q is the perihelion distance. The asteroid has an orbital period of approximately 3.56 years and an absolute magnitude $H = 13.2$. Based upon IRAS (Tedesco, 2004) observations, its effective diameter and geometric albedo are estimated at 8.98 km and 0.1383, respectively. Discovery was on 1990 October 10 by Mizuno and Furuta at Kani Observatory Japan.

5236 Yoko was reported as a lightcurve opportunity in the *Minor Planet Bulletin* (Warner *et al*., 2015). A total of 317 useful data points were used in the calculations, which were obtained over five nights during the period 2015 Oct 8-14. The solar phase angle varied from +14.9° through to +12.0° during observation period. The Earth distance was approximately 1.149 AU during the observation span.

The phased plot of the data demonstrates a classical bimodal shape with two maximums and minimums. The period solution of 2.6175

± 0.0004 h is in close agreement with earlier work by Carbo *et al.* (2009), who found a period of 2.768 ± 0.004 h and amplitude of 0.37 ± 0.05 mag.

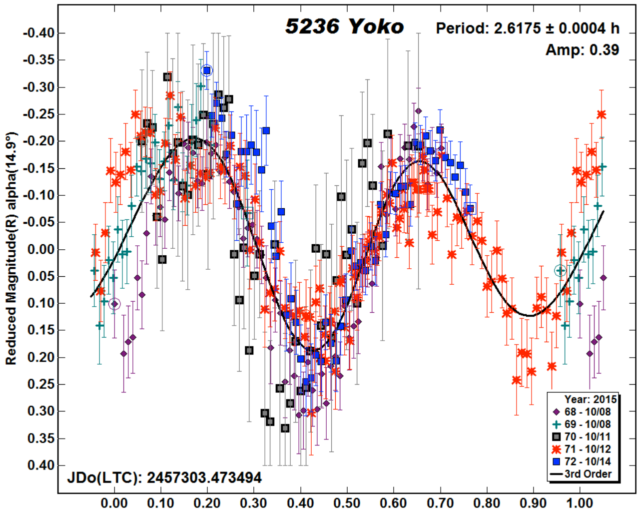

Acknowledgements

The author's wishes to express his gratitude to Professor Richard P. Binzel for his valued guidance and to Brian D. Warner for *MPO Canopus* software, which really makes asteroid lightcurve work much easier, enjoyable, and faster.

References

JPL (2015). Small-Body Database Browser. *http://ssd.jpl.nasa.gov/sbdb.cgi#top*

Carbo, L., Green, D., Kragh, K., Krotz, J., Meiers, A., Patino, B., Pligge, Z., Shaffer, N., Ditteon, R. (2009). "Asteroid Lightcurve Analysis at the Oakley Southern Sky Observatory: 2008 October thru 2009 March." Minor Planet Bulletin **36**, 152-157.

Harris, A.W., Young, J.W., Bowell, E., Martin, L.J., Millis, R.L., Poutanen, M., Scaltriti, F., Zappala, V., Schober, H.J., Debehogne, H., Zeigler, K.W. (1989). "Photoelectric Observations of Asteroids 3, 24, 60, 261, and 863." *Icarus* **77**, 171-186.

Software Bisque (2011). TheSky 6 Professional for Windows and CCDSoft v5.00.216 software. Golden, Colorado. *http://www.bisque.com*

Tedesco, E.F., Noah, P.V., Noah, M., Price, S.D. (2004). "IRAS Minor Planet Survey." IRAS-A-FPA-3-RDR-IMPS-V6.0. NASA Planetary Data System. *http://sbn.psi.edu/pds/resource/imps.html*

Warner, B.D. (2007). "Initial Results of a Dedicated H-G Program." *Minor Planet Bul.* **34**, 113-119.

Warner, B.D. (2015). MPO Software, *MPO Canopus* version 10.7.0.1 Bdw Publishing, *http://minorplanetobserver.com*

Warner, B.D., Harris, A.W., Pravec, P., Durech, J., Benner, L.A.M. (2015). "Lightcurve Photometry Opportunities: 2015 October – December." *Minor Planet Bulletin* **42**, 286-287.

ROTATION PERIOD ANALYSIS FOR 1967 MENZEL

Junda Liu
Suzhou High School Of Jiangsu Province
Suzhou,Jiangsu 215007 P.R. CHINA
824841086jdl@gmail.com

(Received: 2015 Oct 11)

Analysis of photometric observations for minor planet 1967 Menzel shows a synodic rotation period of P = 2.84 ± 0.03 h with an amplitude A = 0.28 mag.

1967 Menzel was discovered at Heidelberg on 1905 Nov 1 by M. Wolf. Its orbit has a semi-major axis of 2.233 AU, eccentricity of 0.1387, and orbital period of 3.34 years (JPL, 2015). The asteroid's synodic period has been reported on numerous occasions: Behrend (2005, 2.83481 h), Pray (2006, 2.8350 h), LeCrone *et al.* (2006, 2.834 h), Pravec *et al.* (2007, 2.8344 h; 2010, 2.8343 h), Higgins (2008, 2.8346 h), and Clark (2015, 2.8364 h).

The observations of 1967 were made at Lvye Observatory (IAU P34) on 2015 Oct 11. The instruments of Lvye Observatory were a Skywatcher 0.25-m *f*/4.4 reflector telescope, QHY9 CCD camera at 10°C, binned 2x2, and unfiltered. The image scale was 1.99 arc seconds per pixel. The exposure time was 60 s. All images were dark, bias, and flat-corrected by *MaxIm DL v5.23*. Differential photometry and period analysis were made with *MPO Canopus.*

200 data points were used for the analysis. The lightcurve shows a period P = 2.84 ± 0.03 h with an amplitude A = 0.28 mag. This is in good agreement with the earlier works.

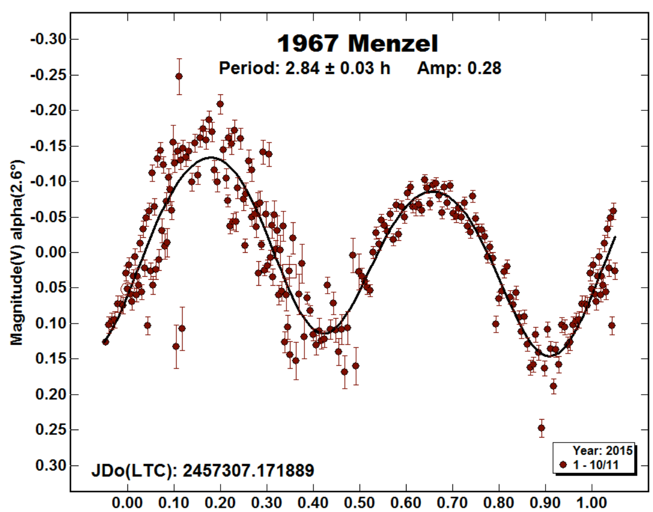

References

Behrend, R. (2005). Observatoire de Geneve web site. *http://obswww.unige.ch/~behrend/page_cou.html*

Clark, M. (2015). "Asteroid Photometry from the Preston Gott Observatory." *Minor Planet Bull.* **42**, 15-20.

Higgins, D. (2008). "Asteroid Lightcurve Analysis at Hunters Hill Observatory and Collaborating Stations: April 2007 – June 2007." *Minor Planet Bull.* **35**, 30-32.

JPL (2015). Small Body Database Browser. *http://ssd.jpl.nasa.gov/sbdb.cgi*

Lecrone, C., Duncan, A., Hudson, E., Johnson, J. Mulvihill, A., Reichert, C., Ditteon, R. (2006). "2005-2006 Fall Observing Campaign at Rose-Hulman Institute of Technology". *Minor Planet Bull.* **33**, 66-67.

Pravec, P. (2007, 2010). Photometric Survey for Asynchronous Binary Asteroids. *http://www.asu.cas.cz/~asteroid/binastphotsurvey.htm*

Pray, D.P. (2006). "Lightcurve analysis of asteroids 326, 329, 426, 619, 1829, 1967, 2453, 10518 and 42267". *Minor Planet Bull.* **33**, 4-5.

Warner, B.D., Harris, A.W., Pravec, P. (2009). "The asteroid lightcurve database." *Icarus* **202**, 134-146. Updated 2015 Oct 10. *http://www.MinorPlanet.info/lightcurvedatabase.html*

Warner, B.D. (2013). MPO Software, MPO Canopus version 10.4.3.17. Bdw Publishing, *http://minorplanetobserver.com/*

LIGHTCURVE ANALYSIS FOR ASTEROID 2310 OLSHANIYA

Caroline E. Odden, Thomas A. Johst, Hyung J. Jin, Walaa M. Alkhanaizi, AJ Augustin, Rocco J. Amorosso, Jamie T. Chen, John C. Duquette, Calvin S. Griffin, Isabella A. Flynn, Ji H. Kwan, Ava A. LaRocca, Samantha G. Lin, Heather F. Mei, Sarp Orgul, Benjamin T. Reinisch, Julia Y. Xia, Allen Zhou
Phillips Academy Observatory (I12)
180 Main Street
Andover, MA 01810 USA
ceodden@andover.edu

Daniel A. Klinglesmith III
Etscorn Campus Observatory
New Mexico Tech
101 East Road
Socorro, NM 87801

(Received: 2015 October 14)

Photometric observations for asteroid 2310 Olshaniya were obtained at the Phillips Academy Observatory during a span of several weeks in 2015 January and February and from the Magdalena Ridge Observatory during four nights in February. A synodic period of $P = 16.169 \pm 0.003$ hours was derived from these data.

2310 Olshaniya is a main-belt asteroid discovered by Lyudmila Zhuravlyova 1974 September 26 at Nauchnyj in the Crimean Astrophysical Observatory (Schmadel, 2003). A search of the Asteroid Lightcurve Database (LCDB; Warner *et al.,* 2009) and other sources did not reveal a previously reported period for the asteroid.

A lightcurve for the asteroid was obtained from Phillips Academy Observatory and the Magdalena Ridge Observatory during 2015 January and February. Observations were taken from Phillips Academy with a 0.40-m *f*/8 Ritchey-Chrétien reflector by DFM Engineering and an Andor Tech iKon DW436 camera with a 2048x2048 array of 13.5-micron pixels cooled to –50ºC. The resulting image scale was 0.86 arcseconds per pixel. The Etscorn Campus Observatory used a 0.35-m *f*/11 Schmidt-Cassegrain telescope and SBIG STL-1001E CCD with 1024x1024 24-micron pixels resulting in a plate scale of 1.25 arcseconds/pixel. The exposure time for all images was 180 seconds through a clear filter. The CCD was cooled to –30ºC or –35ºC depending on the night-time temperature. The images were flat-field corrected using batch image processing within *MPO Canopus* (Warner, 2010).

Images were measured using *MPO Canopus* using a differential photometry technique. All comparison stars were selected to near solar color by using the "comp star selector" tool of *MPO Canopus*. Data merging and period analysis were also done with *MPO Canopus* using an implementation of the Fourier analysis algorithm of Harris (FALC; Harris *et al.,* 1989). The combined data sets from both observatories were analyzed collaboratively by high school students enrolled in an astronomy research class taught by Odden at Phillips Academy. The final lightcurve appearing here was contributed by Jin. The period spectrum strongly suggests a bimodal solution with a synodic period of 16.169 hours ± 0.003 hours and an amplitude of 0.46 mag.

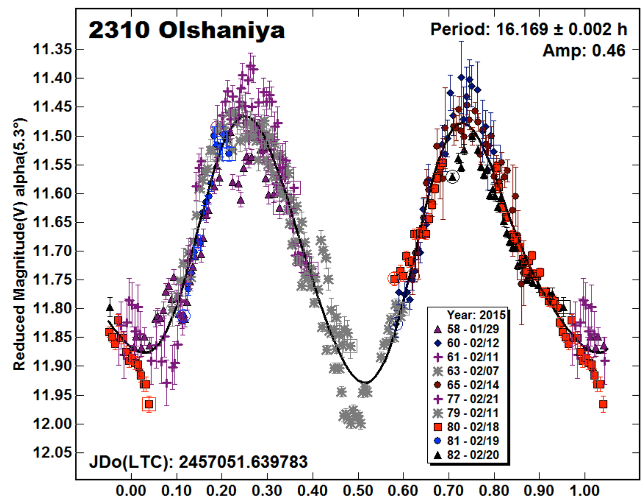

Acknowledgments

Research at the Phillips Academy Observatory is supported by the Israel Family Foundation. Many thanks to the Abbot Academy Association for the generous grant used to purchase the new Andor Tech camera. The Etscorn Campus Observatory operations are supported by the Research and Economic Development Office of New Mexico Institute of Mining and Technology (NMIMT).

References

Harris, A.W., Young, J.W., Bowell, E., Martin, L.J., Millis, R.L., Poutanen, M., Scaltriti, F., Zappala, V., Schober, H.J., Debehogne, H., Zeigler, K. (1989). "Photoelectric Observations of Asteroids 3, 24, 60, 261, and 863." Icarus **77**, 171-186.

Schmadel, L.D. (2003). *Dictionary of Minor Planet Names.* (5th ed., p. 146). Springer, New York, NY.

Warner, B.D., Harris, A.W., Pravec, P. (2009). "The asteroid lightcurve database." *Icarus* **202**, 134-146. Updated 2015 April 7. *http://www.minorplanet.info/lightcurvedatabase.html*

Warner, B.D. (2010). *The MPO Users Guide: A Companion Guide to the MPO Canopus/PhotoRed Reference Manuals*. BDW Publishing, Colorado Springs, CO.

ROTATION PERIOD AND H-G PARAMETERS OF (57868) 2001 YD

Vladimir Benishek
Belgrade Astronomical Observatory
Volgina 7, 11060 Belgrade 38, SERBIA
vlaben@yahoo.com

Frederick Pilcher
4438 Organ Mesa Loop
Las Cruces, NM 88011 USA

(Received: 2015 Oct 15)

For the main-belt asteroid (57868) 2001 YD we report a rotation period 108.10 ± 0.04 hours, amplitude 0.93 ± 0.02 magnitudes, H = 15.472 ± 0.041, and G = 0.069 ± 0.047.

The main-belt asteroid (57868) 2001 YD was discovered on 2001 December 17 at Palomar within the Near-Earth Asteroid Tracking (NEAT) program. Prior to our work no references for a rotation period for the asteroid were found. It was listed as a potential photometric target on the Potential Lightcurve Targets list on the CALL website maintained by Warner (2015a).

In order to determine the synodic rotation period, Benishek started photometric observations at Sopot Astronomical Observatory (SAO) on 2015 August 8 at the phase angle of 14.45 degrees. This was well before the opposition on 2015 August 29, when the phase angle was 4.1 degrees and V ~16.4. The initial sessions by Benishek indicated a slow rotation. To efficiently establish a lightcurve of the asteroid, we formed a collaboration and pooled our data sets.

At the SAO, Benishek used an *f*/6.3 0.35-m Meade LX200GPS Schmidt-Cassegrain telescope (SCT) equipped with a SBIG ST-8 XME CCD camera. At the Organ Mesa Observatory, Pilcher used a 0.35-m *f*/10 Meade LX200GPS SCT with an SBIG STL-1001E CCD camera. Since the target was quite faint, the unguided exposures were not filtered in order to achieve higher signal-to-noise ratio.

A mutually agreed observing approach involved collecting only several, well time-separated small groups of data points per night, which proved to be sufficient to define lightcurve slope for a particular session. Differential aperture photometry with up to five comparison stars of near solar color (0.5 ≤ B-V ≤ 0.9) was performed in *MPO Canopus* software (Warner, 2015b) by using the Comparison Star Selector utility. Johnson V magnitudes were taken from the *AAVSO Photometric All-Sky Survey* (APASS) catalog, Data Release 9 (Henden *et al.*, 2009). Night-to-night calibrations achieved using the APASS V magnitudes show a much lower degree of linkage misfits between individual sessions than when using other catalogs available to the CSS. Adjustments of the magnitude zero-points for individual data sets were almost completely unnecessary in order to achieve a minimum Fourier RMS residual, except in two cases, which could be considered as negligible if one takes into account the size of the data set.

A total of 778 data points distributed in 43 individual data sets was obtained with 10 sets by Pilcher and 33 sets by Benishek. Table I lists the dates, times, phase angle, and observer for each session.

The Fourier period analysis was also conducted in *MPO Canopus*. There are several harmonically related period solutions in the resulting period spectrum (Figure 1). These include a bimodal period of P = 108.10 hours with a lightcurve amplitude of A = 0.93 ± 0.02 mag (see Fig. 2). Since the data were gathered in at relatively small phase angles before and after the opposition, geometric considerations presented in Harris *et al.* (2014) virtually assure that this is the correct solution.

Date	Mid-Time (UT)	Phase (α°)	Obs.
2015/08/06	23:56	-14.45	VB
2015/08/07	23:31	-13.92	VB
2015/08/08	22:07	-13.42	VB
2015/08/10	00:05	-12.83	VB
2015/08/10	23:34	-12.29	VB
2015/08/11	22:37	-11.76	VB
2015/08/13	01:52	-11.13	VB
2015/08/13	23:22	-10.63	VB
2015/08/14	23:14	-10.08	VB
2015/08/18	23:22	-7.87	VB
2015/08/20	06:55	-7.18	FP
2015/08/22	9:29	-6.12	FP
2015/08/23	22:44	-5.43	VB
2015/08/24	20:25	-5.07	VB
2015/08/25	22:38	-4.69	VB
2015/08/26	10:16	-4.55	FP
2015/08/27	01:36	-4.39	VB
2015/08/28	01:37	4.22	VB
2015/08/31	22:07	4.46	VB
2015/09/01	19:37	4.71	VB
2015/09/02	23:13	5.10	VB
2015/09/03	22:20	5:49	VB
2015/09/07	21:52	7.41	VB
2015/09/08	22:08	7.95	VB
2015/09/12	02:26	9.68	FP
2015/09/12	21:59	10.12	VB
2015/09/13	03:52	10.26	FP
2015/09/13	21:52	10.67	VB
2015/09/14	03:56	10.81	FP
2015/09/14	20:08	11.18	VB
2015/09/15	03:14	11.34	FP
2015/09/16	03:48	11.90	FP
2015/09/17	21:35	12.84	VB
2015/09/18	20:54	13.36	VB
2015/09/19	19:00	13.85	VB
2015/09/22	22:37	15.47	VB
2015/09/23	20:22	15.93	VB
2015/10/01	21:48	19.69	VB
2015/10/02	02:48	19.78	FP
2015/10/02	19:40	20.08	VB
2015/10/03	18:21	20.48	VB
2015/10/05	19:55	21.32	VB
2015/10/07	02:36	21.82	FP

Table I. Observation circumstances.

It should be noted that the RMS error differs slightly depending on whether the entire data set or only subsets of data, each with small a small date range, is used. The discrepancies are somewhat lower in the latter cases. This suggests a gradual change of amplitude and shape of the lightcurve with phase angle. However, given the long rotation period, it was impossible to quantify these rather slight changes consistently. This is why the lightcurve encompassing the entire observation time range is taken into consideration for period determination.

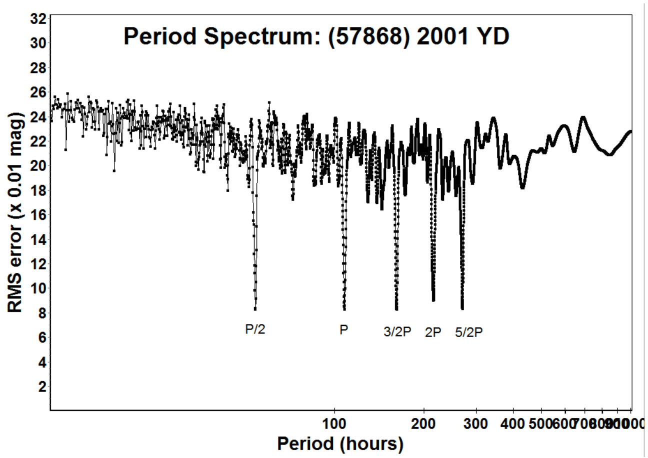

Fig.1. The period spectrum for (57868) 2001 YD

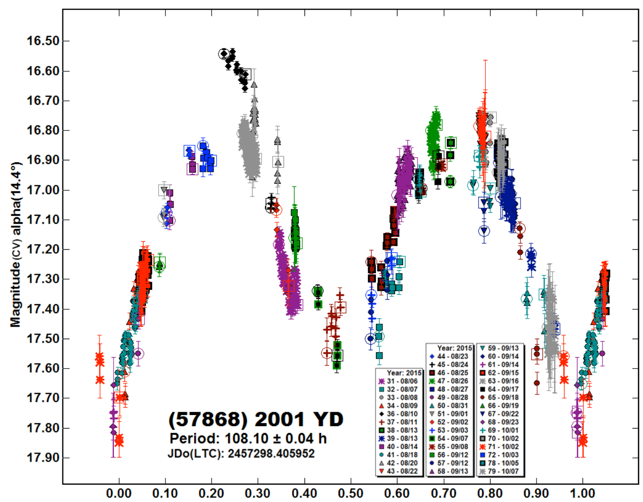

Fig. 2. The composite lightcurve phased to 108.10 hours

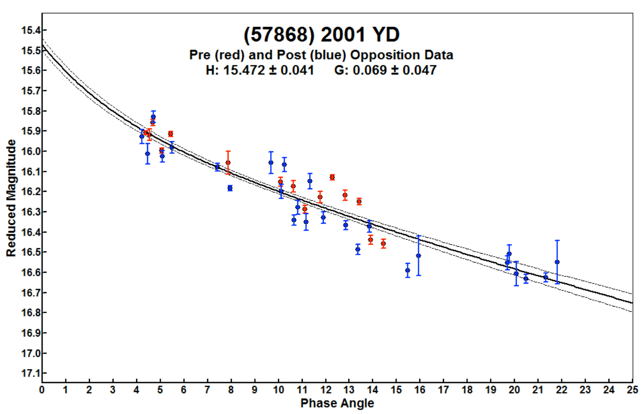

Fig. 3 The phase curve for (57868) 2001 YD

Using the spreadsheet procedure described by Buchheim (2010), the mean magnitude values of the lightcurves for individual nights were obtained. These were converted into reduced magnitudes by applying $-5*\log(r\Delta)$, with r and Δ being, respectively, the asteroid-Sun and asteroid-Earth distances. To establish the phase curve and determine the V-band absolute magnitude (H) and slope parameter (G), the reduced magnitudes were used in the H-G Calculator tool of *MPO Canopus*, which is based on the FAZ algorithm developed by Alan Harris (1989). Our analysis found $H = 15.472 \pm 0.041$ mag and $G = 0.069 \pm 0.047$ (see Fig. 3).

The somewhat large scatter seen in Figure 3 might be partly interpreted as a consequence of the impossibility to account for the likely changes in the Fourier fit model used for the mean light magnitude calculations. Therefore, the values for H and G should be taken with some caution.

Acknowledgements

This research was made possible in part based on data from CMC15 Data Access Service at CAB (INTA-CSIC) and the AAVSO Photometric All-Sky Survey (APASS), funded by the Robert Martin Ayers Sciences Fund. (*http://svo2.cab.inta-csic.es/vocats/cmc15/*).

References

Buchheim, R.K. (2010). "Methods and Lessons Learned Determining the H-G Parameters of Asteroid Phase Curves." in *Proceedings for 29th Annual Symposium on Telescope Science*. pp. 101-115. Society for Astronomical Sciences. Rancho Cucamonga, CA.

Harris, A.W. (1989). "The H-G Asteroid Magnitude System: Mean Slope Parameters." *Abstracts of the Lunar and Planetary Science Conference* **20**, 375.

Harris, A.W., Pravec, P., Galad, A., Skiff, B.A., Warner, B.D., Vilagi, J., Gajdos, S., Carbognani, A., Hornoch, K., Kusnirak, P., Cooney, W.R., Gross, J., Terrell, D., Higgins, D., Bowell, E., Koehn, B.W. (2014). "On the maximum amplitude of harmonics on an asteroid lightcurve." *Icarus* **235**, 55-59.

Henden, A.A., Terrell, D., Levine, S.E., Templeton, M., Smith, T.C., Welch, D.L. (2009). "The AAVSO Photometric All-Sky Survey (APASS)." *https://www.aavso.org/apass*

Warner, B.D. (2015a). Collaborative Asteroid Lightcurve Link website. *http://www.minorplanet.info/call.html*

Warner, B.D. (2015b). *MPO Canopus* software. *http://www.bdwpublishing.com*

TARGET ASTEROIDS! OBSERVING CAMPAIGNS FOR JANUARY THROUGH MARCH 2016

Carl Hergenrother and Dolores Hill
Lunar & Planetary Laboratory
University of Arizona
1629 E. University Blvd.
Tucson, AZ 85721 USA
chergen@lpl.arizona.edu

(Received: 2015 Oct 15)

Asteroid campaigns to be conducted by the Target Asteroids! program during the January-March 2016 quarter are described. In addition to asteroids on the original Target Asteroids! list of easily accessible spacecraft targets, an effort has been made to identify other asteroids that are 1) brighter and easier to observe for small telescope users and 2) analogous to 101955 Bennu and 162173 Ryugu, targets of the OSIRIS-REx and Hayabusa-2 sample return missions.

Introduction

The *Target Asteroids!* program strives to engage telescope users of all skill levels and telescope apertures to observe asteroids that are viable targets for robotic sample return. The program also focuses on the study of asteroids that are analogous to 101955 Bennu and 162173 Ryugu, the target asteroids of the NASA OSIRIS-REx and JAXA Hayabusa-2 sample return missions respectively. Most target asteroids are near-Earth asteroids (NEA) though observations of relevant Main Belt asteroids (MBA) are also requested.

Even though many of the observable objects in this program are faint, acquiring a large number of low S/N observations allows many important parameters to be determined. For example, an asteroid's phase function can be measured by obtaining photometry taken over a wide range of phase angles. The albedo can be constrained from the phase angle observations, as there is a direct correlation between phase function and albedo (Belskaya and Shevchenko, 2000). The absolute magnitude can be estimated by extrapolating the phase function to a phase angle of 0°. By combining the albedo and absolute magnitude, the size of the object can be estimated.

An overview of the *Target Asteroids!* program can be found at Hergenrother and Hill (2013).

Current Campaigns

Target Asteroids! continues to conduct a number of dedicated campaigns on select NEAs and analog carbonaceous MBAs during the quarter. These campaigns have a primary goal of conducting photometric measurements over a large range of phase angles.

Target Asteroids! objects brighter than V = 17.0 are presented in detail. A short summary of our knowledge of each asteroid and 10-day (shorter intervals for objects that warrant it) ephemerides are presented. The ephemerides include rough RA and Dec positions, distance from the Sun in AU (r), distance from Earth in AU (Δ), V magnitude, phase angle in degrees (PH) and elongation from the Sun in degrees (Elong).

We ask observers with access to large telescopes to attempt observations of spacecraft accessible asteroids that are between V magnitude ~17.0 and ~20.0 during the quarter (contained in the table below).

Asteroid Number	Name	Peak V Mag	Time of Peak Brightness
(10302)	1989 ML	19.3	early Jan
(52381)	1993 HA	18.3	early Jan
(163249)	2002 GT	18.9	late Mar
(350713)	2001 XP88	18.9	early Oct
(382758)	2003 GY	19.5	late Mar
	1994 UG	17.3	mid Mar
	2003 GA	19.9	late Feb
	2009 DN1	19.6	late Mar
	2010 WY8	19.6	early Mar

The campaign targets are split up into two sections: carbonaceous MBAs that are analogous to Bennu and Ryugu; and NEAs analogous to the Bennu and Ryugu or provide an opportunity to fill some of the gaps in our knowledge of these spacecraft targets (examples include very low and high phase angle observations, phase functions in different filters and color changes with phase angle).

The ephemerides listed below are just for planning purposes. In order to produce ephemerides for your observing location, date and time, please use the Minor Planet Center's Minor Planet and Comet Ephemeris Service:

http://www.minorplanetcenter.net/iau/MPEph/MPEph.html

or the *Target Asteroids!* specific site created by Tomas Vorobjov and Sergio Foglia of the International Astronomical Search Collaboration (IASC) at

http://iasc.scibuff.com/osiris-rex.php

Analog Carbonaceous Main Belt Asteroid Campaigns

1257 Mora (*a* = 2.49 AU, *e* = 0.08, *i* = 3.9°, *H* = 12.0)
The target asteroids of the OSIRIS-REx and Hayabusa-2 missions originated in the inner part of the main belt (between 2.0 and 2.55 AU) on low inclination orbits. *Target Asteroids!* is conducting many campaigns on objects in this region of the main belt.

The campaign to observe 1257 Mora started during the previous quarter. January will see Mora fading to V ~ 17 and allowing higher phase angles to be observed for the asteroid during this apparition.

DATE	RA	DEC	Δ	r	V	PH	Elong
01/01	02 12	+11 29	2.13	2.69	16.9	19	115
01/11	02 15	+11 42	2.26	2.69	17.0	20	105
01/21	02 21	+12 08	2.39	2.69	17.2	21	96
01/31	02 28	+12 43	2.53	2.69	17.3	21	88

2026 Cottrell (*a* = 2.45 AU, *e* = 0.12, *i* = 2.5°, *H* = 12.9)
Cottrell is presumed to be a carbonaceous based on its very dark albedo (Masiero *et al*., 2011). Though an inner main-belt asteroid, it does not appear to be a member of any known carbonaceous asteroid families. Taxonomy has not been determined for it so spectroscopy and filter photometry is a high priority. It reaches a minimum phase angle of 0.7° and maximum brightness of V = 15.1 on February 20.

DATE	RA	DEC	Δ	r	V	PH	Elong
01/01	10 32	+08 54	1.49	2.19	16.5	22	123
01/11	10 33	+08 34	1.39	2.19	16.3	19	133
01/21	10 31	+08 31	1.31	2.18	16.0	15	144
01/31	10 26	+08 45	1.24	2.18	15.7	10	155
02/10	10 18	+09 13	1.20	2.17	15.4	5	167
02/20	10 08	+09 49	1.18	2.17	15.1	0	178
03/01	09 59	+10 27	1.19	2.17	15.4	5	167
03/11	09 51	+10 59	1.22	2.17	15.7	11	155
03/21	09 45	+11 20	1.28	2.16	16.0	15	144
03/31	09 43	+11 28	1.35	2.16	16.2	19	133

Near-Earth Asteroid Campaign Targets

(7350) 1993 VA (*a* = 1.36 AU, *e* =0.39, *i* = 7.3°, *H* = 17.1)
Carbonaceous and located on a low delta-V orbit, (7350) 1993 VA may make a nice future spacecraft target. Typical of a carbonaceous C-type asteroid, 1993 VA has a very dark albedo of 0.05. Little is known of its rotational properties and this apparition will be a prime opportunity to determine its rotational period. Peak brightness occurs in late March/early April at V = 15.8. It can be observed over phase angles of 40° to 112° during the period when it is brighter than V = 18.

DATE	RA	DEC	Δ	r	V	PH	Elong
02/20	01 28	+09 44	0.29	0.85	18.3	110	53
03/01	02 02	+20 17	0.23	0.88	17.9	112	55
03/11	02 54	+35 33	0.18	0.93	17.2	107	62
03/21	04 46	+53 42	0.15	0.98	16.3	92	78
03/31	08 16	+59 00	0.16	1.04	15.8	72	98

(33342) 1998 WT24 (*a* = 0.72 AU, *e* = 0.42, *i* = 7.3°, *H* = 17.9)
One of the better characterized NEAs, 1998 WT24 is a Xe-type with high albedo (0.34 ± 0.20) and an equivalent diameter of 0.415 ± 0.040 kilometers (Busch *et al.*, 2008). It will be brighter than magnitude V = 18.0 between 2015 Oct. 24 and Jan. 9. During that time, phase function photometry is possible over a phase angle range of 21° to 115°. Peak brightness occurs on Dec. 10 at V = 11.3. During January the asteroid is receding from Earth and rapidly drops in brightness from magnitude 16.6 to 19.7.

DATE	RA	DEC	Δ	r	V	PH	Elong
01/01	22 58	+09 39	0.10	0.95	16.6	103	70
01/11	22 32	+09 00	0.15	0.91	18.1	117	55
01/21	22 12	+07 24	0.19	0.85	19.7	130	41

(294739) 2008 CM (*a* = 0.83 AU, *e* = 0.21, *i* = 8.5°, *H* = 16.9)
Similar to 1998 WT24, this object passed closest to Earth last year and is rapidly fading from a very bright (for an NEA) magnitude 12.9 to 17.6 by the end of January. Past observations have determined a rotation period of 3.05 h and amplitude of ~0.48 magnitudes (Warner, 2014). Little else is known about 2008 CM, so new photometry will shed light on its color, taxonomy and phase function.

DATE	RA	DEC	Δ	r	V	PH	Elong
01/01	08 18	-01 13	0.07	1.04	12.9	32	146
01/11	06 40	-30 17	0.17	1.09	15.4	46	126
01/21	06 14	-34 54	0.29	1.15	16.7	48	118
01/31	06 06	-35 33	0.41	1.21	17.6	48	114

References

Belskaya, I., Shevchenko, V. (2000). "The Opposition Effect of Asteroids." *Icarus* **147**, 94-105.

Busch, M.W., Benner, L.A.M., Ostro, S.J., Giorgini, J.D., Jurgens, R.F., Rose, R., Scheeres, D.J., Magri, C., Margot, J.-L., Nolan, M.C., Hine, A.A. (2008). "Physical Properties of Near-Earth Asteroid (33342) 1998 WT24." *Icarus* **195**, 614-621.

Hergenrother, C., Hill, D. (2013). "The OSIRIS-REx *Target Asteroids!* Project: A Small Telescope Initiative to Characterize Potential Spacecraft Mission Target Asteroids." *Minor Planet Bulletin* **40**, 164-166.

Masiero, J.R., Mainzer, A.K., Grav, T., Bauer, J.M., Cutri, R.M., Dailey, J., Eisenhardt, P.R.M., McMillan, R.S., Spahr, T.B., Skrutskie, M.F., Tholen, D., Walker, R.G., Wright, E.L., DeBaun, E., Elsbury, D., Gautier, T., Gomillion, S., Wilkins, A. (2011). "Main Belt Asteroids with WISE/NeoWISE. I. Preliminary Albedos and Diameters." *Astrophysical Journal* **741**, id. 68.

Warner, B.D. (2014). "Near-Earth Asteroid Lightcurve Analysis at CS3-Palmer Divide Station: 2014 January-March." *Minor Planet Bulletin* **41**, 157-168.

LIGHTCURVE PHOTOMETRY OPPORTUNITIES: 2016 JANUARY-MARCH

Brian D. Warner
Center for Solar System Studies / MoreData!
446 Sycamore Ave.
Eaton, CO 80615 USA
brian@MinorPlanetObserver.com

Alan W. Harris
MoreData!
La Cañada, CA 91011-3364 USA

Josef Ďurech
Astronomical Institute
Charles University in Prague
18000 Prague, CZECH REPUBLIC
durech@sirrah.troja.mff.cuni.cz

Lance A.M. Benner
Jet Propulsion Laboratory
Pasadena, CA 91109-8099 USA
lance.benner@jpl.nasa.gov

(Received: 8 October 2015)

We present lists of asteroid photometry opportunities for objects reaching a favorable apparition and have no or poorly-defined lightcurve parameters. Additional data on these objects will help with shape and spin axis modeling via lightcurve inversion. We also include lists of objects that will be the target of radar observations. Lightcurves for these objects can help constrain pole solutions and/or remove rotation period ambiguities that might not come from using radar data alone.

We present several lists of asteroids that are prime targets for photometry during the period 2016 January-March.

In the first three sets of tables, "Dec" is the declination and "U" is the quality code of the lightcurve. See the asteroid lightcurve data base (LCDB; Warner *et al.*, 2009) documentation for an explanation of the U code:

http://www.minorplanet.info/lightcurvedatabase.html

The ephemeris generator on the CALL web site allows you to create custom lists for objects reaching V ≤ 18.5 during any month in the current year, e.g., limiting the results by magnitude and declination.

http://www.minorplanet.info/PHP/call_OppLCDBQuery.php

We refer you to past articles, e.g., *Minor Planet Bulletin* **36**, 188, for more detailed discussions about the individual lists and points of advice regarding observations for objects in each list.

Once you've obtained and analyzed your data, it's important to publish your results. Papers appearing in the *Minor Planet Bulletin* are indexed in the Astrophysical Data System (ADS) and so can be referenced by others in subsequent papers. It's also important to make the data available at least on a personal website or upon request. We urge you to consider submitting your raw data to the ALCDEF page on the Minor Planet Center web site:

http://www.minorplanetcenter.net/light_curve

We believe this to be the largest publicly available database of raw lightcurve data that contains 2.5 million observations for more than 11400 objects.

Now that many backyard astronomers and small colleges have access to larger telescopes, we have expanded the photometry opportunities and spin axis lists to include asteroids reaching V = 15.5.

In both of those lists, a line in *italics text* indicates a near-Earth asteroid (NEA). In the spin axis list, a line in **bold text** indicates a particularly favorable apparition. To keep the number of objects manageable, the opportunities list includes only those objects reaching a particularly favorable apparition, meaning they could all be set in bold text.

Lightcurve/Photometry Opportunities

Objects with U = 3– or 3 are excluded from this list since they will likely appear in the list below for shape and spin axis modeling. Those asteroids rated U = 1 should be given higher priority over those rated U = 2 or 2+, but not necessarily over those with no period. On the other hand, *do not overlook asteroids with* U = 2/2+ *on the assumption that the period is sufficiently established.* Regardless, do not let the existing period influence your analysis since even high quality ratings have been proven wrong at times. Note that the lightcurve amplitude in the tables could be more or less than what's given. Use the listing only as a guide.

		Brightest			LCDB Data		
Number	Name	Date	Mag	Dec	Period	Amp	U
3299	Hall	01 01.6	15.5	+18			
8348	Bhattacharyya	01 01.7	15.4	+31	19.6	0.06-0.10	2-
1502	Arenda	01 01.9	14.7	+16	45.8	0.4	2
9008	Bohsternberk	01 02.4	15.5	+21			
3999	Aristarchus	01 06.9	14.9	+23	12.58	0.30	2+
1665	Gaby	01 08.8	13.5	+29	66.	0.27	2
58688	1998 BJ4	01 09.3	15.3	+32	20.7887	0.10	1
337866	2001 WL15#	01 09.8	14.1	+14			
43659	2002 FJ1	01 11.2	15.5	+29			
14831	Gentileschi	01 11.4	15.5	+24	46.4744	0.65	2
10566	Zabadak	01 15.3	15.4	+20			
6505	Muzzio	01 18.0	14.7	+3	13.735	0.10	2+
2003	Harding	01 22.3	15.3	+22	2.96	0.18	1
4113	Rascana	01 23.9	15.4	+18	4.4161	0.46	2
32385	2000 QU191	01 23.9	15.0	+28			
4343	Tetsuya	01 24.3	15.3	+8			
5874	1989 XB	01 24.5	15.2	+17		0.06	

		Brightest			LCDB Data		
Number	Name	Date	Mag	Dec	Period	Amp	U
3299	Hall	01 01.6	15.5	+18			
2521	Heidi	01 24.7	14.9	+15	12.	0.02	1
2802	Weisell	01 26.8	14.7	+18	14.683	0.25-0.37	2
741	Botolphia	01 26.9	13.3	+24	23.93	0.12- 0.4	2-
1844	Susilva	01 30.1	14.9	+27		0.47	
41588	2000 SC46	02 01.4	14.6	-23			
6173	Jimwestphal	02 02.0	15.3	+32			
2556	Louise	02 06.0	15.0	+17	3.809	0.39	2+
3260	Vizbor	02 11.9	14.6	+5	72.12	0.64	2+
112493	2002 PR6	02 12.0	15.1	+14			
46875	1998 QD104	02 12.7	15.5	+15	88.7339	0.47	2
2333	Porthan	02 17.0	14.8	+31	27.78	0.58	2
20607	Vernazza	02 17.2	15.2	+18			
5654	Terni	02 21.0	15.0	+21	9.255	0.24-0.41	2
5382	McKay	02 23.8	15.4	+5	21.4862	0.86	2
37586	1991 BP2	02 23.8	15.2	-17			
1597	Laugier	02 25.5	15.1	+8			
2288	Karolinum	02 27.6	14.3	+31	42.16	0.15-0.40	2+
35063	1988 FD	02 27.7	15.4	+34	2.6815	0.11	2
3829	Gunma	02 29.2	14.8	+2			
13581	1993 QX4	03 02.8	15.4	+8			
1859	Kovalevskaya	03 03.1	14.6	+7	11.1084	0.13	2
3311	Podobed	03 06.2	15.5	+6			
17435	di Giovanni	03 10.8	15.4	-15			
2875	Lagerkvist	03 12.7	15.2	+0			
4540	Oriani	03 13.8	15.0	-8			
892	Seeligeria	03 14.7	13.7	+1	41.4	0.15	2
2656	Evenkia	03 17.1	15.3	+7	7.0836	0.72	2
1863	Antinous#	03 20.9	14.7	-53	7.4568	0.12-0.23	2
6917	1993 FR2	03 20.9	15.3	+1			
1715	Salli	03 28.6	14.2	+10	11.1667	0.22	2
2862	Vavilov	03 28.9	14.5	-7	>800.	0.4	2
18404	Kenichi	03 30.8	15.4	+0			

Low Phase Angle Opportunities

The Low Phase Angle list includes asteroids that reach very low phase angles. The "α" column is the minimum solar phase angle for the asteroid. Getting accurate, calibrated measurements (usually V band) at or very near the day of opposition can provide important information for those studying the "opposition effect." Use the on-line query form for the LCDB

http://www.minorplanet.info/PHP/call_OppLCDBQuery.php

to get more details about a specific asteroid.

You will have the best chance of success working objects with low amplitude and periods that allow covering at least half a cycle every night. Objects with large amplitudes and/or long periods are much more difficult for phase angle studies since, for proper analysis, the data must be reduced to the average magnitude of the asteroid for each night. This reduction requires that you determine the period and the amplitude of the lightcurve; for long period objects that can be difficult. Refer to Harris *et al.* (1989; *Icarus* **81**, 365-374) for the details of the analysis procedure.

As an aside, some use the maximum light to find the phase slope parameter (*G*). However, this can produce a significantly different value for both *H* and *G* versus when using average light, which is the method used for values listed by the Minor Planet Center.

The International Astronomical Union (IAU) has adopted a new system, $H\text{-}G_{12}$, introduced by Muinonen *et al.* (2010; *Icarus* **209**, 542-555). However it will be some years before it becomes the general standard and, furthermore, it is still in need of refinement. That can be done mostly through having more data for more asteroids, but only if there are data at very low and moderate phase angles. Therefore, we strongly encourage observers to obtain data for these objects not only at very low phase angles, but to follow them well before and/or after opposition, *i.e.*, out to phase angles of 15-30 degrees.

Num	Name	Date	α	V	Dec	Period	Amp	U
1171	Rusthawelia	01 05.6	0.53	13.4	+21	10.98	0.26-0.31	3
140	Siwa	01 09.2	0.08	12.8	+22	34.407	0.05-0.15	3
112	Iphigenia	01 10.9	0.88	13.1	+24	31.466	0.30	3
1292	Luce	01 11.3	0.48	14.1	+21	6.9541	0.12-0.26	3
383	Janina	01 12.2	0.45	13.5	+23	6.4	0.06-0.17	3
88	Thisbe	01 13.6	0.64	11.4	+20	6.042	0.08-0.25	3
30	Urania	01 14.3	0.41	10.0	+22	13.686	0.11-0.45	3
1319	Disa	01 16.6	0.90	14.5	+18	7.080	0.26 0.27	3
559	Nanon	01 21.7	0.78	13.1	+22	10.059	0.09-0.26	3
33	Polyhymnia	01 21.9	0.73	13.1	+22	18.608	0.13-0.21	3
115	Thyra	01 25.9	0.65	9.8	+20	7.241	0.13-0.20	3
576	Emanuela	01 28.3	0.53	14.2	+17	8.192	0.05-0.06	2-
171	Ophelia	01 30.2	0.69	11.9	+20	6.6654	0.14-0.46	3
570	Kythera	01 31.0	0.69	13.7	+15	8.120	0.15-0.20	2
606	Brangane	02 03.1	0.46	13.7	+18	12.2950	0.20	3-
1118	Hanskya	02 09.6	0.17	14.3	+14	15.61	0.18-0.38	2
130	Elektra	02 12.2	0.49	11.7	+12	5.225	0.19-0.58	3
1069	Planckia	02 12.4	0.16	12.9	+14	8.665	0.14-0.42	3
84	Klio	02 13.0	0.36	13.1	+15	23.562	0.04-0.21	3
5	Astraea	02 15.5	0.41	8.7	+14	16.800	0.10-0.30	3
46	Hestia	02 22.7	0.57	12.2	+09	21.040	0.08-0.12	3
676	Melitta	02 24.4	0.43	14.1	+11	7.87	0.04-0.20	2
1659	Punkaharju	03 01.0	0.28	14.3	+07	5.01	0.26-0.43	3
708	Raphaela	03 03.3	0.51	13.5	+08	20.918	0.25-0.45	3-
279	Thule	03 04.0	0.70	14.4	+09	15.962	0.02-0.10	2+
1145	Robelmonte	03 06.4	0.19	14.0	+06	9.01	0.05-0.18	2
844	Leontina	03 07.9	0.09	14.2	+05	6.7859	0.20-0.26	3
101	Helena	03 08.6	0.45	12.2	+03	23.080	0.09-0.13	3
669	Kypria	03 08.7	0.25	14.4	+04	14.283	0.17-0.74	3
1062	Ljuba	03 09.1	0.36	13.8	+03	33.8	0.17-0.2	3
209	Dido	03 09.6	0.68	12.5	+06	5.7366	0.11-0.33	3
37	Fides	03 09.8	0.57	10.6	+06	7.3335	0.10-0.25	3
1717	Arlon	03 10.0	0.91	14.1	+02	5.1484	0.07-0.12	3
431	Nephele	03 12.4	0.56	13.7	+05	18.821	0.03-0.30	2
263	Dresda	03 13.5	0.44	14.3	+01	16.809	0.32-0.55	3
168	Sibylla	03 13.6	0.96	12.9	+00	47.009	0.16	3
1005	Arago	03 13.6	0.60	14.5	+01	8.7819	0.22	2
892	Seeligeria	03 14.7	0.32	13.7	+01	41.40	0.15	2
169	Zelia	03 15.1	0.10	12.8	+02	14.537	0.13-0.14	3
321	Florentina	03 16.8	0.94	13.9	+04	2.871	0.31-0.52	3
513	Centesima	03 20.9	0.32	14.0	-01	5.23	0.18-0.45	3
801	Helwerthia	03 21.4	0.92	14.4	-02	23.93	0.15	3-
915	Cosette	03 23.0	0.46	14.3	+00	4.445	0.30-1.02	3
94	Aurora	03 23.3	0.11	12.0	-01	7.22	0.03-0.18	3
585	Bilkis	03 24.5	0.46	12.5	-01	8.5751	0.10-0.41	3-
160	Una	03 24.9	0.16	12.7	-01	11.033	0.08-0.23	3
238	Hypatia	03 25.0	0.07	12.3	-02	8.8745	0.07-0.17	3
66	Maja	03 28.4	0.15	13.2	-03	9.73509	0.12-0.45	3
81	Terpsichore	03 29.1	0.47	12.8	-05	10.943	0.06-0.10	3
872	Holda	03 31.2	0.35	12.9	-05	5.945	0.20-0.47	3

Shape/Spin Modeling Opportunities

Those doing work for modeling should contact Josef Ďurech at the email address above. If looking to add lightcurves for objects with existing models, visit the Database of Asteroid Models from Inversion Techniques (DAMIT) web site

http://astro.troja.mff.cuni.cz/projects/asteroids3D

An additional dense lightcurve, along with sparse data, could lead to the asteroid being added to or improving one in DAMIT, thus increasing the total number of asteroids with spin axis and shape models.

Included in the list below are objects that:

1. Are rated U = 3– or 3 in the LCDB
2. Do not have reported pole in the LCDB Summary table
3. Have at least three entries in the Details table of the LCDB where the lightcurve is rated U ≥ 2.

The caveat for condition #3 is that no check was made to see if the lightcurves are from the same apparition or if the phase angle bisector longitudes differ significantly from the upcoming apparition. The last check is often not possible because the LCDB does not list the approximate date of observations for all details records. Including that information is an on-going project.

		Brightest			LCDB Data		
Num	Name	Date	Mag	Dec	Period	Amp	U
533	Sara	01 02.7	13.9	+13	11.654	0.19-0.30	3
1867	Deiphobus	01 02.7	15.2	+24	58.66	0.10-0.30	3-
247	Eukrate	01 04.1	11.4	+62	12.093	0.10-0.18	3
4874	**Burke**	**01 04.7**	**15.0**	**+12**	**3.657**	**0.22-0.23**	**3-**
1171	Rusthawelia	01 05.5	13.4	+21	10.98	0.26-0.31	3
202	Chryseis	01 07.5	11.2	+16	23.67	0.04-0.28	3
1453	Fennia	01 08.4	15.2	+66	4.4121	0.10-0.19	3
811	Nauheima	01 08.7	14.9	+20	4.0011	0.08-0.20	3
1292	Luce	01 11.3	14.1	+21	6.9541	0.12-0.26	3
2650	Elinor	01 11.3	15.0	+36	2.762	0.12-0.18	3
459	Signe	01 11.4	13.4	+39	5.5362	0.25-0.43	3
713	Luscinia	01 14.8	14.2	+7	9.9143	0.09-0.40	3
4224	Susa	01 15.2	15.5	+3	6.178	0.21-0.27	3-
773	Irmintraud	01 16.9	13.5	+32	6.7514	0.05-0.15	3
1319	Disa	01 16.9	14.5	+18	7.08	0.26-0.27	3
2258	**Viipuri**	**01 18.1**	**14.7**	**+21**	**3.81**	**0.25-0.31**	**3**
1689	Floris-Jan	01 19.1	14.4	+20	145.	0.4	3
332	Siri	01 19.2	13.7	+25	8.0074	0.10-0.35	3
939	Isberga	01 19.3	15.3	+22	2.9173	0.22-0.25	3
33	Polyhymnia	01 21.6	13.1	+22	18.608	0.13-0.21	3
453	Tea	01 22.0	13.1	+29	6.812	0.03-0.37	3
305	**Gordonia**	**01 22.5**	**12.0**	**+13**	**12.893**	**0.16-0.23**	**3**
901	Brunsia	01 23.4	14.7	+16	3.1363	0.11-0.28	3
1467	Mashona	01 25.0	14.1	+31	9.76	0.24-0.25	3
913	Otila	01 25.4	15.1	+24	4.872	0.09-0.45	3
2421	Nininger	01 26.4	15.4	+29	6.4058	0.37	3-
654	**Zelinda**	**01 29.7**	**10.1**	**-5**	**31.735**	**0.08- 0.3**	**3**
171	**Ophelia**	**01 30.2**	**11.9**	**+20**	**6.6654**	**0.14-0.46**	**3**
474	Prudentia	02 01.5	15.0	+11	8.572	0.53-0.90	3
333	Badenia	02 02.4	14.1	+20	8.192	0.20-0.33	3-
374	Burgundia	02 03.0	12.7	+4	6.972	0.05-0.18	3
144	Vibilia	02 03.6	11.9	+22	13.819	0.13-0.20	3
611	Valeria	02 03.7	13.1	+0	6.977	0.08-0.16	3
1951	**Lick**	**02 04.5**	**14.1**	**+31**	**5.3016**	**0.15-0.33**	**3**
596	Scheila	02 05.5	13.4	+35	15.848	0.06-0.10	3
592	Bathseba	02 08.7	13.5	+8	7.7465	0.22-0.32	3
841	**Arabella**	**02 08.7**	**15.0**	**+19**	**3.39**	**0.22-0.26**	**3**
677	Aaltje	02 10.2	13.5	+5	16.608	0.10-0.37	3
955	Alstede	02 11.2	14.9	+23	5.19	0.26-0.27	3
1069	**Planckia**	**02 12.4**	**12.9**	**+14**	**8.665**	**0.14-0.42**	**3**
294	Felicia	02 14.2	15.5	+14	10.4227	0.19-0.35	3
715	Transvaalia	02 15.9	14.4	+31	11.83	0.19-0.32	3
2429	Schurer	02 16.7	15.5	+30	6.66	0.12-0.77	3-
706	Hirundo	02 19.8	15.2	+10	22.027	0.39- 0.9	3
2026	**Cottrell**	**02 20.1**	**15.1**	**+10**	**4.4994**	**0.77**	**3**
261	**Prymno**	**02 21.6**	**11.6**	**+16**	**8.002**	**0.13-0.20**	**3**
3913	**Chemin**	**02 21.8**	**14.4**	**+8**	**3.4077**	**0.17-0.53**	**3**
482	Petrina	02 23.5	13.2	+2	11.7922	0.07-0.56	3
1123	Shapleya	02 24.2	14.5	+19	52.92	0.38	3-
1562	**Gondolatsch**	**02 24.2**	**14.0**	**+13**	**8.78**	**0.30-0.35**	**3-**
2048	**Dwornik**	**02 24.2**	**15.1**	**+7**	**3.677**	**0.04-0.22**	**3**
477	Italia	02 24.8	14.1	+14	19.413	0.15-0.20	3
8077	**Hoyle**	**02 24.8**	**14.9**	**+20**	**2.7454**	**0.20-0.23**	**3**
7822	***1991 CS***	***02 25.2***	***14.9***	***-3***	***2.389***	***0.26-0.39***	***3***
563	Suleika	02 26.5	12.2	+22	5.69	0.13-0.28	3
1129	Neujmina	02 27.8	14.6	-3	5.0844	0.06-0.20	3
483	Seppina	03 01.1	13.4	+2	12.727	0.14-0.29	3
633	Zelima	03 01.3	14.3	+11	11.724	0.14-0.53	3-
815	Coppelia	03 04.1	14.3	+26	4.421	0.17-0.24	3
686	Gersuind	03 06.8	14.5	-14	6.3127	0.30-0.37	3
844	Leontina	03 08.0	14.2	+5	6.7859	0.20-0.26	3
2151	Hadwiger	03 08.0	14.1	+21	5.872	0.07-0.38	3
104	Klymene	03 08.2	12.5	+8	8.984	0.26- 0.3	3
101	Helena	03 08.6	12.2	+3	23.08	0.09-0.13	3
1717	Arlon	03 09.9	14.1	+2	5.1484	0.07-0.12	3
2358	Bahner	03 12.4	15.4	+1	10.848	0.33-0.43	3
598	Octavia	03 13.1	14.4	+18	10.8903	0.28-0.35	3
839	Valborg	03 17.1	14.6	-4	10.366	0.14-0.19	3
582	Olympia	03 17.6	12.5	+20	36.312	0.05-0.23	3
219	Thusnelda	03 18.7	13.2	-5	59.74	0.19-0.24	3
967	Helionape	03 19.8	14.9	+9	3.234	0.04-0.12	3
210	Isabella	03 23.6	13.3	+2	6.672	0.09-0.38	3
5925	1994 CP1	03 23.9	14.9	+6	5.4002	0.54	3
860	Ursina	03 24.3	14.7	-16	9.386	0.22-0.50	3
585	**Bilkis**	**03 24.5**	**12.5**	**-1**	**8.5751**	**0.10-0.41**	**3-**
522	Helga	03 25.2	14.4	+3	8.129	0.13-0.30	3
2903	Zhuhai	03 25.7	15.0	-18	5.263	0.32-0.54	3
4607	Seilandfarm	03 26.3	15.5	-6	3.9683	0.15-0.17	3
93768	2000 WN22	03 26.5	15.5	+52	2.6821	0.29-0.33	3
81	Terpsichore	03 29.0	12.8	-5	10.943	0.06-0.10	3
872	**Holda**	**03 31.2**	**12.9**	**-5**	**5.945**	**0.20-0.47**	**3**
368	Haidea	03 31.4	14.7	-10	9.823	0.15-0.23	3

Radar-Optical Opportunities

There are several resources to help plan observations in support of radar.

Future radar targets:
http://echo.jpl.nasa.gov/~lance/future.radar.nea.periods.html

Past radar targets:
http://echo.jpl.nasa.gov/~lance/radar.nea.periods.html

Arecibo targets:
http://www.naic.edu/~pradar/sched.shtml
http://www.naic.edu/~pradar

Goldstone targets:
http://echo.jpl.nasa.gov/asteroids/goldstone_asteroid_schedule.html

However, these are based on *known* targets at the time the list was prepared. It is very common for newly discovered objects to move up the list and become radar targets on short notice. We recommend that you keep up with the latest discoveries using the RSS feeds from the Minor Planet Center

http://www.minorplanetcenter.net/iau/rss/mpc_feeds.html

In particular, monitor the NEA feed and be flexible with your observing program. In some cases, you may have only 1-3 days when the asteroid is within reach of your equipment. Be sure to keep in touch with the radar team (through Dr. Benner's email listed above) if you get data. The team may not always be observing the target but, in some cases, your initial results may change their plans. In all cases, your efforts are greatly appreciated.

Use the ephemerides below as a guide to your best chances for observing, but remember that photometry may be possible before and/or after the ephemerides given below. Note that *geocentric* positions are given. Use these web sites to generate updated and *topocentric* positions:

MPC: *http://www.minorplanetcenter.net/iau/MPEph/MPEph.html*
JPL: *http://ssd.jpl.nasa.gov/?horizons*

In the ephemerides below, ED and SD are, respectively, the Earth and Sun distances (AU), V is the estimated Johnson V magnitude, and α is the phase angle. SE and ME are the great circles distances (in degrees) of the Sun and Moon from the asteroid. MP is the lunar phase and GB is the galactic latitude. "PHA" in the header indicates that the object is a "potentially hazardous asteroid", meaning that at some (long distant) time, its orbit might take it very close to Earth.

Some of the targets listed here may be carry-overs from the previous quarter's photometry opportunities article since they are still reachable targets for at least part of the covered quarter-year.

About YORP Acceleration

Many, if not all, of the targets in this section are near-Earth asteroids. These objects are particularly sensitive to YORP acceleration. YORP (Yarkovsky–O'Keefe–Radzievskii–Paddack) is the asymmetric thermal re-radiation of sunlight that can cause an asteroid's rotation period to increase or decrease. High precision lightcurves at multiple apparitions can be used to model the asteroid's *sidereal* rotation period and see if it's changing.

It usually takes four apparitions to have sufficient data to determine if the asteroid is rotating under the influence of YORP, so while obtaining a lightcurve at the current apparition may not result in immediately seeing a change, the data are still critical in reaching a final determination. This is why observing asteroids that already have well-known periods can still be a valuable use of telescope time. It is even more so when considering BYORP (binary-YORP) among binary asteroids where that effect has stabilized the spin so that acceleration of the primary body is not the same as if it would be if there were no satellite.

Asteroid	Fam/Grp	Period	App	Last	Bin
1998 WT24	NEA	3.698	1	2011	N
Florence	NEA	2.358	6	2011	N
2008 CM	NEA	3.054	1	2014	N
1994 AW1	NEA	2.519	5	2015	Y
Sisyphus	NEA	2.400	4	2015	Y
1991 CS	NEA	2.389	3	2015	N
2006 CJ	NEA	-	-	-	-
1997 XF11	NEA	3.259	1	2002	N
2000 DP107	NEA	2.7754	2	2008	Y
Apollo	NEA	3.065	6	2014	Y
2004 FG11	NEA	<4.	2	2014	Y

Table I. Summary of radar-optical opportunities in 2016 Jan-Mar. Data from the asteroid lightcurve database (Warner *et al.*, 2009; *Icarus* **202**, 134-146).

To help focus efforts in YORP detection, Table I gives a quick summary of this quarter's radar-optical targets. The Fam/Grp column gives the family or group for the asteroid. The period is in hours and, in the case of binary, for the primary. The App columns gives the number of different apparitions at which a lightcurve period was reported while the Last column gives the year for the last reported period. The Bin column is 'Y' if the asteroid has one or more satellites.

(33342) 1998 WT24 (Nov-Jan, *H* = 18.0, PHA)
The period for 1998 WT24 is known to be about 3.698 h. This makes it a potential binary candidate, so higher-precision data are encouraged.

DATE	RA	Dec	ED	SD	V	α	SE	ME	MP	GB
11/01	09 06.6	-05 59	0.19	0.97	17.4	91.1	78	44	-0.75	+26
11/11	08 58.9	-06 07	0.15	1.00	16.6	82.4	89	83	-0.01	+25
11/21	08 43.5	-06 12	0.10	1.01	15.6	72.3	102	139	+0.69	+21
12/01	07 56.9	-05 26	0.06	1.02	13.8	55.5	122	24	-0.72	+12
12/11	04 17.3	+02 24	0.03	1.01	11.3	23.5	156	163	+0.00	-32
12/21	00 01.4	+09 23	0.05	0.99	14.4	81.4	96	28	+0.76	-52
12/31	23 01.3	+09 41	0.10	0.96	16.5	102.2	72	165	-0.70	-45
01/10	22 35.0	+09 06	0.14	0.91	18.0	116.0	57	56	+0.00	-41

3122 Florence (Dec-Feb, *H* = 14.2, PHA)
Here is another potential binary candidate since the rotation period is known to be 2.358 h. Observations throughout the ephemeris period can help establish the H-G parameters. The estimated size is 4.5 km.

DATE	RA	Dec	ED	SD	V	α	SE	ME	MP	GB
12/01	11 16.4	+15 09	1.80	1.97	18.1	29.9	84	34	-0.72	+65
12/11	11 23.3	+13 52	1.72	2.01	18.1	29.2	92	87	+0.00	+66
12/21	11 27.3	+12 48	1.63	2.06	18.0	28.0	101	137	+0.76	+66
12/31	11 28.0	+11 59	1.54	2.10	17.8	26.0	111	9	-0.70	+65
01/10	11 24.9	+11 25	1.46	2.14	17.7	23.1	121	120	+0.00	+64
01/20	11 17.7	+11 06	1.39	2.18	17.5	19.3	133	98	+0.82	+63
01/30	11 06.4	+11 00	1.33	2.22	17.3	14.6	146	33	-0.70	+61
02/09	10 51.7	+11 02	1.30	2.25	17.0	9.0	159	164	+0.00	+58

(294739) 2008 CM (Dec-Jan, *H* = 17.1, PHA)
Warner (2014; *MPB* **41**, 157-168) found a period of 3.054 h. The amplitude was 0.48 mag at a phase angle α = 70°, about the same as during the first few days of the ephemeris below.

DATE	RA	Dec	ED	SD	V	α	SE	ME	MP	GB
12/20	14 35.0	+55 09	0.12	0.99	15.7	84.0	89	117	+0.66	+56
12/25	12 11.8	+50 15	0.08	1.01	14.1	68.1	108	80	+1.00	+66
12/30	09 06.6	+15 09	0.06	1.03	12.7	34.9	143	18	-0.79	+37
01/04	07 32.4	-16 45	0.09	1.06	13.8	37.3	139	95	-0.34	+1
01/09	06 50.8	-28 03	0.15	1.08	15.0	44.7	129	133	-0.01	-12
01/14	06 29.6	-32 30	0.20	1.11	15.9	47.7	124	106	+0.19	-18
01/19	06 17.6	-34 29	0.26	1.14	16.5	48.7	120	63	+0.72	-21
01/24	06 10.8	-35 20	0.32	1.17	17.0	48.8	117	59	+1.00	-23

1994 AW1 (Dec-Jan, *H* = 17.0, PHA)

This is a known binary (Pravec and Hahn, 1997; *Icarus* **127**, 431-440). The primary rotation period is 2.519 h. The orbital period the satellite is 22.3 h, making it difficult for a single station to cover *mutual events* (occultations and/or eclipses) thoroughly, assuming the viewing geometry allows seeing the events. This would be a good project for a group of observers who are widely separated in longitude.

DATE	RA	Dec	ED	SD	V	α	SE	ME	MP	GB
12/01	20 49.8	+62 58	0.36	1.10	17.8	62.0	99	103	-0.72	+12
12/06	21 30.4	+62 30	0.35	1.11	17.7	60.6	101	111	-0.26	+8
12/11	22 14.4	+61 22	0.34	1.12	17.6	59.1	104	101	+0.00	+4
12/16	22 59.6	+59 21	0.33	1.12	17.5	57.5	106	74	+0.22	+0
12/21	23 43.5	+56 25	0.33	1.13	17.5	56.1	108	54	+0.76	-5
12/26	00 24.0	+52 37	0.32	1.13	17.4	54.8	110	79	-0.99	-10
12/31	01 00.1	+48 08	0.32	1.14	17.4	53.9	111	121	-0.70	-15
01/05	01 31.8	+43 14	0.33	1.14	17.5	53.4	111	145	-0.25	-19

1866 Sisyphus (Jan-Apr, *H* = 13.0, Binary)

This is considered a known binary based on radar observations in 1985 (*http://echo.jpl.nasa.gov/asteroids/Sisyphus/sisyphus.html*) that showed a spike in the echo power spectrum on several nights. Stephens *et al*. (2011; *MPB* **38**, 212-213) reported a possible satellite with an orbital period of 25.5 h based on lightcurve photometry. Assuming a binary, the primary has a period of about 2.40 h and amplitude that ranges from 0.01 to 0.15 mag.

DATE	RA	Dec	ED	SD	V	α	SE	ME	MP	GB
01/10	15 10.3	+13 27	2.98	2.82	18.0	19.3	71	68	+0.00	+55
01/25	15 24.2	+13 35	2.76	2.79	17.8	20.4	81	91	-0.99	+52
02/09	15 35.1	+14 16	2.54	2.75	17.7	21.0	92	95	+0.00	+50
02/24	15 41.7	+15 28	2.31	2.71	17.4	20.8	103	66	-0.99	+49
03/10	15 42.7	+17 06	2.09	2.67	17.1	19.7	115	125	+0.01	+49
03/25	15 36.6	+19 00	1.90	2.62	16.8	17.8	127	41	-0.98	+51
04/09	15 22.3	+20 45	1.74	2.57	16.5	15.4	137	146	+0.04	+55
04/24	15 00.3	+21 44	1.63	2.51	16.3	14.0	143	37	-0.97	+60

(7822) 1991 CS (Jan-Mar, *H* = 17.4, PHA)

The rotation period for this NEA is well-established at about 2.390 h. The period makes it an ideal candidate for being a binary, even though the amplitude ranges from 0.26-0.39 mag. This makes it more elongated than many known binary primaries, but there are exceptions; this could be one as well.

DATE	RA	Dec	ED	SD	V	α	SE	ME	MP	GB
01/10	09 56.4	-73 22	0.47	1.02	18.3	71.9	81	85	+0.00	-15
01/20	09 44.5	-69 49	0.39	1.05	17.9	69.8	88	102	+0.82	-13
01/30	09 29.9	-63 30	0.31	1.07	17.3	65.2	98	70	-0.70	-9
02/09	09 14.4	-50 53	0.23	1.10	16.4	54.9	114	118	+0.00	-1
02/19	09 01.5	-25 04	0.18	1.13	15.3	34.3	140	51	+0.86	+14
02/29	08 54.5	+11 02	0.18	1.15	15.1	23.2	153	95	-0.68	+32
03/10	08 54.7	+35 26	0.25	1.18	16.2	37.4	134	122	+0.01	+39
03/20	09 02.0	+47 08	0.34	1.20	17.2	46.2	119	36	+0.89	+41

(364136) 2006 CJ (Feb-Mar, *H* = 20.2)

No rotation period was found in the literature for 2006 CJ. The estimated diameter is only 270 meters, which makes it possible, but not too likely, that 2006 CJ could be a super-fast rotator. For this reason, a larger scope and short exposures will be ideal since the longer exposures required by smaller telescopes might "smear" the lightcurve data, *i.e*., cover more than about 1/5 of a rotation in a single exposure. This makes it difficult if not impossible to find the rotation period of the asteroid.

DATE	RA	Dec	ED	SD	V	α	SE	ME	MP	GB
02/20	10 44.9	-22 48	0.23	1.19	18.7	28.7	145	56	+0.92	+31
02/22	10 24.8	-22 24	0.22	1.18	18.5	27.1	147	35	+0.99	+29
02/24	10 03.7	-21 44	0.22	1.18	18.5	26.4	148	32	-0.99	+27
02/26	09 42.1	-20 48	0.22	1.18	18.4	26.8	148	49	-0.91	+24
02/28	09 20.5	-19 36	0.22	1.17	18.5	28.3	146	73	-0.77	+21
03/01	08 59.4	-18 12	0.22	1.17	18.5	30.8	143	98	-0.59	+18
03/03	08 39.2	-16 38	0.22	1.17	18.6	34.0	139	123	-0.40	+15
03/05	08 20.3	-14 58	0.22	1.16	18.8	37.6	134	145	-0.21	+12

(35396) 1997 XF11 (Mar-May, *H* = 16.3, PHA)

The reported synodic periods for this NEA average about 3.257 h. This is based on observations made by Pravec *et al*. in 2002. You may recall that initial reports soon after its discovery concerning the chances for the asteroid hitting the Earth in the not-to-distant future eventually led to improvements in impact probability monitoring.

DATE	RA	Dec	ED	SD	V	α	SE	ME	MP	GB
03/01	13 50.8	-15 45	0.84	1.65	18.8	27.7	129	30	-0.59	+45
03/11	13 53.0	-15 58	0.70	1.59	18.3	24.4	139	164	+0.06	+44
03/21	13 50.5	-15 39	0.59	1.53	17.6	19.5	149	58	+0.94	+45
03/31	13 42.1	-14 34	0.48	1.46	16.9	12.7	161	65	-0.56	+47
04/10	13 26.3	-12 24	0.39	1.39	15.9	3.8	175	147	+0.10	+50
04/20	13 02.4	-08 46	0.32	1.32	15.7	9.5	167	12	+0.96	+54
04/30	12 31.0	-03 28	0.27	1.24	15.7	25.0	149	120	-0.52	+59
05/10	11 54.1	+03 19	0.23	1.16	15.7	43.3	128	84	+0.14	+63

(185851) 2000 DP107 (Mar, *H* = 18.2, PHA)

This is a known binary with a primary rotation period of 2.775 h and orbital period for the satellite of 42.12 h. Because of the long orbital period, capturing the mutual events (occultations and/or eclipses) caused by the satellite, assuming the viewing geometry is right, will be a hit or miss situation for a single observer. However a coordinated campaign of observers well-separated in longitude should be able to fill in the secondary lightcurve within a relatively short time. The primary lightcurve amplitude ranges from 0.13-0.21 mag.

DATE	RA	Dec	ED	SD	V	α	SE	ME	MP	GB
03/01	11 19.4	+12 05	0.52	1.51	18.1	5.8	171	74	-0.59	+64
03/03	11 14.9	+12 15	0.51	1.50	18.0	4.7	173	99	-0.40	+63
03/05	11 10.2	+12 24	0.50	1.49	17.9	4.4	173	126	-0.21	+62
03/07	11 05.2	+12 32	0.49	1.48	17.9	5.0	173	154	-0.06	+61
03/09	11 00.0	+12 40	0.48	1.47	17.9	6.3	171	171	+0.00	+60
03/11	10 54.6	+12 47	0.47	1.46	17.9	8.0	168	142	+0.06	+59
03/13	10 49.2	+12 52	0.46	1.45	18.0	10.0	165	112	+0.21	+58
03/15	10 43.6	+12 57	0.46	1.44	18.0	12.1	162	82	+0.43	+57

1862 Apollo (Mar-Apr, *H* = 16.3, PHA)

This is the namesake for the Apollo asteroids, those with orbits that lie mostly outside Earth's orbit but also cross it for a short time. This is a binary, the satellite being discovered by Ostro *et al.* (2005). The primary rotation period is 3.066 h. The amplitude of the lightcurve changes dramatically from apparition to the next, ranging from only 0.15 mag up to 1.15 mag. Apollo is one a small number of asteroids where YORP acceleration has been confirmed (Kaasalainen *et al.*, 2007; *Nature* **446**, 420-422). Additional lightcurves can be used to confirm and improve the earlier results.

DATE	RA	Dec	ED	SD	V	α	SE	ME	MP	GB
03/10	17 24.7	-22 17	0.83	1.27	18.4	51.5	88	101	+0.01	+8
03/15	17 50.4	-23 02	0.77	1.22	18.2	54.3	87	167	+0.43	+2
03/20	18 19.2	-23 36	0.72	1.18	18.1	57.5	85	133	+0.89	-4
03/25	18 51.3	-23 51	0.67	1.13	18.0	61.1	83	81	-0.98	-11
03/30	19 26.8	-23 40	0.63	1.08	17.9	65.2	80	30	-0.66	-18
04/04	20 05.2	-22 54	0.61	1.03	17.8	69.6	76	28	-0.17	-26
04/09	20 45.4	-21 29	0.59	0.99	17.8	74.1	71	93	+0.04	-34
04/14	21 26.1	-19 23	0.59	0.94	17.9	78.5	67	153	+0.49	-43

(363599) 2004 FG11 (Mar-Apr, *H* = 20.9, PHA)

Radar observations by Taylor *et al.* (2012) found this to be a binary with a satellite orbital period of 20.4 h. The primary period is not well known, but is believed to be < 4 h. Lightcurve observations in 2014 by Warner may have detected the satellite, but only by forcing the data to the estimated orbital period. There were no indications of the primary's lightcurve at that time.

DATE	RA	Dec	ED	SD	V	α	SE	ME	MP	GB
03/27	14 29.5	+01 47	0.23	1.20	19.4	25.9	148	15	-0.89	+55
03/29	14 34.2	+03 16	0.20	1.18	19.1	26.3	149	35	-0.75	+56
03/31	14 40.2	+05 12	0.17	1.15	18.7	27.2	148	58	-0.56	+56
04/02	14 48.1	+07 52	0.15	1.13	18.4	29.0	147	81	-0.36	+56
04/04	14 59.5	+11 41	0.12	1.10	18.0	32.2	144	105	-0.17	+56
04/06	15 17.4	+17 29	0.09	1.07	17.6	38.1	139	126	-0.03	+55
04/08	15 49.8	+26 52	0.07	1.05	17.2	48.8	128	134	+0.01	+51
04/10	17 01.2	+41 39	0.06	1.02	17.2	68.6	108	121	+0.10	+38

IN THIS ISSUE

This list gives those asteroids in this issue for which physical observations (excluding astrometric only) were made. This includes lightcurves, color index, and H-G determinations, etc. In some cases, no specific results are reported due to a lack of or poor quality data. The page number is for the first page of the paper mentioning the asteroid. EP is the “go to page” value in the electronic version.

THE MINOR PLANET BULLETIN (ISSN 1052-8091) is the quarterly journal of the Minor Planets Section of the Association of Lunar and Planetary Observers (ALPO). Current and most recent issues of the *MPB* are available on line, free of charge from:
http://www.minorplanet.info/mpbdownloads.html
Nonmembers are invited to join ALPO by communicating with: Matthew L. Will, A.L.P.O. Membership Secretary, P.O. Box 13456, Springfield, IL 62791-3456 (will008@attglobal.net). The Minor Planets Section is directed by its Coordinator, Prof. Frederick Pilcher, 4438 Organ Mesa Loop, Las Cruces, NM 88011 USA (fpilcher35@gmail.com, assisted by Lawrence Garrett, 206 River Rd., Fairfax, VT 05454 USA (LSGasteroid@msn.com). Dr. Alan W. Harris (Space Science Institute; awharris@spacescience.org), and Dr. Petr Pravec (Ondrejov Observatory; ppravec@asu.cas.cz) serve as Scientific Advisors. The Asteroid Photometry Coordinator is Brian D. Warner, Palmer Divide Observatory, 446 Sycamore Ave., Eaton, CO 80615 USA (brian@MinorPlanetObserver.com).

The Minor Planet Bulletin is edited by Professor Richard P. Binzel, MIT 54-410, Cambridge, MA 02139 USA (rpb@mit.edu). Brian D. Warner (address above) is Assistant Editor. The *MPB* is produced by Dr. Robert A. Werner, 3937 Blanche St., Pasadena, CA 91107 USA (bwernerca1@att.net) and distributed by Derald D. Nye. Direct all subscriptions, contributions, address changes, etc. to:

Mr. Derald D. Nye - Minor Planet Bulletin
10385 East Observatory Drive
Corona de Tucson, AZ 85641-2309 USA
(nye@kw-obsv.org) (Telephone: 520-762-5504)

Effective with Volume 38, the *Minor Planet Bulletin* is a limited print journal, where print subscriptions are available only to libraries and major institutions for long-term archival purposes. In addition to the free electronic download of the *MPB* noted above, electronic retrieval of all *Minor Planet Bulletin* articles (back to Volume 1, Issue Number 1) is available through the Astrophysical Data System
http://www.adsabs.harvard.edu/.

Authors should submit their manuscripts by electronic mail (rpb@mit.edu). Author instructions and a Microsoft Word template document are available at the web page given above. All materials must arrive by the deadline for each issue. Visual photometry observations, positional observations, any type of observation not covered above, and general information requests should be sent to the Coordinator.

* * * * *

The deadline for the next issue (43-2) is January 15, 2016. The deadline for issue 43-3 is April 15, 2016.